DEVELOPMENT AND APPLICATION OF THE SKIN XENOGRAFT MOUSE MODEL TO STUDY HOST RESISTANCE TO *DEMODEX CANIS*

A Thesis

Presented to

The Faculty of Graduate Studies

of

The University of Guelph

by

KEITH EMERSON LINDER

In partial fulfillment of requirements

for the degree of

Doctor of Philosophy

September, 2000

ABSTRACT

DEVELOPMENT AND APPLICATION OF THE SKIN XENOGRAFT MOUSE MODEL TO STUDY HOST RESISTANCE TO *DEMODEX CANIS*

Keith Emerson Linder
University of Guelph, 2000

Advisor:
Dr. J. A. Yager
Co-Advisor
Dr. R. A. Foster

The objectives of this experimental study were: 1) to develop a reproducible skin xenograft mouse model of canine demodicosis, and 2) to test the hypothesis that lymphocytes affect *Demodex canis* populations *in vivo*. This study compared the healing of full- and split-thickness canine skin xenografts, developed canine peripheral blood lymphocyte mouse chimeras and recreated canine allogeneic skin graft rejection in the murine model. Canine blood lymphocytes survived transfer to immunodeficient mice and produced variable amounts of canine IgG, up to 6.0 mg/mL. Transferred lymphocytes mediated allogeneic skin graft rejection. The full-thickness skin xenografting techniques developed led to well-haired, relatively large, canine skin xenografts. Four types of genetically immunodeficient mice (scid/bg, ICR scid, tgε26 and *Rag2*) were found to support canine skin xenografts and *D. canis* graft infections; however, development of the "leaky" phenotype and/or low survivability limited the use of scid/bg, ICR scid, or tgε26 mice for modeling demodicosis.

To directly test the lymphocyte hypothesis, *D.* canis infected skin grafts on *Rag2* null mice were treated with syngeneic canine lymphocytes and then graft mite numbers were compared. Grafts received either 25×10^6 unstimulated lymphocytes or 15×10^6 lymphocytes that were stimulated *in vitro* with phytohemagglutinin and human

recombinant interleukin-2. Skin xenografts grew abundant hair and did not develop gross lesions after *D. canis* infection or lymphocyte transfer. Inflammation was not associated with *D. canis* infected follicles. Ninety days post infection, the mean (±SEM) calculated number of mites per xenograft sample was significantly higher after treatment with stimulated lymphocytes, 15,330 (±3,583), than with unstimulated lymphocytes, 6,582 (±1,118) ($P=0.016$), or with saline 8,931(±1,716) ($P=0.049$). Canine IgG, measured by ELISA, was significantly higher in mouse sera after treatment of mite infected grafts with stimulated lymphocytes (mean ±SEM, 34.01 ±4.19 μg/mL), than with unstimulated lymphocytes ($P<0.001$). In conclusion, *D. canis* mites proliferated to high numbers on xenografts, confirming the importance of systemic dog factors in controlling mite populations. *D. canis* did not induce lesions of demodicosis in the absence of inflammation. Treatment with *in vitro* stimulated lymphocytes was associated with increased numbers of mites; this was an unexpected finding. Furthermore, the methodology applied herein demonstrates the applicability of the skin xenograft mouse model in veterinary dermatology research.

This work is dedicated to

TRACY ANNE HAMMER

Tracy was the first dual-degree doctoral candidate in veterinary medicine and microbiology at Michigan Stage University. She was a wonderful friend to many.

Tracy died July 17, 1996, with her mother Beverly, on TWA Flight 800, just before she could finish both of her degrees. Tracy was traveling to France to present her research.

ACKNOWLEDGMENTS

First and foremost, I sincerely thank my advisor Dr. J. A. Yager for providing the opportunity, guidance and support that has enabled me to achieve this goal. Indeed, it has been a great privilege to work with Dr. Yager, whom I regard as one of the few world authorities on veterinary dermatopathology. I thank my co-advisor Dr. R. A. Foster, to whom I am indebted for personal mentoring in diagnostic pathology and for setting an intellectual standard for me to follow.

I am also thankful to the members of my advisory committee, Drs. B.A. Croy, W.M. Parker, J.R. Barta, and P. E. Shewen for their continuous support, encouragement and advice throughout my graduate studies. Dr. Croy generously provided the tgε26 transgenic mice used in these experiments.

I am grateful for the technical expertise of many professionals within the Department of Pathobiology, especially Hua Shen, Gaye Smith, and Barb Jefferson, without whom this work would not have been possible. I am grateful for the assistance of Karen Macmillan. A special thanks goes to Gail Kunkle for advice and support.

I thank Janice Greenwood and Pom Chantakru for helping me with the tgε26 mice. I thank Dave Bridle, Jackie Rombeek, Tony Cengija and Angela Pinsonneault for invaluable assistance with mouse husbandry. Mary Martini, Annette Morrison, Panos Mavronicolus and Jennifer Beehler took great care of the dogs enrolled in this study.

I greatly appreciate all of the animals, dogs and mice that made this research possible. While I will remember them all, "Penny" will be forever present in my thoughts. I am also grateful to the pet owners and veterinarians that took the time to assist me with this work.

I thank the many friends and colleagues that have enriched my life over the past few years and special thanks go to Lindsay Tomlinson, Josepha Delay, Cathy Shilton, Darren Wood, Denise Goens, Simon Pearce, Elemir Simko and Andrew Peregrine. The assistance of Josepha and Darren made the dog surgeries possible. I thank John and Joe Foster for good friendship and support.

I thank my family, Vincent, Christine, Benjamin, and Chanse Linder for providing unconditional love and encouragement throughout this project. I thank Connie Chow for her editorial comments and support.

Lastly, I am forever indebted to Dana Randall for her love, patience and many hours spent traveling Highway-401.

DECLARATION OF WORK PERFORMED

I declare that I have performed all of the work in this thesis, with the exception of the items listed below.

Bacterial culture of canine skin graft samples was performed by the Animal Health Diagnostic Laboratory (University of Guelph, Guelph, ON). Immunohistochemical staining of tissues was performed by Prairie Diagnostic Services (Western College of Veterinary Medicine, Saskatoon, SK).

TABLE OF CONTENTS

Acknowledgments i

Declaration of Work Performed ii

List of Figures ix

List of Tables xiii

CHAPTER 1: GENERAL INTRODUCTION AND LITERATURE REVIEW 1

1.1 General Introduction 1

1.2 Part 1: *Demodex canis* and Canine Demodicosis 3

1.2.1 Biology of *Demodex canis* 3

1.2.2 Epidemiology of Canine Demodicosis 7

1.2.2.1 Distribution, Incidence, and Breed Association 7

1.2.2.2 Clinical Presentation, Diagnosis, and Treatment 9

1.2.3 Pathogenesis of Canine Demodicosis 10

1.2.3.1 Mite Factors 10

1.2.3.2 Host Factors 11

1.2.3.2.1 Innate Defense Mechanisms 11

1.2.3.2.2 Acquired Humoral Immunity 12

1.2.3.2.3 Acquired Cellular Immunity 13

1.2.3.3 Histopathology 15

1.2.4 Summary 17

1.3 Part 2: Skin Xenograft Mouse Model 17

1.3.1 Components of the Skin Xenograft Mouse Model 18

1.3.1.1 Graft Recipient – Immunodeficient Mouse..... 19

1.3.1.2 The Skin Xenograft..... 23

1.3.2 Modeling Skin Infections..... 29

1.3.3 Modeling Skin Inflammation..... 31

1.3.3.1 Preexisting Inflammatory Lesions..... 31

1.3.3.2 Recreating Cutaneous Inflammation..... 31

1.3.4 Modeling Canine Demodicosis..... 33

1.4 Summary and Rationale..... 34

1.5 Research Objectives..... 35

Table..... 21

CHAPTER 2: GENERAL MATERIALS AND METHODS..... 36

2.1 Research Animals..... 36

2.1.1 Mice..... 36

2.1.2 Dogs..... 37

2.1.3 Mites..... 38

2.2 Mouse Blood Collection..... 38

2.3 Skin Grafting Procedures..... 39

2.3.1 Canine Donor Skin Collection..... 39

2.3.2 Preparation of Individual Skin Grafts..... 40

2.3.3 Skin Grafting of Mice..... 40

2.3.4 Skin Graft Bandage Procedures..... 41

2.4 *Demodex canis* Infection of Skin Grafts..... 42

2.5 Skin Graft Collection and Evaluation..... 43

2.5.1 Skin Graft Collection..... 43

2.5.2 Histology and Immunohistochemistry..... 44

2.5.3 Skin Graft Digestion and Enumeration of *Demodex canis*..... 45

2.5.4 Mouse Necropsy..... 47

2.6 Isolation of Canine Leukocytes..... 47

2.7 *In vitro* Canine Lymphocyte Blastogenesis..... 48

2.8 Quantification of Murine and Canine Immunoglobulin in Mouse Plasma..... 50

2.9 Statistical Methods..... 51

CHAPTER 3: DEVELOPMENT OF THE SKIN XENOGRAFT MOUSE MODEL FOR THE STUDY OF CANINE DEMODICOSIS..... 52

3.1 Introduction..... 52

3.2 Use of Tgε26 Mice to Support Canine Skin Xenografts and Identification of Factors Important for Xenograft Success..... 54

3.2.1 Materials and Methods..... 54

3.2.2 Results..... 58

3.2.3 Discussion..... 61

Figures..... 67

3.3 Canine Leukocyte Reconstitution of Tgε26 Mice..... 73

3.3.1 Materials and Methods..... 74

3.3.2 Results..... 76

3.3.3 Discussion..... 77

Figures..... 83

3.4 Demonstration of Canine Lymphocyte Function in the Skin Xenograft Environment..... 87

3.4.1 Materials and Methods..... 88

3.4.2 Results..... 89

3.4.3 Discussion..... 90

Figures..... 94

CHAPTER 4: APPLICATION OF THE SKIN XENOGRAFT MOUSE MODEL TO STUDY HOST RESISTANCE TO *DEMODEX CANIS* AND THE PATHOGENESIS OF CANINE DEMODICOSIS..... 97

4.1 Introduction..... 97

4.2 Use of Canine Skin Xenograft-ICR Scid Mouse Chimeras to Model Canine Demodicosis..... 98

4.2.1 Materials and Methods..... 99

4.2.2 Results..... 102

4.2.3 Discussion..... 105

Figures..... 109

Tables..... 114

4.3 Use of Canine Skin Xenograft-Tgε26 Mouse Chimeras to Model Canine Demodicosis..... 117

4.3.1 Materials and Methods..... 117

4.3.2 Results..... 120

4.3.3 Discussion..... 126

Figures..... 130

Tables..... 142

4.4 Use of Canine Skin Xenograft-*Rag2* Mouse Chimeras to Model Canine Demodicosis..... 148

4.4.1 Materials and Methods..... 149

4.4.2 Results..... 151

4.4.3 Discussion..... 155

Figures..... 162

Tables..... 172

CHAPTER 5: GENERAL DISCUSSION AND CONCLUSIONS..... 174

5.1 Introduction..... 174

5.2 Development of the Skin Xenograft Mouse Model..... 174

5.2.1 Immunodeficient Mice..... 175

5.2.2 Canine Skin Xenografting..... 177

5.2.3 Canine Leukocyte Mouse Chimeras..... 179

5.2.4 Newer Immunodeficient Mice..... 181

5.3 Application of the Skin Xenograft Mouse Model to Study Canine Demodicosis..... 183

5.3.1 The Skin Xenograft Mouse Model of Canine Demodicosis..... 182

5.3.2 Investigating the Pathogenesis of Canine Demodicosis..... 185

5.3.2.1 Host Resistance to *Demodex canis* Overgrowth..... 185

5.3.2.2 Skin Lesion Development in Canine Demodicosis..... 189

5.3.3 Future Investigations of Canine Demodicosis..... 192

5.4 Conclusions..... 195

Table..... 175

REFERENCES..... 299

Appendix 1: Fabricated Skin Punch Biopsy Tools..... 223

Appendix 2: Mouse Plasma Canine IgG Levels (μg/mL) for PBMC Reconstituted Tgε26 mice, Section 3.3..... 224

Appendix 3: Mouse Plasma Canine IgG Levels (μg/ml) for the ICR Scid Experiment, Section 4.2..... 226

Appendix 4: Hair Growth Score for Canine Xenografts in the *Rag2* Experiment, Section 4.4..... 227

Appendix 5: Mouse Serum Canine IgG Levels (μg/ml) for the *Rag2* Experiment, Section 4.4..... 228

Appendix 6: Bacterial Culture Results for the *Rag2* Experiment, Section 4.4..... 229

LIST OF FIGURES

CHAPTER 3

SECTION 3.2

Figure 3.2-1: Line graph showing the surface eschar score (mean ± standard error) for canine thin split-thickness skin grafts on tgε26 mice at 3, 6, and 9 weeks post transplantation .....**Page 67**

Figure 3.2-2: Line graph showing the diameter (mm) of canine skin grafts on tgε26 mice at 1, 3, 6 and 9 weeks post transplantation .....**Page 68**

Figure 3.2-3: Appearance of representative canine skin grafts on tgε26 mice at 9 weeks post transplantation.....**Page 69**

Figure 3.2-4: Photomicrographs of a thin split-thickness canine skin graft (Group-I) from a tgε26 mouse at 10 weeks post transplantation.....**Page 70**

Figure 3.2-5: Photomicrographs of a full-thickness canine skin graft (Group-III) from a tgε26 mouse at 10 weeks post transplantation.....**Page 71**

Figure 3.2-6: Photomicrographs of a thick split-thickness canine skin graft (Group-II) from a tgε26 mouse at 10 weeks post transplantation.....**Page 72**

SECTION 3.3

Figure 3.3-1: Line graph showing canine IgG concentration (μg/mL) over time in plasma from IgG positive tgε26 mice after intraperitoneal transfer of canine PBMC.....**Page 83**

Figure 3.3-2: Line graph showing the packed cell volume for tgε26 mice taken prior to and at weekly intervals after intraperitoneal transfer of canine PBMC.....**Page 84**

Figure 3.3-3: Line graph showing canine IgG concentration (mg/mL; mean ± SD) over time in plasma from tgε26 mice (n=6) after intraperitoneal transfer of canine IgG.....**Page 85**

Figure 3.3-4: Line graph showing the packed cell volume for tgε26 mice (n=6) taken prior to and at weekly intervals after intraperitoneal transfer of canine IgG.....**Page 86**

SECTION 3.4

Figure 3.4-1: Photomicrographs of a canine skin graft from a tgε26 mouse at 4 weeks after direct graft inoculation with allogeneic canine PBMC (Group-I).....**Page 94**

Figure 3.4-2: Photomicrographs of a canine skin graft from a tgε26 mouse at 4 weeks after direct inoculation with PBS (Group-II).....**Page 95**

Figure 3.4-3: Photomicrographs of CD3 immunostained canine skin grafts from tgε26 mice at 4 weeks after direct inoculation with allogeneic canine PBMC (Group-I) or PBS (Group-II).....**Page 96**

CHAPTER 4

SECTION 4.2

Figure 4.2-1: Timeline for ICR scid experiment.....**Page 100**

Figure 4.2-2: Appearance of two representative full-thickness canine skin grafts on ICR scid mice prior the development of graft lesions.....**Page 109**

Figure 4.2-3: Appearance of six representative full-thickness canine skin grafts on ICR scid mice at experiment completion.....**Page 109**

Figure 4.2-4: **(A)** Bar graph showing the calculated total number of *D. canis* per digest sample (mean ± standard error) recovered from canine skin grafts on ICR scid mice by NaOH digestion.....**Page 110**

Figure 4.2-5: Photomicrographs of less severely affected full-thickness canine skin grafts from ICR scid mice at experiment completion.....**Page 111**

Figure 4.2-6: Photomicrographs of skin grafts from ICR scid mice with prominent dermal infiltrate of mononuclear inflammatory cells.....**Page 112**

Figure 4.2-7: Photomicrographs showing inflammation in skin grafts from two ICR scid mice that did not receive canine PBMC.....**Page 113**

SECTION 4.3

Figure 4.3-1: Timeline for experiment one with tgε26 mice.....**Page 118**

Figure 4.3-2: Timeline for experiment two with tgε26 mice.....**Page 118**

Figure 4.3-3: Appearance of representative canine skin grafts on tgε26 mice that received canine PBMC (Group-I) or PBS (Group-II) once after *D. canis* infection (experiment one).....**Page 130**

Figure 4.3-4: Bar graph showing the results of *D. canis* enumeration, by NaOH digestion, for canine skin grafts on tgε26 mice that received canine PBMC or PBS once after mite infection (experiment one).....**Page 131**

Figure 4.3-5: Bar graph showing the results of *D. canis* enumeration, by NaOH digestion, for canine skin grafts on tgε26 mice that received canine PBMC or PBS once after mite infection (experiment one).....**Page 133**

Figure 4.3-6: Bar graph showing the results of *D. canis* enumeration, by NaOH digestion, for canine skin grafts on tgε26 mice that received canine PBMC or PBS twice, before and after mite infection (experiment two).....**Page 134**

Figure 4.3-7: Bar graph showing the results of *D. canis* enumeration, by NaOH digestion, for canine skin grafts on tgε26 mice that received canine PBMC or PBS twice, before and after mite infection (experiment two).....**Page 135**

Figure 4.3-8: Photomicrographs of a representative canine skin graft from a tgε26 mouse that received PBMC once (Group-I), after mite infection (experiment one).....**Page 136**

Figure 4.3-9: Photomicrographs of a representative canine skin graft from a tgε26 mouse that received PBS once (Group-II), after mite infection (experiment one).....**Page 137**

Figure 4.3-10: Photomicrographs of a representative canine skin graft from a tgε26 mouse that received PBMC (Group-I) or PBS (Group-II) once, after mite infection (experiment one).....**Page 138**

Figure 4.3-11: Photomicrographs of a canine skin graft from a tgε26 mouse that had received canine PBMC twice (Group-I) before and after mite infection (experiment two).....**Page 139**

Figure 4.3-12: Photomicrographs of a canine skin graft on a tgε26 mouse that had received canine PBS twice (Group-II), before and after mite infection (experiment two).....**Page 140**

Figure 4.3-13: Photomicrographs of CD3 immunostained canine skin grafts from tgε26 mice that had received canine PBMC (Group-I) or PBS (Group-II) before and after mite infection (experiment two).....**Page 141**

Figure 4.3-14: Photomicrographs of CD 45 immunostained canine skin grafts from tgε26 mice that had received canine PBMC (Group-I) or PBS (Group-II) before and after mite infection (experiment two).....**Page 142**

SECTION 4.4

Figure 4.4-1: Timeline for *Rag2* experiment.....**Page 149**

Figure 4.4-2: Appearance of canine skin grafts on *Rag2* null mice in Group-I at experiment completion.....**Page 162**

Figure 4.4-3: Appearance of canine skin grafts on *Rag2* null mice in Group-II at experiment completion.....**Page 163**

Figure 4.4-4: Appearance of canine skin grafts on *Rag2* null mice in Group-III at experiment completion.....**Page 164**

Figure 4.4-5: Appearance of canine skin grafts on *Rag2* null mice in Group-IV at experiment completion.....**Page 165**

Figure 4.4-6: Bar graphs showing the results of *D. canis* enumeration for canine skin grafts, by NaOH digestion, at completion of the *Rag2* experiment.....**Page 166**

Figure 4.4-7: Photomicrographs of a representative canine skin graft, treated with *in vitro* stimulated PBL (Group-I), from a *Rag2* null mouse.....**Page 167**

Figure 4.4-8: Photomicrographs of a representative canine skin graft, treated with unstimulated PBMC (Group-II), from a *Rag2* null mouse.....**Page 168**

Figure 4.4-9: Photomicrographs of a representative canine skin graft, treated with PBS (Group-III), from a *Rag2* null mouse.....**Page 169**

Figure 4.4-10: Photomicrographs of a representative canine skin graft, treated with *in vitro* stimulated PBL (Group-IV) but not infected with *D. canis*, from a *Rag2* null mouse.....**Page 170**

Figure 4.4-11: Bar graph showing canine IgG concentration (μg/mL, mean ± standard error) in sera from *Rag2* mice at experiment completion, approximately 4 weeks after intragraft transfer of canine leukocytes.....**Page 171**

LIST OF TABLES

CHAPTER 1

Table 1: Animal Skin Donors and Immunodeficient Recipient Mice Used for Skin Xenograft Experiments .....**Page 21**

CHAPTER 4

SECTION 4.2

Table 4.2-1: Calculated Number of *D. canis* Per Skin Graft Digest Sample Collected from Skin Grafts on ICR Scid Mice.....**Page 114**

Table 4.2-2: Calculated Number of *D. canis* Per Gram of Digest Sample Collected from Skin Grafts on ICR Scid Mice.....**Page 115**

Table 4.2-3: PCV Values for ICR Scid Mice at Experiment Onset and Completion.....**Page 116**

SECTION 4.3

Table 4.3-1: Calculated Number of *D. canis* Per Follicle Unit on Digest Samples from Skin Grafts on Tgε26 Mice that Received PBMC or PBS Once After Mite Infection (Experiment One).....**Page 142**

Table 4.3-2: Calculated Number of *D. canis* Per Skin Graft Digest Sample from Grafts on Tgε26 Mice that Received PBMC or PBS Once After Mite Infection (Experiment One).....**Page 143**

Table 4.3-3: Calculated Number of *D. canis* Per Follicle Unit on Digest Samples Collected from Skin Grafts on Tgε26 Mice that Received PBMC or PBS Before and After Mite Infection (Experiment Two).....**Page 144**

Table 4.3-4: Calculated Number of *D. canis* Per Skin Graft Digest Sample Collected from Grafts on Tgε26 Mice that Received PBMC or PBS Before and After Mite Infection (Experiment Two).....**Page 145**

Table 4.3-5: Tgε26 Mouse PCV Values at the Onset and at Completion of Experiment One Where Mice Received PBMC or PBS Once Before Mite Infection.....**Page 146**

Table 4.3-6: Tgε26 Mouse PCV Values at the Onset and at Completion of Experiment Two Where Mice Received PBMC or PBS Before and After Mite Infection.....**Page 147**

SECTION 4.4

Table 4.4-1: Calculated Number of *D. canis* Per Skin Graft Digest Sample Collected from Grafts on *Rag2* Mice at Experiment Completion.....**Page 172**

Table 4.4-2: *Rag2* Mouse PCV Values at the Onset and at Experiment Completion.....**Page 173**

CHAPTER 5

SECTION 5.2

Table 5.1: Comparison of skin xenografting results, *D. canis* infection rates and outcomes for the different strains of mice used to model canine demodicosis.....**Page 175**

CHAPTER 1: GENERAL INTRODUCTION AND LITERATURE REVIEW

1.1 GENERAL INTRODUCTION

The ectoparasite *Demodex canis* is responsible for canine demodicosis, a common skin disease afflicting dogs in North America. Overgrowth of *D. canis* has the potential to induce severe disease that requires months of treatment to effect a clinical cure, after which a proportion of cases will relapse. The expense of treatment, discomfort associated with the disease, and disruption of the human-animal bond lead owners, not infrequently, to elect euthanasia for affected animals.

The literature describing canine demodicosis reaches back more than a century, however the basic details regarding its pathogenesis remain poorly understood. Demodicosis is an inflammatory skin disease associated with *D. canis* overgrowth, yet the causal relationship of these factors remains uncertain. What role does inflammation play in controlling cutaneous mite numbers on the skin and in skin lesion development? Do mites directly damage hair follicles and induce hair loss? Why do some dogs develop generalized disease while others do not? These questions remain unanswered.

The current consensus is that dogs with generalized disease suffer from an inherited or acquired defect in T-cell function. In juvenile dogs, this T-cell defect is thought to result from a genetic predisposition. In adult dogs, this defect is considered acquired, as a result of immunosuppressive therapy or a concurrent debilitating disease. Although the T-cell dysfunction hypothesis is supported by descriptive and *in vitro* experimental studies published during the last 30 years, the ability of T-cells to control

mite populations has not been directly tested. Other potentially significant pathogenic factors, such as local mechanisms of skin resistance, have received little attention.

Investigations of the pathogenesis of canine demodicosis have been hampered by the lack of a suitable experimental system. *Demodex canis* can not be cultured *in vitro* and mites rapidly die when removed from the host. Generalized demodicosis is difficult, if not impossible, to recreate experimentally in the natural host without severe immunosuppression, a condition that limits *in vivo* investigations of host immunity.

The availability of the skin xenograft mouse model has provided a new approach to study canine demodicosis. The model takes advantage of the ability of genetically immunodeficient mice to support skin grafts from different species for many months. Skin xenografts retain a high degree of structural and biochemical integrity and thus provide an *in vivo* test system with biologic relevance. Canine skin xenografts will support *D. canis* infections. Finally, the immunodeficient recipient mice used in this model can be reconstituted with specific elements of the donor host immune system, such as lymphocytes. Combining these features of the xenograft model provides a method to address fundamental questions about the pathogenesis of demodicosis. The first objective of this thesis was to develop the canine skin xenograft model of demodicosis. The second objective was to directly test the ability of lymphocytes to limit *D. canis* populations on canine skin.

The first half of this chapter summarizes aspects of demodicosis in dogs, including the biology of *D. canis*. The second portion of this chapter reviews the components of the skin xenograft mouse model and the relevant literature pertaining to its application in dermatology research.

1.2 PART 1: *DEMODEX CANIS* AND CANINE DEMODICOSIS

1.2.1 BIOLOGY OF *DEMODEX CANIS*

The mite responsible for canine demodicosis was originally identified by Tulk in 1844 and was subsequently given its current species name, *Demodex canis,* by Leydig in 1859 (Nutting & Desch, 1978). It was not until the second half of the 19th century that French provided more complete morphologic description of *D. canis* (French, 1962; French, 1963). French's work was later expanded by Desch and Nutting (Desch, 1973; Nutting & Desch, 1978).

In 1843, Owen coined the genus name *Demodex*, which is derived from the Greek "demos" for lard and "dex" for boring worm (Desch, 1973). Members of this large genus, with more than 50 species already described (Nutting, 1985), share several features. Demodicids are obligate mammalian symbiotes, host species specific and highly host adapted to occupy a particular niche on the body, usually located within a cutaneous environment (Nutting, 1976a). Many of these mites, like *D. canis*, primarily occupy the pilar canal of hair follicles (e.g., *D. folliculorum* of humans, *D. caprea* of goats, and *D. phylloides* of pigs), whereas some species inhabit sebaceous glands (*D. brevis* in humans) or meibomian glands (Nutting, 1976a). A few, such as *D. criceti* in the hamster and *D. gatoi* in the cat, have adapted to live on the skin surface (Desch & Stewart, 1999).

Several mammals are known to host more than one species of *Demodex*, a condition termed synhospitality. More than one species has been described for humans (*D. folliculorum* and *D. brevis*), cats (*D. cati* and *D. gatoi*) and horses (*D. caballi* and *D. equi*). Nutting provides more examples including an extensive list of the host

specificities of different *Demodex spp.* (Nutting, 1985). Dogs may be host to at least three *Demodex spp.* *Demodex canis* is well described and is the common species found on normal dogs as well as dogs with demodicosis (Scott *et al.*, 1995). Recently, two unnamed, potentially new *Demodex spp.* have been identified from dogs with dermatitis, including a short-bodied surface dwelling mite (Mason, 1993b; Lemmens *et al.*, 1994; Chen, 1995; Chesney, 1999; Saridomichelakis *et al.*, 1999) and a long-bodied mite inhabiting hair follicles and sebaceous glands (Hillier & Desch, 1997).

Demodex spp. are considered a component of the normal body fauna of most mammals. In humans, *Demodex spp.* are readily found on the skin of healthy individuals and the prevalence of infestation can range from less than 10% to nearly 100% depending on the methods of detection and the human population studied (Riechers & Kopf, 1969; Rufli & Mumcuoglu, 1981; Sengbusch & Hauswirth, 1986; Sengbusch, 1991). Survey studies have identified the prevalence of mite infestation in the skin of clinically normal swine (35% to 50%), horses (16% to 59%), goats (8% to 11%) and cattle (2% to 11%) (Baker & Fisher, 1969; Qintero, 1978). Similarly, *D. canis* is present in digested skin samples from healthy dogs and the prevalence has been reported as 5% (Gafaar *et al.*, 1958), 10% (Unsworth, 1946), 17% (Himonas *et al.*, 1975), or 53% (Koutz *et al.*, 1960). The skin sample size and number of skin sites examined were limited (and non-uniform) in these studies and the prevalence of *D. canis* is expected to be higher than 53% in some populations of normal dogs. In a study of 204 normal dogs, Koutz and coworkers did not find any association between age, sex, breed, or coat type and *D. canis* colonization (Koutz *et al.*, 1960). *Demodex canis* primarily inhabit the skin around the eyes and

mouth with fewer mites present on the face and head (Koutz *et al.*, 1960). Few, if any, *D. canis* are recovered from the trunk and limbs of healthy dogs.

Demodicids have undergone extensive morphologic adaptation for survival in the host skin environment. All *Demodex spp.* have developed a tubular, spindle-shaped, body. Compared to free-living or other parasitic mites, the body surface features of *Demodex spp.* are greatly reduced. Adults possess few shortened setae and spines as well as greatly shortened legs (Bukva, 1991). A typical adult *Demodex sp.* has stump-like legs with only 3 segments compared to 5 or more segments in the relatively long legs of myobid or psorergatid mites (Nutting, 1985). Mouthparts are shortened and eyes are absent. The exoskeleton of demodecids, like psorergatid mites, is very thin compared to other parasitic mites. Because of this, *D. canis*, when removed from the hair follicle, desiccate within 45 to 60 minutes at 20°C and a relative humidity of 40% (Nutting, 1965). The digestive tract of demodicids terminates in a blind-ended sac with no known species having an anus (Nutting, 1985; Desch *et al.*, 1989). The lack of fecal excretion may decrease the antigenic stimulus provided by the mite, facilitating its survival on the host. More extensive description of structural adaptations have been reported (Nutting, 1985; Bukva, 1991).

Demodex spp. are thought to feed on the cellular contents of keratinocytes (and/or sebocytes) and possibly glandular secretions (Desch & Nutting, 1978; Desch *et al.*, 1989). Stylet-like retractable chelicerae present in the preoral cavity are available to puncture cells. Large, paired salivary glands possibly supply enzyme rich secretions for preoral digestion. The esophagus is less than 1 μm in diameter, strongly suggesting that mites ingest only liquid substrate.

Demodicids are considered holostadial; all life-cycle stages of *D. canis* develop on the dog within the pilar canal of hair follicles and occasionally within sebaceous glands (Nutting & Desch, 1978). *Demodex canis* development follows the usual acarine life cycle of ovum, larva, protonymph, nymph, and adult (Nutting & Desch, 1978). Morphologic data, used for identifying individual stages in this study, were taken from several sources (French, 1962; French, 1963; Desch, 1973; Nutting & Desch, 1978). A taxonomic key is available to distinguishing *D. canis* from other *Demodex spp.* of veterinary importance (Nutting, 1976a; Nutting & Desch, 1978).

The duration of the demodicid life cycle is poorly understood. Spickett (1961) used *in vitro* survival data and histological analysis of infested human tissues to estimate the complete life-cycle for *D. folliculorum* to last 14.5 days (ovum, 60 hr; larva, 36 hr; protonymph, 72 hr; deutonymph (nymph), 60 hr; and adult, 120 hr). Spickett's estimates should be interpreted with caution, however. Spickett most certainly combined data for *D. folliculorum* with that for *D. brevis*. *Demodex brevis* was not assigned the status of a distinct species (from *D. folliculorum*) until 1972, many years after Spickett's studies (Desch & Nutting, 1972). Furthermore, demodicids generally do not reproduce or survive for long periods *in vitro*. Sako (1964) estimated the generation time for *D. canis* to be between 20 and 34 days. Unsworth (1946) reported similar findings that were based on a limited number of observations.

Transmission of demodicid mites occurs through direct contact. *Demodex canis* has been recovered from the hair follicles of puppies as early as 24 hours after birth, (Sako, 1964; Greve & Gaafar, 1966) indicating that puppies acquire *D. canis* from the dam as early as the first few hours of life. Pups can readily acquire mites from clinically

normal dams or dams with demodicosis (French *et al.*, 1964; Greve & Gaafar, 1966). Mites are detected first on the face and head of puppies, a finding that has led some to conclude that mite transfer occurs during nursing (Greve & Gaafar, 1966; Scott *et al.*, 1995). Puppies delivered by cesarean section or removed from fetal membranes by hand from heavily infected dams and hand reared did not harbor mites (French *et al.*, 1964; Greve & Gaafar, 1966).

Experimental transmission of *D. canis* has been performed, after which a proportion of neonatal dogs generally develop transitory skin lesions that spontaneously resolve (Scott *et al.*, 1995, Sheahan, 1970 #876). Skin lesions that developed in a transmission study by French and coworkers were not described in detail and mites were not demonstrated in cutaneous tissues (French *et al.*, 1964). It is considered difficult, if not impossible, to consistently reproduce skin lesions associated with canine demodicosis in healthy adult dogs, especially the lesions of generalized demodicosis (Scott *et al.*, 1995). Sako (1964) went as far as to bind the legs of a clinically normal dog to those of a dog with demodicosis in attempts to reproduce the disease. Folz (1978) coinfected beagle dogs with *D. canis* and *Sarcoptes scabiei* and then repeatedly stressed dogs in an 8-week protocol to recreate generalized disease. Studies of experimentally immunosuppressed dogs are discussed below (Section 1.2.3.2.3).

1.2.2 EPIDEMIOLOGY OF CANINE DEMODICOSIS

1.2.2.1 Distribution, Incidence, and Breed Association

Demodicosis has a truly protean distribution and is recognized worldwide (Unsworth, 1946; Reddy *et al.*, 1992; Lemarie & Horohov, 1996; Caswell *et al.*, 1997). A survey of

veterinary teaching hospitals reported demodicosis as the sixth most commonly diagnosed skin disease of dogs in North America, and the third most common in the southeast and southwest regions (Sischo *et al.*, 1989). Similarly, a retrospective study by Scott and Paradis reported demodicosis to be one of the ten most commonly diagnosed skin diseases of dogs at the veterinary teaching hospital of the University of Montreal in Saint-Hyacinthe, Quebec (Scott & Paradis, 1990).

All dogs, mixed or purebred, are considered susceptible to developing demodicosis. However, purebred dogs are generally over represented in study populations and a higher prevalence of demodicosis has been reported for several breeds (Scott *et al.*, 1974; Scott, 1979; Scott & Paradis, 1990; Miller *et al.*, 1992; Scott *et al.*, 1995; Lemarie *et al.*, 1996). Lemarie and colleagues (1996) also found that mixed bred dogs and certain pure bred dogs (Cocker spaniel, Labrador retriever, German shepherd) were under-represented in an affected population. Short-coated breeds are considered more susceptible to developing demodicosis (Unsworth, 1946; Baker, 1970); however, not all investigators report such a trend (Scott *et al.*, 1974). Regional variation in dog populations, patterns of breed presentation, and variability in case handling likely contribute to reported differences in breed susceptibilities. Male and female dogs appear equally susceptible to developing generalized demodicosis (Lemarie *et al.*, 1996).

Although a specific mode of inheritance has not been established, it is generally accepted that genetic factors play a role in the susceptibility of dogs to generalized disease. Investigators have describe kennels with a high incidence of demodicosis that could be increased or decreased by selective breeding or culling of affected animals (Scott, 1979; Wilkie *et al.*, 1979). Scott reported a familial history of generalized

demodicosis in 89% of 27 cases (Scott, 1979). Breed associations of disease incidence provide further support for a genetic component in demodicosis.

1.2.2.2 Clinical Presentation, Diagnosis and Treatment

Clinical cases of canine demodicosis are classified as localized or generalized based on the number, area and distribution of skin lesions (Kwochka, 1987; Scott *et al.*, 1995). Localized cases present with 1 to 4 well-circumscribed lesions, typically a few centimeters in diameter, more common on the head (especially around the eyes), neck, and forelimbs, but may develop on any haired area of the body. Individual lesions consist of partial or complete alopecia, scaling, mild erythema, follicular plugging and hyperpigmentation. Pruritus or concurrent bacterial pyoderma is rare. Dogs with localized disease are usually between 3 and 12 months of age and lesions may wax and wane for weeks to months, but dogs are otherwise healthy and the prognosis is good. Most dogs spontaneously recover; approximately 10% progress to generalized demodicosis.

Dogs have generalized disease when skin lesions affect 5 or more areas of the body, a whole body region (such as the head), or involve 2 or more feet. Generalized cases are further classified as squamous or pustular. Lesions of the squamous form are similar in character to those of localized disease; however, secondary lesions such as lichenification or seborrhea may develop in chronic cases. Pustular demodicosis results when generalized disease occurs concurrently with superficial or deep bacterial skin infection (i.e., bacterial pyoderma). Generalized pustular demodicosis is a life-threatening condition and affected dogs are clinically ill, usually have a peripheral

lymphadenopathy, and may show signs of septicemia. Although up to 50% of generalized cases spontaneously resolve, the prognosis is guarded and dogs progress to chronic disease, lasting years if untreated. Relapse of treated generalized demodicosis is common.

Generalized demodicosis is typically apparent before 2 years of age, but often these cases do not present until 2 to 4 years of age, and are classified as juvenile-onset demodicosis. Dogs that develop skin lesions after four years of age have adult-onset demodicosis. Adult-onset demodicosis has been associated with concurrent immunosuppressive treatment or debilitating disease, discussed below (Section 1.2.3.2.3).

In demodicosis, mite numbers increase in association with skin lesions. Normal dogs, and dogs suffering from other skin diseases, harbor very few mites. A diagnosis of canine demodicosis is confirmed by demonstrating increased numbers of adult *D. canis* or immature stages by microscopic examination of deep skin scrapings (Scott *et al.*, 1995). To confirm generalized disease, mites must be recovered from multiple areas.

Localized demodicosis is a benign disease and treatment does not alter the clinical course. The treatment of generalized demodicosis was recently reviewed (Paradis, 1999).

1.2.3 PATHOGENESIS OF CANINE DEMODICOSIS

1.2.3.1 Mite Factors

Little specific information is available regarding mite factors in development of canine demodicosis. Scott (1995) reasoned that mite virulence factors did not contribute to disease as not all pups in a litter develop demodicosis. Because most dogs harbor *D. canis*, host factors are considered to limit disease and the mere presence of mites is not

sufficient. Although direct evidence is lacking, this feature has led most investigators to consider demodicosis as a non-contagious disease (Lemarie, 1996). Clearly, basic questions remain regarding the contribution of mite factors to the development or severity of disease. Do mites directly damage hair follicles and contribute to alopecia and the formation of skin lesions? In generalized demodicosis, mite numbers increase dramatically and thousands of mites may be present per gram of skin (Unsworth, 1946). Do mite or host factors control this proliferation? It is reasonable to assume that not all *D. canis* populations are uniform, even on the same host.

1.2.3.2 Host Factors

Few studies have addressed systemic mechanisms of innate defense and local skin mechanisms of resistance have not been evaluated. Research has focused on characterizing the ceilular immune response, and little is known about the role of acquired antibody-mediated immunity (humoral immunity) in the pathogenesis of canine demodicosis.

1.2.3.2.1 *Innate Defense Mechanisms*

A few components of systemic innate defenses have received limited attention. Abnormalities in circulating neutrophils in cases of generalized demodicosis have not been identified (Scott *et al.*, 1974; Scott *et al.*, 1976). Toman *et al.* (1998) found a normal respiratory burst index (by chemiluminescence assay) for neutrophils and macrophages from dogs with generalized demodicosis. Moore and coworkers (1987) described the deposition of the complement component C3 in cutaneous lesions of

demodicosis (2 of 8 cases); however, complement deposition was a common finding in dermatitis reactions due to other causes. Wolfe and Halliwell (1980) and Tomen *et al.* (1998) did not find low hemolytic complement levels in dogs with demodicosis. In Toman's study, 2 of 25 dogs with demodicosis had reduced ability for complement-mediated lysis of sheep erythrocytes. Serum protein electrophoretic patterns observed in cases of demodicosis are common to many inflammatory conditions (Scott *et al.*, 1974; Reddy *et al.*, 1992) and specific protein fractions have not been evaluated.

1.2.3.2.2 *Acquired Humoral Immunity*

No studies have characterized or measured antibody specific to *Demodex spp.* mite-antigens or evaluated protective humoral immune responses. Elevated serum IgA concentrations was reported in dogs with demodicosis (8 cases), as well as in dogs with other inflammatory skin conditions, including pyoderma (Day & Penhale, 1988). In contrast, a survey that included parasitized dogs, of which three had demodicosis, did not find an increase in either serum IgA or IgG and serum IgE was not detectable (Hill *et al.*, 1995). Healey and Gaafar (1977) observed increased numbers of mast cells in skin lesions of demodicosis, although the number of IgE bearing mast cells was not increased. Dogs with demodicosis have increased IgG autoantibody to IgE which are associated with IgG × IgE immune complexes (Hammerberg *et al.*, 1997). This finding indicates that direct measures of serum or tissue IgE may be misleading and that the role of IgE in canine demodicosis may be more complex. Moore and coworkers (1987) reported deposition of IgA (2 of 8 cases), IgG (4 of 8 cases) and IgM (4 of 8 cases) in skin lesions of generalized demodicosis. None of these studies adequately address the role of

secondary pyoderma, making it difficult to draw specific conclusions about humoral response in demodicosis, except to say that severe deficiencies have not been identified.

1.2.3.2.3 *Acquired Cellular Immunity*

Owen (1972) first reported that immunosuppression with antilymphocyte serum led to generalized demodicosis in 8 out of 15 dogs. Subsequently, Healey and Gafaar designed an experiment to test Owen's observation. All 10 of their neonatal dogs receiving antilymphocyte serum and topically applied *D. canis* developed generalized squamous demodicosis (Healey & Gaafar, 1977b). None of the neonatal dogs that received antilymphocyte serum alone (9 dogs) or no treatment (8 dogs) developed lesions. Two dogs out of an additional 9 that received *D. canis* only developed squamous lesions; the extent of these lesions was not described. The findings suggest that a cellular immune response involving lymphocytes limited *D. canis* proliferation and protected dogs from demodicosis.

Several investigators assessed cellular immunity in dogs with naturally occurring demodicosis using *in vitro* mitogen stimulation of blood lymphocytes. Suppression of lymphocyte proliferation was found in response to phytohemaglutanin, concanavalin-A, pokeweed mitogen, or lipopolysaccharide (Scott *et al.*, 1974; Corbett *et al.*, 1975; Hirsh *et al.*, 1975; Scott *et al.*, 1976; Krawiec & Gaafar, 1980; Barta *et al.*, 1982; Barta *et al.*, 1983; Barriga *et al.*, 1992; Burkett *et al.*, 1996; Paulik *et al.*, 1996). By using combinations of serum and lymphocytes from normal dogs and those with demodicosis, the several of these studies attributed lymphocyte suppression to a serum factor and not to lymphocyte function directly. The degree of immunosuppression tended to correlate with

skin lesion extent and disappeared after successful treatment of demodicosis, suggesting that the suppressive factor was associated with overt disease (Scott *et al.*, 1974; Hirsh *et al.*, 1975; Scott *et al.*, 1976; Krawiec & Gaafar, 1980; Barriga *et al.*, 1992).

The immunosuppressive activities in serum are unknown. It is heat stable (at 56°C for 30 minutes) and not adsorbed by lymphocytes (Barta *et al.*, 1982). Lymphocytes exposed to known suppressive serum respond normally after washing (Scott *et al.*, 1976). These sera also negatively regulate neutrophils and macrophages (Latimer *et al.*, 1983). Support has been obtained that the serum suppressive factor(s) are immune complexes formed with staphylococcal antigens (DeBoer *et al.*, 1988; Mason, 1993a; DeBoer, 1994). Barriga and others have attributed immunosuppression to both *D. canis* and pyoderma (Barta *et al.*, 1983; Barriga *et al.*, 1992). One study reported that lymphocytes from dogs with generalized demodicosis exhibited a decreased *in vitro* proliferative response to interleukin-2 as well as decreased interleukin-2 receptor expression (Lemarie & Horohov, 1996). The authors concluded that the deficit in demodicosis results from an abnormal T-helper-2 immune response.

Intradermal mitogen testing has been used as an alternative to *in vitro* techniques to assess cell-mediated reactions. When dogs with active lesions of demodicosis were tested with PHA or Con-A, skin reactions at 24- and 48-hours post injection were decreased compared to controls (Scott *et al.*, 1974; Corbett *et al.*, 1975; Healey & Gaafar, 1977b; Bhalerao & Bose, 1990; Reddy & Rao, 1992), suggesting a decreased delayed-type hypersensitivity response. Dogs with localized disease had a skin response similar to that of normal dogs (Reddy & Rao, 1992), indicating that immunosuppression was a consequence of generalized disease rather than a predisposing factor. In general, the

cutaneous response of affected dogs to mitogens supports a defect in cell-mediated immunity.

Links between generalized demodicosis and immunosuppression are supported by clinical findings. Dogs presenting with adult onset demodicosis often have concurrent debilitating disease or have received immunosuppressive medications (Kwochka, 1987; Scott *et al.*, 1995). Seventy percent of dogs in one study of adult onset disease and 44% in another showed these correlations (Duclos *et al.*, 1994; Lemarie *et al.*, 1996).

1.2.3.3 Histopathology

The histological changes in canine demodicosis include follicular and surface epidermal hyperplasia, sebaceous hyperplasia, and follicular keratosis with perifollicular melanosis and/or epidermal hyperpigmentation (Baker, 1969; Sheahan & Gaafar, 1970; Baker, 1975; Cayatte *et al.*, 1992; Kamboj *et al.*, 1993). More specific degenerative changes of hair follicles include thinning of the follicular wall with follicular rupture as well as hydropic degeneration, spongiosis, pyknosis and necrosis of external root sheath keratinocytes.

Using the pattern analysis approach, Caswell and coworkers distinguished three major patterns of inflammation associated with *D. canis* infection: (1) neutrophilic folliculitis and furunculosis, (2) mural folliculitis, and (3) nodular dermatitis (Caswell *et al.*, 1995; Caswell *et al.*, 1997). Neutrophilic folliculitis and furunculosis is a reaction pattern attributable to bacterial pyoderma and it signals the development of pustular demodicosis (Sheahan & Gaafar, 1970; Yager & Wilcock, 1994). Lymphocytic mural folliculitis was identified in nearly half of the cases of either localized or generalized

disease. In these cases, the interface sub-type of mural folliculitis predominated. The lymphocytic interface reaction pattern is associated with cell-mediated immune attack on epidermal cells and is seen, for example, in graft-versus-host disease (Yager & Wilcock, 1994). Lymphocyte phenotyping supported this observation and revealed CD3+ and CD8+ cells infiltrating the external root sheath of hair follicles, consistent with a cytotoxic T-cell response (Caswell *et al.*, 1995). Day and coworkers reported similar results and also characterized perifollicular B-cell infiltrates (Day, 1997). The nodular dermatitis results from perifollicular granulomas centered on mites released into the dermis through the follicle wall (Sheahan & Gaafar, 1970; Gross *et al.*, 1992). In a prospective evaluation of skin lesions, Caswell *et al.* (1997) demonstrated that the presence of perifollicular granulomas, was associated with resolution of clinical disease and elimination of mites on the skin. Together these findings suggest that a predominately lymphocyte-associated, cell-mediated immune attack on *D. canis*-infected hair follicles with disruption of the follicular wall contributes to elimination of mites and/or skin lesion development. The consequent release of some mites into the dermis leads to the development of perifollicular granulomas. Lymphocytes have not been shown to directly limit mite numbers on the skin and the alternative possibility that lymphocytes target hair follicle epithelium as a result of altered self or mite antigen presentation (similar to an autoimmune response) must be considered.

Controversy remains regarding the exact contribution of *D. canis* to gross and histological changes in demodicosis. It has been reported that mite proliferation and feeding activity induces erosions of the follicle wall, epidermal hyperplasia, follicular keratosis, hair loss, and follicle rupture (Nutting, 1976b; Nutting *et al.*, 1989). Many of

the histological changes reported for demodicosis are non-specific and can be observed in a variety of infectious and/or inflammatory skin conditions in the dog (Yager & Wilcock, 1994; Scott *et al.*, 1995).

1.2.4 SUMMARY

Canine demodicosis is a common and often devastating inflammatory skin condition associated with *D. canis* overgrowth. While multiple host factors appear to be important in disease pathogenesis, little is known about basic *Demodex spp.* biology and the contribution of mite factors to disease. What does appear certain is that *D. canis* has undergone extensive morphological coevolutionary adaptation with the dog and it is likely that this host-parasite relationship involves complex molecular interactions.

Generalized demodicosis appears to result from alterations in cellular immunity that may be related to genetic and acquired forms of immunosuppression. The literature points to a defect in lymphocyte function. However, the work to date has been largely descriptive and based mostly on *in vitro* studies. The host immune response to *D. canis* specific antigens has not been addressed and the role of lymphocytes in controlling mite populations has not been directly tested. Local mechanisms of skin resistance have not been examined and the contribution of mite factors to skin lesion development has gone unexplored. Investigations into the functional aspects of host resistance to *D. canis* have been hampered by the lack of a suitable experimental system.

1.3 PART 2: THE SKIN XENOGRAFT MOUSE MODEL

The first attempt to graft heterologous skin to genetically immunodeficient mice occurred

in the late 1960s, when Rygaard grafted nude mice with rat skin (Rygaard, 1969). During the next 5 years, skin from a number of sources, including humans and cats, was successfully grafted to nude mice (Manning *et al.*, 1973; Reed & Manning, 1973; Shaffer *et al.*, 1973; Rygaard, 1974). These xenograft experiments addressed the immunologic status of the nude mouse. Researchers soon realized that the system also provided an opportunity to study the xenograft itself. In the mid-1970s, Kreuger *et al.* (1975) grafted human psoriatic skin to nude mice (Krueger *et al.*, 1975)and soon after, Briggaman and colleagues (1976) studied xenografts of human ichthyotic skin on nude mice. Cubie (1976) was the first to utilize the model to study an infectious skin disease, attempting to induce viral papillomas in human skin grafts on nude mice. Successful reproduction of virally induced skin lesions was not reported until 1979, when Kreider *et al.* demonstrated that the Shope papillomavirus induced "typical" papillomas in rabbit skin grafts on nude mice.

Between the 1975 and 1985, several reviews discussed grafting human skin to nude mice (Reed & Manning, 1978; Krueger & Briggaman, 1982; Briggaman, 1985). In a paper published in 1980 titled *Localization of the Defect in Skin Diseases Analyzed in the Human Skin Graft-Nude Mouse Model,* Briggaman (1980) considers the model to be a general experimental tool for investigating human skin diseases. For the purposes of this thesis, the name "skin xenograft mouse model" was adapted from Briggaman's paper.

1.3.1 COMPONENTS OF THE SKIN XENOGRAFT MOUSE MODEL

A **xenograft** is defined as transplanted tissue derived from a different species than the graft recipient. In the skin xenograft mouse model, skin collected from the animal under

study represents the xenograft (for example, canine or human skin) and is transplanted to the dorsum of a minimally T-cell deficient mouse—the recipient. When healed, the skin grafts are available for manipulation. The skin xenografts and the immunodeficient recipient mouse comprise the two basic components of the model.

The model is versatile as other components, including other tissue grafts can be added. For example, the modeling of inflammatory processes requires that leukocytes from the skin graft donor be transferred to the recipient mouse. The term **chimera** is used when an immunodeficient mouse is reconstituted with leukocytes from a different species. Severe combined immunodeficient (scid) mice reconstituted with viable human peripheral blood lymphocytes (PBL), by either intravenous or intraperitoneal injection, constitute human-PBL-scid chimeras (McCune *et al.*, 1988; Mosier *et al.*, 1988). Chimera also describes the intermixing of cells from different species within a tissue, **tissue chimerism**. Tissue chimerism occurs when cells of mouse origin migrate into a xenogenic skin graft.

The mice used in the skin xenograft model are genetically immunodeficient as a result of a spontaneous mutation or an experimentally directed mutation to create a transgenic mouse. A **transgenic** mouse is created when a stabile DNA sequence is introduced into the germ cells and it is referred to as a gene **knockout mouse** when a directed mutation, usually achieved by homologous recombination, disrupts the function of a known gene (Davisson, 1996). Both types of animals were used in this thesis.

1.3.1.1 Graft Recipient – The Immunodeficient Mouse

The majority of skin xenograft work has been performed with just two mouse mutants:

the athymic nude mouse (Flanagan, 1966) used in the original xenogenic skin grafting experiments of the late 1960s, or the scid mouse discovered in the early 1980s (Bosma *et al.*, 1983).

1.3.1.1.1 *Nude Mouse*

The nude mouse phenotype, originally described by Flanagan in 1966, is due to an autosomal recessive mutation located on chromosome 11 (Flanagan, 1966; Anonymous, 1989). The nude locus contains a single point mutation in the *Foxn1* gene, coding for a winged-helix / forkhead transcription factor that is likely expressed in epithelial components of skin and thymus (Nehls *et al.*, 1994; Segre *et al.*, 1995; Kaestner *et al.*, 2000). Nude mice ($Foxn1^{nu}/Foxn1^{nu}$) fail to develop a normal thymus or hair and, as a result, appear "nude" (Wortis *et al.*, 1971; Eaton, 1976; Van Vliet *et al.*, 1985). Because of thymic dysplasia, nude mice do not produce mature T-cells and are generally unable to respond to thymus-dependent antigens (Anonymous, 1989). They retain other components of the immune system (Holub, 1989) including abnormally high NK-cell lytic activity (Minato *et al.*, 1980), B-cells and serum immunoglobulins (Mond *et al.*, 1982). In addition to the thymus and skin defects, nude mice have alterations in other systems, such as the endocrine system (Holub, 1989).

The nude mouse remains useful for xenogenic skin grafting, a fact that is evident from many recent publications (Bosca *et al.*, 1988; Scott & Rhodes, 1988; Eming *et al.*, 1995; Lin *et al.*, 1995; Sullivan *et al.*, 1995; Medalie *et al.*, 1996; Short *et al.*, 1996; White *et al.*, 1999). The primary benefits of using the nude mouse in veterinary studies is the wealth of information detailing its biology (Anonymous, 1989; Holub, 1989;

Rygaard, 1991) and the comparative information available from extensive use in human xenograft models. The nude mouse will support skin grafts from a variety of donor species (Table 1).

Table 1: Animal Skin Donors and Immunodeficient Recipient Mice Used for Skin Xenograft Experiments

SKIN DONOR	MOUSE TYPE	REFERENCES
Dog	Nude mouse	[Rosenquist, 1988 #697]
	Scid/bg mouse	[Caswell, 1996 #495]
Cat	Nude mouse	[Manning, 1973 #632]
Pig	*Rag1* mouse	[Friedman, 1999 #70]
	Rag1 mouse	[Sawada, 1997 #71]
	Nude mouse	[Krueger, 1980 #614]
	Nude mouse	[Rosenquist, 1988 #697]
Fetal sheep	Nude mouse	[McCloghry, 1993 #92]1
Cow	Scid mouse	[Greenwood, 1997 #566]
Guinea Pig	Nude mouse	[Green, 1982 #562]
Rat	Nude mouse	[Rosenquist, 1988 #697]
		[Rygaard, 1974 #700]
		[Yamane, 1996 #756]
		[Shaffer, 1973 #713]
Rabbit	Nude mouse	[Rosenquist, 1988 #697]
		[Shaffer, 1973 #713]
Syrian Hamster	Nude mouse	[Shaffer, 1973 #713]
Chicken	Nude mouse	[Manning, 1973 #632]
		[Rygaard, 1974 #702]
		[Shaffer, 1973 #713]
Lizard	Nude mouse	[Rygaard, 1974 #702]
Pigeon	Nude mouse	[Rygaard, 1974 #702]
Grass Snake	Nude mouse	[Rygaard, 1974 #702]
Chameleon	Nude mouse	[Manning, 1973 #632]
Tree frog	Nude mouse	[Manning, 1973 #632]

The nude mouse is not immunologically quiescent. This mouse produces immunoglobulins in response to xenografts, and if an external source of complement is supplied, these mice will reject the foreign grafts (Holub, 1989). Older nude mice can produce some functional T-cells, particularly mice with microbial infections (Holub, 1989). The presence of some T-cells, NK-cells, and B-cells, as well as serum immunoglobulin make nude mice poor candidates for experiments modeling inflammatory reactions, especially those involving chimeric leukocyte reconstitution. Endogenous immunoglobulin, interferes with immunohistochemical techniques using anti-mouse monoclonal antibodies (Yan *et al.*, 1993). One further disadvantage of the nude mouse is the high incidence of spontaneous lymphoid neoplasia (Holub, 1989).

1.3.1.1.2 *Severe Combined Immunodeficient (scid) Mouse*

Murine severe combined immunodeficiency (scid) is an autosomal recessive mutation originally described by Bosma *et al.* (1983). The scid mutation maps to the gene for a DNA-dependent protein kinase (*Prkdc*) (Blunt *et al.*, 1995a; Blunt *et al.*, 1995b). This protein kinase facilitates the repair of DNA damage, particularly double-strand breaks, including the recombination of the variable (V), diversity (D), and joining (J) segments of the B-cell receptor and T-cell receptor genes. As a consequence, scid mice ($Prkdc^{scid}/Prkdc^{scid}$) fail to produce mature T-cells, have significantly reduced numbers of B-cells, and produce little or no serum immunoglobulin. NK-cells and other leukocytes, however, do not appear affected (MacDougall *et al.*, 1990; Bancroft *et al.*, 1991; Watanabe *et al.*, 1996).

In the xenograft model, the scid phenotype is an improvement in some respects over the nude mouse. The lack of mature T-cells, most B-cells, and immunoglobulin provides a "cleaner" immunodeficient mouse. Scid mice, but not nude mice, can be successfully engrafted with xenogenic leukocytes (Taylor, 1994), making them useful for experiments modeling inflammatory skin diseases (Petzelbauer *et al.*, 1996). Without interfering antibodies, xenografts and tissues from scid mice are more easily evaluated with immunohistochemical techniques using anti-mouse antibodies.

Use of scid mice has some drawbacks. The mutation exhibits incomplete penetrance (Hendrickson, 1993), and a percentage of scid mice (up to 25%) eventually develop a degree of immunocompetence—a condition referred to as the "leaky" phenotype. "Leaky" scid mice produce immunoglobulin and restricted numbers of T-cell clones and are able to reject foreign skin grafts (Bosma *et al.*, 1988; Carroll & Bosma,

1988; Carroll *et al.*, 1989; Bosma, 1992; Kotloff *et al.*, 1993a). Thus, before an experiment commences, scid sera should be screened for endogenous immunoglobulin levels. Incidence of the "leaky" phenotype was reduced by the addition of the beige (*Lyst*^{bg}) mutation (Mosier *et al.*, 1993), or by crossing the scid mutation onto a different inbred mouse strain (Nonoyama *et al.*, 1993). The incidence of the "leaky" phenotype and spontaneous thymic lymphoma increases with age, which complicates long-term experiments (Custer *et al.*, 1985).

1.3.1.1.3 *Newer Types of Immunodeficient Mice*

The enormous expansion in immunology has stimulated development of numerous immunodeficient transgenic or gene knockout mice. Selection from this expanding pool of mice will minimize the potential for mouse-related complications in applications of the skin xenograft model. Few of the newer mouse mutants have been used for skin xenografting. Examples include the *Rag1* and *Rag2* knockout mice. Both mutants lack T-cells and B-cells due to inactivation of the recombinase activating gene-1 or -2 (*Rag1* or *Rag2*) and an inability to complete V(D)J immunoglobulin gene recombination (Mombaerts *et al.*, 1992; Shinkai *et al.*, 1992). *Rag1* null mice have been shown to support human or porcine skin grafts for extended periods (Atillasoy *et al.*, 1997; Friedman *et al.*, 1999).

1.3.1.2 <u>The Skin Xenograft</u>

1.3.1.2.1 *Skin Xenograft Source*

Numerous protocols have been applied to skin xenografting. Split-thickness grafts are

common; however full-thickness grafts are used when attempting to retain adnexa. Cultured keratinocytes in combination with artificially constructed dermis or normal acellular dermis have been grafted (Medalie *et al.*, 1996). Human xenografts have been derived from a variety of donors and anatomical sites including fetal (Lane *et al.*, 1989), neonatal (common), young adult or aged skin (Gilhar *et al.*, 1991a), foreskin (common), trunk, face, (Petersen *et al.*, 1984) and scalp (Gilhar & Krueger, 1987). Finally, mice have been grafted with lesional skin from different diseases including psoriasis, lichen planus, alopecia areata and several genodermatoses (Krueger *et al.*, 1975; Briggaman & Wheeler, 1976; Gilhar *et al.*, 1989a; Gilhar *et al.*, 1992; Kim *et al.*, 1992; Van Neste *et al.*, 1993; Vailly *et al.*, 1998).

Although human skin xenografts have been the most studied, as early as the 1970s, skin from different animal donors was transplanted to immunodeficient mice (Table 1). Only two studies report grafting canine skin to immunodeficient mice. Rosenquist *et al.* (1988) assessed the effects of cold storage conditions on graft take using canine split-thickness grafts on nude mice. Although some canine grafts survived transplantation, a loose definition of graft survival was accepted and details regarding graft morphology were not provided. Caswell *et al.* (1996) used full-thickness canine skin grafts on scid/bg mice to recreate *D. canis* infections.

1.3.1.2.2 *Retention of the Xenograft Donor Phenotype*

In general, healed skin grafts retain a high degree of cellular and structural integrity for extended periods, usually for the life span of the mouse (one to two years). Unlike *in vitro* systems, xenogenic human grafts resemble normal skin grossly and histologically,

and maintain the complex relationships of cellular and extracellular components, including basement membranes, adnexa, and blood vessels.

The epidermal architecture resembles normal human skin, complete with epidermal strata and rete ridges (Yan *et al.*, 1993; Nickoloff *et al.*, 1995; Boehncke *et al.*, 1997). Immunohistochemical staining for the keratinocyte differentiation antigen involucrin in grafts on scid mice is similar to that of normal human skin (Brandsma *et al.*, 1995). Melanocytes can be detected in the basal layer of the epidermis (Kaufmann *et al.*, 1993). The epidermal basement membrane retains a normal ultrastructure, as well as expression of collagen-IV, collagen-VII and bullous pemphigoid antigen in full-thickness grafts on scid mice (Kim *et al.*, 1992). Normal human skin grafted to scid mice retains native vascular endothelium when evaluated at 8 (Yan *et al.*, 1993), 24, (Kim *et al.*, 1992) and 52 weeks (Kaufmann *et al.*, 1993). Graft chimerism does occur however, and is discussed below. Phenotypic characteristics associated with anatomical sites are maintained in the xenografts. Palmar-derived keratinocytes retained site-specific expression of keratin-9 after grafting to nude mice (Limat *et al.*, 1996).

Kaufman *et al.* (1993) demonstrated that in addition to keratinocytes, endothelial cells, and fibroblasts, components of the skin immune system remain in grafts for up to 12 months on scid mice. CD1a+ epidermal dendritic cells remain confined to the epidermis, whereas dermal macrophages were located adjacent to vessels. CD3+ T-cells, expressing a memory cell pattern for CD45, were also retained in the dermis for 12 months. Mast cells were present but appeared to be decreased in number in grafts evaluated with toluidine-blue staining; however, the number of degranulated mast cells was not measured. Other investigators report similar or low carrier leukocyte status of

human skin grafts in the process of modeling inflammatory conditions or physiologic reactions (Yan *et al.*, 1993; Nickoloff *et al.*, 1995; Christofidou-Solomidou *et al.*, 1996; Juhasz *et al.*, 1996; Christofidou-Solomidou *et al.*, 1997b; Gilhar *et al.*, 1997; Delhem *et al.*, 1998).

Physiologically, skin xenografts resemble normal human skin, providing further evidence that grafted normal skin remains representative. Yan *et al.* (1993) demonstrated that human full-thickness skin graft endothelium responds to cytokine injection with a similar pattern of E-selectin and intercellular adhesion molecule-I (ICAM-I) expression as normal human skin. Wound healing in human xenografts resembles that seen in normal skin (Juhasz *et al.*, 1993).

1.3.1.2.3 *Retention of Adnexa*

Demodex canis reside within hair follicles and sebaceous glands and retention of these structures in xenografts is important for the purposes of modeling demodicosis. Between 30% and 50% of human scalp plug xenografts (normal or diseased) survive with a few hair follicles after transplantation (Gilhar & Krueger, 1987; Van Neste *et al.*, 1989; Hashimoto *et al.*, 1996; Van Neste, 1996). Greater technical success has been achieved with an alternative method using human fetal skin grafts; 90% of grafts had hair growth >1 year post transplantation (Kyoizumi *et al.*, 1998).

Reports have not specifically addressed the hair growth potential, or its optimization, for xenografts from veterinary species. However, brief descriptions and published photographs show that hair growth does occur on xenografts derived from different donors. Thick hair growth was observed for feline skin grafts 1 cm in diameter

(Manning *et al.*, 1973). Rygaard (1974) described a similar level of hair growth from rat skin grafts on nude mice. Krueger and Briggaman (1982) published a photograph of several hairs growing from a pig skin graft. While investigating fungal infection of xenografts, Green *et al.* (1982) reported growth of hairs from a guinea pig skin graft. Greater than 90% of fetal sheep skin xenografts on nude mice produced hair (McCloghry *et al.*, 1993a; McCloghry *et al.*, 1993b). The follicular density decreased in grafted fetal sheep skin, especially in central areas, as compared to control fetuses. A common feature of skin donors (with the exception of the pig) is that grafts were from animals with relatively thin skin compared to humans or dogs. Hair growth on canine skin xenografts was not described in detail and was highly varible (Caswell *et al.*, 1996).

Sebaceous glands and eccrine glands, retained in human skin xenografts, were responsive to chemical (pilocarpine) and endocrine (testosterone) manipulation (Petersen *et al.*, 1984; Robertson *et al.*, 1986).

1.3.1.3.4 *Alterations in Skin Xenografts after Transplantation*

The skin xenograft, although biologically representative of the donor in many ways, is an artificial construct. Hyperpigmentation, excessive fibrosis, or changes in dermal mast cell numbers occur in some skin xenografts (Gilhar *et al.*, 1991b; Kaufmann *et al.*, 1993; Farooqui *et al.*, 1995; Matsumoto *et al.*, 1996; Christofidou-Solomidou *et al.*, 1997b). Fibroplasia occurs at the interface between the skin xenograft and mouse tissue as part of the healing process and this area may be infiltrated by inflammatory cells in small numbers (Pilewski *et al.*, 1995; Christofidou-Solomidou *et al.*, 1996).

In general, skin xenografts do not develop significant graft chimerism. The

morphologic demarcation that is readily apparent (grossly and microscopically) between scid mouse and human skin has been confirmed by species specific immunohistochemical staining for the MHC-I antigen (Kim *et al.*, 1992). Similar findings were reported for nude mice (Demarchez *et al.*, 1986; Demarchez *et al.*, 1987a; Demarchez *et al.*, 1987b). Gream *et al.* (1984) described epidermal chimerism in only one skin graft out of 32 on nude mice evaluated over a 48-week period. Kaufman *et al.* (1993) evaluated 28 skin grafts on scid mice and described focal epidermal chimerism only in the margin of one graft using anti-mouse MHC-I antibody. In that one graft, mouse epidermis had overgrown human dermis and was indistinguishable morphologically from adjacent human epidermis. Boehncke *et al.* (1994) described more extensive replacement of human epidermis by mouse keratinocytes in psoriatic xenografts. Again, the chimeric epidermis took on characteristics of the human epidermis including lesions of psoriasis.

Tissue chimerism also has been established by vascular endothelium in skin grafts on nude mice but not scid mice. Demarchez *et al.* (1987) described replacement of human graft endothelial cells with nude mouse endothelium. Human lymphocytes and monocytes are capable of migrating across murine microvasculature in multiple tissues including the skin and are likely able to transmigrate murine endothelial lined human vessels in skin grafts. This is supported by studies of human leukocytes in human-PBL-scid chimeras (Taylor, 1994), chemokine and antigen challenge studies in murine skin of human-PBL-scid chimeras (Murphy *et al.*, 1994; Taub *et al.*, 1996; Herz *et al.*, 1998), and endothelial receptor binding studies using human lymphocytes and murine endothelium (Frey *et al.*, 1998; Wang *et al.*, 1998b; Evans *et al.*, 2000). Greenwood *et*

al.(1993, 1996, 1997) have observed similar results with bovine lymphocyte chimeras. Recent work by Evans and colleagues showed that canine leukocytes will specifically bind to murine endothelial receptors and are likely capable of crossing vessels lined by murine endothelial cells (Evans, personal communication).

In response to inflammatory stimuli, murine inflammatory cells transmigrate human vascular endothelium into skin grafts on immunodeficient mice. Murine neutrophils (and possibly monocytes) enter human skin grafts after tumor necrosis factor alpha (TNFα) injection or chemically-induced mast cell degranulation (Yan *et al.*, 1993; Christofidou-Solomidou *et al.*, 1996). Murine neutrophils and eosinophils infiltrated human skin grafts after injection with a poxvirus carrying the HIV-1 *LAIgp160* gene (Delhem *et al.*, 1998). There are similar reports of murine Langerhans cells migrating into human skin grafts on nude mice (Demarchez *et al.*, 1993; Hoefakker *et al.*, 1995).

1.3.2 MODELING SKIN INFECTIONS

A number of fastidious dermatotropic viruses that are difficult to culture or to study *in vivo* have been investigated using the skin xenograft model. These include *Molluscum contagiosum* (Buller *et al.*, 1995; Fife *et al.*, 1996; Paslin *et al.*, 1997), varicella-zoster (Moffat *et al.*, 1995; Moffat *et al.*, 1998a; Moffat *et al.*, 1998b) and several papillomaviruses (Kreider *et al.*, 1987; Christensen & Kreider, 1990; Brandsma *et al.*, 1995). In some of the earliest experiments, Kreider *et al.* (1985, 1986, 1987) employed a renal subcapsular transplant model for human papillomavirus-11 (HPV-11) infection of foreskin and cervical tissues, that supported virus replication. Brandsma *et al.* (1995) used normal foreskin grafted to the backs of scid mice to obtain replication of HPV-16

and wart development. Other viruses cultured using the skin xenograft model include HPV-1, HPV-18, bovine papillomavirus-1 (BPV-1), cottontail rabbit papillomavirus (CRPV), and herpes simplex virus-1 (HSV-1) (Kreider *et al.*, 1979; Van Genderen *et al.*, 1987; Kreider *et al.*, 1990; Christensen & Kreider, 1993; Randazzo *et al.*, 1996; Lobe *et al.*, 1998). Virally infected skin grafts, usually, reproduce the histological lesions of naturally occurring infections.

The ability to replicate these viruses in skin xenografts naturally led to *in vivo* studies. Christensen and others (1990, 1991, 1993) studied *in vivo* antibody-mediated neutralization of viral host cell attachment for HPV-11, BPV-1, and CRPV using skin xenografts. Utilizing the capacity of scid mice to accept lymphocyte, thymus, and liver grafts in addition to skin grafts, Moffat and coworkers (1995, 1998a, 1998b) were able to experimentally demonstrate components of the "pathogenic cycle" of VZV throughout different human host tissues. Wild-type HSV-1 caused ulceration and typical histopathological lesions with immunohistochemical evidence of replication in human skin grafts on scid mice, while a deletional mutant vaccine candidate (HSV-1716) developed restricted replication (Randazzo *et al.*, 1996).

Fungal skin infections reproduce well using the xenograft model. Chronic infection of guinea pig skin grafts with *Trichophyton mentagrophytes*, after topical application, led to comparable histological changes to chronic dermatophytosis in humans (Green *et al.*, 1982). Kakutani and Takahashi (1987) obtained similar results after human skin xenografts were puncture inoculated with *T. mentagrophytes*.

One author applied the skin xenograft model to investigate a human parasitic disease –the early events of *Schistosoma mansoni* larval migration through human skin were successfully studied (Roye *et al.*, 1998).

1.3.3 MODELING SKIN INFLAMMATION

1.3.3.1 Preexisting Inflammatory Lesions

Psoriatic skin was one of the first examples of lesional skin to be transplanted to nude mice (Krueger *et al.*, 1975). Subsequently, lesional skin from patients with either alopecia areata/universalis (Gilhar & Krueger, 1987), or lichen planus (Gilhar *et al.*, 1989b) was successfully grafted to immunodeficient mice. Inflammatory cell infiltrates within xenogenic skin grafts survive transplantation, and grafts retain lesions for many weeks. Prolonged engraftment with lesional skin is associated with resolution of lesions, normalization of graft morphology, and dissipation of graft inflammation. In the case of alopecia areata/universalis, skin grafts derived from alopecic areas on patients begin to regrow hair after grafting. Such experiments illustrate the utility of the skin xenograft mouse model in demonstrating that skin lesions associated with these diseases are dependent on continued inflammation.

1.3.3.2 Recreating Cutaneous Inflammation

The skin xenograft model has been applied to study induction of cutaneous inflammation in normal skin. Yan and coworkers (1993) took advantage of the ability of murine leukocytes to cross human skin graft endothelium in response to inflammatory stimuli. Graft injection of tumor necrosis factor alpha (TNFα) led to reversible up-regulation of

several adhesion molecules on human graft endothelium and murine leukocyte infiltration of the dermis. Several researchers subsequently used this approach to study the role of cytokines, adhesion molecules, mast cells, and other factors considered important in the initiation of inflammation (Yan *et al.*, 1994; Pilewski *et al.*, 1995; Christofidou-Solomidou *et al.*, 1996; Yan *et al.*, 1996).

Cograftment of autologous leukocytes provides a source of donor inflammatory cells that are needed to recreate dermatitis reactions with skin xenografts. Reconstitution of scid mice with human leukocytes was first reported in the late 1980s (McCune *et al.*, 1988; Mosier *et al.*, 1988). In addition to human leukocytes, partial reconstitution of scid mice has been reported using bovine, equine, and feline leukocytes (Balson *et al.*, 1993; Greenwood & Croy, 1993; Johnson *et al.*, 1994; Greenwood *et al.*, 1997). Transferred lymphocytes produced immunoglobulin within scid mice for weeks to months, thus providing components of the humoral immune system. Results of experiments modeling allogenic graft rejection indicate that transferred human or bovine lymphocytes retain functional capabilities—lymphocytes recirculate to skin grafts and mediate graft rejection (Alegre *et al.*, 1994; Christofidou-Solomidou *et al.*, 1997a; Greenwood *et al.*, 1997).

In one of the first experiments employing this approach to study skin inflammation (other than allograft rejection), Petzelbauer *et al.* (1996) modeled delayed-type hypersensitivity (DTH). Scid mice were grafted with patient skin of a high or low tetanus toxoid responder and subsequently were reconstituted with autologous lymphocytes. Upon intradermal skin graft injection of tetanus toxoid, a perivascular human CD4+ lymphocytic infiltrate developed in grafts from high-responders. The induced reaction was considered antigen specific because it was not observed for low

responders. In a similar study, known tuberculin-reactive donors, demonstrated a DTH-like reaction 72 hours after intradermal tuberculin challenge of human skin grafts on autologous lymphocyte reconstituted scid mice (Tsicopoulos *et al.*, 1998). A perivascular infiltrate of CD4+ and CD8+ lymphocytes developed in response to tuberculin but not saline injection and there was a relative increase in the number of IL-2 and IFN-gamma mRNA-expressing cells within xenografts (Tsicopoulos *et al.*, 1998).

The development of graft-versus-host disease (GVHD) is a recognized complication of xenogenic leukocyte scid mouse chimeras (Taylor, 1994). Inflammatory targeting of mouse tissues by principally grafted lymphocytes leads to organ pathology, usually affecting the liver, skin and lymphoid organs. Affected mice may become ill or even moribund. Some mice develop hemolytic anemia, as was observed in an early attempt to create canine leukocyte scid chimeras (Caswell, 1995).

1.3.4 MODELING CANINE DEMODICOSIS

Caswell *et al.* (1996) reported that canine skin xenografts would support *D. canis* infections. Full-thickness normal canine skin grafts were transplanted to scid/bg mice and subsequently exposed to *D. canis*. Mites actively invaded hair follicles and reproduced all life-cycle stages on skin grafts. Two skin donor dogs were used and mites were recovered from 4 of 4 grafts for the first donor, and from 4 of 11 grafts from the second donor. Two to 3 month incubation times were required to detect mites on grafts. This experiment demonstrated that full-thickness canine skin can be grafted to scid/bg mice and suggests that the xenograft mouse model might be a viable system for studying

the pathobiology of canine skin. If optimized, the xenograft model could provide a new and much-needed method for culturing *D. canis* and for experimentally recreating *D. canis* skin infections.

1.4 SUMMARY AND RATIONALE

The skin xenograft mouse model is well-established in human dermatology and offers several experimental advantages for investigating the pathogenesis of skin diseases. First, the skin xenograft model provides an *in vivo* experimental system to address functional questions in a biologically relevant manner. Skin grafts retain the donor phenotype, including hair follicles and adnexa. The utility of the model for studying skin infections has been demonstrated, particularly for those organisms that cannot be cultured *in vitro* such as *D. canis*. Inflammatory skin conditions have been successfully modeled using the xenograft model.

Use of the xenograft model should permit basic, unresolved questions about the pathogenesis of canine demodicosis to be directly addressed in a functional manner. The question of lymphocyte function in host resistance to *D. canis*, considered central to the pathogenesis of canine demodicosis, could be directly tested. Infection of skin xenografts with *D. canis*, in the absence of host influences, provides a means to assess the contribution of mites to skin lesion formation. Development of a reproducible canine skin xenograft model of demodicosis has wider implications as the model could be applied to develop new treatments for demodicosis or to study other canine skin diseases.

Caswell's experiment, showing that *D. canis* could survive on canine skin grafts, has not been repeated (Caswell *et al.*, 1996). Limitations of that study were variable mite

infection rates, low numbers of mites recovered from grafts and surgical technique problems with grafting full-thickness canine skin to scid/bg mice. The preliminary findings justified development of the skin xenograft mouse model of canine demodicosis.

1.5 RESEARCH OBJECTIVES

The experiments undertaken were directed towards two major objectives: (1) To develop and validate basic components of the skin xenograft mouse model for use with canine tissues and thereby establish the model's usefulness as an investigative tool for studying canine skin disease. (2) To use the skin xenograft mouse model to directly assess the effect of canine lymphocytes on *D. canis* populations on canine skin.

CHAPTER 2: GENERAL MATERIALS AND METHODS

2.1 RESEARCH ANIMALS

Animals were maintained according to the Canadian Council of Animal Care guidelines.

2.1.1 Mice (*Mus musculus*)

Male transgenic tgε26 mice (B6;CBA-TgN(*CD3E*)26Cpt), raised at the University of Guelph, were a kind gift of Dr. Anne Croy (University of Guelph, Guelph, Ontario, Canada). Male ICR scid mice (Tac:Ucr:Ha(ICR)-*Prkdc*^{scid}) and *Rag2* knockout mice (129S6/SvEvTac-*Rag2*^{tm1}) were obtained from Taconic (Germantown, New York, USA).

Mice were housed in a barrier facility within the Isolation Unit at the University of Guelph (Guelph, Ontario, Canada). One to five mice were housed per cage on a Micro-isolator® rack (Laboratory Products Inc., Maywood, New Jersey, USA) and were exposed to a 14 hour light-cycle. Cages, bedding, and water were autoclaved and mice received gamma irradiated mouse chow (Charles River Laboratories, St. Constant, Quebec, Canada). The drinking water was acidified (approx. pH=3) and supplemented with sulfamethoxyzole (0.5 mg/mL) and trimethoprim, (0.01 mg/mL) (Novo-timel®, Novopharm Ltd., Toronto, Ontario, Canada).

Mice were allowed 7 to 10 days to acclimate to housing conditions prior to experimentation. All procedures using mice were performed in a laminar flow hood using sterilized instruments and aseptic technique.

2.1.2 Dogs (*Canis familiaris*)

Random source adult male dogs, weighing 25 to 35 kg, were purchased from and maintained by Animal Care Services (University of Guelph). Dogs were provided an enriched environment and 3 to 5 outdoor leash walks per week. Dogs were housed individually in raised floor cages in a room with other dogs, and were allowed intermittent direct contact.

Within the two months preceding the start of experiments, dogs were vaccinated against rabies, canine distemper, adenovirus type-2, parainfluenza, parvovirus, leptospirosis, and bordetella (IMRAB®, Merial Canada Inc., Baie d'Ure', Quebec, Canada; Bronchi-Shield® III, Ayerst Veterinary Laboratories, Guelph, Ontario, Canada; and either Vanguard® 5, Pfizer Canada Inc., London, Ontario, Canada or Galaxy® DA2 PPvL, Ayerst Veterinary Laboratories, Montreal, Quebec, Canada).

Fecal samples were monitored on a monthly basis for evidence of intestinal parasites by standard fecal flotation methods. To eliminate intestinal parasites, dogs were treated appropriately with pyrantel pamoate (Strongid®-T, Pfizer Canada Inc., London, Ontario, Canada) and/or praziquantel (Droncit®, Bayer Inc., Toronto, Ontario, Canada) when required. Dogs were examined for evidence of ear mites and were treated when necessary with a borate-containing ear astringent (Veterinary Pharmacy Inc., Guelph, Ontario, Canada). All dogs lacked evidence of infection with other external parasites and tested negative for canine heartworm infection (*Dirofilaria immitis*) utilizing a modified Knott's technique to identify circulating microfilaria.

Prior to experimentation, each dog had a normal physical examination and was deemed to lack evidence of skin disease. Blood smear, differential count and packed cell

volume (PCV) were within normal limits (reference limits, Animal Health Laboratory, Guelph, Ontario, Canada).

2.1.3 Mites (*Demodex canis*)

Demodex canis were collected from dogs with squamous demodicosis that had high mite burdens, including multiple life-cycle stages, lacked clinical and/or histopathological evidence of bacterial pyoderma, and had not been treated with an acaricide within the previous 2 months. Only mites with a compatible size and morphology for *D. canis*, as described by Nutting and Desch (1978), were utilized.

The majority of mites were collected by plucking hairs from lesional skin using Kelly forceps. Ten to 30 hairs were fixed at the skin surface with forceps and removed by applying traction. The apical portion of the plucked hairs was trimmed away with scissors and the basilar portions along with the mites were deposited in sterile 50 mL conical polypropylene centrifuge tubes (Fisher Scientific Ltd., Ottawa, Ontario, Canada). Alternatively, mites were collected in sterile mineral oil by skin scraping with a #10 scalpel blade (Scott *et al.*, 1995) and transported on glass microscope slides (Surgipath, Winnipeg, Manitoba, Canada) in a covered sterile container.

2.2 MOUSE BLOOD COLLECTION

Blood samples were collected from the orbital sinuses of mice using micro-hematocrit capillary tubes (Fisher Scientific Ltd.) (Bivin & Smith, 1984), while mice were anesthetized with methoxyflurane (Metafane®, Pitman Moore, Mississauga, Ontario, Canada). The PCV was recorded and plasma was collected into sterile microcentrifuge

tubes (Fisher Scientific Ltd.) and stored at –40°C. To obtain serum samples, blood was collected by intracardiac puncture with a 1 mL syringe and a 25 gauge needle (Bivin & Smith, 1984), while mice were anesthetized with Avertin (0.03 mL/g) (Wixson & Smiler, 1997). Serum was collected after centrifugation at 500 × g for 20 minutes using a serum separator (Sure-Sep Jr., Organon Teknika, Scarborough, Ontario, Canada).

2.3 SKIN GRAFTING PROCEDURES

2.3.1 Canine Donor Skin Collection

Dogs were sedated with 0.05 mL/kg of Premix (atropine 0.24 mg/mL, acepromazine 1 mg/mL, and meperidine 20 mg/mL; Ontario Veterinary College, Guelph, Ontario, Canada) prior to anesthetic induction with thiopental (Abbott Laboratories Inc., Montreal, Quebec, Canada). Dogs were maintained under general anesthesia with isoflurane (Aerrane®, Janssen Animal Health, Toronto, Ontario, Canada) using a rebreathing anesthetic machine. All surgical procedures were performed using sterile technique. A surgical site over the mid-dorsolateral back was shaved and surgically prepared with a chlorhexidine based surgical scrub (Steri-Stat® 4%, Ingram & Bell, Don Mills, Ontario, Canada) and 70% isopropyl alcohol (Commercial Alcohols Inc., Brampton, Ontario, Canada). Dogs received 1 g of cefazolin (Novopharm Ltd.) intravenously prior to surgery. A single full-thickness elliptical skin sample (14 × 6 cm) was removed by incising the skin with a #10 scalpel blade followed by blunt dissection immediately superficial to the panniculus carnosus. The excised skin sample was placed into 400 mL of fresh tissue culture medium (Roswell Park Memorial Institute 1640 (RPMI), Life Technologies, Burlington, Ontario, Canada) containing penicillin (200 IU/mL) (ICN

Biomedicals Canada Ltd., Mississauga, Ontario, Canada) and streptomycin (80 µm/mL) (Life Technologies) and chilled on ice. After the surgical wound was closed a multi-layered bandage was applied, and the dogs were monitored during the recovery period. Post-operative pain was managed with butorphanol (Torbugesic®, Ayerst Veterinary Laboratories). All surgical wounds healed without significant complications.

2.3.2 Preparation of Individual Skin Grafts

Skin grafts were prepared in a laminar flow hood using sterile technique. Tissues were kept moist at all times with fresh culture medium containing antibiotics as described in the previous section. Subcutaneous and deep dermal fat was trimmed away with curved Mayo scissors. Skin grafts were trimmed to a round shape (10 to 12 mm in diameter) on a sterile plastic cutting board using a #10 scalpel blade. Grafts were placed in fresh culture medium (5 mL/graft) containing antibiotics and chilled on ice until grafting.

Three to five skin samples (6 × 6 mm, full-thickness) were collected from the excisional canine skin biopsies (used to create skin grafts) and were evaluated for the presence of preexistent inflammation or *D. canis* infection by histology (see below). Three additional skin samples (6 × 6 mm, full-thickness) were also assessed for the presence of mites by NaOH digestion (see below). None of the donor skin samples had evidence of preexistent inflammation or mite infection.

2.3.3 Skin Grafting of Mice

The surgical site (dorsolateral thorax) was shaved on each mouse 24 hours prior to surgery (Clippers, Wahl® Professional, Model 6120, Swenson Canada Inc., Toronto, Ontario, Canada). Immediately prior to skin grafting, mice were anesthetized with

Avertin (IP, 0.02 to 0.03 mL/g). Buprenorphene (SQ, 1.0 mg/kg) (Buprenex®, Reckitt & Colman Pharmaceuticals Inc., Richmond, Virginia, USA) was administered for postoperative analgesia. A circular graft bed, 4 to 6 mm in diameter larger than the canine skin graft, was created with small curved Metzenbaum scissors. The tips of the scissors were held perpendicular to the skin surface and interconnecting shallow skin incisions were made in an outline of the graft bed margin to a level just superficial to the panniculus carnosus. The skin over the graft bed was removed by fixing the anterior ventral margin with forceps and pealing the skin away in the caudal direction, parallel with the lateral thoracic artery. This technique was required to maintain the panniculus carnosus, and associated vasculature, intact as the floor of the graft bed. The skin graft was blotted with sterile gauze, seated on the graft bed, and anchored at the epidermal margin to adjacent mouse skin (at four to six points) using minimal tissue adhesive (Vetbond®, 3M Animal Care Products, St. Paul, Minnesota, USA) delivered with a 1 mL syringe and a 30 gauge needle. Care was taken to prevent tissue glue from contacting the dermal surface of the skin graft. Skin grafts were immediately bandaged (see below).

It was possible to apply an average of four grafts per hour. The time between skin collection and final graft application for a group of mice ranged from 6 to 9.5 hours.

2.3.4 Skin Graft Bandage Procedures

Two bandaging methods were used. **Method A:** Based on the report by Caswell *et al.* (1996), skin grafts on anesthetized mice were covered by two layers (15 × 15 mm) of sterile paraffin-impregnated gauze dressing (Jelonet®, Smith & Nephew, Lachine, Quebec, Canada). The gauze was held in place by one layer (20 mm wide) of adhesive

elastic bandage (Elastoplast®, Smith & Nephew) wrapped around the trunk. Finally, one or two layers of plaster-of-paris casting material (18 mm wide) (Gypsona®, Smith & Nephew) were applied using sterile water. Here after, these are referred to as cast bandages. **Method B:** Skin grafts were covered by two layers of paraffin-impregnated gauze (15 × 15 mm). The gauze was held in place with a single sterile waterproof elastic bandage (Comfort Strips, 3M Canada, London, Ontario, Canada), followed by two layers of 25.4 mm wide hospital tape (Renfrew Tape Ltd., Renfrew, Ontario, Canada). When bandaged >5 days, bandages were fixed to mouse skin using surgical staples (Auto Suture®, United States Surgical Corp., Norwalk, Connecticut, USA) placed at the anterior dorsal margin (2 staples) and the caudal dorsal margin (1 staple). Bandages were trimmed ventrally (5 to 10 mm wide) and in the axillary and inguinal regions. Here after, these are referred to as tape bandages.

Bandages were removed at 7 to 24 days after grafting, while mice were anesthetized with methoxyflurane. If cast bandages were used, then mouse hair was trimmed with scissors to release the bandage and remove adhesive residue.

2.4 *DEMODEX CANIS* INFECTION OF SKIN GRAFTS

Demodex canis were separated into individual infective doses in 100 to 150 μL of mineral oil on non-coated glass microscope slides (Surgipath). Each inoculum was standardized by intermixing mites on microscope slides and by including a similar number of viable mites in each dose, confirmed by microscopic examination of slides at 100X magnification. Mites were considered viable if they were moving or were

refractive and lacked obvious exoskeletal or internal organ disruption. More than 85% were moving prior to inoculation of grafts.

Mites were transferred to shaved skin grafts on anesthetized mice by directly wiping the mite-coated surface of a glass slide over the graft surface. Using the short edge of a clean slide, any mineral oil remaining on a slide was drawn into a drop and transferred to the skin graft. Skin grafts were immediately bandaged as above. The order of graft infection ensured a similar average mite collection to transfer time-interval for each group. Non-infected control grafts received only mineral oil prior to bandaging.

The efficiency of mite transfer was determined by counting the mites remaining on glass slides after infection and was estimated to be greater than 90% for all experiments. The few remaining mites were usually moving and considered viable. The duration between mite collection and graft infection ranged from 2.5 to 7.5 hours.

2.5 SKIN GRAFT COLLECTION AND EVALUATION

2.5.1 Skin Graft Collection

Mice were anesthetized with Avertin (0.03 mL/g), plasma or serum was collected and mice were immediately euthanized. A packed cell volume (PCV) was obtained and recorded. Skin grafts were subjectively evaluated for the degree of hair growth, erythema, scaling, crusting, scarring, or pigmentation. Pictures were taken while mice were awake or anesthetized. Using aseptic technique, skin grafts were removed by incising around the margin with Mayo scissors. Approximately half of the skin graft was collected into a Whirl-pac® bag (Nasco Plastics Inc., New Hamburg, Ontario, Canada) and stored at 4°C for subsequent enumeration of mites, described below. The remainder

of the skin graft was placed in 10% neutral buffered formalin. In some experiments, a 2 by 4 mm full-thickness sample was excised from the center of the skin graft with a #10 scalpel blade and submitted to Animal Health Laboratory (University of Guelph, Guelph, Ontario, Canada) for bacterial culture.

2.5.2 Histology and Immunohistochemistry

For histological evaluation, tissues were embedded in paraffin using standard methods. Five μm sections were prepared using a rotary microtome and stained with hematoxylin and eosin (H&E).

Immunohistochemical detection of T-cells was performed on formalin fixed, paraffin embedded canine skin grafts and mouse tissues using polyclonal rabbit anti-human CD3 antiserum (Dako, Carpinteria, California, USA). Tissues were screened for the presence of mouse leukocytes using mouse specific anti-CD45 antibody (Pharmagen, Mississauga, Ontario, Canada) using similar techniques. Briefly, tissue sections were deparaffinized, washed in automation buffer (Biomedia, Foster City, California, USA) with 10% acetone and 0.15% Brij 35 (ICN Biomedicals Inc., Aurora, Ohio, USA) and then blocked with 3% hydrogen peroxide in methanol at room temperature (RT) for 10 min. Antigen retrieval was performed by incubating sections in 0.05% protease XIV (Sigma, St. Louis, Missouri, USA) at 42°C for 20 min. Sections were blocked with 4% normal goat serum in automation buffer before overnight incubation at 4°C with rabbit anti-human CD3 antiserum (Dako), diluted to 1:500 and 1:1000. Prior to staining, the CD3 antiserum was pre-adsorbed with canine liver acetone powder (Sigma) (1 mL of a 1:50 dilution of antiserum with 0.5 g of liver powder for 24 hour at 4°C) to reduce non-

specific tissue staining. The secondary antibody was biotinylated goat anti-rabbit (Vector, Burlingame, California, USA) and was diluted to 1:400. Staining was completed using a peroxidase-labeled avidin-biotin complex (Vectastain ABC Elite, Vector). Diaminobenzidine (Sigma) was used as a chromagen substrate and sections were counterstained with hematoxylin.

2.5.3 Skin Graft Digestion and Enumeration of *Demodex canis*

Graft digestion samples were trimmed of hair and subcutaneous fat and stored at 4°C for <24 hours. Samples were standardized by either the number of active hair follicle units per sample or by sample weight. The total number of active hair follicle units was derived by counting the follicles that contained a hair shaft using a dissecting microscope with graft samples chilled on ice. The sample weight was measured with an electronic balance (Model AT261, Mettler Instrument Co., Hightstown, New Jersey, USA).

Just prior to digestion, each skin sample was sectioned into uniform 2 to 3 mm cubes, using a new #10 scalpel blade. Samples were suspended in 3 mL of 4% sodium hydroxide (NaOH) in 15 mL round bottom pyrex test tubes (Fisher Scientific Ltd), and then placed in a boiling water bath for 25 min. The digestion reaction was stopped with 3 mL cold distilled water and samples were immediately decanted into pre-weighed 15 mL conical centrifuge tubes. The tubes were washed with three distilled water rinses (RT) of 3 mL each. Mites were concentrated into a pellet by centrifugation of combined digestion reaction contents and washes at 822 × g for 10 min. The supernatant was removed by careful aspiration with a Pasteur pipette and digestion samples were resuspended in 500 µL of distilled water using an electronic balance (Model AT261,

Mettler Instrument Co.). Finally, tubes were centrifuged at 100 × g for 3 min. If samples retained abundant melanin pigment or particulate debris after digestion, samples were resuspended in 1,000 or 2,000 µL of distilled water to allow visualization of mites. Similarly, samples were diluted to these larger volumes if high mite numbers interfered with mite enumeration.

Digested samples were assigned a random number prior to enumeration of mites. Each sample was thoroughly mixed by a gentle vortex before a 10 µL aliquot was placed on glass microscope slide and covered with a 22 × 22 mm glass cover slip (Fisher Scientific Ltd.). Alternatively, a 40 µL aliquot was collected and viewed under a 22 × 50 mm cover slip. The entire content of each aliquot was examined and recorded; this process was repeated two to five times with additional aliquots from each digest sample. More than two aliquots were examined in this manner if the mite count from one aliquot was low in order to increase the total observations per sample. All slides were examined at 40X and 200X magnification, except for fragments of mites, which were assessed at 400X, using the same light microscope calibrated to Kohler illumination.

Mite stages were identified using published morphologic criteria (Nutting & Desch, 1978). The total occurrence of each life cycle stage, including the egg, larva, nymph, and adults was recorded for each aliquot. The process of NaOH tissue digestion induced minor structural artifacts in mites that led to certain limitations in the counting procedure. The protonymphal stage could not be reliably differentiated from the larval stage, and as a consequence, any observation of this stage was included in counts for the larval stage. Adult mites were counted and recorded without reference to sex.

Fragmented mites that were identifiable to a particular life-cycle stage were counted. Rarely, a mite fragment was not identifiable to a specific stage and was not counted.

Digested samples were monitored for the presence of fragmented mites as an indicator of sample handling. In all experiments, mite fragments were rarely seen, and when observed, mite fragments accounted for less than 1-2% of the total mite count per sample.

2.5.4 Mouse Necropsy

Necropsies were performed at the time of euthanasia. The following tissues were collected and prepared for histological evaluation: liver, kidney, spleen, pancreas, lung, heart, tongue, skeletal muscle (cranial tibialis), esophagus, stomach (glandular and non-glandular), small intestine (duodenum, jejunum, ileum), cecum, colon, skin, and bladder. Tissue sections were prepared and stained with H&E as described above.

2.6 ISOLATION OF CANINE LEUKOCYTES

Canine peripheral blood mononuclear cells (PBMC) were isolated by discontinuous density gradient centrifugation using sterile techniques (Barta & Barta, 1993). Blood (150 to 250 mL) was collected into 10 mL ethylenediaminetetraacetic acid (EDTA) coated Vacutainer® tubes (Becton Dickinson, Franklin Lakes, New Jersey, USA) using an 18-gauge jugular catheter. After thorough mixing, the blood was centrifuged (1500 × g, 30 min) (Sorvall®, RT6000B centrifuge, Dupont Co., Newtown, Connecticut, USA) and the buffy coats from 3 tubes (approx. 3 mL) were combined with three parts phosphate-buffered saline (PBS) at RT in 15 mL conical polypropylene centrifuge tubes

(Fisher Scientific Ltd.). Using an 18-gauge spinal needle, the buffy coat mixture was under-layered with 3.5 mL of Histopaque®-1077 (Sigma, St. Louis, Missouri, USA) and centrifuged (400 × g, 30 min). The mononuclear cell layer was isolated from the gradient interface using a Pasteur pipette and cells were washed in 10 mL of PBS followed by centrifugation (100 × g, 10 min). Erythrocyte cell lysis was performed by exposing the loosened cell pellet to 500 µL of distilled water for 5 sec followed immediately by a second PBS wash. PBMC were combined in PBS and held on ice until injection into mice, or were resuspended in lymphocyte culture medium for lymphocyte blastogenesis as described below. Cell counts were performed on a Coulter counter® (Beckman Coulter Canada Inc., Mississauga, Ontario, Canada). A 200-cell differential was performed using a cytospin preparation (Cytospin-2, Shandon Southern Products Ltd., Astmoor, Cheshire, UK). The percent cell viability was assessed by trypan blue dye exclusion (Fisher Scientific Ltd.) on a 200-cell differential.

2.7 *IN VITRO* CANINE LYMPHOCYTE BLASTOGENESIS

Canine lymphocytes were stimulated *in vitro* to undergo blastogenesis in a 72-hour protocol with phytohemagglutinin (PHA) and human recombinant interleukin-2 (hr-IL-2) (Somberg *et al.*, 1992; Barta & Barta, 1993; Mizuno *et al.*, 1993). This protocol was refined prior to experiments using PBMC from three different healthy adult mixed breed dogs in order to determine optimal doses of PHA-P and hr-IL-2 as well as optimal incubation times. Canine PBMC were resuspended at a concentration of 1×10^6 cells/mL in RPMI culture medium containing 15% heat-inactivated fetal bovine serum (Cansera, Rexdale, Ontario, Canada), 10 mM Hepes buffer (Sigma Chemical Co.), 2mM L-

glutamine (Life Technologies), penicillin (100 IU/mL) and streptomycin (100 μg/mL). PBMC used for inoculation of mice were maintained in 75 cm^2 tissue culture flasks (Corning, New York, USA), containing 50 mL of culture medium, at 5% CO_2 and 37°C in a humidified tissue culture incubator (Model 3158, Forma Scientific, Macietta, Ohio, USA). After culture for one hr, PHA (10 μg/mL) (Sigma) was added. Forty-eight hours later, hr-IL-2 (1000 units/mL) (PharMingen) was added and cells were cultured for an additional 24 hr. The PBMC used for mouse injections were collected into 50 mL conical polypropylene centrifuge tubes (Fisher Scientific Ltd.), washed once in 20 mL of PBS (RT), centrifuged (100 × g, 10 min), and resuspended in PBS.

To determine a lymphocyte stimulation index, an aliquot of PBMC, were maintained in 96-well plates (Evergreen Scientific, Los Angeles, California, USA) at 0.2 mL per well. Tritiated thymidine (ICN Biomedicals Inc., Aurora, Ohio, USA) was added to each well (25 μCi/mL) 18 hours prior freezing plates (–40°C), cells were analyzed with a beta-plate cell harvester, and thymidine incorporation was determined with a scintillation counter (Becton Dickinson). Six control wells containing PBMC did not receive PHA-P or hr-IL-2 and provided readings for background thymidine incorporation. The stimulation index was calculated as follows:

$$\frac{\text{Average cpm of 6 replicates with PHA-P and hr-IL-2}}{\text{Average cpm of 6 replicates without PHA-P or hr-IL-2}} = \text{Stimulation Index}$$

2.8 QUANTIFICATION OF MURINE AND CANINE IMMUNOGLOBULIN IN MOUSE PLASMA

Canine and murine immunoglobulin concentrations in mouse plasma or serum samples were quantified by direct sandwich ELISA using methods adapted from the Animal Health Laboratory (University of Guelph, Guelph, Ontario, Canada).

Canine IgG was quantified in mouse plasma samples using flat bottom 96 well plates (Immunol® 1B, Dynatech, Laboratories Inc., Chantilly, Virgnia, USA). The 96 well plates were coated with an affinity purified goat anti-dog IgG, at 100 µL/well (ICN Biomedicals Inc.) diluted to 2 µg/mL in coating buffer and incubated for 24 hours at 4°C. Plates were washed 5 times with 200 µl/well of PBS containing 0.05 % Tween-20 (Fisher Scientific Ltd.) before being blocked with 1% bovine serum albumin in washing buffer for 1 hour at RT. All subsequent incubations occurred at RT. Reagent dilutions were performed with washing buffer and incubations were preceded by the washing step listed above. Test sera (or plasma) were serially diluted and incubated at 50 µL/well on plates for 2 hr. The biotinylated secondary antibody, goat anti-dog IgG (ICN Biomedicals Inc.) was diluted at 1:4000 and incubated on plates at 100 µL/well for 1 hr. Plates were incubated for 30 minutes at 100 µL/well of ExtrAvidin® peroxidase conjugate (Sigma) diluted to 1:8000. The chromagen reaction was performed with 100µL/well of ABTS peroxidase substrate (Kirkegaard & Perry Laboratories Inc., Gaithersburg, Maryland, USA) and plates were read at dual wavelength absorbance (405/620 nm) using an automated ELISA plate reader (Ceres UV900Hdi, Biotec Instruments Inc., Winooski, Vermont, USA). Endpoint absorbance was recorded at an optical density (OD) reading of 1.0 for a standard well and the average background absorbance was subtracted from all readings. All dilutions were run in triplicate. For each plate, positive control serum

containing known concentrations of canine IgG (ICN Biomedicals Inc.) were evaluated and PBS replaced test serum to determine background absorbance. Murine serum or plasma collected prior to experimentation served as a control to confirm the lack of murine cross reactivity.

Murine immunoglobulin concentrations in mouse serum or plasma were determined using the methods described above. The capture antibody was an affinity purified rabbit anti-mouse immunoglobulin (Dako, Carpinteria, California, USA), and the secondary antibody was an affinity purified biotinylated goat anti-mouse IgG (Dako). A standard curve was generated using serial dilutions of mouse serum with a known concentration of murine immunoglobulin (Dako). Positive control serum was used that contained known quantities of murine IgG (ICN Biomedicals Inc.) and PBS was used to determine background absorbency readings. Canine serum was used to confirm the absence of cross reactivity. Checkerboard titration was performed to determine optimum antibody dilutions (Carpenter, 1992).

2.9 STATISTICAL METHODS

The computer software packages SAS®, version 6.12 for Windows (SAS Institute Inc., Cary, North Carolina, USA), and GraphPad Prism, version 3.00 for Windows (GraphPad Software, San Diego, California, USA), were used for statistical analyses. P-values less than or equal to 0.05 were considered significant for statistical tests.

CHAPTER 3: DEVELOPMENT OF THE SKIN XENOGRAFT MOUSE MODEL FOR THE STUDY OF CANINE DEMODICOSIS

3.1 INTRODUCTION

The skin xenograft mouse model, used almost exclusively to advance human dermatology, has received little attention in veterinary research. Consequently, there are no well-established experimental techniques for a canine model.

The work by Caswell *et al.* (1996) provided a starting point for developing the skin xenograft mouse model to study canine demodicosis. The requirements for a good model were that recipient mice support canine skin grafts and that grafts support comparable numbers of *D. canis*. Further, after an extended mite incubation period, coengraftment of autologous leukocytes was needed. The experimental techniques used by Caswell *et al.* (1996) did not produce adequately sized grafts or consistent results for the experiments envisioned herein.

In the study by Caswell *et al.* (1996) healed canine skin grafts developed widely variable hair growth on scid/bg mice—some grafts grew only a few hairs, and healed grafts varied in size by as much as 30 to 50%. Healed grafts were generally small, 5 to 8 mm in diameter. Preliminary experiments performed in the current study with scid/bg mice, using the same techniques, reproduced these findings. The few human studies that have addressed the issue of hair growth in skin xenografts have not been promising. Full-thickness human scalp grafts must be limited to small punch grafts, usually 1 to 3 mm in diameter in order to achieve even a few actively growing hairs (Van Neste *et al.*, 1989; Hashimoto *et al.*, 1996; Van Neste, 1996). These small grafts are inadequate for

experiments modeling canine demodicosis. In contrast, split-thickness human skin grafts (up to 2 cm in diameter) heal well on immunodeficient mice, although, these lack adnexa and do not grow hair.

In a second experiment by Caswell (1995), scid/bg mice were grafted with canine peripheral blood mononuclear cells (PBMC) by intraperitoneal injection. Canine immunoglobulin was measured in mouse (5/6) sera 14 to 118 days after cell transfer, suggesting that scid/bg mice were at least partially reconstituted with canine lymphocytes. However, the majority of mice became moribund after canine PBMC transfer (8/9) and developed evidence of graft-versus-host disease (GVHD), including hemolytic anemia, died or were euthanized. Furthermore, the presence of murine immunoglobulin in serum indicated that all of the mice had developed the "leaky" phenotype (Bosma *et al.*, 1988). Preliminary experiments in the current study using scid/bg mice reproduced the findings of Caswell. The scid mutation exhibits incomplete penetrance (Hendrickson, 1993) and, as a result, a percentage of scid mice (up to 25%) acquire a degree of immunocompetence and are referred to as "leaky". "Leaky" scid mice are able to mount immune responses and reject xenogenic skin grafts (Bosma *et al.*, 1988).

Several objectives were identified to develop the skin xenograft mouse model for the study of canine demodicosis. The first was to choose an alternative recipient mouse for xenograft studies to reduce or eliminate the "leaky" phenotype and possibly GVHD. The tgε26 transgenic mouse is T-cell and NK-cell deficient and was chosen for this study (Wang *et al.*, 1994). The second objective was to evaluate canine skin xenografting techniques and identify factors important to improving grafting success. Because *D.*

canis develop in hair follicles, skin grafts must be uniform in terms of size and hair growth in order to create comparable mite populations. Larger skin grafts were needed to facilitate graft infection and to provide adequate tissues for evaluation. The third objective was to evaluate canine leukocyte engraftment of tgε26 mice to determine whether the mouse strain could support functioning canine T-lymphocyte grafts.

Development of these fundamental components of the canine skin xenograft mouse model provides the foundation to then address important issues specific to modeling demodicosis.

3.2 USE OF Tgε26 MICE TO SUPPORT CANINE SKIN XENOGRAFTS AND IDENTIFICATION OF FACTORS IMPORTANT FOR XENOGRAFT SUCCESS

To identify factors important for the healing of canine skin xenografts, the healing of different thickness canine skin grafts on tgε26 mice was compared.

3.2.1 MATERIALS AND METHODS

3.2.1.1 Animals

Twenty-one male immunodeficient tgε26 mice, age 10 to 12 weeks, were housed with three to five per micro-isolator cage. Random-source, adult intact-male mongrel dogs with a normal physical examination were chosen and skin samples were collected immediately after euthanasia; dogs were euthanized for reasons other than this study.

3.2.1.2 Experimental Design

Three types of grafts were prepared, each with a different thickness. Each graft type was transplanted to seven mice. Mice in Group-I received thin split-thickness grafts and mice

in Group-II received thick split-thickness skin grafts; both graft types were collected with a dermatome. Group-III received full-thickness skin grafts collected by surgical dissection.

3.2.1.3 Experimental Protocol

Skin collection and preparation: Prior to experimentation, skin samples were collected from three different fresh cadaver dogs to determine the appropriate settings for the dermatome and to insure repeatability of split-thickness sample collection. The anatomic level of skin separation and the thickness of collected skin samples were confirmed by routine histology. The donor skin samples, each 5.5 cm × 8 cm, were collected from the dorsolateral back using sterile surgical techniques. The skin was shaved and prepared with a chlorhexidine based surgical scrub (Section 2.3.1). Thin split-thickness samples (Group-I) were collected using a Padgett manual dermatome (Padgett Instruments Inc., Kansas City, Missouri, USA) at setting 5 using dermatome cement (Padgett Instruments Inc.). Thick split-thickness samples (Group-II) were collected with the dermatome set at 20 and using a new blade. Dermatome-collected samples were harvested by cutting posterior to anterior. Full-thickness skin samples (Group-III) were harvested according to Section 2.3.1. Each skin sample was placed immediately in 300 mL of tissue culture medium (RPMI) containing antibiotics and chilled on ice as per Section 2.3.1.

In a laminar flow hood, individual grafts were excised from the central area of full-thickness and dermatome-harvested samples using 12 mm in diameter skin punches. Biopsy punches were hand-fabricated in order to create larger skin grafts of a uniform diameter while avoiding crush-induced trauma during graft cutting (see Appendix I for

skin punch design). While cutting each graft, skin samples were gently held flat on a plastic cutting board using an applicator to prevent twisting and traumatization of skin samples (see Appendix I for applicator design). Individual grafts were again placed in fresh RPMI (chilled on ice) containing penicillin and streptomycin (Section 2.3.1). Excess dermal fat was trimmed from the base of the full-thickness skin sample using Mayo scissors prior to preparation of individual grafts. Care was taken to prevent drying of tissues. Three to five additional biopsies were collected from each sample for histology to confirm the anatomic depth of skin grafts in each group.

Skin grafting: Skin grafting was performed as previously described with minor modification (Caswell *et al.*, 1996). Recipient mice were shaved with electric clippers 24 hours prior to grafting (see Section 2.3.3). Mice were randomly allocated to groups and the order of grafting insured a similar average time from skin collection to graft application for each group. Mice from different groups were housed together.

Mice were anesthetized with Avertin (Wixson & Smiler, 1997) (IP, 0.02 mL/g) and placed in the ventral recumbent position. Iridotomy scissors were used to remove a tent of skin creating a 12 to 14 mm in diameter graft bed on the dorsolateral chest wall just caudal to the elbow. Pre-trimmed grafts were lightly blotted with sterile gauze to remove transport media and placed in the graft bed. Skin grafts were attached to the adjacent mouse skin with tissue adhesive (Vetbond®, 3M Animal Care Products, St. Paul, Minnesota, USA) at 4 to 6 focal areas along the graft epidermal margin using a 1 mL syringe and a 30 gauge needle. Cast bandages were applied for 7 days (Method A, Section 2.3.4). Mouse toenails were trimmed at the time of bandage removal to decrease the risk of graft trauma.

Skin graft and mouse evaluation: Skin graft parameters were evaluated starting on the day that bandages were removed (1 week), and subsequently at weeks 3, 6, and 9. The area of surface crusting, or eschar formation, was graded as 0 (no crusting), 1 (less than 1/3 of the surface), 2 (between 1/3 to 2/3 of the surface), or 3 (greater than 2/3 of the surface). The general depth of crusting and changes in surface morphology were recorded. Surface color changes were recorded and provided an indication of vascular perfusion. Grafts were monitored for pigmentary changes. The diameter of each graft was measured in millimeters at two locations (oriented at 90 degrees) on the graft and the average of these two measurements was recorded. Hair growth was subjectively evaluated and the onset, location, and quality of hair regrowth after transplantation were recorded. Grafts were monitored for evidence of self-trauma.

Ten weeks after grafting, three grafts from three animals in each group were collected in 10% neutral buffered formalin for histology. A necropsy was performed on all mice and histological evaluation of tissues was performed for mice that did not complete the study.

3.2.1.4 Statistical Methods

ANOVA analyses of linear regression equations were performed using the SAS® statistical software package (Section 2.9). Log transformations of the data were performed when necessary. Skin graft eshar scores were compared using the nonparametric Wilcoxon signed rank test using Graphpad Prism (GraphPad Software, San Diego, California, USA).

3.2.2 RESULTS

The biopsies taken at the time of graft preparation confirmed the anatomical depth of skin grafts. Thin split-thickness grafts in Group-I were 0.8 to 1.2 mm thick, and the deep margin of grafts was located in the reticular dermis with primary hair follicles transected in the mid-isthmal region. Group-II thick split-thickness grafts were 1.8 to 2.2 mm thick and extended to the bulbs of primary hair follicles. Group-III full-thickness grafts were 2.4 to 2.8 mm thick and included a complete complement of skin adnexa, as well as a thin continuous layer of fat along the deep margin, absent from grafts in Group-I or -II. Biopsies lacked inflammation or other evidence of preexistent donor skin disease.

Skin grafts remained viable on 17 of 21 mice at week 10. Two mice died and one mouse became ill and was euthanized. Graft trauma, caused by the cage rack, resulted in the loss of one graft.

When bandages were removed, skin grafts were white to pale-pink, pliable, and smooth with normal surface texture. Mice were observed to clean and groom over the skin graft surface. This activity did not cause graft ulceration. However, mice did pull on the graft surface in the process of removing of tissue-glue residue. After this initial grooming, mice did not appear to be irritated by grafts and only occasionally scratched grafts with a hind foot.

Skin grafts in Group-I healed most quickly and with minimal scarring. Group-I grafts healed within 10 to 14 days and the thin dry central surface crust, or eschar, that had developed after bandage removal disappeared within three to four weeks. Group-II and Group-III grafts healed by approximately 3 weeks but developed thicker, more extensive, central surface eschar after bandage removal that lasted, on average, for seven

weeks in Group-II and nine weeks in Group-III. Figure 3.2-1 illustrates the mean eschar score for skin grafts in each of the three groups. There was a significantly lower eschar score for grafts in Group-I than in Group-II ($P = 0.001$) or Group-III ($P = 0.031$) at 3 weeks post transplantation. The eschar scores for Group-II and Group-III were not significantly different at three weeks ($P > 0.05$) and the more prominent surface changes in these two groups were associated with scar formation. The slopes for the regression equations for the three groups did not differ significantly ($P > 0.05$), indicating that the eschar score dropped at a similar rate during the observation period. Grafts were tan to pale-pink initially, and progressively became more pink starting at the graft margin.

Grafts in each group contracted similarly during the observation period (Figure 3.2-2). Average graft diameter at nine weeks was determined by linear regression. The average percent decrease in graft diameter was 23.15% (Group-I), 26.36% (Group-II) and 21.30% (Group-III). These were significant decreases over the course of the experiment: Group-I, $P < 0.001$; Group-II, $P < 0.001$; and Group-III, $P < 0.001$. The slopes of the regression equations and the y-intercepts did not differ significantly between each of the three groups ($P > 0.05$), indicating that grafts decreased in size at a similar rate and to a similar extent over the course of the trial. Graft contraction was generally gradual and continued throughout the duration of the trial. Two skin grafts (one in Group-I and one in Group-III) were considered to have suffered minor cage-related trauma and were not included in the summary statistics but the diameter values for these grafts are shown in Figure 3.2-3.

The short (shaved) hairs present at grafting did not appear to grow, but were shed with the eschar or as new hair growth developed. Hair grew along the margin of grafts in

each group starting between five and six weeks post-transplantation. In Group-I, only very fine secondary hairs grew and were present over the entire graft by week 10 but were not densely packed. Group-II and Group-III grafts grew primary and secondary hairs that were densely packed at the margin (most prominent in Group-III), but were scant or absent in central areas. In these two groups, hair growth was more variable and the limited hair growth in central areas appeared to be associated with the degree of crusting and scarring. Figure 3.2-3 shows surface architecture and degree of hair growth for three skin grafts from each group at 9 weeks post transplantation.

Histology results were comparable to the gross findings. Split-thickness grafts in Group-I (Figure 3.2-4) contained regularly spaced individual to small clusters of secondary hair follicles, with associated sebaceous and apocrine gland remnants, in central and peripheral areas. Some secondary hairs were actively growing and in the anagen phase, but others were distorted or atrophied. In contrast, full-thickness grafts in Group-III (Figure 3.2-5) retained clusters of primary and secondary hairs in follicle units that appeared normal at the margins of grafts, while extensive dermal fibrosis and scarring replaced adnexa centrally. More than 95% of hair follicles were in the anagen phase. The intermediate-thickness grafts in Group-II (Figure 3.2-6) most resembled those in Group-III, but with fewer primary follicles and occasional follicle remnants retained centrally. Follicular keratosis was mild to moderate in Group-I and Group-II.

Additional histological findings included mild, diffuse epidermal hyperplasia with normal basket-weave orthokeratotic keratinization in grafts from all groups. Mast cells were present individually throughout the superficial and deep dermis. A few grafts in each group contained occasional small aggregates of predominately histiocytes, with

occasional giant cells, that were associated with fragments of keratin or canine hair shafts. This feature was more evident in the thin split-thickness grafts where dermatome-transected hair follicles likely released fragments of canine hair shafts. Free mouse hair shafts were rarely observed in the dermis. Melanomacrophages were scattered individually in the dermis or in small clusters near the epidermis in all groups. The mouse panniculus carnosus was absent beneath all grafts.

At necropsy, one sick mouse and one mouse that died had splenic lymphoma. One mouse that died of anesthetic complications at the time of bandage removal had no other findings at necropsy.

3.2.3 DISCUSSION

This study shows that tgε26 mice support split-thickness and full-thickness canine skin grafts for 10 weeks. Adult canine thin split-thickness grafts retain surface architecture and heal within 14 days (Figure 3.2-3, A) as do human skin grafts of similar thickness and anatomical origin on nude mice (Black & Jederberg, 1985; Briggaman, 1985).

There are only two reports of grafting canine skin to immunodeficient mice. While evaluating cold storage techniques for skin grafts from different species, Rosenquist *et al.* (1988) grafted nude mice with 10 mm diameter split-thickness canine skin. Canine grafts were reported to survive after immediate grafting (6/6) and after 10 days of cold storage (5/5). However, the criterion for graft survival was not stringent (only 50% of the graft area had to remain recognizable) and no specific morphologic data were provided. Caswell and coworkers (1996) demonstrated that full-thickness canine skin xenografts (10 mm) could grow hair. As discussed previously, graft quality was

variable. Graft size and hair growth varied by as much as 50% and some grafts retained only a few hairs (Caswell, personal communication). Gross or histological descriptions of healed grafts were not reported. In the current study, larger skin grafts of consistent appearance were successfully grafted to tgε26 mice (Figure 3.2-3). Twelve millimeter diameter grafts contracted between 21.3 and 26.3% over nine weeks, resulting in grafts that were 8.8 to 9.5 mm in diameter, as size better suited for studying demodicosis. Additionally, in this study, shaving the mouse skin prior to surgery decreased the number of mouse hairs contaminating the mouse graft bed. Hair fragments induced histiocyte infiltration, which is undesirable in studies using xenografts to model inflammation.

Unlike these previous studies, canine thin split-thickness skin grafts healed well. Thus, the difficulties associated with full-thickness grafting likely resulted from characteristics of the thicker grafts and not from an inherent inability of canine skin to heal on immunodeficient mice. The gross and histological changes observed in the thicker skin grafts of Group-II and Group-III were consistent with the consequences of ischemic damage. Grafts developed superficial central ischemic necrosis that led to the formation of a central crust, or eschar, and the subsequent replacement of adnexa with a central scar. The melanin pigment dispersal and melanomacrophage formation in the graft dermis were also consistent with ischemic damage (Yager & Wilcock, 1994). None of the grafts showed evidence of ischemic damage at their margins and all grafts grew hair in this region. Therefore, healing along the graft margin appears to be unique compared to central areas. The tissue glue did not interfere with graft blood supply in this area.

Reports in the literature point to two aspects of skin xenografting that could interfere with central graft blood supply. First, excess fatty tissue on the ventral surface is thought to interfere with healing of skin grafts to mice (Billingham & Medawar, 1951). Fat is a poorly transplantable tissue that suffers ischemic damage easily (Coleman, 1997). In medium-split-thickness grafts (Group-II) a fat layer was absent along the ventral margin, unlike the full-thickness grafts (Group-III). However, healing was not significantly different between Group-II and Group-III. Although fat may interfere with healing, additional factors hampered the healing of canine full-thickness grafts.

Secondly, the panniculus carnosus muscle is thought to contribute blood supply to the ventral surface of skin grafts on mice (Billingham & Medawar, 1951; Breyere, 1972). The lateral thoracic artery travels with this muscle in the pannicular fascia to supply blood to the skin over the lateral and dorsal thorax (Billingham & Medawar, 1951). Histology revealed that the methods used did not retain the panniculus carnosus in the graft bed, which can be difficult because a natural tissue plane does not exist between this muscle layer and the overlying panniculus adiposus in the mouse (Billingham & Medawar, 1951). Because thin split-thickness grafts healed relatively well compared to full-thickness grafts in spite of this layer being absent, additional factors contributed to ischemic damage and are related to graft thickness.

Ischemic damage occurred mostly after bandage removal, which suggested that an acquired problem contributed graft ischemia, this most likely being mouse-induced graft trauma. Paradoxically, mice were not observed to intentionally traumatize skin grafts. Grafts that developed central necrosis were not ulcerated, which would be expected if mice were chewing or extensively scratching their grafts when not being observed. Mice

did, however, clean material from the graft surface and were seen to pull on grafts to remove adhesive material. Mice cleaned grafts variably; this finding could explain why grafts varied in terms of the extent of ischemic damage. The act of grooming grafts likely traumatized underlying vessels, perhaps by stretching fragile anastamoses and inducing ischemic damage. Full-thickness grafts were more susceptible to this form of trauma (or to the development of ischemic damage) than were thin split thickness grafts.

Architectural differences between full-thickness and thin split-thickness grafts could explain their different susceptibilities to developing ischemia. Human microvasculature of the superficial dermis is qualitatively and quantitatively different than that of the deep dermis and panniculus; a similar situation likely exists in dogs (Braverman, 1989; Pavletic, 1991). For instance, the panniculus adiposus and/or deep dermis (ventral surface of full-thickness skin grafts) has fewer, larger diameter, blood vessels than the superficial dermis (ventral surface of thin split-thickness grafts). The deep blood vessels may not favor stable anastomosis with the smaller mouse vessels; these anastomoses are essential in the first 24 to 72 hours after grafting (Lambert, 1971; Sumi *et al.*, 1984; Heslop & Shaw, 1986; Okada, 1986; Plenat *et al.*, 1992; Young *et al.*, 1996). Once anastomosis has occurred, intravascular hydrostatic pressure may drop in full-thickness grafts, which require a relatively larger blood volume per gram of tissue than do split-thickness grafts (Heslop & Shaw, 1986). As a consequence of potentially fewer anastomoses and low hydrostatic pressure, full-thickness grafts may be poorly perfused during the early stages of healing compared to the thinner grafts. If this poorly perfused tissue is subjected to the trauma of mouse grooming, then disruption of the fragile anastomoses may induce visible evidence of ischemic damage.

Stabilization of the tissue plane between the graft and the graft bed is essential to protect the newly forming vascular anastomoses (Breyere, 1972; Ratner, 1998). The ability of the panniculus at the base of full-thickness grafts to contribute to stable granulation is hampered by the presence of relatively fewer fibroblasts, blood vessels, and collagen bundles, and by the presence of adipose tissue. For this reason, full-thickness grafts are likely to be more susceptible to minor trauma during healing than split-thickness grafts.

Why then did the margins of full-thickness grafts heal without ischemic damage and readily grow hair? The rim of a full thickness graft shares many characteristics of a thin split-thickness graft. Here, the superficial dermis is exposed where numerous small vessels are available for anastomosis and stabilization of these fragile structures is maximized. Early vascularization at the graft margin is consistent with the finding that this area turns pink and regrows hair before the central area does.

To improve grafting success, procedures should address factors affecting revascularization of the graft. The panniculus carnosus should be retained in the graft bed and fatty tissue should be excluded from the base of grafts. The application of excessive tissue glue to the graft surface, or other materials that induce grooming related trauma, should be avoided. The hair growth on canine grafts appears to be most affected by ischemic damage. Factors that decrease ischemic damage during early graft healing will likely have the greatest positive impact on graft hair growth.

Although specific data were not provided, Billingham and Medawar (1951) (working with immune competent mice) described an approach to improve the healing of full-thickness grafts on mice by creating a graft bed of granulation tissue. Presumably,

this method would provide conditions that favor increased stabilization of the graft and the formation of vascular anastomoses. This procedure, however, is less practical when working with fragile immunodeficient mice. In the current study, graft factors were identified as important for successful transplantation of full-thickness skin. Thus, creating vascular rich granulation tissue on the donor skin prior to grafting may be more productive.

This is the first report of skin xenografting to tgε26 mice and the results demonstrate that these mice will support canine skin grafts for extended time periods. Tgε26 mice are an good candidate for experiments modeling canine demodicosis and provide an alternative to the use of scid mice. This is the first description of the gross and histological changes that occur in canine skin xenografts, as well as the first comparison of split-thickness and full-thickness canine skin xenografts. In addition to delineating technical considerations, the results reinforce the concept that manipulation of skin graft revascularization events is the most significant factor affecting both the morphologic quality of healed full-thickness canine skin grafts and the development of uniform hair growth.

Figure 3.2-1: Line graph showing the surface eschar score (mean ± standard error) for canine thin split-thickness skin grafts on tgε26 mice at 3, 6, and 9 weeks post transplantation; Group-I, n=5, (□); medium split-thickness skin grafts, Group-II, n=5, (*); and full-thickness skin grafts, Group-III, n=7, (•). (Score: 0 = no eschar, 1 = less than 1/3 of the surface, 2 = between 1/3 and 2/3 of the surface, and 3 = greater than 2/3 of the surface).

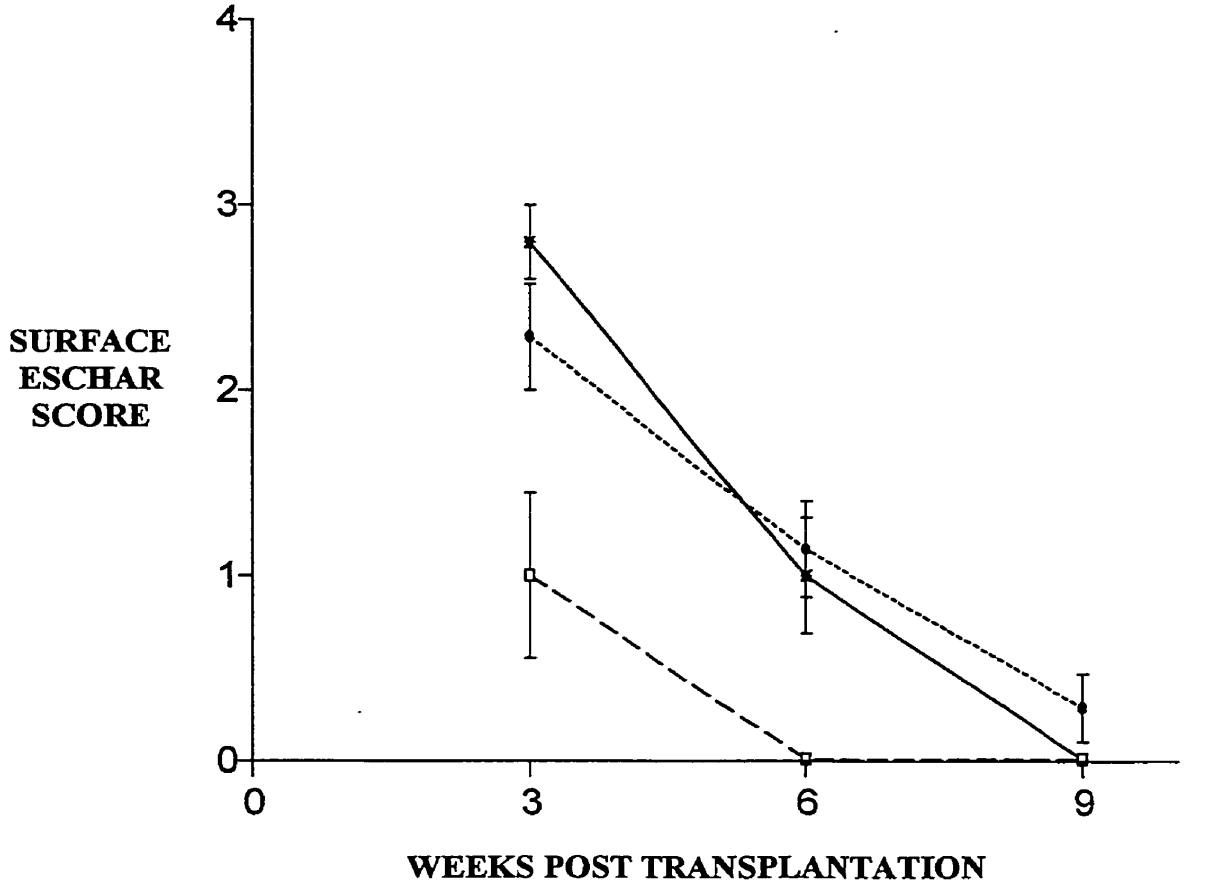
SURFACE
ESCHAR
SCORE
4
3
2
1
0
0
3
6
9
WEEKS POST TRANSPLANTATION

Figure 3.2-2: Line graph showing the diameter (mm) of canine skin grafts on tgε26 mice at 1, 3, 6 and 9 weeks post transplantation; **(A)** Split-thickness skin grafts, Group-I (n=6); **(B)** medium split-thickness skin grafts, Group-II (n=5); and **(C)** full-thickness skin grafts, Group-III (n=7). The linear regression equation is plotted for each group (bold line). The two low responders shown (one in Group-I and one in Group-III) were excluded from the calculation of the regression equation (see text).

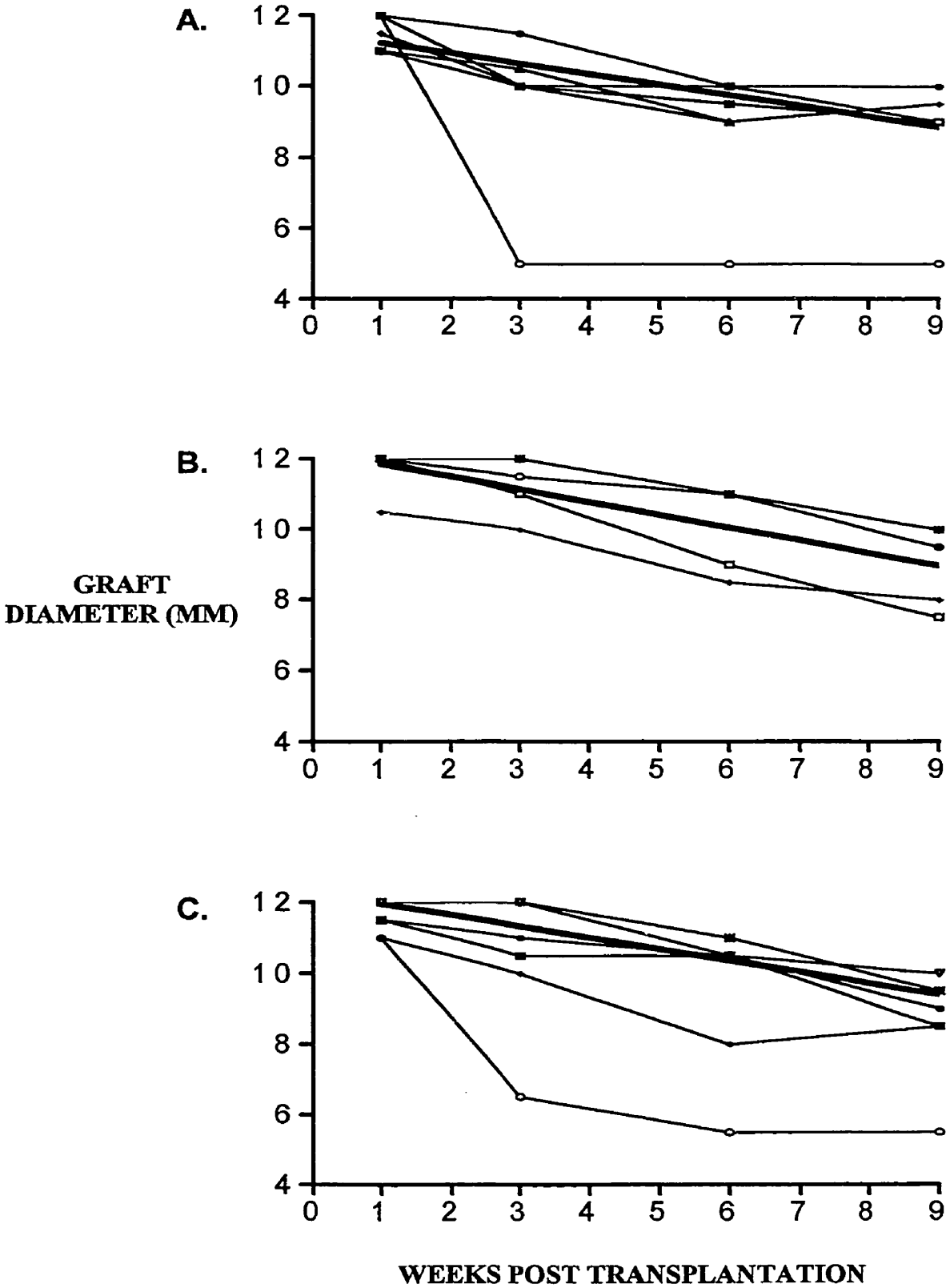
A.
B.
C.
12
10
8
6
4
0
1
2
3
4
5
6
7
8
9
GRAFT DIAMETER (MM)
WEEKS POST TRANSPLANTATION

Figure 3.2-3: Appearance of representative canine skin grafts on tgε26 mice at 9 weeks post transplantation; thin split-thickness grafts, Group-I (**A,B,C**); thick split-thickness skin grafts, Group-II (**D,E,F**); and full-thickness skin grafts, Group-III (**G,H,I**). In Group-I, follicular pores are readily evident and the surface architecture is relatively normal, whereas central radial scarring is evident in grafts from Group-III and follicular pores are not evident.

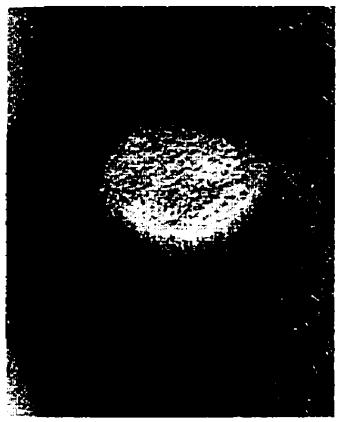

A

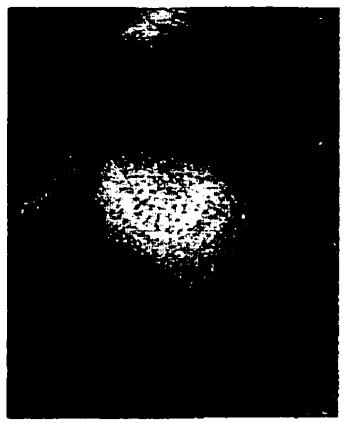

B

C

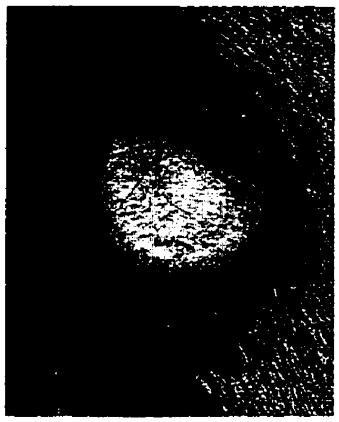

D

E

F

G

H

I

Figure 3.2-4: Photomicrographs of a thin split-thickness canine skin graft (Group-I) from a tgε26 mouse at 10 weeks post transplantation. **(A)** Secondary hair follicles, sebaceous and apocrine glands survive in the graft. The junction between mouse skin, on the left, and canine skin, on the right, is marked with an arrow (magnification = X10). **(B)** Higher magnification shows a canine hair follicle unit (magnification = X25). Hematoxylin and eosin stained, paraffin embedded, tissue section

A

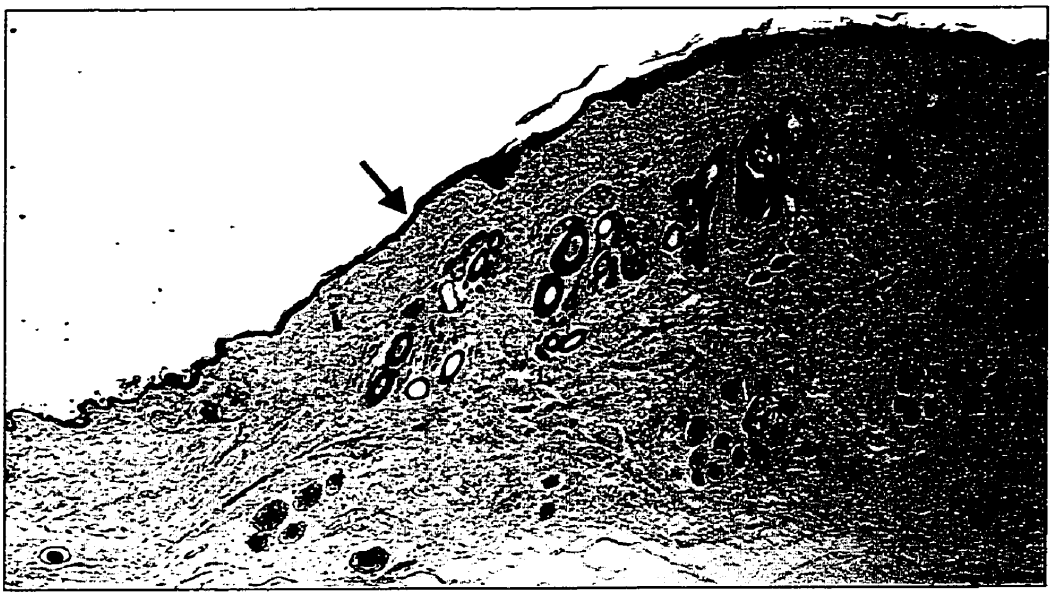

B

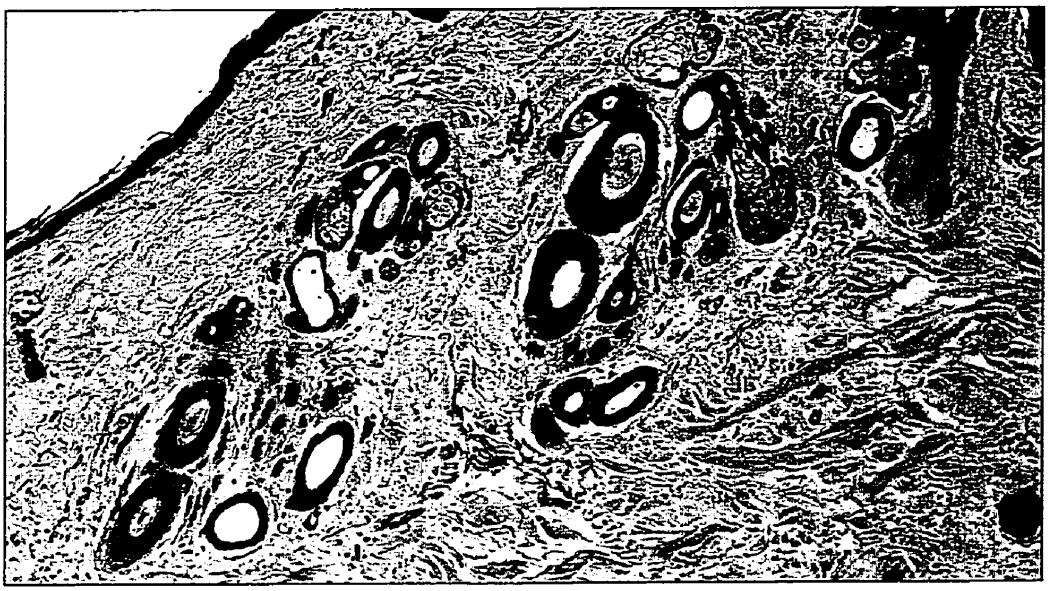

Figure 3.2-5: Photomicrographs of a full-thickness canine skin graft (Group-III) from a tgε26 mouse at 10 weeks post transplantation. **(A)** Many primary hairs and some secondary hairs, as well as sebaceous and apocrine glands, survive in the graft. The junction between mouse skin, on the left, and canine skin, on the right, is marked with an arrow (magnification = X10). **(B)** Higher magnification shows a canine hair follicle unit (magnification = X25). Hematoxylin and eosin stained, paraffin embedded, tissue section

A

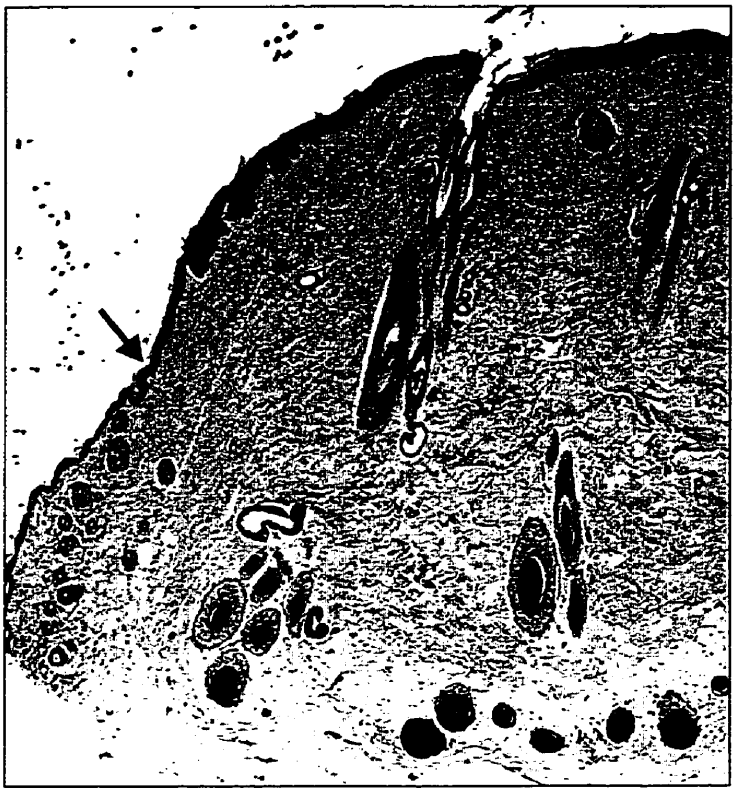

B

Figure 3.2-6: Photomicrographs of a thick split-thickness canine skin graft (Group-II) from a tgε26 mouse at 10 weeks post transplantation. **(A)** Secondary hairs and a few primary hairs, as well as sebaceous and apocrine glands, survive in the canine skin graft. The junction between mouse skin, on the left, and canine skin, on the right, is marked with an arrow (magnification = X10). **(B)** Higher magnification shows a canine hair follicle unit (magnification = X25). Hematoxylin and eosin stained, paraffin embedded, tissue section

A

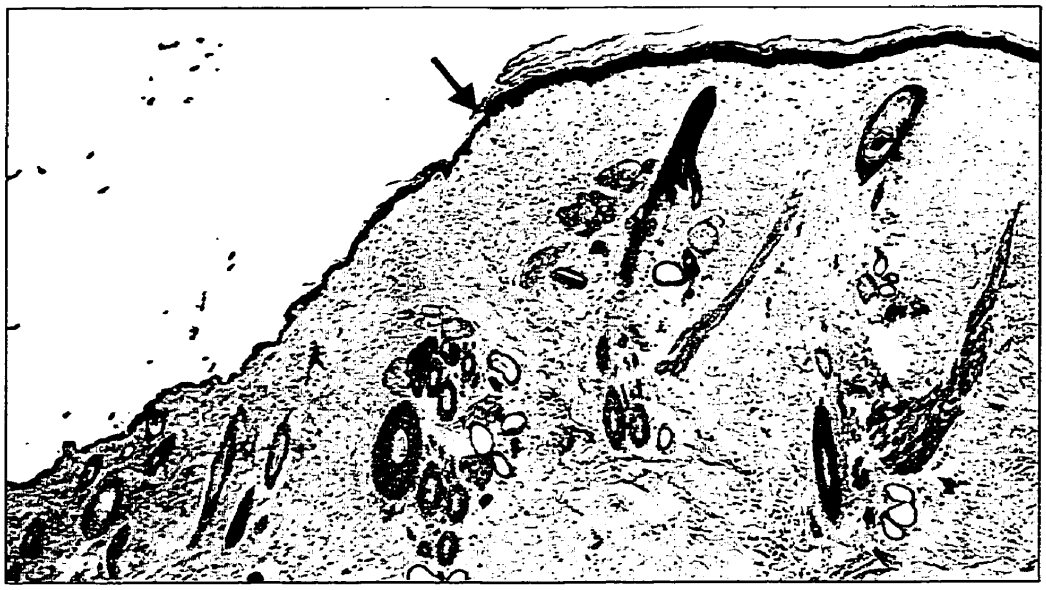

B

3.3 CANINE LEUKOCYTE RECONSTITUTION OF Tgε26 MICE

The skin xenograft mouse model is useful for investigating the pathogenesis of inflammatory skin diseases because recipient mice are able to support leukocyte xenografts in addition to skin xenografts (Alegre *et al.*, 1994; Petzelbauer *et al.*, 1996). The majority of leukocyte reconstitution experiments have utilized scid mice, or scid mice supporting an additional mutation known to augment immunodeficiency, such as the beige mutation (*Lyst*^{bg}) (Mosier *et al.*, 1993). Successful leukocyte engraftment of scid lines has been reported using human, bovine, porcine, equine, and feline lymphocytes (Abedi *et al.*, 1992; Balson *et al.*, 1993; Johnson *et al.*, 1994; Revilla *et al.*, 1994; Greenwood *et al.*, 1997). Although engraftment is variable, transplanted leukocytes remain functional and mediate lymphocyte driven inflammatory reactions in skin xenografts, such as allogeneic skin graft rejection (Alegre *et al.*, 1994; Greenwood *et al.*, 1997) and delayed-type hypersensitivity response to tetanus toxoid (Petzelbauer *et al.*, 1996).

As previously discussed, scid/bg mice were shown to support canine lymphocytes after intraperitoneal transfer PBMC by detecting canine immunoglobulin in serum from mice (5/6) that had received canine leukocyte grafts (Caswell, 1995)(personal observation). However, these mice developed fatal GVHD, including hemolytic anemia, and developed the "leaky" phenotype. Tgε26 mice, (Wang *et al.*, 1994), are T- and NK-cell deficient and were shown in the current study to support canine skin xenografts for 10 weeks (Section 3.2). Experiments were designed to evaluate the ability of tgε26 mice to support canine leukocytes, necessary for modeling inflammation in demodicosis.

Measurement of circulating immunoglobulin was performed to assess leukocyte engraftment, an established method of assessing lymphocyte chimerism in scid mice (Taylor, 1994; Greenwood *et al.*, 1997). These experiments had three objectives: (1) to evaluate the reconstitution of tgε26 mice with canine lymphocytes using PBMC from different dogs, (2) to evaluate the survival and health of tgε26 mice after canine PBMC transfer, and (3) to determine the half-life of canine immunoglobulin in tgε26 mice after intraperitoneal injection. Information about the kinetics of canine immunoglobulin clearance in tgε26 mice was required in order to interpret canine circulating immunoglobulin concentrations.

3.3.1 MATERIALS AND METHODS

3.3.1.1 Animals

Male tgε26 mice, age 9 to 12 weeks were housed with two to five per micro-isolator cage. Random-source, adult, intact-male dogs were purchased from Animal Care Services (University of Guelph, Guelph, Ontario, Canada).

3.3.1.2 Intraperitoneal Reconstitution of Tgε26 Mice with Canine Peripheral Blood Mononuclear Cells

Three groups of five tgε26 mice (Group-I, -II and -III) and one group of four tgε26 mice (Group-IV) were bled prior to leukocyte engraftment to provide control plasma samples and a baseline PCV. Canine blood was collected and PBMC were isolated according Section 2.6. PBMC from one dog were divided equally to reconstitute all mice in a group. Mice were anesthetized with methoxyflurane (Metafane®, Pitman Moore, Mississauga, Ontario, Canada) and between 12 to 25 $\times$ 10^6 peripheral blood lymphocytes

(PBL) (Group-I = 22 x 10^6, Group-II = 12 x 10^6, Group-III = 25 x 10^6, and Group-IV = 14 x 10^6), resuspended in 0.75 to 0.85 ml of PBS, were slowly injected (over one minute) intraperitoneally using a 25 gauge needle. The leukocyte inocula contained between 70 and 90% lymphocytes and cell viability was always greater than 95%. Mice were bled for monitoring immunoglobulin concentration at biweekly intervals for 8 (Group-I) or 12 weeks (Group-II, -III, and -IV) and plasma samples were stored at –40°C. The PCV for each mouse was measured at the time of each blood collection. All samples from a particular group were evaluated with the same ELISA assay.

Mice were monitored daily for evidence of illness until completion of the experiment. All mice were necropsied and tissues were processed for histology.

3.3.1.3 Half-life Determination for Canine Immunoglobulin in Tgε26 Mice

Six tgε26 mice were bled prior to canine immunoglobulin transfer and PCVs were recorded. Lyophilized, affinity purified, canine IgG (Bayer Diagnostics Inc., Etobicoke, Ontario, Canada) was dissolved in PBS, centrifuged at 12,800 × g (10 min) to remove immunoglobulin aggregates (Sigounas *et al.*, 1994) and the supernatant was filter sterilized using a 0.22 μm millipore filter (Millex®-GV brand, Bedford, Maryland, USA). Mice were inoculated by slow intraperitoneal injection with 5 mg of canine IgG in 0.5 mL of PBS. After IgG transfer, mice were bled at 8 hr, 24 hr, and then at 1 week intervals for 5 weeks. The PCV was recorded at each blood collection and plasma samples were stored at –40°C. Canine immunoglobulin was quantified in mouse plasma samples by ELISA and all samples were evaluated within the same assay.

Mice were monitored daily for evidence of clinical illness.

3.3.1.4 Statistical Methods

Regression analyses and calculation of IgG half-life were performed using GraphPad Prism (GraphPad Software, San Diego, California, USA).

3.3.2 RESULTS

3.3.2.1 Canine Peripheral Blood Mononuclear Cell Transfer

A total of 15 out of 19 mice survived the duration of the experiment in good health; four mice died within nine weeks of canine leukocyte engraftment. Two mice in Group-II died prior to the initial blood collection: one of these mice had gross and histological lesions of splenic lymphoma; diagnostic samples were not available for the second mouse. The two mice in Group-III that died lacked histological changes and a cause of death was not determined. Mice completing the study did not have gross or histological abnormalities or evidence of hemolytic anemia. The PCV for mice in each group were similar to pre-PBMC transfer values (Figure 3.3-2). A low PCV was observed on one occasion for one mouse in Group-IV (Figure 3.3-2D).

Plasma samples were available from 17/19 mice that received canine PBMC. Plasma from 16/17 mice (94.1%) had detectable levels of canine IgG between two to 12 weeks post canine PBMC transfer (Appendix 2). Canine IgG was detected for an average of 6.62 weeks post inoculation. All mice in Group-I had detectable levels of canine IgG up until the final collection of samples at eight weeks; in the remaining three groups, the median week for detection was four weeks. Canine IgG was detected in at least two mice in each group and ranged from a low 0.31 μg/mL to more than 6,000 μg/mL. The mean

value (± SD) of canine IgG for all positive samples at two weeks was 409.93 µg/mL (± 1340.08). Canine IgG concentration steadily declined in 13 mice after a peaking at either two or four weeks. In another mouse, canine IgG was detected only in the two-week sample. In two mice (both in Group-I), canine IgG was measured in milligram quantities and increased gradually. The individual mouse plasma canine IgG values for each of the four groups are plotted in Figure 3.3-1.

3.3.2.2 Half-life Determination

The clearance data for canine IgG following intraperitoneal inoculation of six tgε26 mice are summarized in Figure 3.3-3. Canine IgG concentration decreased rapidly during the first week and more gradually during the final four weeks. An IgG half-life of 2.9 days was calculated based on the regression equation. Canine IgG was not detected in plasma samples collected prior to experimentation.

All six tgε26 mice survived the duration of the experiment and remained healthy. The PCV did not appear to change over the course of the trial and anemia was not observed (Figure 3.3-4).

3.3.3 DISCUSSION

The results demonstrate that tgε26 mice supported canine PBL and that these cells survived and were able to produce IgG for 56 days. The concentration of canine IgG in tgε26 mouse plasma (0.0003 to > 6.0 mg/mL) was similar in range and variability to that observed in scid mice reconstituted with PBL from human (0.2 to 3.0 mg/mL) (Taylor, 1994), equine (0.002 to 1.0 mg/mL) (Balson *et al.*, 1993), or bovine (0.001 to > 10.0

mg/mL) (Greenwood & Croy, 1993) donors. The mean peak concentration of canine IgG (0.41 mg/mL) was similar to that for equine IgG (0.38 mg/mL) but less than that for bovine chimeras (2.06 mg/mL, without prior radiation treatment). In human PBL-scid chimeras, IgG increased for the first 28 to 56 days before gradually declining (Mosier *et al.*, 1988; Duchosal *et al.*, 1992). Similarly, bovine IgG increased for the first 14 to 35 days before declining (Greenwood & Croy, 1993). In the present study, canine IgG concentration steadily increased in the plasma of two mice during the 56-day study period, while for the remaining 14 mice, IgG concentrations steadily declined after peaking at 14 or 28 days.

The percentage of tgε26 mice supporting canine lymphocyte engraftment was high, but the extent and duration of engraftment was variable and limited as measured by canine IgG production. Detectable levels of immunoglobulin were not present in isolates of washed PBMC (Balson *et al.*, 1993), and immunoglobulin producing plasma cells are exceedingly rare in peripheral blood of veterinary species (Jain, 1993). Therefore, the presence of canine IgG in mouse plasma in 94.1% of tgε26 mice at 2 weeks post PBMC transfer indicates that canine lymphocytes survived isolation and transfer, and subsequently produced IgG in a high percentage of mice. However, canine IgG concentration was relatively low and measurable over a limited duration after engraftment (six weeks or less) in eight mice (Figure 3.3-1, Figure 3.3-2). The majority of these mice were from Group-II and Group-III, suggesting that donor factors affected engraftment, as measured by immunoglobulin levels. Canine IgG concentration in mouse plasma was higher and detected for a longer duration (more than six weeks) in eight mice

from Group-I and Group-IV; two of these mice had approximately 10-fold or higher levels of canine IgG (Figure 3.3-2).

The clearance data for canine IgG in tgε26 mice indicated a half-life of approximately 2.9 days, which provides comparative information for assessing canine IgG plasma concentration in canine PBMC reconstituted mice. The half-life data confirms that canine lymphocytes survived transfer to tgε26 mice and actively produce IgG for weeks after transfer, despite the fact that total plasma canine IgG levels declined shortly after transfer in the majority of mice.

The calculated half-life of human IgG in scid mice ranges between 5.3 and 12 days compared to 21.2 days in humans (Taylor, 1994). Balson *et al.* (1993) reported the half-life of equine IgG in scid mice as 12.1 days, compared with 19 to 25 days in the horse. Similarly, at 2.9 days, the half-life of canine IgG is shorter in tgε26 mice compared to 8 days in the dog (Waldmann & Strober, 1969). The early rapid decline in canine IgG concentration indicates that more than one mechanism may contribute to early clearance. Immune-complex formation or aggregation of immunoglobulin molecules can result in rapid clearance and may have resulted in the early rapid phase of clearance measured in this experiment (Waldmann & Strober, 1969). Precautions were taken to reduce aggregates in the canine IgG inocula. Similarly, immunoglobulin receptor cross-reactivity after injection may have led to selective clearance of an antibody subset and resulted in the early rapid elimination phase.

The decreased half-life of xenogenic antibodies in mice has been attributed to the increased metabolic rate of this small species (Balson *et al.*, 1993). The half-life of murine IgG in the mouse is 2 to 5 days (Waldmann & Strober, 1969). A consequence of

an accelerated half-life for transferred xenogenic antibodies is that the rate of immunoglobulin production by transferred lymphocytes is considered higher than what is reflected by mouse plasma levels. The measurement of immunoglobulin levels in mouse plasma, as an indicator of chimerism, likely underestimates the success of xenogenic lymphocyte engraftment. Furthermore, the xenogenic immunoglobulin plasma levels are not directly comparable to donor plasma levels.

Canine IgG plasma concentration varied between and within groups of tgε26 mice, suggesting that both donor and recipient factors affected reconstitution of mice with canine lymphocytes. Similar results were reported by Abedi and coworkers studying human scid chimeras (Abedi *et al.*, 1992). The number of lymphocytes transferred affects the level of engraftment of human lymphocytes in scid mice. Only a minority of scid mice that received 5×10^6 lymphocytes or less were successfully reconstituted; however, when 20×10^6 lymphocytes were transferred, nearly 100% engraftment was achieved (Mosier *et al.*, 1988; Torbett *et al.*, 1991). In the current study, 12 to 25×10^6 canine lymphocytes were transferred to tgε26 mice. This number was similar to the human experiments with high reconstitution rates and the number of lymphocytes transferred did not appear to correlate with the level of immunoglobulin production. Second, pretreatment of scid mice with antisera to eliminate murine NK-cells, or the use of scid/bg mice that have reduced NK-cell function, is associated with improved engraftment of human PBL (Taylor, 1994). The tgε26 mice used in these experiments are NK-cell deficient by virtue of the transgene. Third, irradiation of scid mice increased leukocyte graft success and IgG production using human or equine PBL, but did not offer significant benefit when used in conjunction with bovine, pig, or cat

PBL (Balson *et al.*, 1992; Balson *et al.*, 1993). Others have not observed a significant increase in human PBL engraftment using irradiated scid mice (Abedi *et al.*, 1992) and some investigators reported increased mortality in studies using irradiated scid mice (Balson *et al.*, 1993; Greenwood & Croy, 1993). Preconditioning by irradiation can contribute to the development of GVHD in human scid chimeras (Xun *et al.*, 1994; Tsuchida *et al.*, 1997). Finally, tgε26 mice retain B-cells and produce murine immunoglobulin (Wang *et al.*, 1995). Murine B-cells could potentially interact with grafted cells and affect canine lymphocyte survival as well as canine IgG production or clearance.

The development of GVHD has been reported in human PBL scid chimeras (Taylor, 1994). The development of GVHD in canine PBMC scid/bg chimeras limited the use of scid mice for experiments modeling canine demodicosis (Caswell, 1995). Mice that develop GVHD may be clinically ill or even moribund. Affected mice may become anemic, as was the case when canine PBMC were transferred to scid/bg mice (Taylor, 1994; Caswell, 1995). At necropsy, organ pathology has been identified in skin, liver and lymphoid organs such as the spleen in mice with xenogenic GVHD (Taylor, 1994; Caswell, 1995). In addition, investigators using mouse models of allogenic GVHD have identified lesions in the tongue, intestine and skin (Taylor, 1994). In the current study, evidence of GVHD in canine PBMC reconstituted mice was not detected by clinical evaluation, full necropsies, or measurement of serial PCV. In the study by Caswell (1995), and in preliminary experiments in this study, high canine immunoglobulin titers were associated with development of anemia in scid/bg mice. Two tgε26 mice in this study developed comparable high canine immunoglobulin titers

after PBMC transfer (Group-I) but did not develop anemia. Tgε26 mice appear to be less susceptible than scid mice to developing GVHD after transfer of canine PBMC. The presence of murine B-cells and immunoglobulin in tgε26 mice (absent or greatly reduced in scid/bg mice) might alter canine immunoglobulin binding or clearance and protect tgε26 mice from developing immunoglobulin mediated aspects of GVHD such as hemolytic anemia (Taylor, 1994). Alternatively, other mouse differences, such as the ability to fix complement with xenoreactive antibodies, or differences between dogs (although several dogs were used), could account for the lack of hemolytic anemia in the current study.

In summary, the results provide evidence that canine lymphocytes are able to survive transfer and produce IgG within tgε26 mice and that the highest engraftment of immunoglobulin producing cells occurs 2 to 4 weeks post inoculation. The half-life of canine IgG in tgε26 mice is shorter than the half-life for IgG in dogs. Tgε26 mice did not develop GVHD after canine PBMC transfer and therefore are suitable for experiments modeling canine demodicosis.

Figure 3.3-1: Line graph showing canine IgG concentration (μg/mL) over time in plasma from IgG positive tgε26 mice after intraperitoneal transfer of canine PBMC: Group-I **(A, B)** Group-II **(C)**; Group-III **(D)**; and Group-IV **(E)**. Note that two high responders in Group-I have been plotted separately **(B)**, and that the scale on the y-axis is not the same for each graph. One 4-week data point for one high responding mouse (18,103 μg/mL) in Group-I was plotted separately in **(B)** and was considered a measurement error.

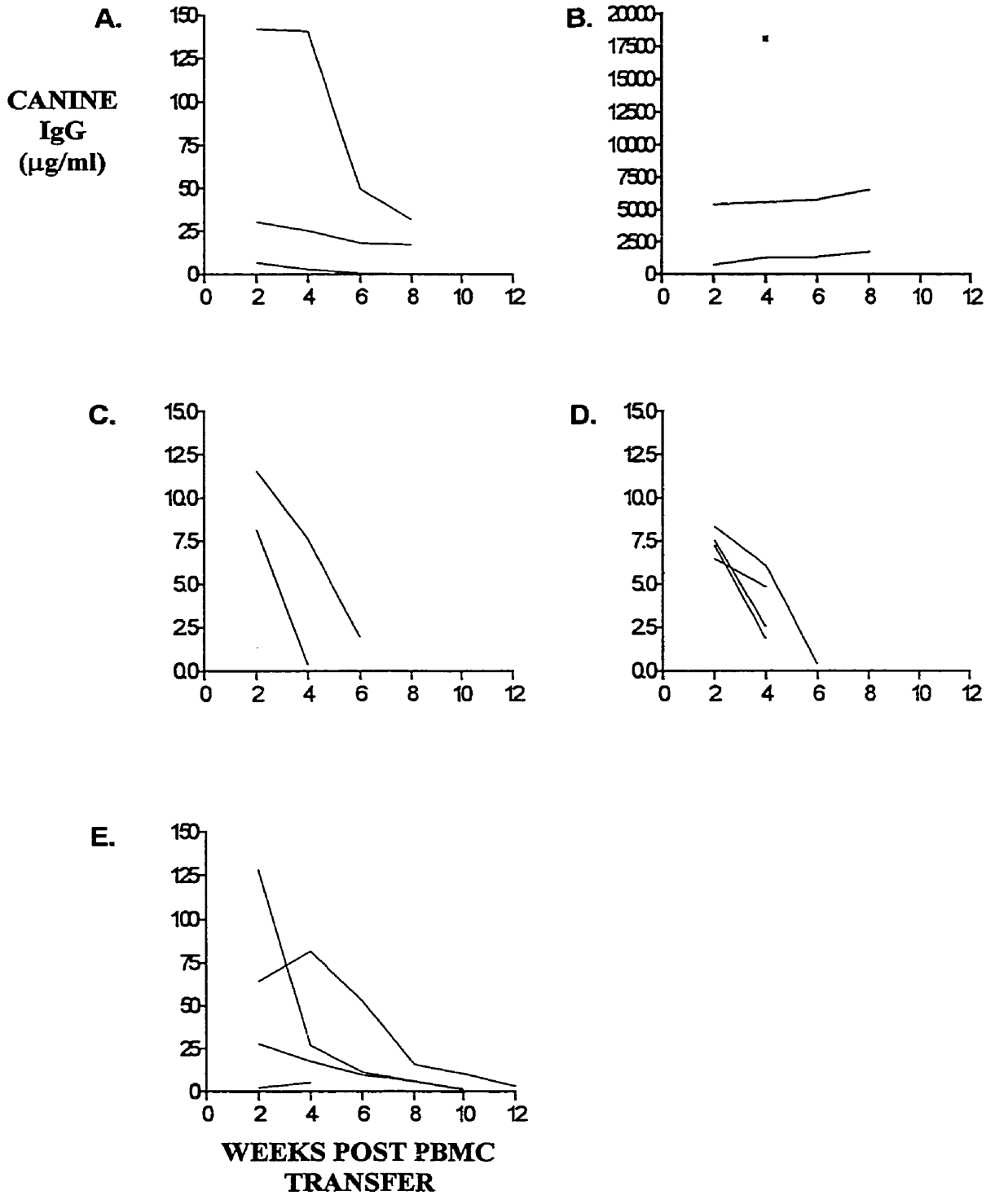
A.
B.
C.
D.
E.
CANINE
IgG
(µg/ml)
WEEKS POST PBMC
TRANSFER

Figure 3.3-2: Line graph showing the packed cell volume for tgε26 mice taken prior to and at weekly intervals after intraperitoneal transfer of canine PBMC; Group-I, n=5 (**A**); Group-II, n=3 (**B**); Group-III, n=5 (**C**); and Group-IV, n=4 (**D**).

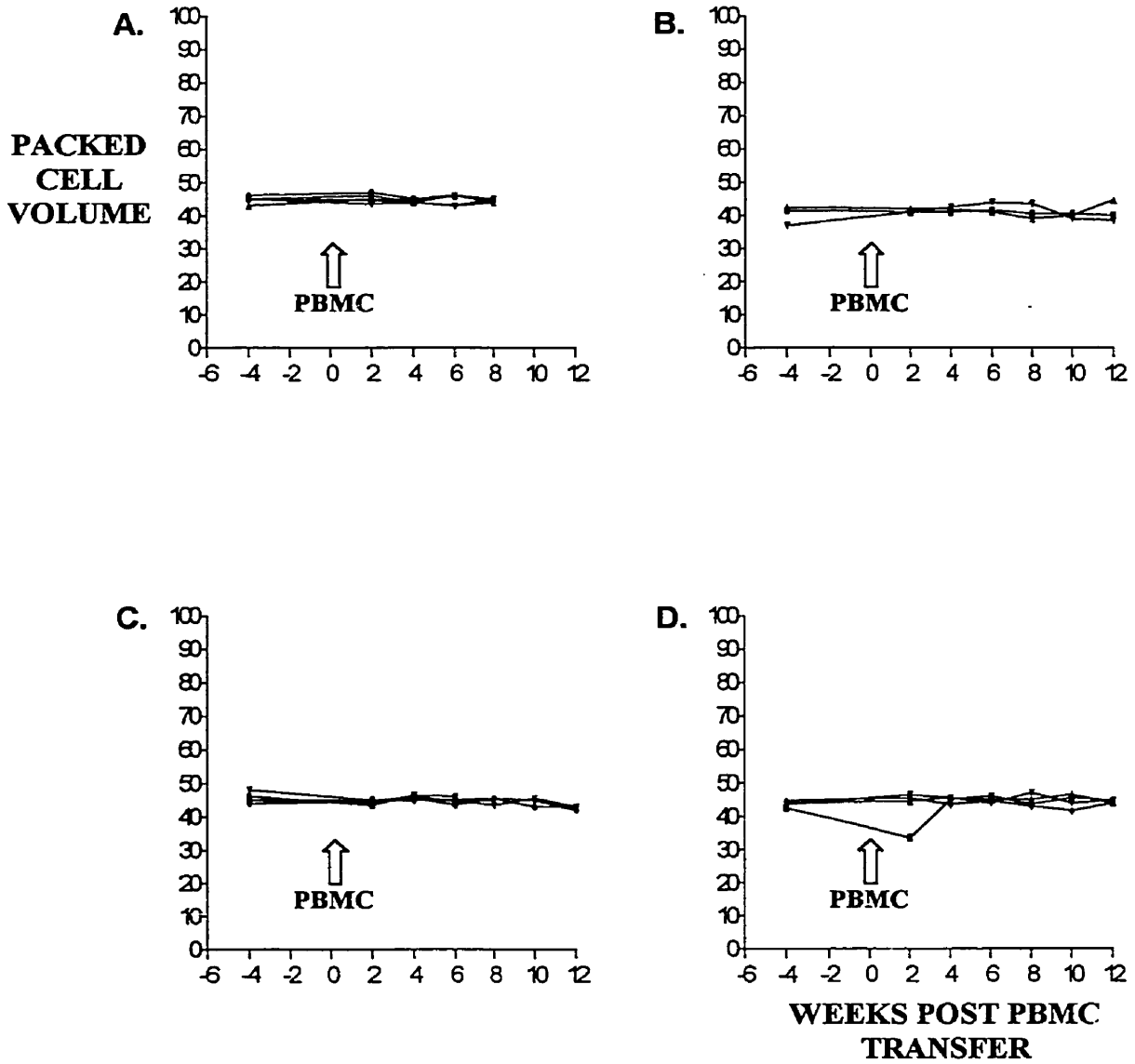
A.
B.
C.
D.
PACKED CELL VOLUME
PBMC
100
90
80
70
60
50
40
30
20
10
0
-6 -4 -2 0 2 4 6 8 10 12
WEEKS POST PBMC TRANSFER

Figure 3.3-3: Line graph showing canine IgG concentration (mg/mL; mean ± SD) over time in plasma from tgε26 mice (n=6) after intraperitoneal transfer of canine IgG. The regression equation is plotted along with the summary statistics.

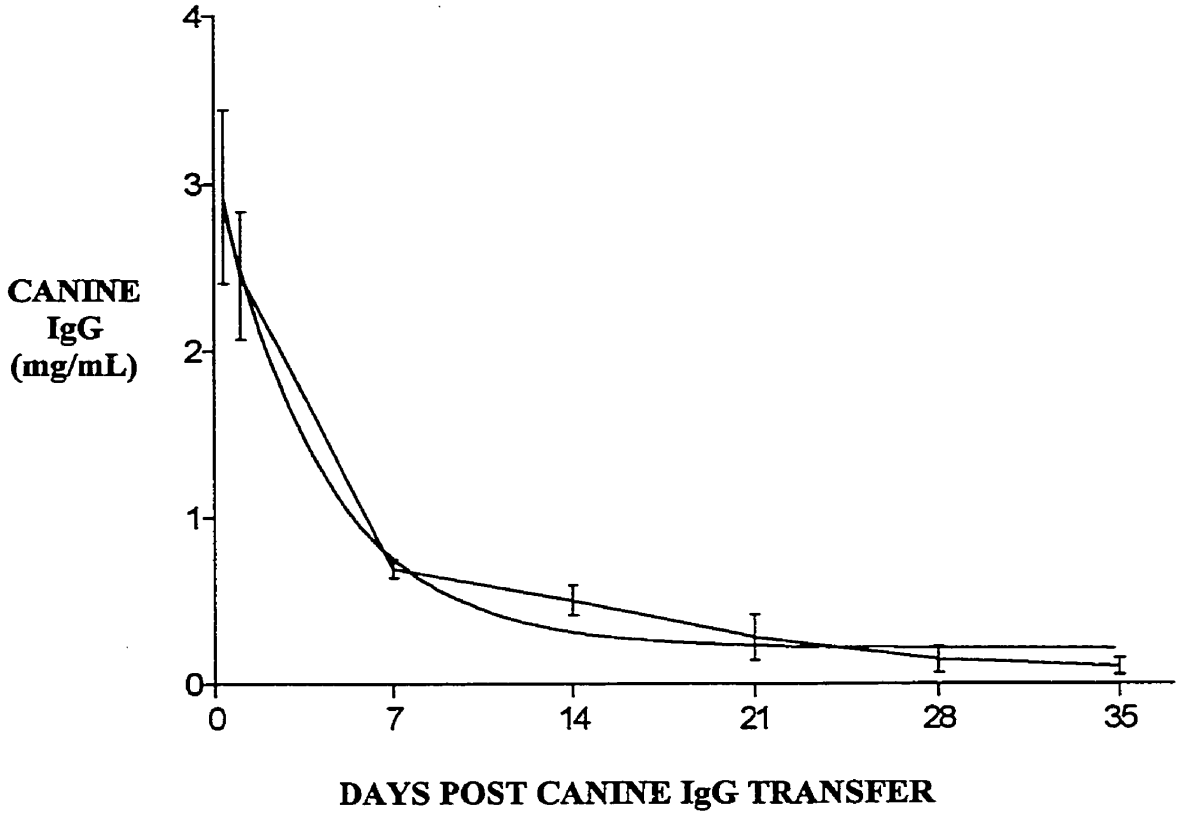
CANINE
IgG
(mg/mL)
4
3
2
1
0
0
7
14
21
28
35
DAYS POST CANINE IgG TRANSFER

Figure 3.3-4: Line graph showing the packed cell volume for tgε26 mice (n=6) taken prior to and at weekly intervals after intraperitoneal transfer of canine IgG.

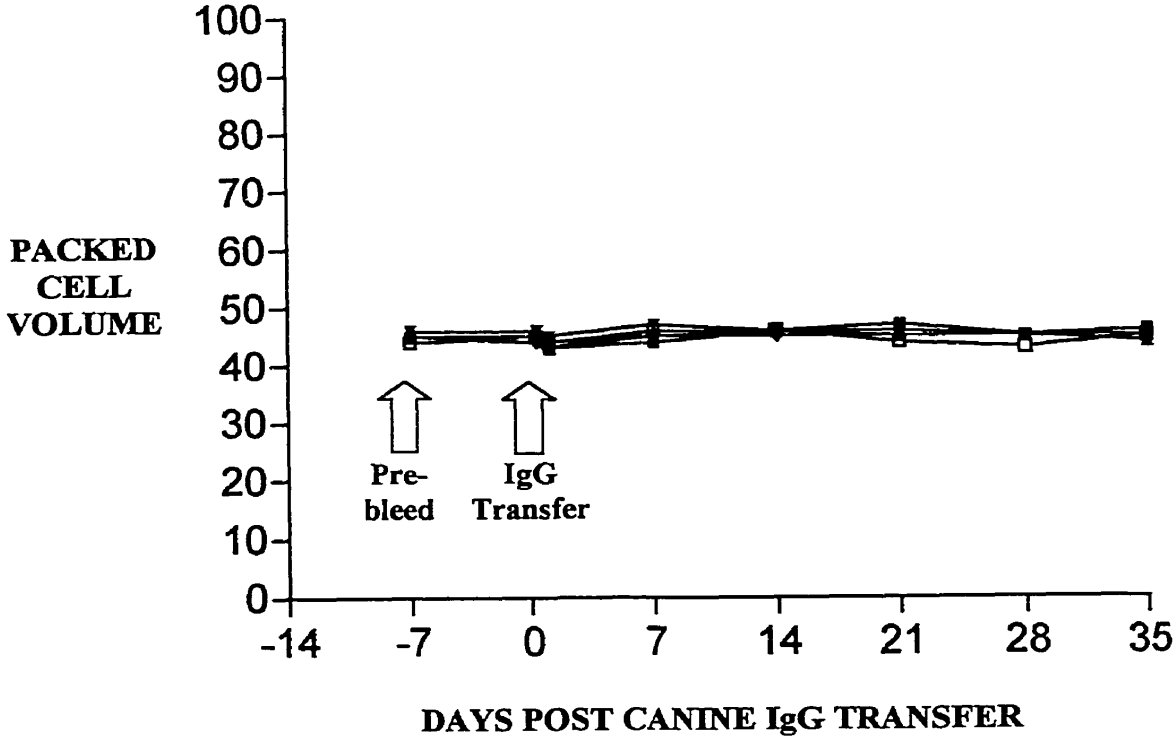
PACKED CELL VOLUME
100
90
80
70
60
50
40
30
20
10
0
-14
-7
0
7
14
21
28
35
Pre-bleed
IgG Transfer
DAYS POST CANINE IgG TRANSFER

3.4 DEMONSTRATION OF CANINE LEUKOCYTE FUNCTION IN THE SKIN XENOGRAFT ENVIRONMENT

The skin xenograft mouse model provides an investigative tool for studying mechanisms involved in specific inflammatory processes or skin diseases of animals and humans. Skin biopsies from the animal being studied can be isolated on immunodeficient mice after which specific skin donon factors, such as leukocyte subsets, can be reintroduced to skin grafts in a controlled manner. Using this approach, basic questions about the contribution of different factors to the pathogenesis skin diseases can be addressed.

Of particular interest in this study is the use of the xenograft model to assess the role of lymphocytes in canine demodicosis. In order to use the skin xenograft model for this purpose, it is important to determine if engrafted T-lymphocytes retain functional capabilities in the skin xenograft environment. Several studies have shown that human lymphocytes are capable of driving cell-mediated immune reactions in skin xenografts on scid mice. Petzelbauer *et al.* (1996) demonstrated that scid mice receiving human lymphocytes from tetanus toxoid sensitive patients were able to generate a delayed-type hypersensitivity response in skin xenografts after challenge with tetanus toxoid. Alegre *et al.* (1994) showed that human PBMC scid chimeras rejected allogenic human skin xenografts. In similar work by Greenwood *et al.* (1997), bovine leukocytes mediated allogeneic skin graft rejection on scid mice. There are no studies demonstrating the function of canine T-lymphocytes in this situation.

A skin allograft rejection experiment was chosen to determine if canine lymphocytes are capable of mediating a cell-mediated immune response and remain functional in the xenograft environment. The development of allograft rejection provides

a readily observable endpoint that indicates the presence of functional canine lymphocytes in the xenograft. A second objective of this experiment was to determine if direct injection of lymphocytes into skin grafts is a viable alternative to intraperitoneal delivery used in previous experiments. This method would insure that canine lymphocytes reach the xenograft.

3.4.1 MATERIALS AND METHODS

3.4.1.1 Animals

Male tgε26 mice, age 9 to 12 weeks, were housed with one mouse per micro-isolator cage. A random-source, adult, intact-male dog was selected as the skin donor. Skin was collected immediately after the dog was euthanized for reasons other than this study. The blood donor was a second random-source, adult, intact-male dog purchased from Animal Care Services (University of Guelph, Guelph, Ontario, Canada).

3.4.1.2 Experimental Protocol

Eight tgε26 mice were bled prior to experimentation and grafted with canine skin (Section 3.2). Allogenic canine PBMC were isolated and injected directly into skin grafts on four mice. During PBMC injections, mice were anesthetized with methoxyflurane and 15×10^6 lymphocytes, suspended in PBS, were deposited in three equally spaced parallel tracks in the graft using a 22-gauge needle. The inoculum contained 77% lymphocytes and 92% PBMC. Cell viability was 98%. Four control mice received similar injections of PBS only. Skin grafts were monitored daily for gross evidence of an allograft rejection reaction.

Four weeks post PBMC transfer, skin grafts were fixed in 10% neutral buffered formalin, trimmed perpendicular to injection tracts and processed for histology. Skin grafts were evaluated for the presence of T-cells by immunohistochemistry using anti-CD3 antibody (Section 2.5.2). The PCV was recorded and canine IgG was measured in mouse plasma samples by ELISA. All mice were necropsied and tissues were processed for histology.

3.4.1.3 Statistical Methods

Using SAS® software package (SAS Institute Inc., Cary, North Carolina, USA) the non-parametric Mann-Whitney test was used to compare plasma canine IgG concentrations from this experiment to those observed for tgε26 mice previously (Section 3.3).

3.4.2 RESULTS

Skin grafts lacked evidence of inflammation prior to the injection of cells. By two weeks, the four grafts that received allogenic PBMC developed patchy areas of erythema and crusting on the surface, were as control grafts remained unchanged. Histological evaluation of PBMC injected grafts revealed lymphocytic interface dermatitis (Figure 3.4-1A). Lymphocytes infiltrated the basilar epidermis and there was vacuolar degeneration, single cell necrosis, and a disruption of the architecture of the stratum basale (Figure 3.4-1B). These grafts developed epidermal ulceration and surface crusting. The dermis contained a diffuse cellular infiltrate of mononuclear cells, including large numbers of lymphocytes. Control grafts lacked these histological changes and did not contain an inflammatory cell infiltrate (Figure 3.4-1C).

Immunohistochemical staining of sections for CD3 identified T-cells in injected grafts. There were 100 to 200 CD3 immunoreactive cells per 10 high power fields (HPF) in PBMC treated grafts (Figure 3.4-2A). A rare positive cell was detected in control grafts (Figure 3.4-2B). A membrane pattern of staining ranged from light to intense. In all grafts, a few scattered positively stained cells were present in the mouse skin adjacent to skin grafts.

Six out of eight mice survived the duration of the experiment. One mouse in the control group became anorexic and was found dead. This mouse lacked significant histological changes at necropsy. One mouse in the PBMC treated group had an enlarged spleen, a focal area of coagulative necrosis in the liver, and reactive changes in the lung and was thought to have died from complications of a bacterial infection. Significant histological lesions were not observed for the six mice that completed the trial. There was no gross or histological evidence of hemolytic anemia in any mouse.
Canine IgG concentration in plasma (collected at four weeks post inoculation) from the three surviving treated mice was 270, 150, and 260 μg/mL (mean ± SD, 226.66 ± 66.58 μg/mL). Canine IgG was not detected in samples taken prior to experimentation or in samples from control mice collected at the conclusion of the experiment. The PCV of treated and control mice at the termination of the experiment were similar to pre-experiment values and anemia was not detected.

3.4.3 DISCUSSION

The results of this experiment are consistent with an allograft rejection response mediated by transferred canine lymphocytes. Treated skin grafts developed gross and histological

changes consistent with skin graft rejection by two weeks post inoculation of allogenic canine PBMC. The time to onset of graft rejection was similar to that observed in human skin allograft rejection experiments using human leukocyte scid chimeras (Alegre *et al.*, 1994; Christofidou-Solomidou *et al.*, 1997a; Murray *et al.*, 1998), but sooner than the onset of bovine skin allograft rejection using bovine leukocyte scid chimeras (Greenwood *et al.*, 1997). The route of leukocyte delivery to mice differed in these experiments and direct inoculation of grafts in the current study may have led to an accelerated response. In the study by Greenwood *et al.* (1997), the inflammatory reactions were graded as a measure of the rejection response. The canine allograft rejection response in the current study was comparable in all grafts to the highest histological score of graft rejection used to characterize bovine skin allograft rejection. Similar to human skin allograft rejection on scid mice, large numbers of lymphocytes infiltrated allogenic grafts and were associated with epidermal cytotoxicity (Christofidou-Solomidou *et al.*, 1997a).

CD3 staining indicated that a large number of T-cells were retained in canine skin grafts and that these cells were much more numerous in grafts in the PBMC treated group. This finding supports a T-cell mediated allograft rejection reaction in treated grafts. Rare cells stained positive for CD3 in the control group. These cells were either carrier leukocytes, as described for human skin grafts on scid mice (Kaufmann *et al.*, 1993), or possibly murine cells. The lack of an inflammatory reaction or evidence of cytotoxicity in the control grafts supported a canine skin donor origin for these cells.

Canine IgG concentration in tgε26 mouse plasma at four weeks post allogenic canine PBMC transfer further indicated that a canine lymphocyte mediated inflammatory response developed in skin grafts. There was a trend for higher canine IgG plasma

concentration at four weeks post PBMC transfer in tgε26 mice supporting a skin allograft rejection response than plasma concentrations at four weeks for tgε26 mice reconstituted with canine PBMC previously in this study (Section 3.3). The mean plasma canine IgG level in mice supporting allograft rejection reactions (n=3) was 226.66 μg/mL ± 38.44 (mean ± SEM) at four weeks, whereas that of non-skin grafted tgε26 mice (Section 3.3) at four weeks (n=14) was 114.58 ± 90.33 μg/mL (mean ± SEM). Because of within experiment variation, there was no significant difference ($P > 0.05$) between these two experiments. The presence of an antigenic stimulus–the allogenic skin grafts– is expected to either increase engraftment of canine lymphocytes, as measured by plasma canine IgG concentration, and/or increase production of canine IgG in the mouse environment. In addition, the finding of 150 to 270 μg/mL of canine IgG in tgε26 mouse plasma four weeks post PBMC transfer (given a half-life of 2.9 days for canine IgG in tgε26 mice; see Section 3.3) indicates that canine IgG was actively being produced in mice after PBMC transfer.

Greenwood *et al.* (1997) reported a similar finding when evaluating bovine skin allograft rejection on scid mice. Gross evidence of skin allograft rejection was observed on bovine-PBL-scid-chimeras with a bovine IgG concentration greater than 200 μg/mL and peak bovine IgG concentrations were associated with onset of graft rejection. Skin grafts on chimeric mice with bovine IgG serum levels less than 200 μg/mL did not show gross evidence of graft rejection, suggesting that IgG levels in mouse plasma are representative of the ability of the chimeric lymphocyte population to mount a graft rejection response.

The development of inflammation in grafts mediated by canine lymphocytes indicates that direct intra-graft transfer of canine leukocytes is possible and provides an alternative approach to delivering cells to skin grafts in the canine xenograft model. This method of lymphocyte transfer to skin xenografts was employed in experiments successfully modeling human inflammatory reactions (Gilhar *et al.*, 1998).

This study demonstrates that the skin xenograft model is an appropriate system for investigating the functional aspects of lymphocyte-mediated reactions in canine skin. The lymphocyte-mediated allograft rejection response is similar in character to the histological changes observed in the wall of *D. canis* infected hair follicles in demodicosis (reviewed in Chapter 1). Both skin inflammatory reactions are characterized by a lymphocytic interface reaction with epidermal cell cytotoxicity. Thus, the skin xenograft mouse model should be useful for evaluating the functional role of canine lymphocytes in demodicosis.

Figure 3.4-1: Photomicrographs of a canine skin graft from a tgε26 mouse at 4 weeks after direct graft inoculation with allogenic canine PBMC (Group-I). **(A)** Large numbers of mononuclear inflammatory cells infiltrate the margin of the canine graft (large asterisks) and target hair follicles (small asterisks) (magnification = X10). **(B)** At higher magnification, lymphocytic interface folliculitis is associated with vacuolation (arrows) and degeneration of the basal keratinocytes (magnification = X25). Hematoxylin and eosin stained, paraffin embedded, tissue sections

A

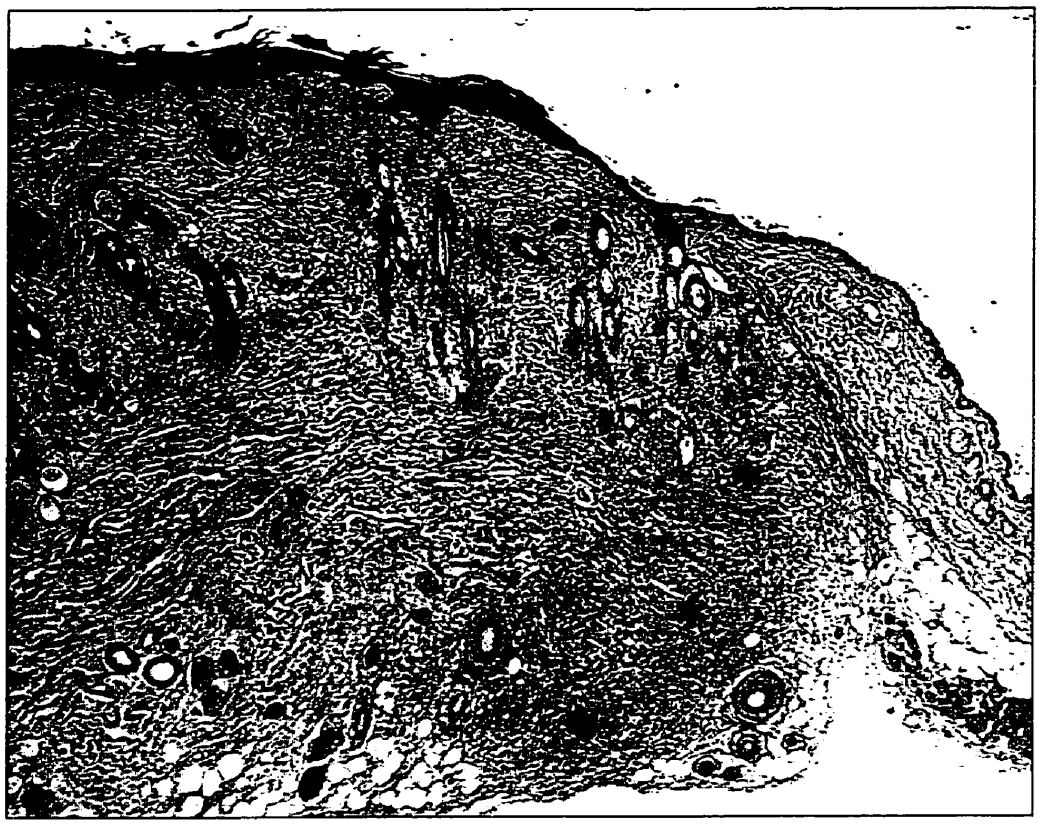

B

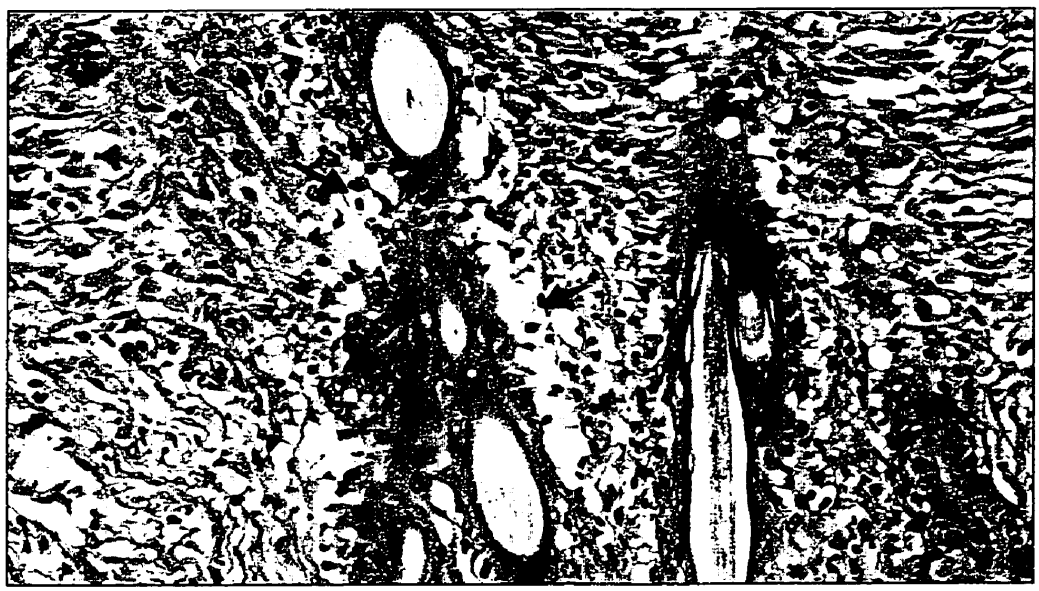

Figure 3.4-2: Photomicrographs of a canine skin graft from a tgε26 mouse at 4 weeks after direct inoculation with PBS (Group-II). **(A)** Inflammation is absent (magnification = X10). **(B)** Higher magnification confirms the lack of inflammation and shows the normal appearing follicle structure (magnification = X25). Hematoxylin and eosin stained, paraffin embedded, tissue sections

A

B

Figure 3.4-3: Photomicrographs of CD3 immunostained canine skin grafts from tgε26 mice at 4 weeks after direct inoculation with allogenic canine PBMC (Group-I) or PBS (Group-II). **(A)** Many infiltrating lymphocytes with positive immunoreaction to CD3 antigen (arrow) are present (Group-I). **(B)** Rare lymphocyte with positive immunoreaction to CD3 antigen (arrow) in the control graft (Group-II). Avidin-biotin complex peroxidase method, diaminobenzidine (DAB) chromagen, hematoxylin counterstain. (magnification = X100)

A

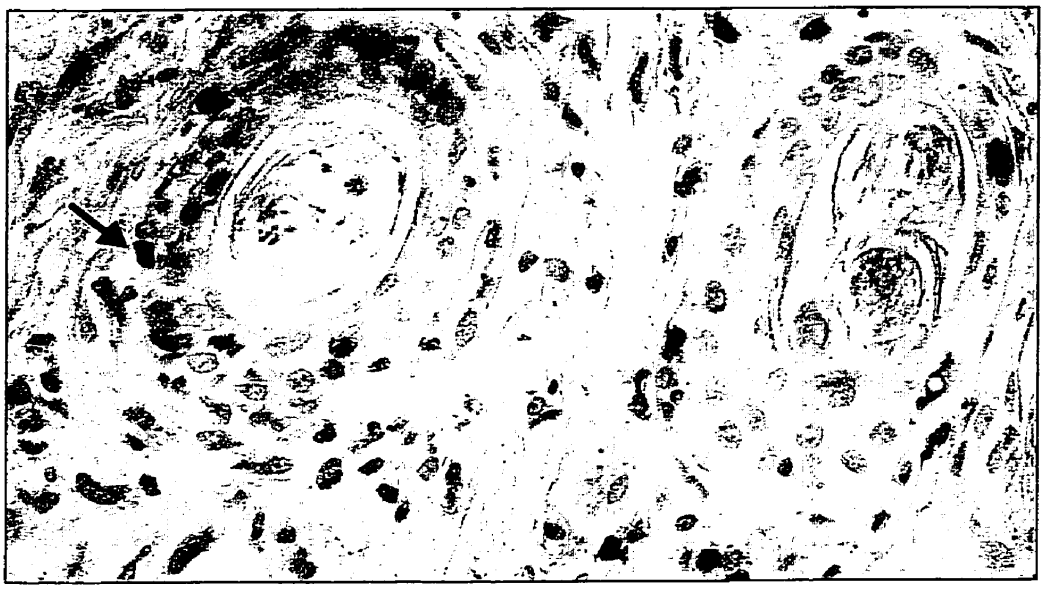

B

CHAPTER 4: APPLICATION OF THE SKIN XENOGRAFT MOUSE MODEL TO STUDY HOST RESISTANCE TO *DEMODEX CANIS* AND THE PATHOGENESIS OF CANINE DEMODICOSIS

4.1 INTRODUCTION

Factors controlling *D. canis* populations on the skin of dogs are not well understood. Previous studies suggest that a defect in cell-mediated immunity allows mites to proliferate unchecked and results in generalized demodicosis (reviewed in Chapter 1). However, there is little specific information about the mechanisms of host resistance to *D. canis* in particular or to *Demodex spp.* in general.

Dogs with generalized demodicosis exhibit a decreased cutaneous response to mitogens and a decreased *in vitro* lymphocyte proliferation assay response (Scott *et al.*, 1995). Puppies that received antilymphocyte serum and challenged with *D. canis* developed generalized disease (Healey & Gaafar, 1977b). Similarly, adult onset demodicosis occurs in association with acquired immunosuppression (Duclos *et al.*, 1994; Lemarie *et al.*, 1996). This evidence has led to the widely referenced hypothesis that generalized demodicosis results from a specific defect in T-cell immunity (Scott, 1979; Mason, 1993a; Scott *et al.*, 1995; Lemarie, 1996; Hill *et al.*, 1999).

Lymphocytic interface folliculitis was identified as the significant inflammatory reaction pattern in canine demodicosis (Caswell *et al.*, 1995; Caswell *et al.*, 1997). As part of this reaction pattern, CD8+ lymphocytes infiltrate the wall of *D. canis* infected hair follicles (Caswell *et al.*, 1995; Caswell *et al.*, 1997). This observation suggests that a host lymphocyte response plays an important role in the pathogenesis of skin lesion

development and/or protective immunity in demodicosis. These and previous studies have not evaluated the immune response to *D. canis* specific antigens and there is no direct evidence for a specific T-cell defect in generalized demodicosis.

Investigations into the factors that control mite populations on dogs have been limited by the lack of a viable experimental test system. *Demodex canis* is a fragile obligate symbiote that does not survive off the host and *in vitro* culture techniques have not been developed. *In vivo* experiments are limited by difficulties associated with reproducing lesions of demodicosis in healthy dogs.

The isolation of mites on skin xenografts, away from donor systemic factors, allows for controlled introduction of lymphocytes. The comparison of mite numbers on infected syngeneic xenografts between lymphocyte treated and control groups provides a direct quantitative measure of the effect of lymphocytes on mite populations. In addition, infection of skin xenografts provides an assessment of local skin innate defense mechanisms in resistance to *D. canis* colonization and the contribution of mites to skin lesion development in the absence of inflammation.

4.2 USE OF CANINE SKIN XENOGRAFT-ICR SCID MOUSE CHIMERAS TO MODEL CANINE DEMODICOSIS

The majority of studies that have utilized the skin xenograft mouse model to investigate inflammatory skin conditions have used the scid mouse or the scid mouse with a combined mutation known to augment immunodeficiency, such as the beige ($Lyst^{bg}$) mutation. Early attempts to model canine demodicosis using scid/bg mice were limited by the development of the "leaky" phenotype in these mice and/or graft-versus-host

disease (GVHD) (Caswell, 1995) (personal observations). An alternative mouse, the ICR scid, was developed at the laboratories of Taconic (Germantown, New York, USA) and was found to have a decreased incidence of the "leaky" phenotype and is commercially available. For this reason, the ICR scid mouse was chosen for an experiment using the skin xenograft mouse model to assess the role of canine lymphocytes in host resistance to *D. canis*. This experiment with ICR scid mice was performed concurrent with those assessing tgε26 mice for use in the xenograft model.

4.2.1 MATERIALS AND METHODS

4.2.1.1 Animals

Male ICR scid mice, aged six to eight weeks, were housed with two to five per micro-isolator cage. An adult, intact-male, mixed-breed dog was purchased from and maintained by Animal Care Services (University of Guelph, Ontario, Canada). *Demodex canis* were collected from three different dogs in the Province of Ontario

4.2.1.2 Experimental Design

In general, the experimental design outlined here was followed for each of the experiments in this chapter with variation in specific components as indicated.

Recipient mice were grafted with full-thickness canine skin and grafts were allowed to heal for several weeks. After topical application, mites were incubated on skin grafts to allow populations to expand. After the last mite transfer, *D. canis* infected skin grafts (Group-I) received autologous PBMC by intraperitoneal injection from the skin donor dog. *D. canis* infected control grafts (Group-II) received PBS. A second

control group (Group-III) received only PBMC and no mites. Following a second incubation period after lymphocyte transfer, skin grafts were collected and evaluated for differences in mite populations. Grafts were monitored for development of gross and histological changes. The second control group that received only PBMC was evaluated for the development of graft inflammation in the absence of *D. canis*. The timeline for the ICR scid experiment is given below (Figure 4.2-1).

Figure 4.2-1: Timeline for ICR scid experiment

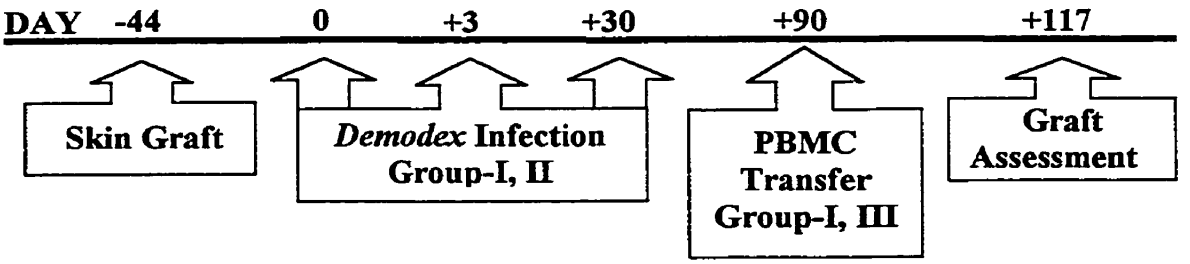

4.2.1.3 Experimental Protocol

Plasma samples from 30 ICR scid mice were screened by ELISA for murine immunoglobulin and the "leaky" phenotype. Twenty-seven mice were selected that had undetectable murine immunoglobulin (undetectable was defined as less than 2 times the average background absorbency reading on the ELISA plate).

Skin grafting: The 27 ICR scid mice were grafted with full-thickness canine skin according to section 2.3 and were bandaged for 12 days (Method-B, Section 2.3.4).

Demodex graft infection: Twenty-five mice, supporting grafts with more prominent hair growth, were subjectively allocated to three groups with comparable grafts. Skin grafts in Group-I (10 mice) and Group-II (10 mice) were infected on three occasions with *D.*

canis collected from different dogs, while Group-III (5 mice) received mineral oil only and were bandaged. At 44 days after grafting, Group-I and -II mice each received 40 to 60 viable mites with 95% adults and only occasional nymphs, protonymphs, larvae, and eggs. Three days after the first *D. canis* transfer, each graft received an additional 60 to 80 viable mites with 80% adults, 10 to 15% nymphs, and occasional protonymphs, larvae, and eggs. Thirty days after the first *D. canis* transfer, each graft received 80 to 120 viable mites with 85% adults and 15% mixed nymphs, protonymphs, larvae, and eggs. Grafts were protected with tape bandages for five days (Method-B, Section 2.3.4).

Lymphocyte transfer: At 60 days after the last mite transfer, skin donor PBMC were transferred by intraperitoneal injection to mice in Group-I and Group-III. Each mouse received 18×10^6 PBL. Each inoculum contained 75% lymphocytes and 85% PBMC. The cell viability was 97%. Mice in Group-II received PBS only.

Skin graft and mouse evaluation: At 87 days after the last *D. canis* transfer, plasma and skin grafts were collected. Skin graft digest samples were standardized by weight and tissue samples were collected for bacteriologic culture. A necropsy was performed on all mice, including histological evaluation of tissues.

4.2.1.4 Statistical Methods

Numbers of mites were compared between groups by ANOVA using the SAS® computer software package (Section 2.9) and the model chosen fit the ANOVA assumptions. The means and confidence intervals for PCV values were calculated using Graphpad Prism (GraphPad Software, San Diego, California, USA).

4.2.2 RESULTS

Fifteen out of 25 ICR scid mice survived the duration of the trial: five out of 10 mice remained in Group-I; eight out of 10 mice remained in Group-II; and two out of five mice remained in Group-III. Ten mice died or were euthanized due to illness or skin graft complications. An additional mouse was found dead on the trial completion date and was included with the data for mice completing the trial.

Skin grafts healed well after transplantation. Compared to previous experiments, there was reduced central eschar formation after bandage removal and although hair regrowth started at the graft margins, it soon involved central areas of the graft (Figure 4.2-2). Subsequently, the majority of skin grafts in each group developed extensive surface crusting with hair loss (Figure 4.2-3). Crusts were composed of a mixture of proliferative keratin scale and serocellular exudate. Surface crusts developed primarily after *D. canis* transfer; however, crusts were also observed on non-*D. canis* treated grafts of Group-III. Ulceration of some grafts necessitated euthanasia of affected mice.

Demodex canis were recovered by NaOH digestion from 18/20 mite inoculated grafts. Thirteen mice that survived the trial and that had grafts supporting mites are described. In the PBMC treated group (Group-I, n = 5), the calculated total number of mites per skin graft digest sample ranged between 1,480 and 10,640 (mean ± SEM; 4,512 ± 1,588.12). For the PBS control group (Group-II, n = 8), mite numbers ranged between 40 and 3,720 (mean ± SEM; 1,065 ± 442). *Demodex canis* were not recovered from mice in Group-III. There was a significant treatment effect ($P = 0.0174$) on mite numbers between Groups-I and II. The presence of a significant interaction between treatment and stage type ($P = 0.029$) indicated that this treatment effect was not uniform for the

different stages. This interaction occurred because there was a significant difference between the number of eggs ($P < 0.001$), larvae ($P = 0.014$), and nymphs ($P = 0.032$) but not adults ($P > 0.05$) for the two groups. There was no significant association ($P > 0.05$) between weight of the digest samples and calculated mite totals and for this reason Figure 4.2-4 shows the calculated mite and stage totals per digest sample. Adults and nymphs tended to be more numerous than eggs and immature stages (Figure 4.2-4B). Table 4.2-1 lists the calculated total mites per skin graft digest sample and the calculated totals for each life-cycle stage. Table 4.2-2 lists the calculated total mites per gram of skin graft digest sample and the stage totals per gram.

Histological analysis revealed extensive inflammation affecting the majority of grafts in all groups. Prominent aggregates of coccoid bacteria, typical of *Staphylococcus spp.*, were associated with neutrophilic folliculitis and furunculosis as well as exudation, crusting, and epidermal ulceration (Figure 4.2-5). Micro-abscesses, vascular thrombosis and/or regional coagulation necrosis were present in the dermis of more severely affected grafts. A perivascular to diffuse lymphohistiocytic infiltrate was present in the dermis of grafts in the treatment group and both control groups and was generally more pronounced in PBMC treated grafts (Figure 4.2-6). Lymphocytes infiltrated the interfollicular and follicular epidermis and were associated with vacuolation and single cell necrosis of keratinocytes in several grafts that did not receive canine PBMC (Figure 4.2-7). This lymphocytic interface reaction was often associated with focal infiltration by eosinophils. *Demodex canis* were observed in scattered hair follicles in sections from 11 of the 20 grafts receiving mites and in sections from eight of the 13 grafts on mice that completed the trial. A few mites were visible in sections from one skin graft that was negative for

mites by NaOH digestion, making the overall *D. canis* infection rate 95%. Hair follicles containing mites did not appear to be directly targeted by inflammation. In sections from several grafts, inflammation and ulceration disrupted skin graft architecture and only a few intact follicles were available for examination.

Bacterial culture of 19/25 skin grafts recovered 2 to 4+ pure growth of *Staphylococcus intermedius* from 15 grafts. No bacteria were recovered from 2/2 grafts cultured from Group-III that did not receive mites.

Plasma samples were available from 19/25 mice for immunoglobulin evaluation. Murine IgG was detectable in plasma samples from 12 mice. The calculated concentration of murine IgG in mouse plasma ranged from 0.62 to 478.16 μg/mL (mean ± SD, 58.19 ± 142.2 μg/mL). Canine IgG was detected in 6/7 mice that received PBMC (4/5 in Group-I, and 2/2 in Group-III). The calculated concentration of canine IgG ranged from 0.2 to 5,290 μg/mL. For Group-I, the mean detectable canine IgG concentration (± SD) was 11.42 μg/mL (± 10.32) and for Group-III, 0.2 μg/mL was detected in one mouse and 5290 μg/mL was detected in a second mouse (Appendix 3). Canine IgG was not detected in plasma samples from mice in Group-II that did not receive canine PBMC or in pre-experiment plasma samples from all mice. Anemia was not detected and the PCV for mice at completion of the trial was similar to that of pre-experimental values and ranged between 41 and 49 (Table 4.2-3). Hemolysis, observed in one blood sample (PCV = 36), was attributed to sample handling.

Necropsy evaluation revealed that three mice died of thymic lymphoma. The remaining seven mice that became ill and were euthanized, or that died, had necropsy findings consistent with systemic bacterial infection. Affected mice had multifocal areas

of hepatic necrosis and/or neutrophilic hepatitis, splenic enlargement, and prominent cellularity of pulmonary parenchyma. Affected mice supported skin grafts with extensive bacterial colonization and suppurative inflammation. GVHD was not detected.

4.2.3 DISCUSSION

PBMC administration was associated with a measurable effect on the *D. canis* populations on skin grafts. More mites were recovered from grafts on PBMC treated mice suggesting that lymphocytes had a trophic effect on mite populations.

The basic elements required to model demodicosis were successfully accomplished. Full-thickness canine skin grafts were developed with improved hair growth compared to previous experiments. A high *D. canis* infection rate (95%) was achieved on skin grafts and mites were actively replicating on skin grafts, producing all life cycle stages. Canine lymphocytes survived transfer to ICR scid mice as indicated by the presence of circulating canine IgG (6/7) at four weeks post PBMC inoculation. The concentrations of canine IgG detected were similar in range to those observed for tgε26 mice (Section 3.3). Although many of the conditions required for testing the hypothesis were accomplished, the development of inflammation and extensive graft disruption, attributable to factors other than canine lymphocyte transfer or mite infection, made it difficult to interpret a causal relationship between the differences in mite numbers and lymphocyte transfer. Skin lesions started after *D. canis* infection and prior to leukocyte transfer on many grafts and grafts in Group-III that did not receive mites also developed lesions. These changes were primarily attributed to two causes. First, *S. intermedius* graft infection was associated with suppurative graft inflammation and considerable

architectural disruption. Repeated *D. canis* infection of skin grafts likely contributed to the high incidence of bacterial infection.

Second, a significant percentage of the ICR scid mice developed a degree of immunocompetence and were considered to have acquired the "leaky" phenotype. Murine IgG was detected by ELISA assay in 63% of mice (12/19) over the course of the experiment. The graft rejection reaction, identified as an interface dermatitis and spontaneous infiltration of grafts with lymphocytes and macrophages in non-canine lymphocyte treated grafts, provided further evidence of the "leaky" phenotype. Graft rejection was considered to have directly contributed to gross lesions.

The development of the "leaky" phenotype in scid/bg and ICR scid mice was a limiting factor for the use of these strains in the skin xenograft mouse model of canine demodicosis (Caswell, 1995). Typically, 2 to 25% of C.B.-17 scid mice become "leaky", have antigen receptor positive B and T lymphocytes, and produce immunoglobulin (Bosma *et al.*, 1988; Carroll & Bosma, 1989; Mosier *et al.*, 1993). In this experiment, we attempted to minimize any effect of the "leaky" phenotype by prescreening mice and by choosing a mouse strain (ICR scid) considered more resistant to this complication than C.B.-17 scid mice (Taconic, Germantown, New York, USA).

The results of this experiment and preliminary experiments using scid/bg mice suggest that experimental conditions in this study favored the development of the "leaky" phenotype in scid mice. The incidence of the "leaky" phenotype in C.B.-17 scid mice increases with age and therefore the long duration of the current grafting experiments (over 5 months) could have been a contributing factor (Bosma *et al.*, 1988; Carroll & Bosma, 1989; Mosier *et al.*, 1993). One theory regarding the development of the "leaky"

phenotype is that the V(D)J recombinase altered by the scid mutation could revert to the wild-type phenotype under selective pressure (Petrini *et al.*, 1990; Kotloff *et al.*, 1993a; Kotloff *et al.*, 1993b). An increased incidence of the "leaky" phenotype might be expected in long-term experiments in which mice are exposed to foreign antigens and/or inflammation (Taylor, 1994). In the current study, scid mice were exposed multiple times to foreign antigens, including xenogeneic skin grafts and PBMC, *D. canis* infection, and, for several mice, bacterial infection, all of which were likely associated with some degree of inflammation / tissue damage at the time of exposure. Finally, there is limited information on the properties of canine scid xenografts; this species interaction could favor the development of the "leaky" phenotype.

Given the number of changes that were present in skin grafts, other possible causes were considered that could have contributed to the differences in mite numbers between experimental groups. However, because of the low numbers of mice and within group variation, a clear association could not be made between mite numbers and such changes as bacterial infection, evidence of graft rejection, detection of murine IgG, etc.

Canine skin grafts healed well on ICR scid mice and the early healing period was considered improved over the results of full-thickness grafting to tgε26 mice (Section 3.2). Central eschar development occurred after bandage removal but was not as severe. This decrease in ischemic damage was attributed to the extended bandaging times (12 versus 7 days) and not to the difference in mouse types or skin donors. This conclusion is supported by the observation that full-thickness canine skin grafts on scid/bg mice, when bandaged for 7 days, healed similarly to those on tgε26 mice (data not shown).

The survival rate for ICR scid mice in this experiment was low. Necropsy results identified systemic bacterial infection as the most common cause of mouse mortality, which developed secondarily to skin graft infection. Thymic lymphoma was associated with the death of 3 out of 25 ICR scid mice (12%) and a similar incidence was reported for C.B.-17 scid mice (up to 15%) (Custer *et al.*, 1985).

Evidence of GVHD was not identified, although the extent of systemic bacterial infection in some mice complicated this interpretation. Hemolytic anemia, a significant complications of previous experiments with scid/bg mice, was not observed (Caswell, 1995). Caswell (1995) concluded that "leakiness" in scid/bg mice contributed to the development of GVHD. However, in the current experiment, a high incidence of the "leaky" phenotype was detected, suggesting that other factors related to dog, mouse strain, or mouse immunodeficiency contribute to the development of GVHD in canine PBMC scid chimeras.

Despite the complications of "leakiness" and *S. intermedius* pyoderma, there was a significant difference in the mite populations in Group-I that received canine lymphocytes compared to Group-II that did not. This raises the interesting question of the effects of local inflammation on mite reproduction. Further experiments to address this issue require the use of a new immunodeficient mouse strain with the skin xenograft mouse model in order to limit the effects of "leakiness".

Figure 4.2-2: Appearance of two representative full-thickness canine skin grafts on ICR scid mice prior the development of graft lesions. Improved grafting results are evident as skin grafts developed hair growth in central and peripheral areas.

Figure 4.2-3: Appearance of six representative full-thickness canine skin grafts on ICR scid mice at experiment completion; Group-I **(A, B)**, Group-II **(C, D)** and Group-III **(E, F)**. Skin grafts in each group have developed extensive surface crusting and hair loss.

Figure-4.2-2

A

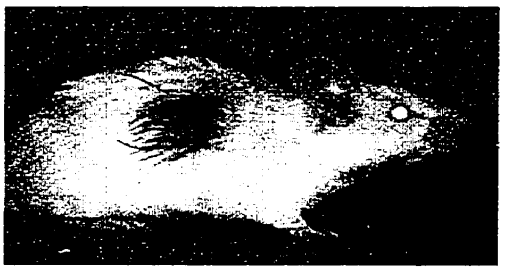

B

Figure-4.2-3

A

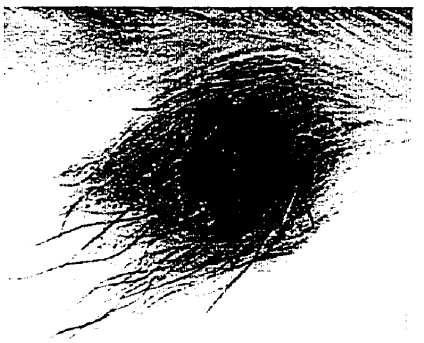

B

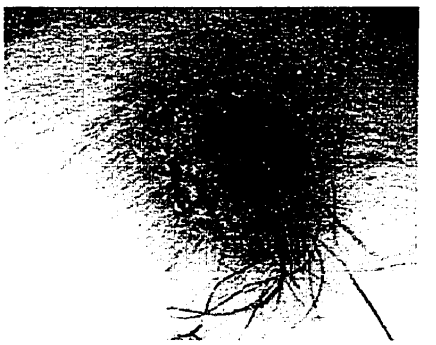

C

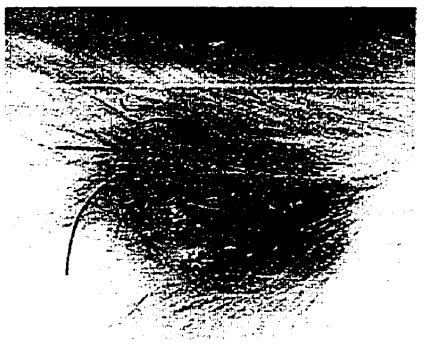

D

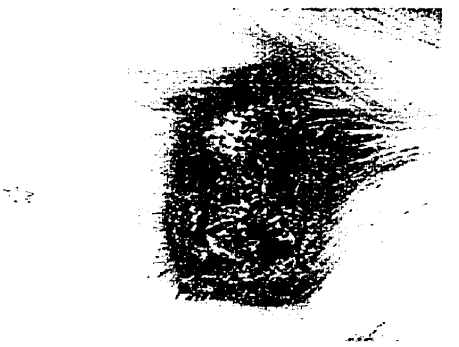

E

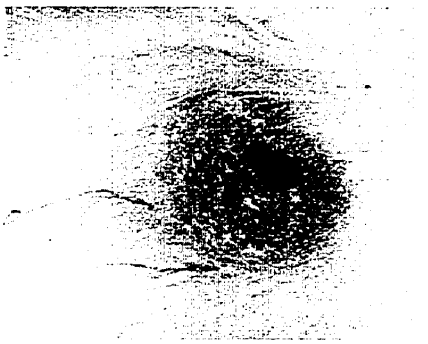

F

Figure 4.2-4: (A) Bar graph showing the calculated total number of *D. canis* per digest sample (mean ± standard error) recovered from canine skin grafts on ICR scid mice by NaOH digestion; PBMC treated group (Group-I) and PBS control group (Group-II). Mites were not recovered from skin graft digest samples for Group-III (not shown). **(B)** The calculated total number of each *D. canis* life-cycle stage per digest sample (mean ± standard error) recovered from grafts in Group-I and Group-II.

(A)

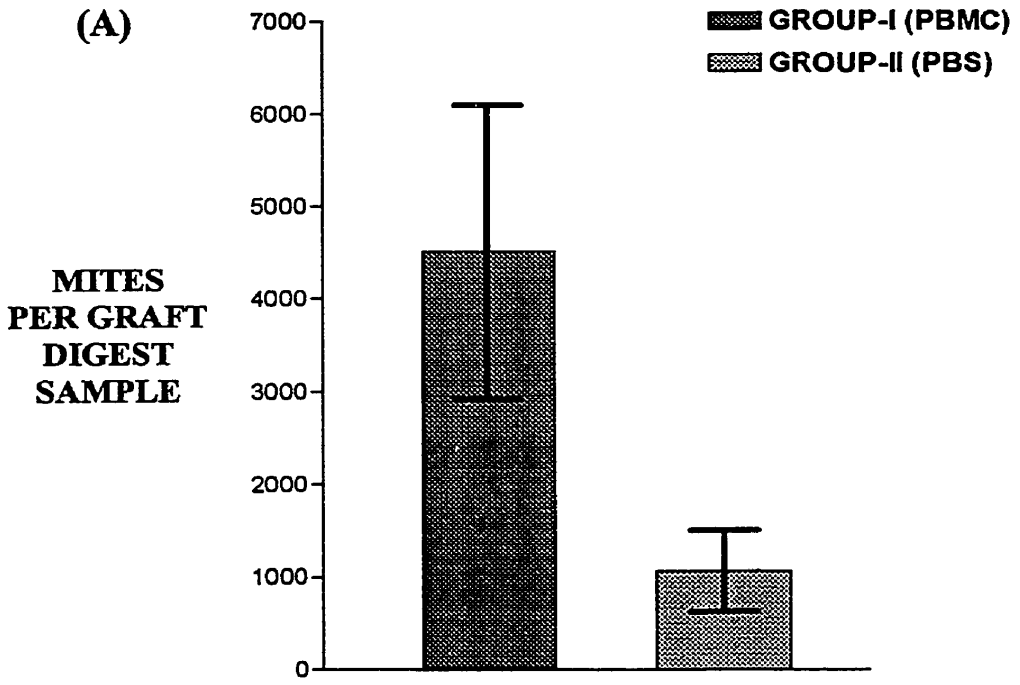
GROUP-I (PBMC)
GROUP-II (PBS)
MITES PER GRAFT DIGEST SAMPLE
7000
6000
5000
4000
3000
2000
1000
0

(B)

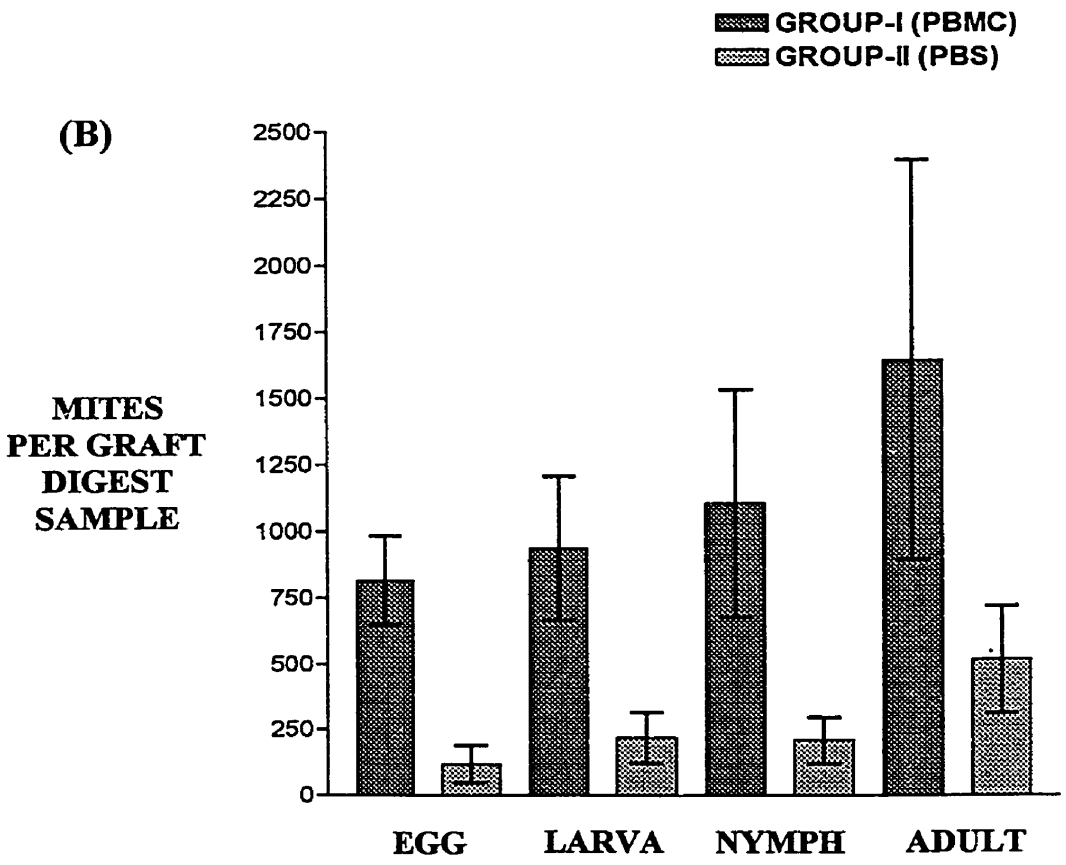
GROUP-I (PBMC)
GROUP-II (PBS)
MITES PER GRAFT DIGEST SAMPLE
2500
2250
2000
1750
1500
1250
1000
750
500
250
0
EGG
LARVA
NYMPH
ADULT

Figure 4.2-5: Photomicrographs of less severely affected full-thickness canine skin grafts from ICR scid mice at experiment completion; **(A)** *D. canis* and PBMC treated graft (Group-I); **(B)** *D. canis* and PBS treated graft (Group-II); **(C)** PBMC treatment only (Group-III). Neutrophilic folliculitis and furunculosis (A, arrow), as well as extensive surface crusting, are evident. Many large bacterial colonies are present (B, within circle). A perivascular to diffuse lymphohistiocytic infiltrate is present in the dermis of all grafts. Hematoxylin and eosin stained, paraffin embedded, tissue sections (magnification = X5)

A

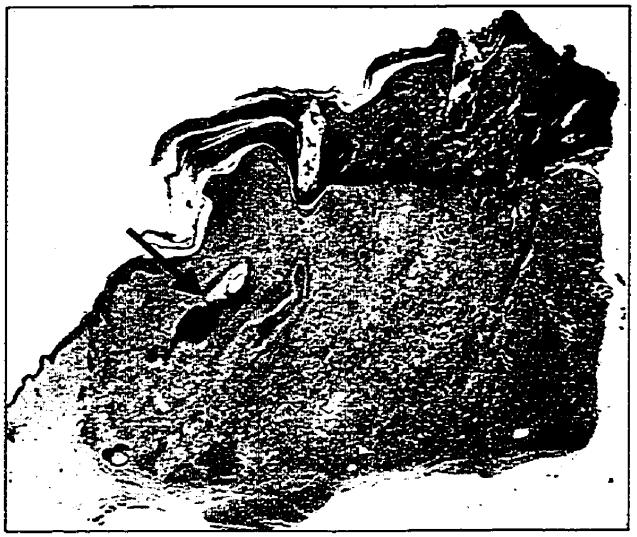

B

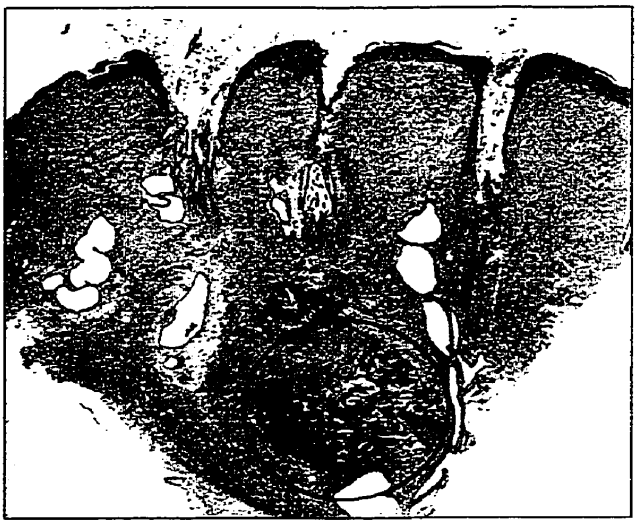

C

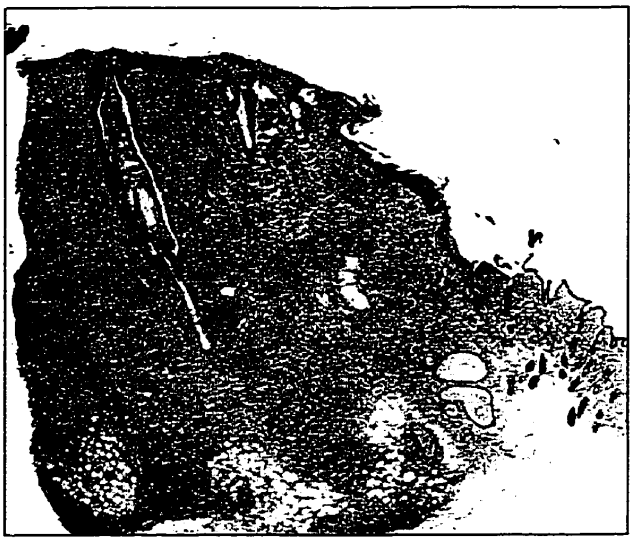

Figure 4.2-6: Photomicrographs of skin grafts from ICR scid mice with prominent dermal infiltrate of mononuclear inflammatory cells; *D. canis* infection and PBMC treatment, Group-I **(A)** and after PBMC treatment only, Group-III **(B)**. Hematoxylin and eosin stained, paraffin embedded, tissue sections (magnification = X75)

A

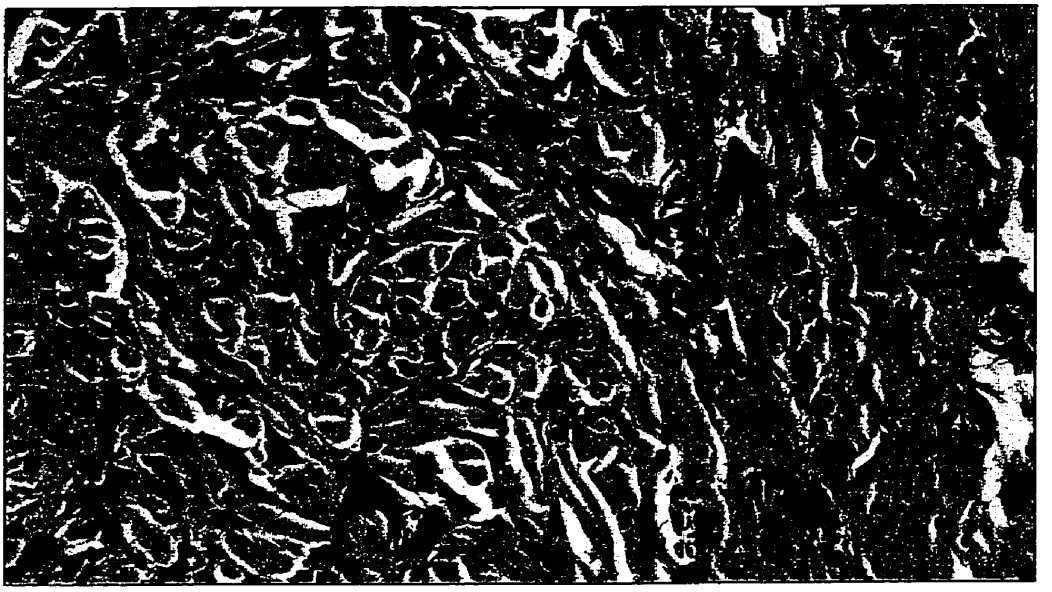

B

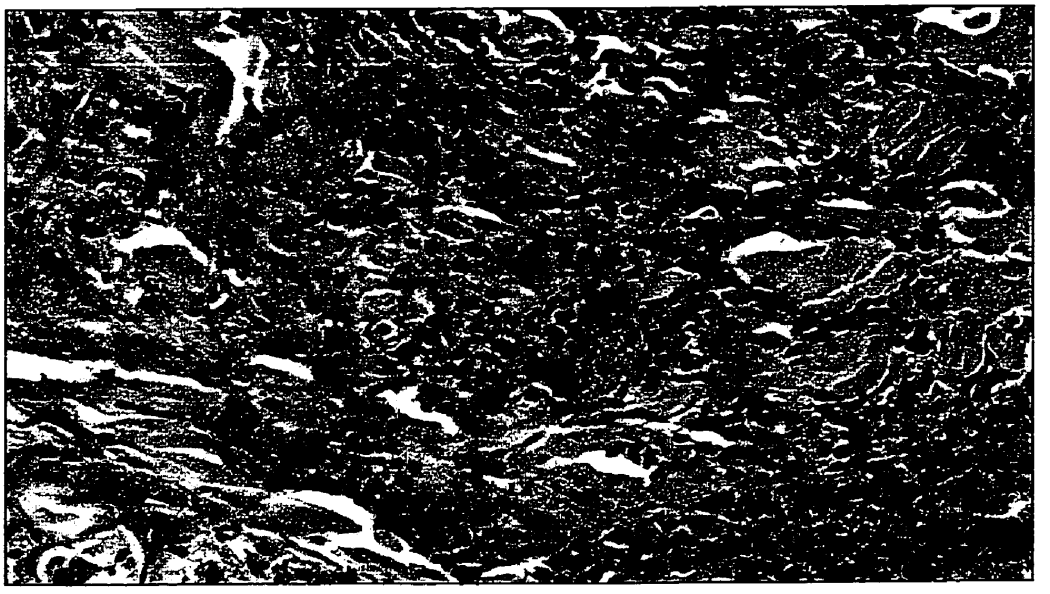

Figure 4.2-7: Photomicrographs showing inflammation in skin grafts from two ICR scid mice that did not receive canine PBMC. A lymphocytic interface dermatitis **(A)** and interface folliculitis **(B)** are evident. Lymphocytes infiltrate the epithelium and are associated with vacuolation and occasional single cell necrosis of basal keratinocytes. Hematoxylin and eosin stained, paraffin embedded, tissue sections (magnification = X75)

A

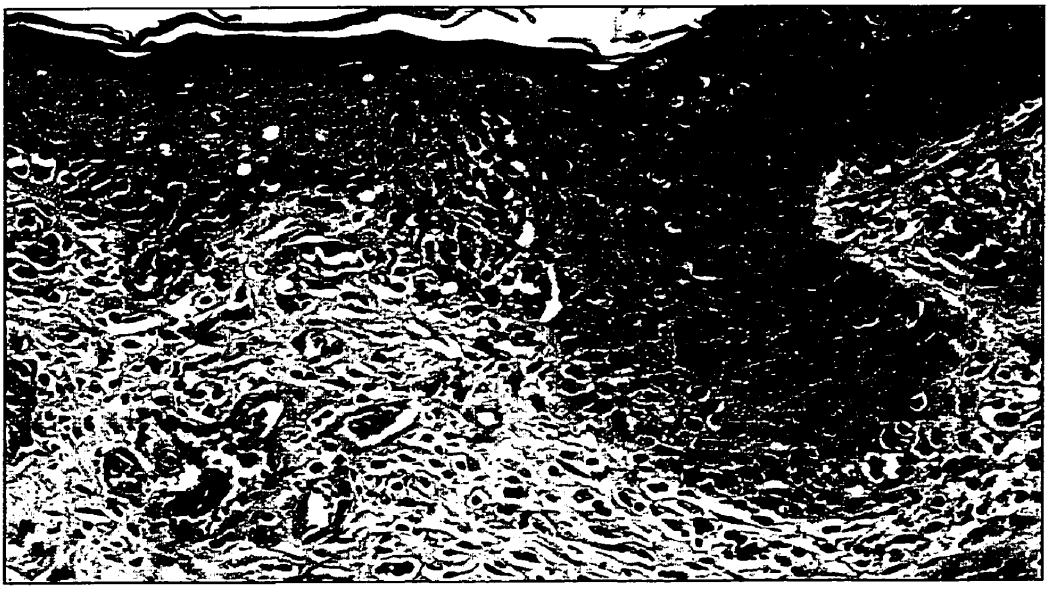

B

Table 4.2-1: Calculated Number of *D. canis* Per Skin Graft Digest Sample Collected from Skin Grafts on ICR Scid Mice

Mouse	Calculated Stage Totals				Calculated Mite Totals
	Egg	Larva	Nymph	Adult	
Group-I (*D. canis* plus PBMC)					
1	640	480	280	80	1480
2	1320	2000	2760	4500	10640
3	640	680	760	920	3000
4	1080	800	840	1280	4000
5	400	720	880	1440	3440
Mean ± SEM	816 ± 167.14	936 ± 271.17	1104 ± 427.75	1644 ± 751.70	4512 ±1588.12
Group-II (*D. canis* plus PBS)					
1	0	80	80	240	400
2	0	0	40	240	280
3	80	40	40	200	360
4	0	0	0	40	40
5	600	800	720	1600	3720
6	160	320	440	480	1400
7	120	360	240	1200	1920
8	0	160	120	120	400
Mean ± SEM	120 ± 72.11	220 ± 96.21	210 ± 88.72	515 ± 201.76	1065 ± 442

Group-III (PBMC treatment only)
Demodex canis was not recovered from any skin grafts in Group-III that were not infected with mites.

Table 4.2-2: Calculated Number of *D. canis* Per Gram of Digest Sample Collected from Skin Grafts on ICR Scid Mice

Mouse	Calculated Stage Totals Per Gram				Mite Totals Per Gram
	Egg	Larva	Nymph	Adult	
Group-I (*D. canis* plus PBMC)					
1	3472.59	2604.44	1519.26	434.07	8030.36
2	11924.11	18066.84	24932.24	40650.40	95573.59
3	5786.61	6148.28	6871.60	8318.26	27124.75
4	7826.08	5797.10	6086.95	9275.36	28985.49
5	3189.79	5741.62	7017.54	11483.25	27432.20
Mean ± SEM	6439.83 ±1609.23	7671.65 ±2676.71	9285.51 ±4039.40	14032.27 ±6910.90	37537.70 ±15142.24
Group-II (*D. canis* plus PBS)					
1	0.00	650.41	650.41	1951.22	3252.03
2	0.00	0.00	161.16	966.96	1128.12
3	918.48	459.24	459.24	2296.21	4133.18
4	0.00	0.00	0.00	220.63	220.63
5	2477.29	3303.06	2972.75	6606.11	15359.21
6	1054.02	2108.04	2898.55	3162.06	9222.66
7	1315.79	3947.37	2631.58	13157.89	21052.63
8	0.00	868.15	651.11	651.11	2170.37
Mean ± SEM	720.69 ±318.13	1416.52 ±538.50	1269.34 ±443.39	3626.52 ±1535.55	7587.19 ±2579.76

Group-III (PBMC treatment only)
Demodex. canis was not recovered from any skin grafts in Group-III that did not receive mites.

Table 4.2-3: PCV Values for ICR scid Mice at Experiment Onset and Completion

Mouse	PCV at Onset of Experiment	PCV at Completion
Group-I (*D. canis* plus PBMC)		
1	43	36*
2	44	45
3	46	44
4	39	46
5	43	45
6	48	†
7	41	†
8	46	†
9	45	†
10	44	†
Group-II (*D. canis* plus PBS)		
1	49	44
2	39	43
3	44	44
4	45	41
5	46	49
6	43	42
7	47	†
8	42	43
9	38	42 e
10	45	†
Group-III (PBMC treatment only)		
1	48	42
2	41	43
3	44	45 e
4	47	46 e
5	45	47 e

Mean PCV and 95% Confidence Intervals (CI) for mice (n=25) at the onset of the ICR scid experiment: Mean = 44.08, Lower 95% CI = 42.88, Upper 95% CI = 45.28

* - Sample hemolyzed after blood collection
† - Mouse died prior to completion of the experiment

4.3 USE OF CANINE SKIN-XENOGRAFT Tgε26 MOUSE-CHIMERAS TO MODEL CANINE DEMODICOSIS

The use ICR scid or scid/bg mice for xenograft experiments modeling canine demodicosis was complicated by the development of the "leaky" phenotype (Section 4.2) (Caswell, 1995). Other mouse mutants have not been investigated in detail for modeling inflammatory skin conditions with the xenograft model, particularly not with canine tissues. The current study identified the tgε26 transgenic mouse (Wang *et al.*, 1994; Wang *et al.*, 1995) for use in the xenograft model, demonstrating that it could support canine skin grafts and lymphocytes.

Two experiments were performed with tgε26 mice. The first followed the design of the ICR scid mouse experiment (Section 4.2). In the second experiment, canine lymphocytes were transferred to tgε26 mice before and after *D. canis* infection was established on skin grafts, to more closely mimic naturally occurring demodicosis where lymphocytes are present prior to mite population expansion.

4.3.1 MATERIALS AND METHODS

4.3.1.1 Animals

Male transgenic tgε26 mice, aged eight to 12 weeks, were housed with two to three mice per micro-isolator cage. Adult, intact-male, mixed-breed dogs were purchased from Animal Care Services (University of Guelph, Ontario, Canada). *Demodex canis* were collected from dogs in the Province of Ontario.

4.3.1.2 Experimental Design

Experiment one: The experimental design followed that of the ICR scid experiment (Section 4.2), except that skin grafts were infected with *D. canis* only once. Group-I received *D. canis* and autologous PBMC intraperitoneally, after mite infection had been established. Group-II received *D. canis* and PBS. A time-line for experiment one with tgε26 mice is given below (Figure 4.3-1).

Figure 4.3-1: Timeline for experiment one with tgε26 mice

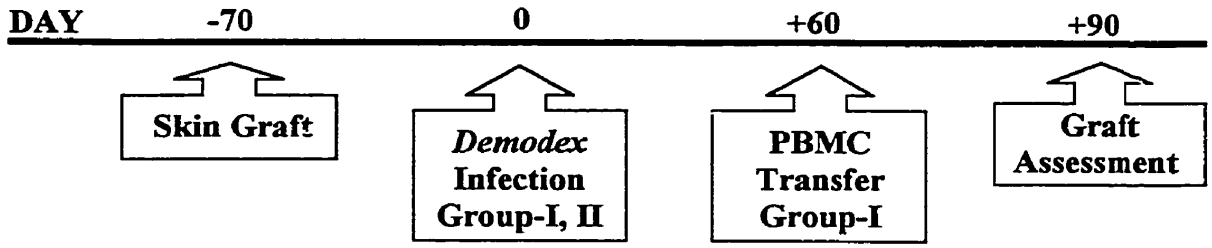

Experiment two: Skin grafts were infected with *D. canis* only once. Group-I received autologous PBMC by intraperatoneal injection one day prior to *D. canis* infection and again after infection. Group-II received *D. canis* and PBS. A timeline for experiment two is given below (Figure 4.3-2).

Figure 4.3-2: Timeline for experiment two with tgε26 mice

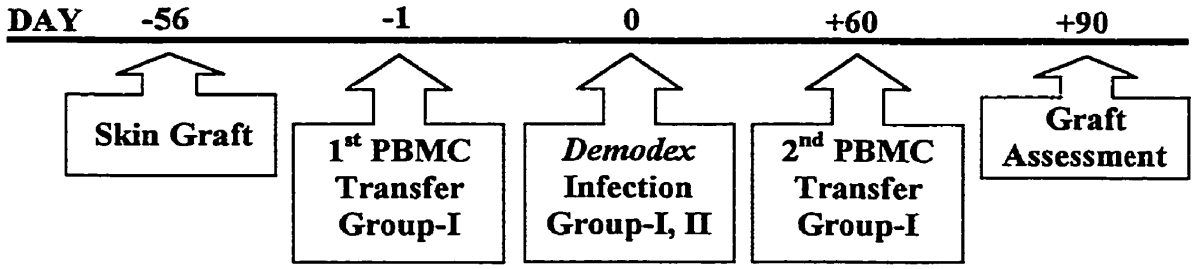

4.3.1.3 Experimental Protocol

Skin grafting: **Experiment one:** Twenty tgε26 mice were grafted with full-thickness canine skin according Section 3.2. Skin grafts were protected with cast bandages for nine

to 12 days (Method-A, Section 2.3.4). **Experiment two:** Fifteen tgε26 mice were grafted according to Section 2.3.3 and were protected with tape bandages for seven to nine days (Method-B, Section 2.3.4).

Demodex graft infection: **Experiment one:** Twelve mice, supporting grafts with adequate hair growth, were subjectively allocated to two groups (six mice each) with grafts of comparable quality. Skin grafts were infected with *D. canis* 70 days after grafting. Each graft received 250 to 350 mites with 80% viable adults, 15% nymphs, and occasional protonymphs, larvae, and eggs. Grafts were protected with cast bandages for five days (Method-A, Section 2.3.4). **Experiment two:** Ten skin grafts were selected and distributed into two groups with comparable grafts. At 56 days after grafting, each graft received 90 to 110 *D. canis* composed of 85% viable adults, 10% nymphs, and occasional protonymphs, larvae, and eggs. Grafts were protected with tape bandages for five days (Method-B, Section 2.3.4).

Lymphocyte transfer: **Experiment one:** At 60 days post *D. canis* infection, PBMC were transferred from the skin donor dog to six mice in the treatment group (Group-I) by intraperitoneal injection. Each mouse received 29×10^6 PBL. The inoculum contained 70% lymphocytes and 90% PBMC. The cell viability was 98%. The remaining six mice (Group-II) received PBS. **Experiment two**: Five mice in Group-I were inoculated with PBMC one day prior to *D. canis* infection and then again 60 days after infection. On the first leukocyte inoculation, each mouse received 36×10^6 viable PBL by intraperitoneal injection. This inoculum contained 71% lymphocytes and 90% PBMC. Cell viability was 97%. On the second leukocyte inoculation, each mouse received 35×10^6 viable

PBL. This second inoculum contained 65% lymphocytes and 86% PBMC. The cell viability was 98%. Mice in Group-II received PBS at both transfer times.

Skin graft and mouse evaluation: **Experiment one and two:** plasma samples and skin grafts were collected 90 days after *D. canis* infection. Skin graft digest samples were standardized by the number of active hair follicle units. For **experiment two**, graft tissue sections were stained with anti-CD3 antibody to identify T-cells (Section 2.5.2). Tissue sections were also stained with mouse specific anti-CD45 antibody.

4.3.1.4 Statistical Methods

Statistical evaluation was performed according to Section 4.2.1.4.

4.3.2 RESULTS

In experiment one, 10 out of 12 tgε26 mice survived the duration of the experiment; six mice remained in the PBMC treated group and four mice remained in the control group. In experiment two, six mice survived and three out of five mice remained in both the PBMC treated group and the control group. Four mice died or were euthanized due to illness prior to the second leukocyte transfer.

Skin grafts healed on mice and hair density and length were variable between skin grafts and were most prominent for all grafts at the completion of the trial (Figure 4.3-3). A central eshar developed on most grafts and was associated with scarring and alopecia. This change was less prominent in skin grafts in experiment one. In experiment one, the surface appearance or hair growth did not change appreciably after *D. canis* infection or after PBMC transfer. In experiment two, the majority of skin grafts developed very mild

scaling prior to *D. canis* infection or lymphocyte transfer and this became slightly more prominent on skin grafts by completion of the trial.

In experiment one, NaOH digestion of skin graft samples recovered *D. canis* from 12/12 grafts. The following information pertains to the 10 mice that completed the experiment. For the PBMC treated mice (Group-1), the calculated number of mites per skin graft digest sample ranged from 540 to 6,153.27 (mean ± SEM, 2,100.56 ± 858.96). For the controls (Group-II), the calculated number of mites per skin graft sample ranged between 185 and 4,959.50 (mean ± SEM, 1,691.12 ± 1,115.64). In Group-I, the average number of mites per active hair follicle unit ranged between 10.57 and 60.32 (mean ± SEM; 25.75 ± 7.85). For Group-II, the average number of mites per follicle unit ranged from 7.5 to 59.75 (mean ± SEM, 26.20 ± 11.49). There was no significant difference ($P > 0.05$) between Group-I and Group-II when calculated mite totals or mites per follicle unit were compared, nor was there a significant difference between individual life-cycle stages. There was a significant positive linear association ($P = 0.017$) between the number of hair follicle units and the calculated numbers of mites per skin graft digest sample. For this reason, Figure 4.3-4 illustrates the calculated mite and stage totals per hair follicle unit for each group. Immature stages were more numerous and more eggs were recovered than larva ($P < 0.001$) nymphs ($P < 0.001$) or adults ($P < 0.001$) on skin grafts within a group (Figure 4.3-4B). The average number of each life cycle stage had a similar distribution in the control and PBMC treated groups (Figure 4.3-4B). For comparison to other experiments in this chapter, Figure 4.3-5 shows the calculated mite and stage totals per digest sample for both groups. Table 4.3-1 lists the calculated

number of mites and stages per digest sample and Table 4.3-2 lists these numbers per hair follicle unit.

In experiment two, mites were recovered from 7/10 skin grafts by NaOH digestion. Of the 6 mice completing the trial, mites were recovered from 2/3 grafts in the PBMC treated group and from 3/3 grafts in the control group. For the PBMC treated group, the calculated total mites, per graft sample, ranged between 0 and 787.5 (mean ± SEM, 420.83 ± 228.93). In the control group, the calculated mite totals per graft sample ranged between 175 and 550 (mean ± SEM, 337.50 ± 111.10). For the PBMC treated group, the calculated number of mites per active hair follicle ranged between 0 and 8.85 (mean ± SEM, 4.68 ± 2.56). In the control group, the calculated number of mites per follicle unit ranged from 2.43 to 5.91 (mean ± SD, 4.11 ± 1.00). Because of the low numbers surviving in experimental groups and because analysis was sensitive to the smoothing factor chosen, statistical evaluation of treatment effect was not possible. There did not appear to be a difference between the calculated mite (or stage) totals per digest sample, or between the number of mites (or stages) per follicle unit, for Group-I and Group-II (Figure 4.3-6). Despite the smoothing factor chosen (1, 0.1, or 0.01), there was a significant positive association between the number of mites and the number follicle units ($P = 0.014$, smoothing factor = 1). Figure 4.3-6 shows the mite and stage totals per hair follicle unit. Immature stages tended to be more numerous than mature stages (Figure 4.4-6B). There were significantly more eggs on skin grafts than nymphs ($P = 0.006$) or adults ($P < 0.001$), and although there tended to be more eggs than larvae, this difference was not significant ($P = 0.201$, smoothing factor = 1). The number of each life cycle stage had a similar distribution in the PBMC treated and control groups (Figure

4.4-6B). Figure 4.3-7 shows the calculated mite and stage totals per digest sample for the Group-I and Group-II. Table 4.3-3 lists the calculated number of mites and stages for each skin graft digest sample and Table 4.3-4 reports these totals per hair follicle unit. The number of active hair follicle units ranged between 18 and 115 for experiment one and between 63 and 91 for experiment two (Table 4.3-1 and 4.3-3)

Histological analysis confirmed *D. canis* infection in all grafts in experiment one and in 8/10 grafts in experiment two. One mouse that completed experiment two, and that was negative for mites when assessed by NaOH digestion, had several mites in histological section and therefore the infection rate was 80%. Mites were located in the superficial 1/3 to 1/2 of primary and secondary hair follicles (Figure 4.3-8 and Figure 4.3-9). Mites were also observed in sebaceous ducts and occasionally in sebaceous glands (Figure 4.3-10). Mites led to mild dilation of the follicle lumen and thinning of the external root sheath epithelium but were separated from viable follicular keratinocytes by an intact keratinized layer, even when located in thin walled sebaceous ducts. In experiment one, inflammation was absent or minimal in skin grafts and was not associated with PBMC treatment and did not target *D. canis* infected hair follicles. Occasional aggregates of mixed inflammatory cells, predominately histiocytes, were present at the margins of some grafts, often around a hair shaft free in the dermis. In a few skin grafts, mild focal disruption of the epidermis (likely by mild graft trauma) was accompanied by focal granulocyte infiltration.

In experiment two however, a more prominent inflammatory cell infiltrate was observed in skin grafts from both the treatment and control groups. In one graft in the PBMC treated group (Group-I), a lymphocytic mural folliculitis targeted follicles,

including those containing mites (Figure 4.3-11). Lymphocytes infiltrated the follicle epithelium and were associated with vacuolation, occasional single cell necrosis and disorganization of the external root sheath keratinocytes. Eosinophils infiltrated the perifollicular dermis around several affected follicles. A similar lymphocytic reaction targeted patchy areas of the surface epidermis and a perivascular infiltrate of lymphocytes and macrophages was present in the dermis (Figure 4.3-11). A skin graft in the control group (Group-II) had a similar prominent mononuclear cell infiltrate in the dermis that was associated with scattered lymphocytic exocytosis in the surface epidermis and occasional single cell necrosis of keratinocytes (Figure 4.3-12). Additional skin grafts in the control group had a mild perivascular mononuclear cell infiltrate, as did grafts in the treatment group.

In both treatment and control groups for the two experiments, graft architecture resembled pregrafted skin. Primary and secondary hair follicles were present (usually near the margin of grafts) and 25 to 75% of follicles were in the anagen phase of the hair cycle. Hair follicles, sebaceous glands and apocrine glands were morphologically similar to donor skin. Normal basket weave orthokeratotic keratinization predominated. Additional histological findings included the presence regional to diffuse dermal fibrosis with central atrophy of adnexa in several grafts. Mast cells were scattered individually throughout the superficial and deep dermis. Aggregates of melanomacrophages were present in areas where hair follicles had atrophied. Mild irregular epidermal hyperplasia was common. Follicular keratosis was mild to moderate, affected the majority of skin grafts and was associated with cystic dilation of follicles in some grafts. Similar changes were observed in uninfected grafts that were not included in the trial.

Immunohistochemical staining of sections with anti-CD3 antibody confirmed the presence of T-lymphocytes in grafts from both the treatment and control groups for experiment two (Figure 4.3-13). CD3 positive cells surrounded hair follicles and infiltrated external root sheath epithelium. Positive cells also infiltrated the surface epidermis and were scattered in the dermis. Staining of serial sections with mouse specific anti-CD45 antibody identified mouse cells in the same areas as the CD3 positive cells (Figure 4.3-14).

In experiment one, canine IgG was detected (0.70 μg/mL) in 1/6 PBMC treated mice. In experiment two, canine IgG was detected in 3/3 surviving PBMC treated mice and the concentrations were 2,270 μg/ml, 0.3 μg/mL and 3.66 μg/ml. Canine IgG was also detected (1.32 μg/mL) in plasma from one mouse in the control group. Canine IgG was not detected in plasma samples from all other control mice in both experiments or from pre-graft plasma samples for all mice.

Anemia was not detected. The PCV at completion of the trial was similar to that of pre-treatment values and ranged between 42 and 47 (Table 4.3-5 and Table 4.3-6).

At total of six tgε26 mice died over the course of the two experiments. In experiment one, two mice died in Group-II and these mice lacked gross or histological tissue changes; a cause of death was not determined. For experiment two, one mouse in Group-I died with splenic lymphoma, while a second mouse died from complications of incisor overgrowth. In Group-II of this second experiment, the cause of death for one mouse was not determined and adequate diagnostic samples were not available from a another mouse. Gross and histological examinations did not reveal evidence of GVHD.

4.3.3 DISCUSSION

PBMC treatment of mice with *D. canis* infected skin grafts did not have a significant effect on mite numbers compared to controls. The highest numbers of mites recovered from a graft in experiment one was from the only mouse that had measurable plasma levels of canine IgG. Similarly, in experiment two, the highest numbers of mites were associated with a mouse with the highest levels of canine IgG, suggesting that lymphocytes may have interacted with mites.

Canine IgG was measured in only 1/6 mice (16%) in experiment one this was considered a low reconstitution rate compared to previous experiments with tgε26 mice where 15/17 (88%) mice had measurable IgG at four weeks after inoculation (Section 3.3). If this result reflects reconstitution of mice with canine T-cells, then the low survival of canine lymphocytes in tgε26 mice in experiment one could explain the lack of a significant treatment effect on mite numbers.

All of the mice (3/3) in experiment two had detectable levels of circulating canine IgG and this was expected given that mice were inoculated on two occasions with canine PBMC. In this experiment, the introduction of canine lymphocytes into tgε26 mice just prior to *D. canis* infection more closely parallels the interaction of mites and the host during naturally occurring disease. Few mice survived this experiment and wide intragroup variation in mite numbers made it difficult to determine if PBMC treatment affected the number of mits on skin grafts. The impact of PBMC treatment was further complicated by evidence that some tgε26 mice developed functional lymphocytes.

Tgε26 mice were considered to have functional lymphocytes because histological evidence of graft rejection was present in skin grafts from both the PBMC treated and

control group. An interface dermatitis and interface folliculitis was associated with infiltration of CD3+ T-cells. IHC staining with murine specific anti-CD45 monoclonal antibody identified murine cells within these lesions. Similar to the graft rejection reaction observed with ICR scid mice (Section 4.2), eosinophils accompanied the lymphocytes targeting the epidermis. CD3+ T-cells were subsequently identified in lymphoid tissues of tgε26 mice that did not receive any foreign tissues (neither canine skin grafts nor PBMC) (personal observation, data not shown). This would suggest that T-cell "leakiness" is intrinsic to the tgε26 mice and was not induced by experimental conditions.

As part of this graft rejection reaction, a prominent murine lymphocytic interface folliculitis developed in a canine skin graft supporting *D. canis*. This graft supported the highest number of *D. canis* and the graft rejection reaction, similar histological changes of naturally occurring demodicosis, did not appear to limit mite colonization (Caswell *et al.*, 1997).

Similar to the previous experiment with ICR scid mice (Section 4.2), high *D. canis* infection rates were achieved using tgε26 mice in experiment one (100%) and experiment two (80%). In contrast to the ICR scid experiment, more immature stages were present than adult mites on skin grafts in both experiments with tgε26 mice, suggesting that the kinetics of mite replication was different. Because mites were collected from different sources, the differences in mite populations between experiments could not be attributed to other experimental parameters. There was a significant positive linear association between mites recovered from skin graft digest samples and the number of follicle units on each digest sample. This finding was expected because *D. canis*

require the hair follicle environment to survive and reinforces the need for uniform hair growth on grafts when modeling canine demodicosis.

In experiment one, skin grafts did not develop gross lesions after *D. canis* infection or after lymphocyte transfer. Grafts continued to grow hair, despite the presence of large numbers of actively proliferating mites, and, by histological evaluation, mites did not appear to directly damage hair follicles. This observation provided evidence that *D. canis* overgrowth on skin grafts is not associated with morphologic or functional alterations of hair follicles. Surface scaling was considered to be slightly more prominent for the majority of skin grafts in experiment two at the end of the trial and this change was attributed to inflammation associated with graft rejection.

After healing, skin grafts varied in quality in both experiments. Central eschar formation, indicative of ischemic damage, was similar to that observed for full-thickness skin grafts on tgε26 mice (Section 3.2). This finding confirmed that the variability in graft quality was not due to differences between canine skin donors. However, graft healing in experiment one was considered improved, showing less severe eshar formation and better hair regrowth, compared to experiment two. This improvement was attributed to longer bandaging times (9-12 days versus 7-9 days) and was similar to that observed for grafts on ICR scid mice bandaged for 12 days (Section 4.2).

Tgε26 mice were not hardy and did not tolerate the multiple procedures and long-term nature of these experiments well. Death of tgε26 mice over the course of experiments (17 and 40%) was a significant complication. Mice were lost for a variety of reasons and no common, preventable, cause of death was identified. One mouse died due to splenic lymphoma, which was observed previously for two tgε26 mice (Section 3.3).

As with previous experiments using tgε26 mice, the development of GVHD was not observed and hemolytic anemia was not identified.

In summary, a significant difference in mite numbers was not observed after the introduction of canine PBMC to mice supporting *D. canis* infected grafts. Although, higher numbers of mites were associated with higher mouse plasma canine IgG levels suggesting that, like the experiment with ICR scid mice, canine PBMC stimulated mite proliferation. The grafting results point to increasing the bandaging time to improve the quality full-thickness canine skin xenografts and reinforce the need to develop well haired uniform skin grafts for the purposes of modeling demodicosis. The development of functional mouse lymphocytes, similar to "leaky" scid/bg and ICR scid mice, and the decreased longevity of tgε26 mice makes this mouse type unsuitable for experiments modeling demodicosis; a new immunodeficient mouse must be sought for these purposes.

Figure 4.3-3: Appearance of representative canine skin grafts on tgε26 mice that received canine PBMC (Group-I) or PBS (Group-II) once after *D. canis* infection (experiment one); Group-I **(A)**, and Group-II **(B)**. Skin grafts did not develop gross changes after *D. canis* infection or after canine PBMC transfer.

A

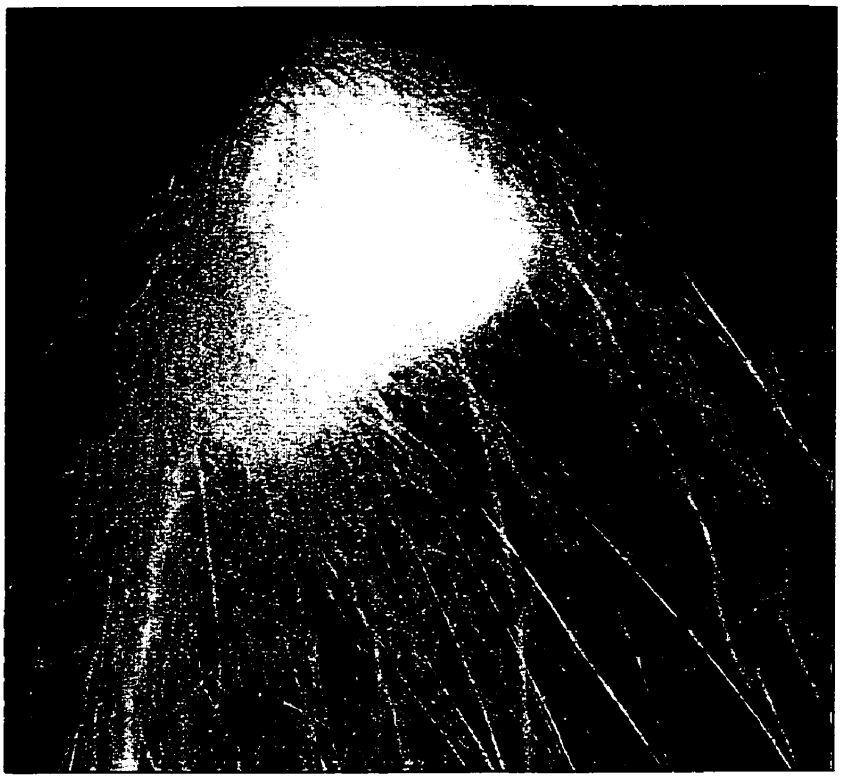

B

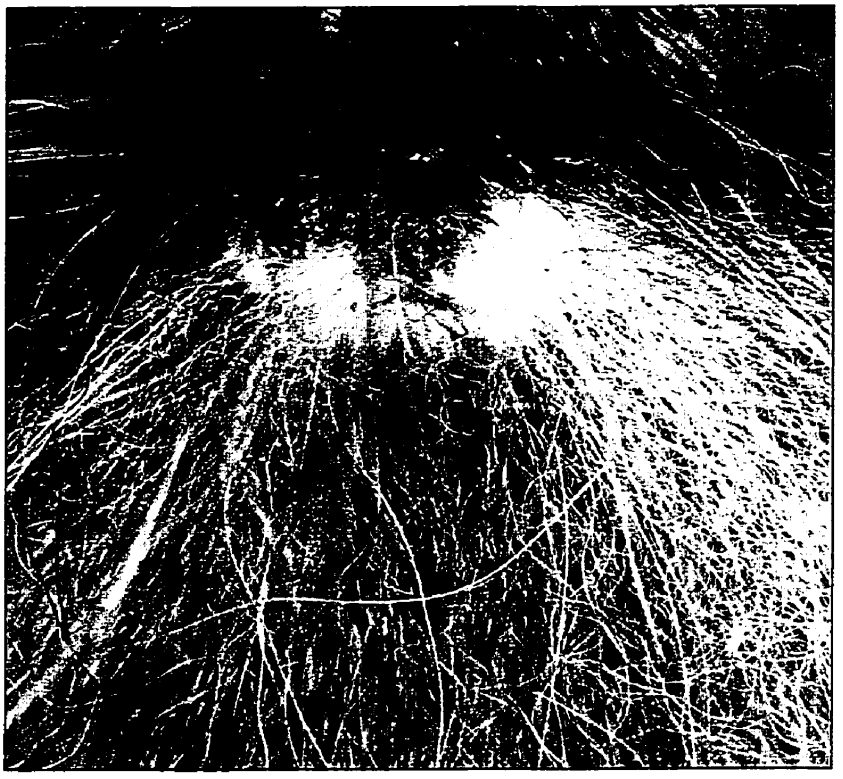

Figure 4.3-4: Bar graph showing the results of *D. canis* enumeration, by NaOH digestion, for canine skin grafts on tgε26 mice that received canine PBMC or PBS once after mite infection (experiment one). **(A)** Calculated total number of *D. canis* per hair follicle unit (mean ± standard error) recovered grafts in the PBMC treated group (Group-I) and PBS control group (Group-II). **(B)** The calculated total number of each *D. canis* life-cycle stage per hair follicle unit (mean ± standard error) recovered from graft samples for Group-I and Group-II.

(A)

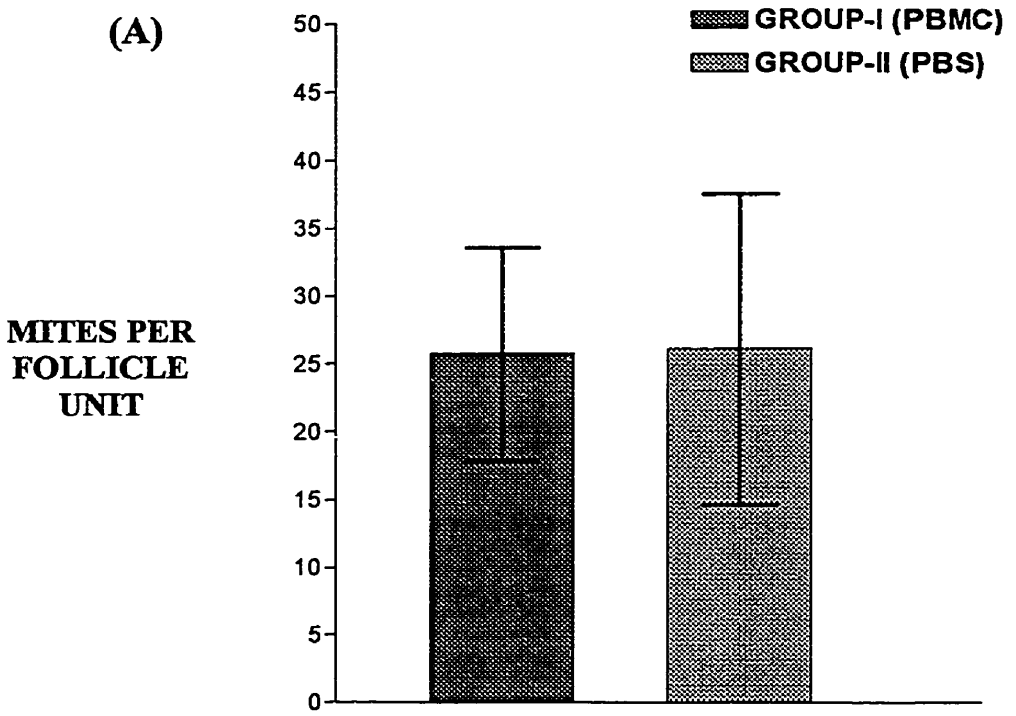
GROUP-I (PBMC)
GROUP-II (PBS)
MITES PER FOLLICLE UNIT
50
45
40
35
30
25
20
15
10
5
0

(B)

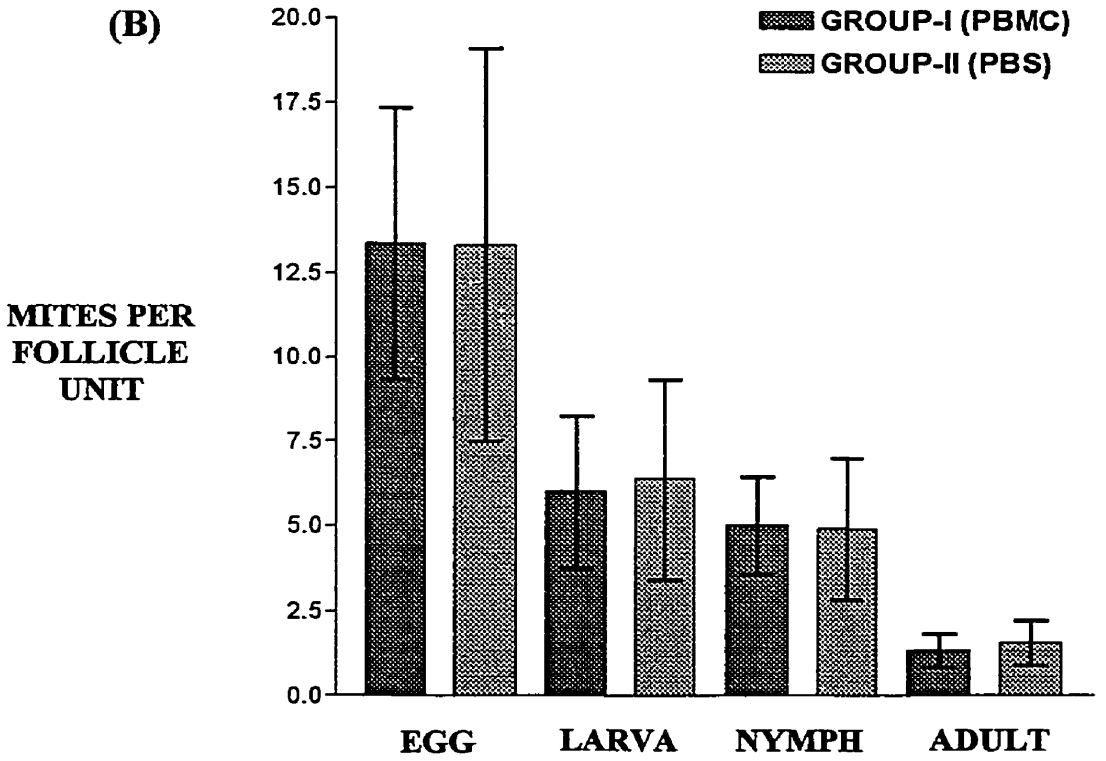
GROUP-I (PBMC)
GROUP-II (PBS)
MITES PER FOLLICLE UNIT
20.0
17.5
15.0
12.5
10.0
7.5
5.0
2.5
0.0
EGG
LARVA
NYMPH
ADULT

Figure 4.3-5: Bar graph showing the results of *D. canis* enumeration, by NaOH digestion, for canine skin grafts on tgε26 mice that received canine PBMC or PBS once after mite infection (experiment one). **(A)** Calculated total number of *D. canis* per graft digest sample (mean ± standard error) recovered from grafts in the PBMC treated group (Group-I) and PBS control group (Group-II). **(B)** The calculated total number of each *D. canis* life-cycle stage per graft digest sample (mean ± standard error) recovered from graft in Group-I and Group-II.

(A)

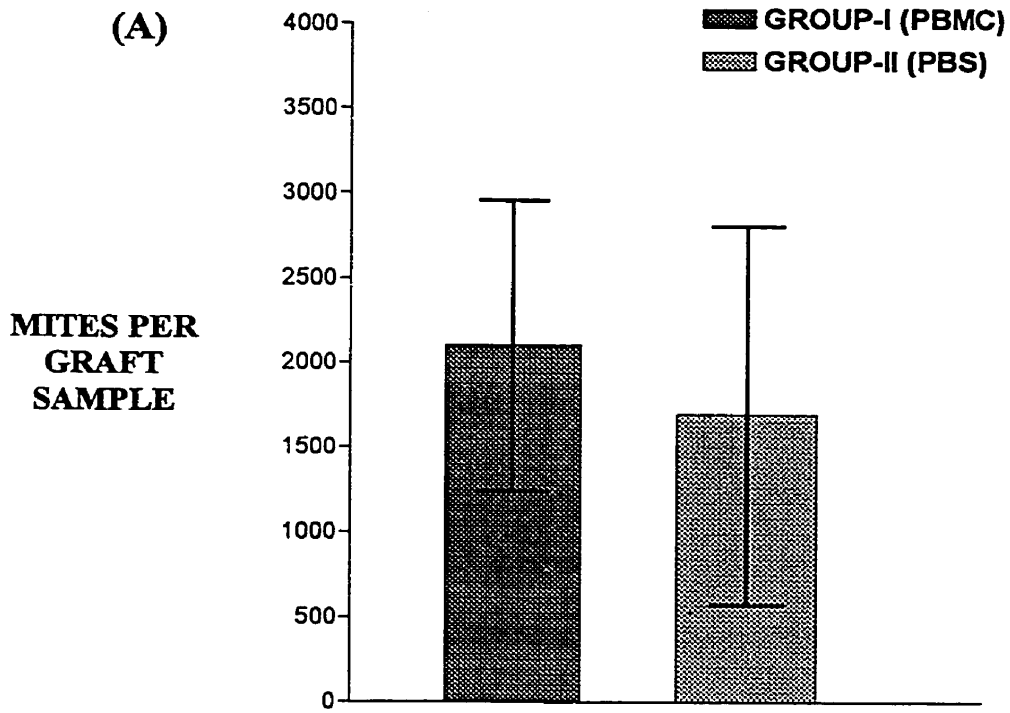
GROUP-I (PBMC)
GROUP-II (PBS)
MITES PER GRAFT SAMPLE
4000
3500
3000
2500
2000
1500
1000
500
0

(B)

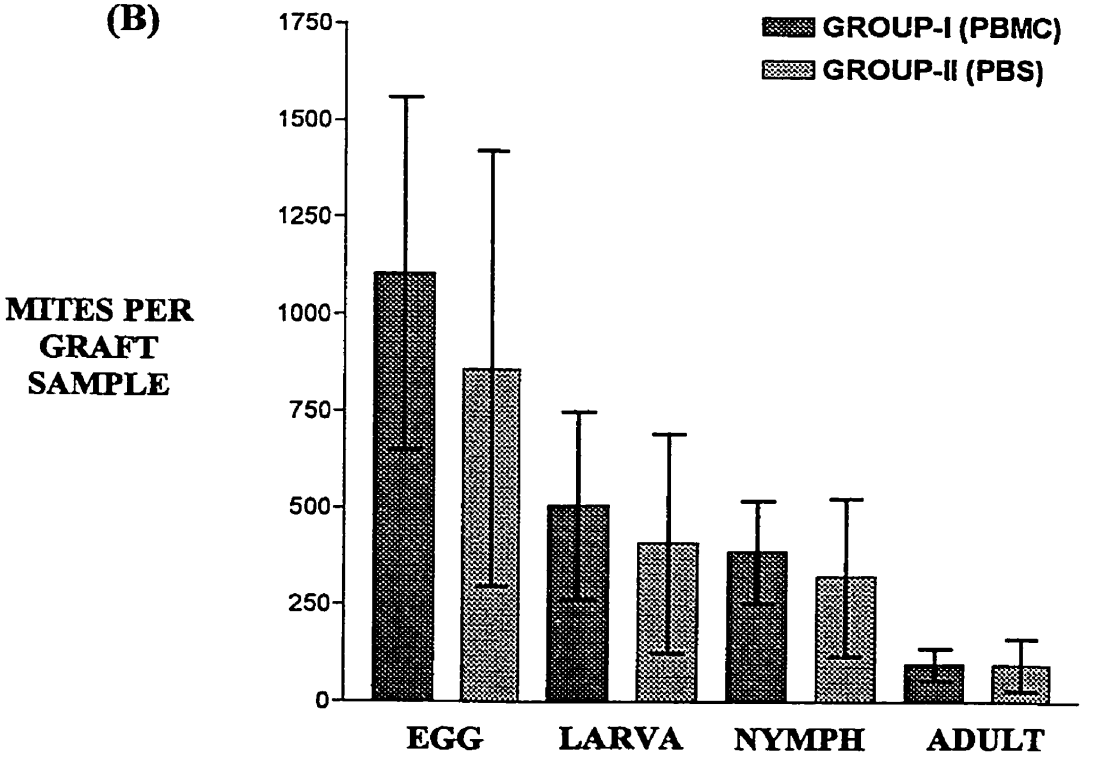
GROUP-I (PBMC)
GROUP-II (PBS)
MITES PER GRAFT SAMPLE
1750
1500
1250
1000
750
500
250
0
EGG
LARVA
NYMPH
ADULT

Figure 4.3-6: Bar graph showing the results of *D. canis* enumeration, by NaOH digestion, for canine skin grafts on tgε26 mice that received canine PBMC or PBS twice, before and after mite infection (experiment two). **(A)** The calculated total number of *D. canis* per follicle unit (mean ± standard error) recovered from grafts in the PBMC treated group (Group-I) and PBS control group (Group-II). **(B)** The calculated total number of each *D. canis* life-cycle stage per follicle unit (mean ± standard error) recovered from grafts in Group-I and Group-II.

(A)

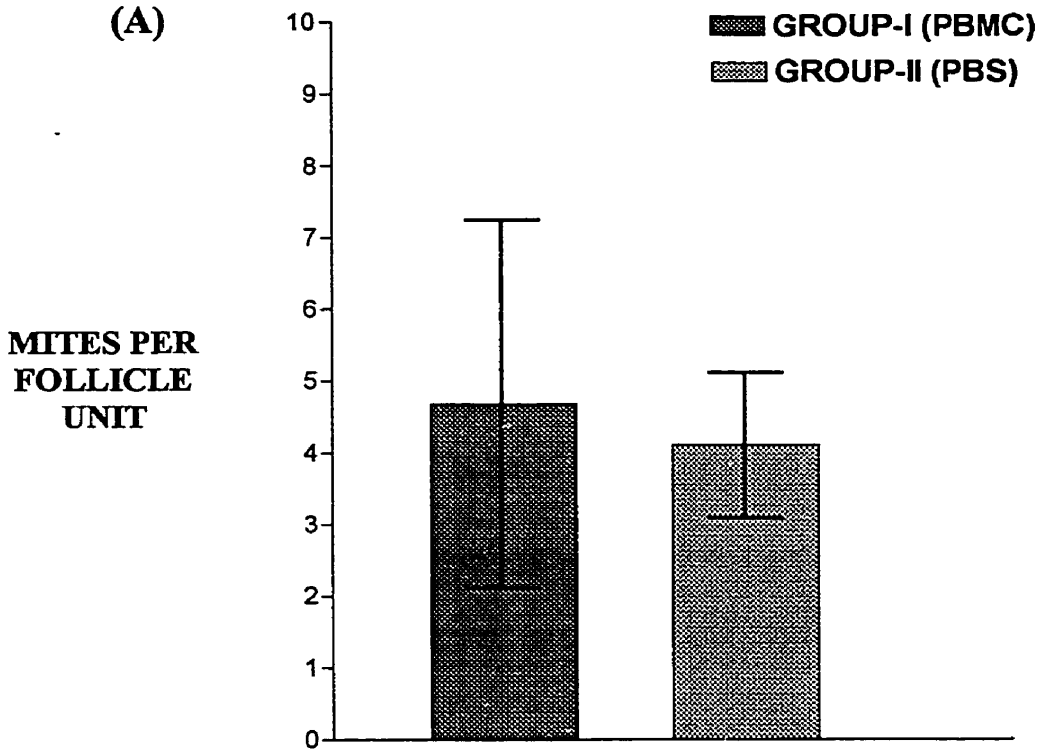
GROUP-I (PBMC)
GROUP-II (PBS)
MITES PER FOLLICLE UNIT
10
9
8
7
6
5
4
3
2
1
0

(B)

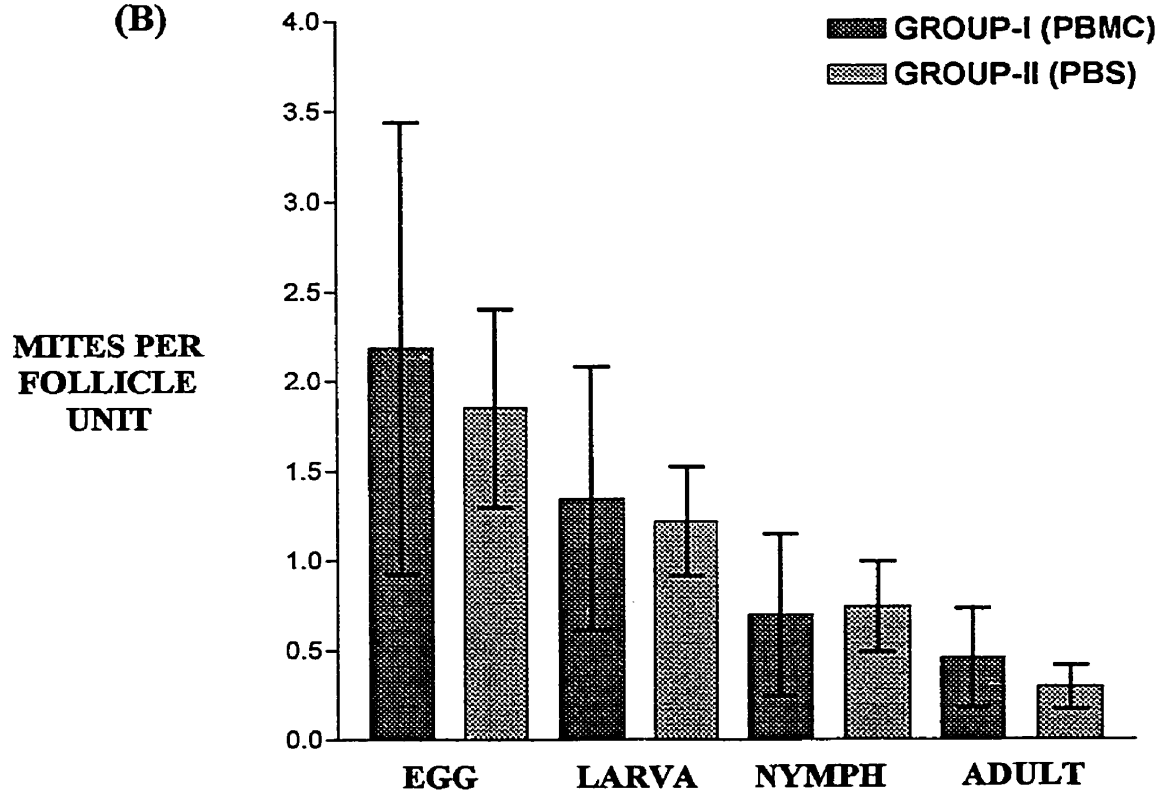
GROUP-I (PBMC)
GROUP-II (PBS)
MITES PER FOLLICLE UNIT
4.0
3.5
3.0
2.5
2.0
1.5
1.0
0.5
0.0
EGG
LARVA
NYMPH
ADULT

Figure 4.3-7: Bar graph showing the results of *D. canis* enumeration, by NaOH digestion, for canine skin grafts on tgε26 mice that received canine PBMC or PBS twice, before and after mite infection (experiment two). **(A)** The calculated total number of *D. canis* per skin graft digest sample (mean ± standard error) for the PBMC treated group (Group-I) and PBS control group (Group-II). **(B)** The calculated total number of each *D. canis* life-cycle stage per graft digest sample (mean ± standard error) recovered from grafts in Group-I and Group-II.

(A)

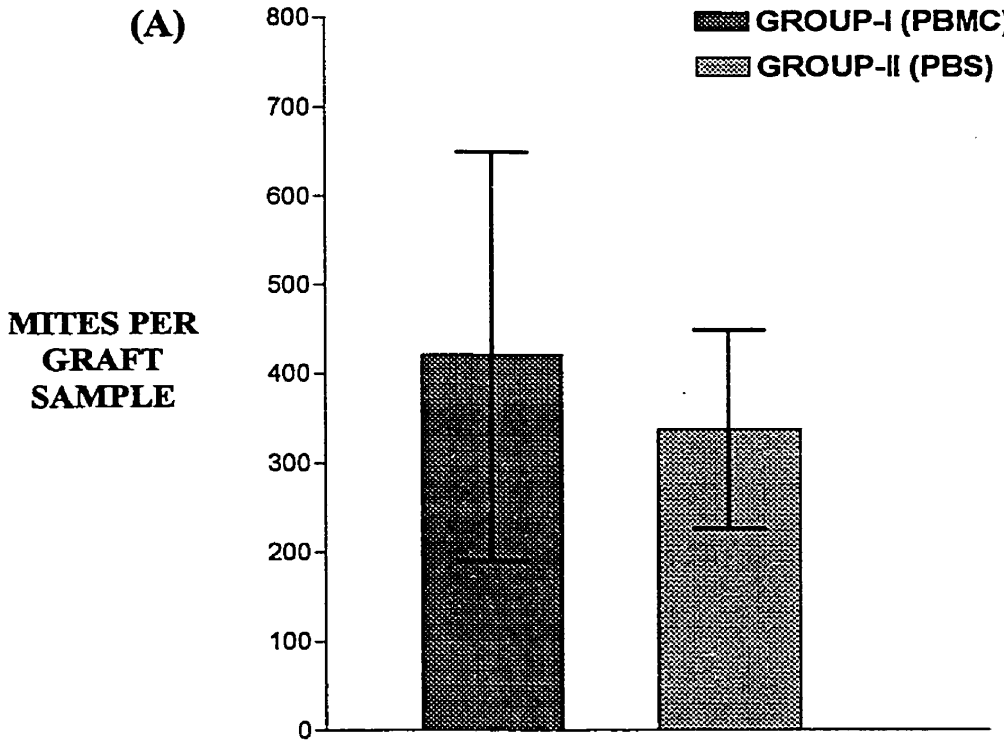
GROUP-I (PBMC)
GROUP-II (PBS)
MITES PER GRAFT SAMPLE
800
700
600
500
400
300
200
100
0

(B)

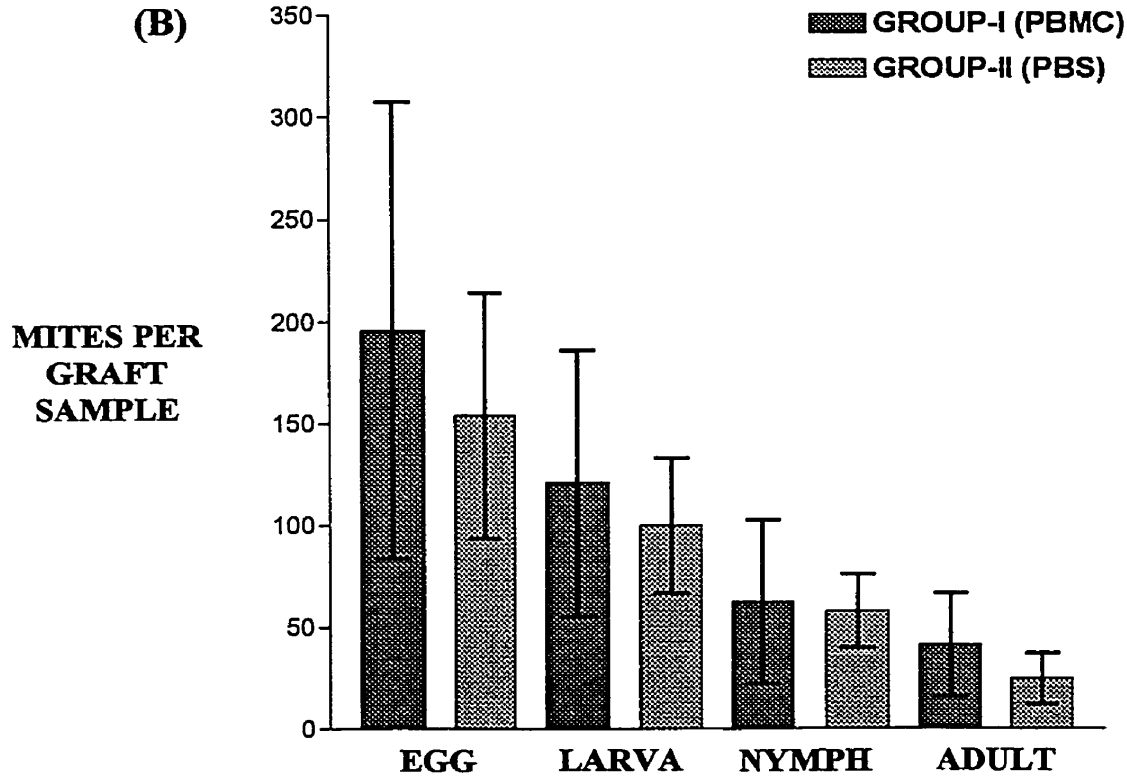
GROUP-I (PBMC)
GROUP-II (PBS)
MITES PER GRAFT SAMPLE
350
300
250
200
150
100
50
0
EGG
LARVA
NYMPH
ADULT

Figure 4.3-8: Photomicrographs of a representative canine skin graft from a tgε26 mouse that received PBMC once (Group-I), after mite infection (experiment one). **(A)** Low magnification shows the overall graft morphology and lack of inflammatory cell infiltrates (magnification = X10). **(B)** At higher magnification, numerous cross sections of *D. canis* (arrow) are visible within follicle lumens (magnification = X25). Hematoxylin and eosin stained, paraffin embedded, tissue sections

A

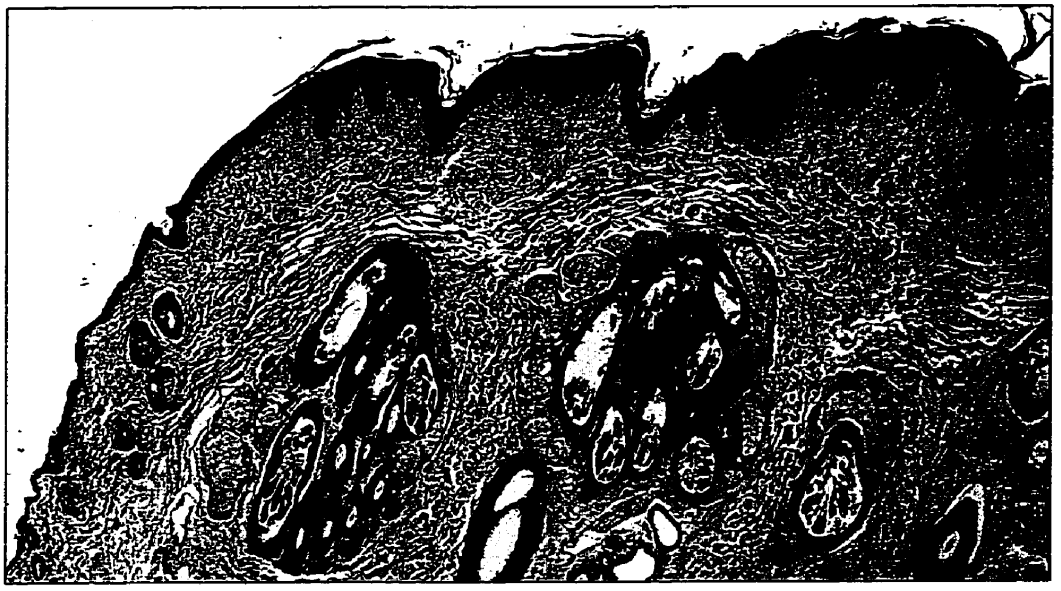

B

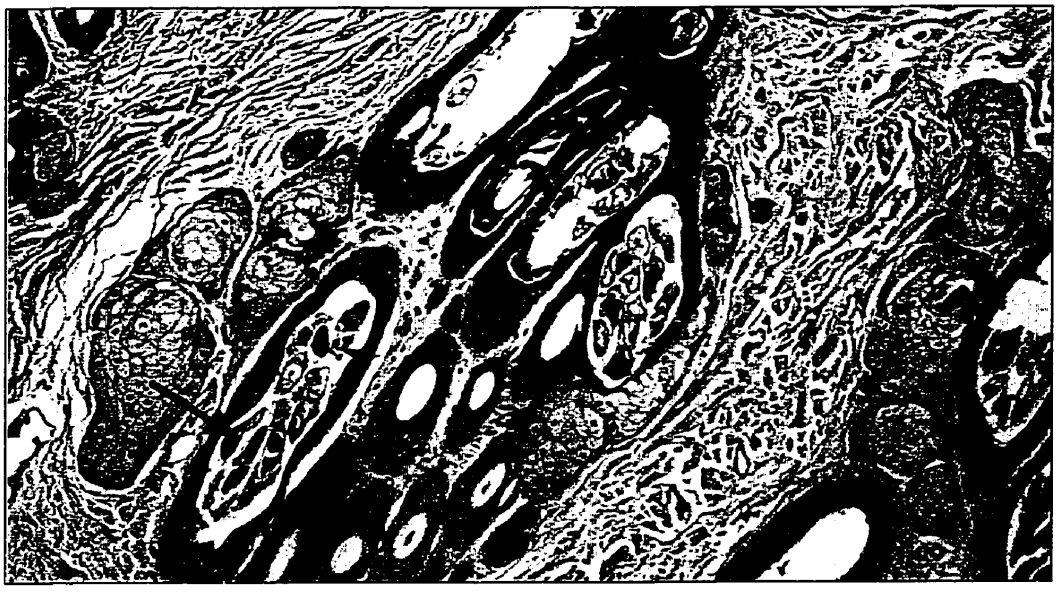

Figure 4.3-9: Photomicrographs of a representative canine skin graft from a tgε26 mouse that received PBS once (Group-II), after mite infection (experiment one). **(A)** Low magnification shows the overall graft morphology and lack of inflammatory cell infiltrates (magnification = X10). **(B)** At higher magnification, numerous cross sections of *D. canis* (arrow) are visible within follicle lumens (magnification = X25). Hematoxylin and eosin stained, paraffin embedded, tissue sections

A

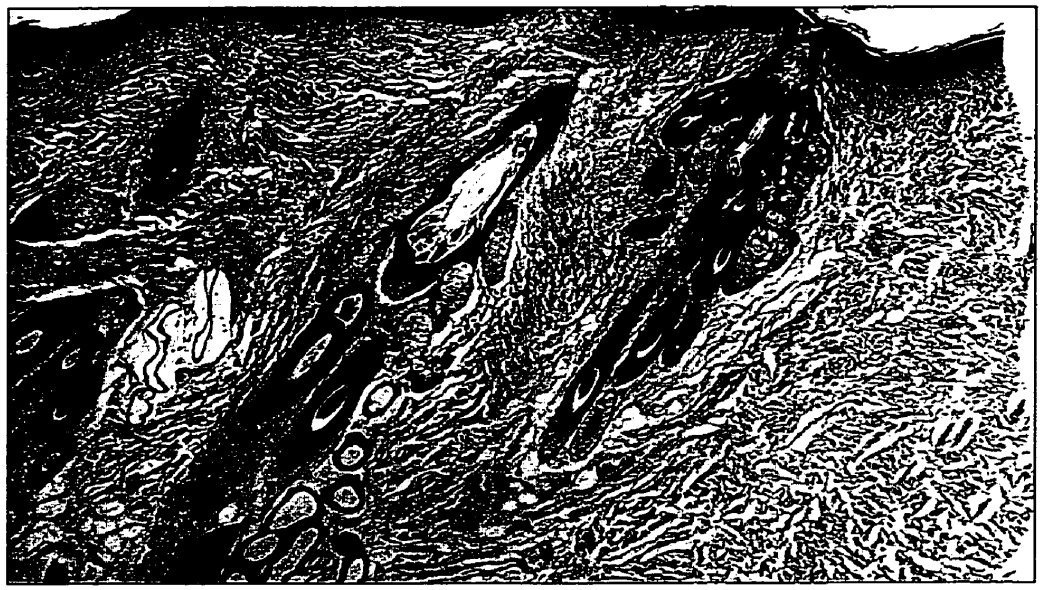

B

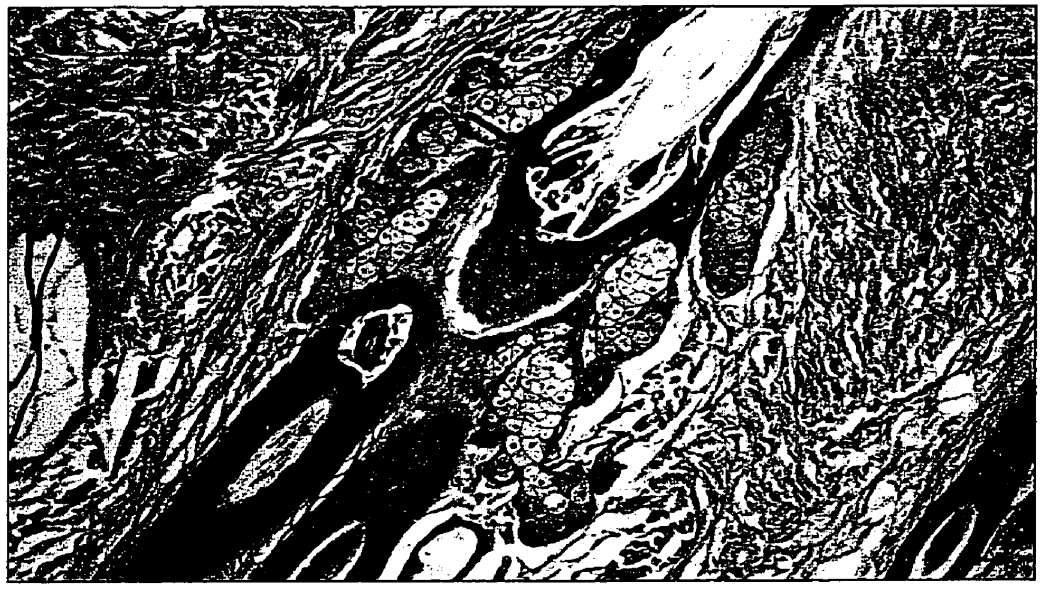

Figure 4.3-10: Photomicrographs of a representative canine skin graft from a tgε26 mouse that received PBMC (Group-I) or PBS (Group-II) once, after mite infection (experiment one). **(A)** Tissue section from a graft in Group-I with several *D. canis* (arrow) within a dilated sebaceous gland duct (magnification= X50). **(B)** Tissue section from a graft in Group-II shows *D. canis* (arrow) within a sebaceous gland lobule (magnification = X40). Hematoxylin and eosin stained, paraffin embedded, tissue sections

A

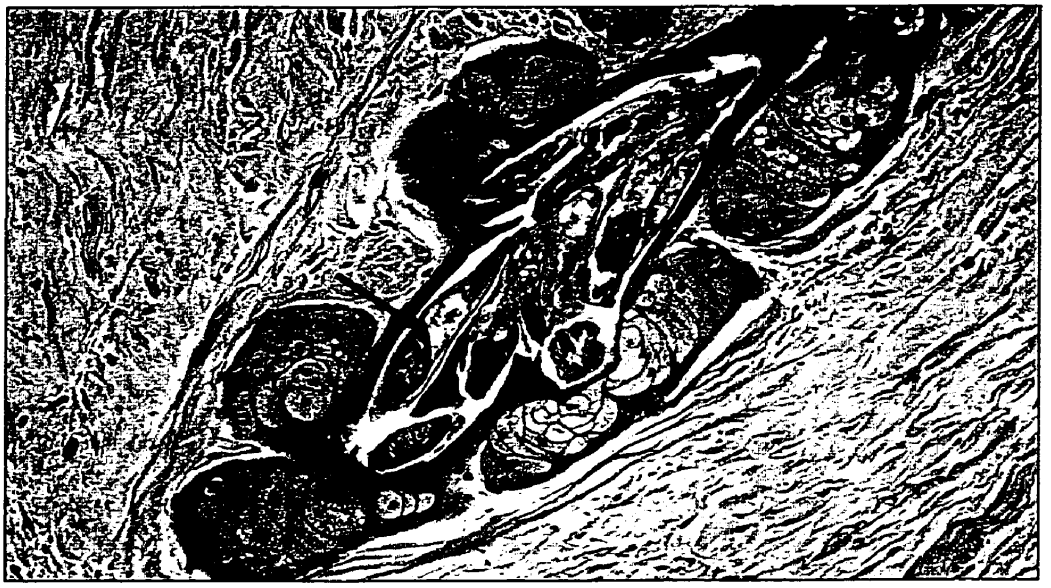

B

Figure 4.3-11: Photomicrographs of a canine skin graft from a tgε26 mouse that had received canine PBMC twice (Group-I), before and after mite infection (experiment two). **(A)** Low magnification shows the overall graft morphology and generalized nature of inflammatory cell infiltrates (magnification = X10). **(B)** At higher magnification, a lymphocytic interface folliculitis is observed to target a follicle containing *D. canis* (arrow) (magnification = X70). **(C)** Lymphocytes also infiltrate the surface epidermis (magnification =X70). Hematoxylin and eosin stained, paraffin embedded, tissue sections

A

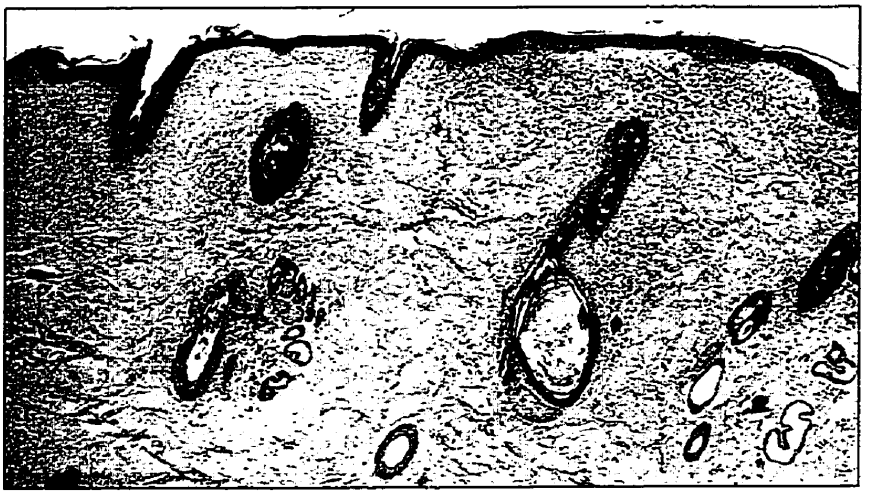

B

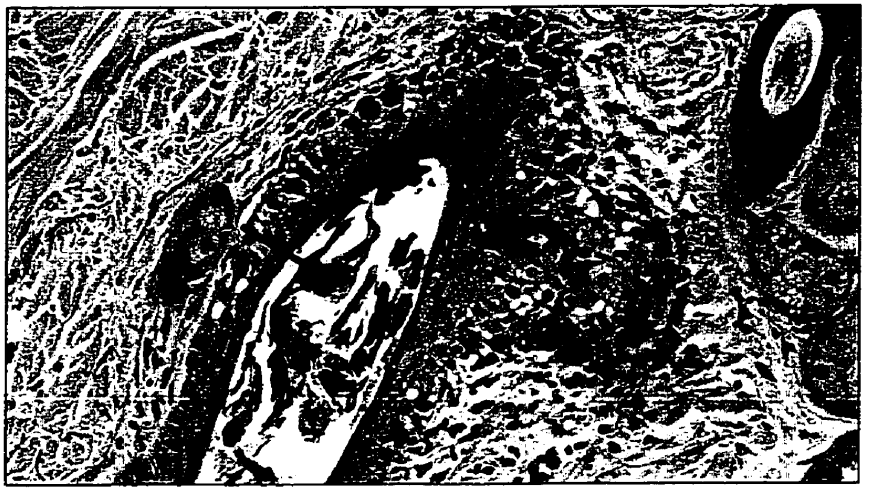

C

Figure 4.3-12: Photomicrographs of a canine skin graft on a tgε26 mouse that had received canine PBS twice (Group-II), before and after mite infection (experiment two). **(A)** Low magnification shows the overall graft morphology and generalized nature of inflammatory cell infiltrates (magnification = X10). **(B, C)** Higher magnification shows lymphocytes infiltrating the epidermis. Lymphocytes are associated with occasional single cells necrosis of keratinocytes (arrows)(magnification = X50). Hematoxylin and eosin stained, paraffin embedded, tissue sections

A

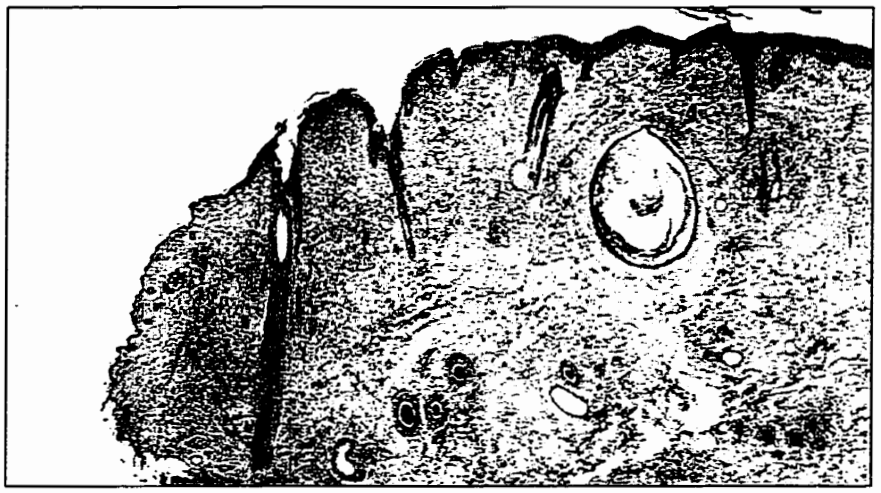

B

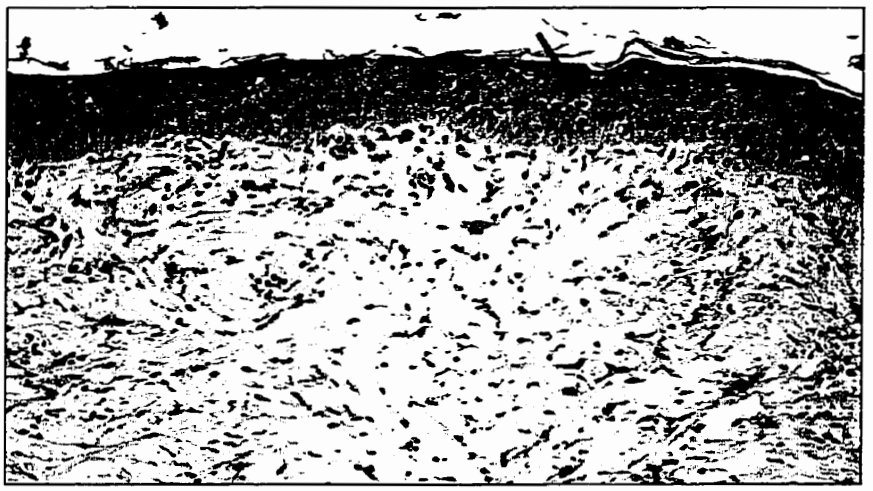

C

Figure 4.3-13: Photomicrographs of CD3 immunostained canine skin grafts from tgε26 mice that had received canine PBMC (Group-I) or PBS (Group-II), before and after mite infection (experiment two). Positive immunoreaction with anti-CD3 antibody identifies many T-cells (arrows) in skin grafts from Group-I **(A)** and Group-II **(B)** (magnification = X100). Avidin-Biotin complex peroxidase method, diaminobenzidine (DAB) chromagen, hematoxylin counterstain.

A

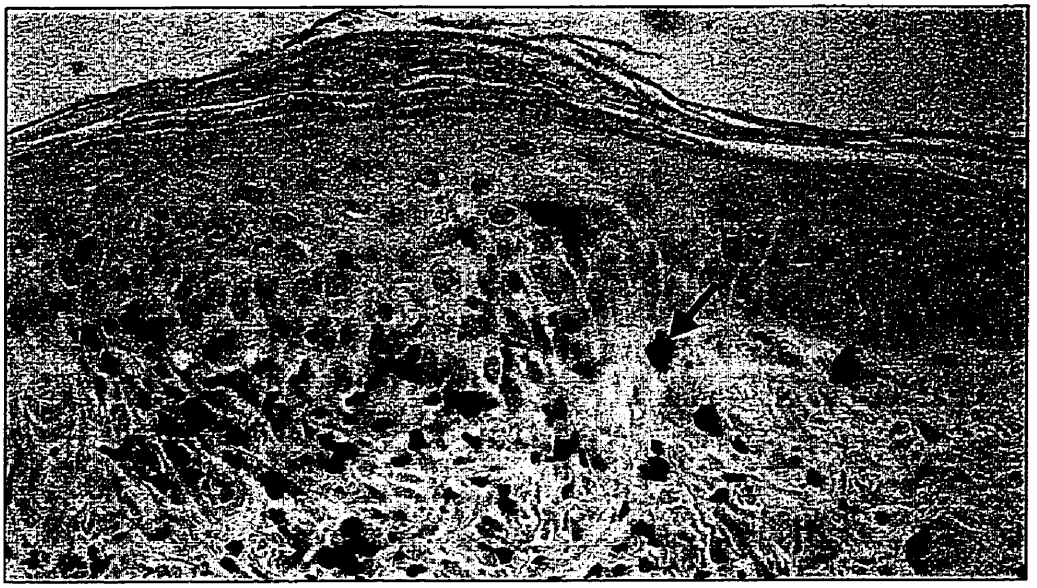

B

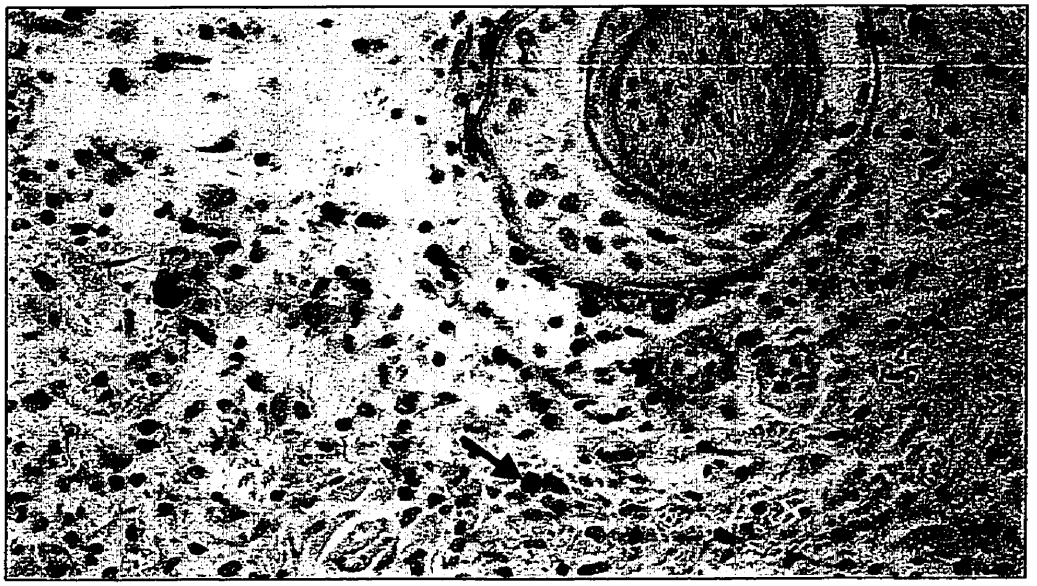

Figure 4.3-14: Photomicrographs of CD45 immunostained canine skin grafts from tgε26 mice that had received canine PBMC (Group-I) or PBS (Group-II), before and after mite infection (experiment two). Positive immunoreaction with anti-CD45 antibody identifies murine mononuclear cells consistent with T-cells (arrows) in canine skin grafts from Group-I **(A)** and Group-II **(B)** (magnification = X100). Avidin-Biotin complex peroxidase method, diaminobenzidine (DAB) chromagen, hematoxylin counterstain.

A

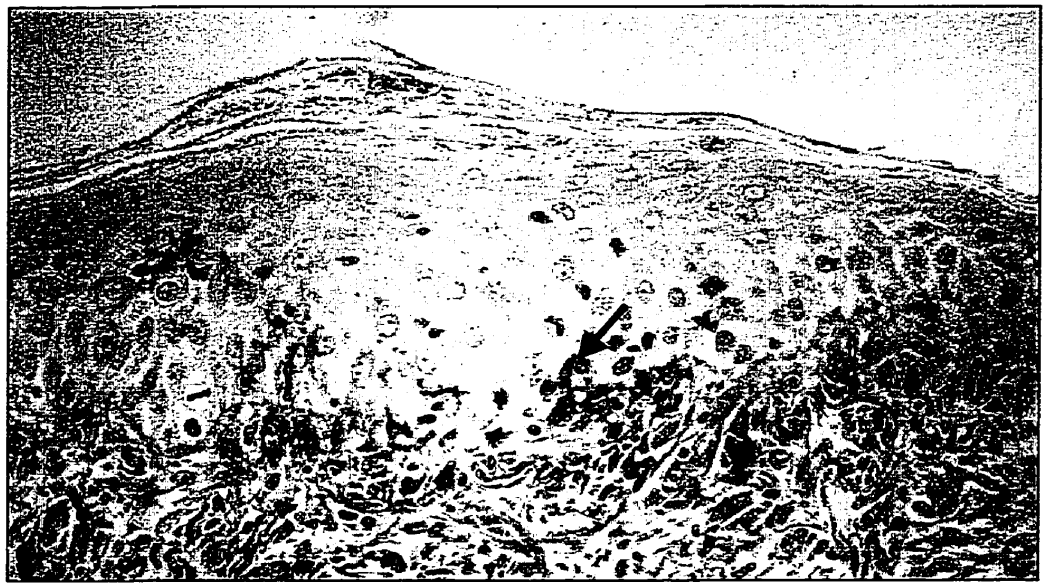

B

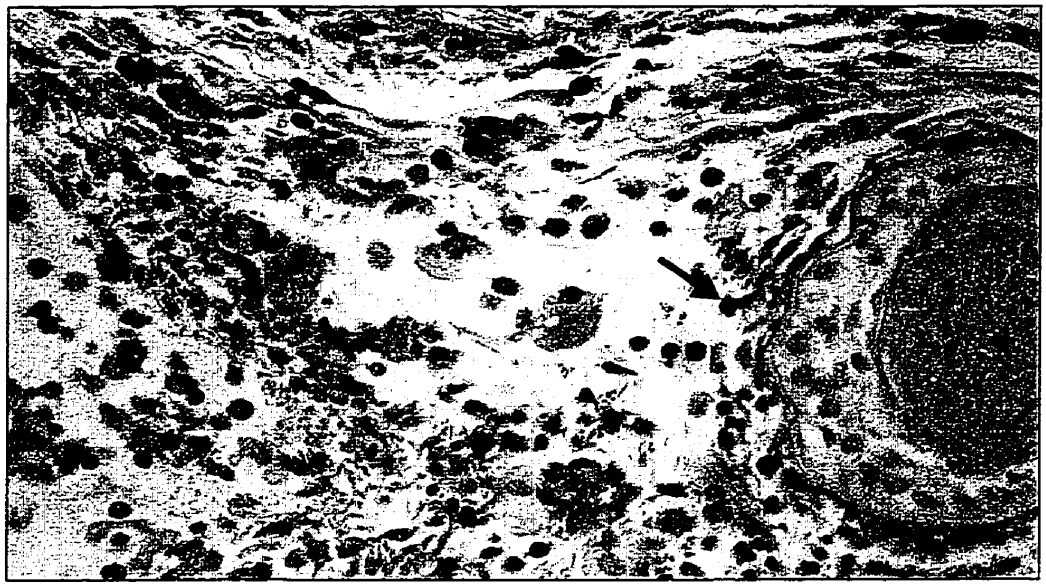

Table 4.3-1: Calculated Number of *D. canis* Per Follicle Unit on Digest Samples from Skin Grafts on Tgε26 Mice that Received PBMC or PBS Once After Mite Infection (Experiment One)

Mouse (FU / Graft)	Calculated Stage Totals / Follicle				Calculated Mite Totals / FU
	Egg	Larva	Nymph	Adult	
Group-I (*D. canis* plus PBMC)					
1 (51)	5.72	2.86	1.58	0.30	10.65
2 (102)	32.19	16.01	9.21	2.81	60.32
3 (98)	11.42	7.07	5.50	0.82	24.82
4 (48)	15.00	6.88	9.06	2.81	33.85
5 (115)	7.28	1.27	1.79	0.23	10.57
6 (44)	8.52	1.93	2.84	1.02	14.31
Mean ± SEM	13.35 ± 3.99	6.004 ± 2.242	4.99 ± 1.42	1.33 ± 0.48	25.75 ±7.85
Group-II (*D. canis* plus PBS)					
1 (83)	30.09	15.02	10.91	3.53	59.75
2 (18)	9.82	4.91	3.00	1.09	18.81
3 (25)	3.45	1.82	1.42	0.81	7.50
4 (68)	9.85	3.75	4.34	0.81	18.75
Mean ± SEM	13.30 ± 5.79	6.37 ± 2.95	4.91 ± 2.08	1.56 ± 0.66	26.20 ±11.49

FU – Active hair follicle unit

Table 4.3-2: Calculated Number of *D. canis* Per Skin Graft Digest Sample from Grafts on Tgε26 Mice that Received PBMC or PBS Once After Mite Infection (Experiment One)

Mouse	Calculated Stage Totals				Calculated Mite Totals
	Egg	Larva	Nymph	Adult	
Group-I (*D. canis* plus PBMC)					
1	290.00	145.00	80.00	15.00	540.00
2	3283.38	1633.17	939.06	286.64	6153.27
3	1118.88	693.26	539.46	79.99	2433.33
4	720.00	330.00	435.00	135.00	1625.00
5	839.16	146.65	206.46	26.66	1219.98
6	375.00	85.00	125.00	45.00	630.00
Mean ± SEM	1104.40 ±453.19	505.514 ±243.12	387.49 ±132.38	98.04 ±41.65	2100.26 ±858.96
Group-II (*D. canis* plus PBS)					
1	2497.50	1246.54	905.76	293.30	4959.50
2	180.00	90.00	55.00	20.00	345.00
3	85.00	45.00	35.00	20.00	185.00
4	670.00	255.00	295.00	55.00	1275.00
Mean ± SEM	858.12 ±561.28	409.13 ±282.76	322.69 ±203.13	97.07 ±65.92	1691.12 ±1115.64

Table 4.3-3: Calculated Number of *D. canis* Per Follicle Unit on Digest Samples Collected from Skin Grafts on Tgε26 Mice that Received PBMC or PBS Before and After Mite Infection (Experiment Two)

Mouse (FU / Graft)	Calculated Stage Totals / Follicle				Calculated Mite Totals / FU
	Egg	Larva	Nymph	Adult	
Group-I (*D. canis* plus PBMC)					
1 (91)	2.20	1.51	0.55	0.96	5.22
2 (89)	4.35	2.53	1.54	0.42	8.85
3 (63)	0.00	0.00	0.00	0.00	0.00
Mean ± SEM	2.18 ±1.25	1.34 ±0.73	0.69 ±0.45	0.46 ±0.27	4.68 ±2.56
Group-II (*D. canis* plus PBS)					
1 (72)	1.22	0.69	0.35	0.17	2.43
2 (72)	1.39	1.22	1.22	0.17	3.99
3 (93)	2.96	1.75	0.67	0.54	5.91
Mean ± SEM	1.85 ±0.55	1.21 ±0.30	0.74 ±0.25	0.29 ±0.12	4.11 ±1.00

FU – Active hair follicle unit

Table 4.3-4: Calculated Number of *D. canis* Per Skin Graft Digest Sample Collected from Grafts on Tgε26 Mice that Received PBMC or PBS Before and After Mite Infection (Experiment Two)

Mouse	Calculated Stage Totals				Calculated Mite Totals
	Egg	Larva	Nymph	Adult	
Group-I (*D. canis* plus PBMC)					
1	200.00	137.50	50.00	87.50	475.00
2	387.50	225.00	137.50	37.50	787.50
3	0.00	0.00	0.00	0.00	0.00
Mean ± SEM	195.83 ±111.88	120.83 ±65.48	62.50 ±40.18	41.66 ±25.34	420.83 ±228.93
Group-II (*D. canis* plus PBS)					
1	87.50	50.00	25.00	12.50	175.00
2	100.00	87.50	87.50	12.50	287.50
3	275.00	162.50	62.50	50.00	550.00
Mean ± SEM	154.16 ±60.52	100.00 ±33.07	58.33 ±18.16	25.00 ±12.50	337.50 ±111.10

Table 4.3-5: Tgε26 Mouse PCV Values at the Onset and at Completion of Experiment One Where Mice Received PBMC or PBS Once Before Mite Infection

Mouse	PCV at Onset of Experiment	PCV at Completion
Group-I (*D. canis* plus PBMC)		
1	38	46
2	42	42
3	47	43
4	46	43
5	44	44
6	45	46
Group-II (*D. canis* plus PBS)		
1	40	46
2	45	43
3	43	46
4	53	47
5	42	†
6	49	†

Mean PCV and 95% Confidence Intervals (CI) for mice (n=12) at the onset of tgε26 experiment one: Mean = 44.42, Lower 95% CI = 41.97, Upper 95% CI = 46.86

† - Mouse died prior to completion of the experiment

Table 4.3-6: Tgε26 Mouse PCV Values at the Onset and at Completion of Experiment Two Where Mice Received PBMC or PBS Before and After Mite Infection

Mouse	PCV at Onset of Experiment	PCV at Completion
Group-I (*D. canis* plus PBMC)		
1	43	43
2	44	47
3	43	45
4	43	†
5	45	†
Group-II (*D. canis* plus PBS)		
1	45	45
2	44	46
3	43	44
4	44	†
5	46	†

Mean PCV and 95% Confidence Intervals (CI) for mice (n=10) at the onset of tgε26 experiment two: Mean = 44.00, Lower 95% CI = 43.25, Upper 95% CI = 44.75

† - Mouse died prior to completion of the experiment

4.4 USE OF CANINE SKIN-XENOGRAFT *RAG2* MOUSE-CHIMERAS TO MODEL CANINE DEMODICOSIS

Sufficient numbers of tgε26 mice did not survive the lengthy experiments modeling demodicosis and some mice developed functional lymphocytes; both factors limiting the use of this mouse mutant for this study.

The *Rag1* and *Rag2* knockout mice have nearly an identical phenotype and lack T-cells and B-cells and do not suffer from the "leaky" phenotype (Mombaerts *et al.*, 1992; Shinkai *et al.*, 1992). *Rag1* null mice will support human skin grafts for 10 months without evidence of rejection (Atillasoy *et al.*, 1997). Both of these mouse mutants are sold commercially; only *Rag2* mice were available for this study.

In order to ensure that canine lymphocytes accessed skin grafts in adequate numbers, direct intragraft injection (instead of intraperitoneal injection) was chosen as the method of delivering canine PBMC for this experiment. Canine lymphocytes were previously shown to survive intragraft inoculation and remained functional after transfer (Section 3.4). To ensure that adequate numbers of lymphocytes were activated in skin grafts, and in an attempt to increase engraftment, an experimental group was added in which lymphocytes were stimulated *in vitro* prior to injection into skin grafts. A lymphocyte stimulation protocol using human recombinant interleukin-2 (hr-IL-2) and phytohemagglutinin (PHA) was chosen for this purpose. The primary objective of this experiment was to evaluate the effect of canine lymphocytes on *D. canis* populations on canine skin.

4.4.1 MATERIALS AND METHODS

4.4.1.1 Animals

Male *Rag2* knockout mice, aged five to six weeks, were housed with two to three per micro-isolator cage. An adult, intact-male, golden retriever dog was purchased from Animal Care Services (University of Guelph, Ontario, Canada). *Demodex canis* were collected from a dog in the Province of Quebec.

4.4.1.2 Experimental Design

The experimental design followed that of the ICR scid experiment (Section 4.2), except for the route of lymphocyte transfer. Skin grafts were infected with *D. canis* only once and leukocytes were transferred once by direct intragraft injection instead of by intraperitoneal injection. There were four experimental groups; two received leukocytes and one received PBS after *D. canis* infection. Group-I received PBL that were stimulated *in vitro*, while Group-II received unstimulated PBMC. Group-III received PBS. Group-IV received *in vitro* stimulated PBL only, but no mites. The timeline for the *Rag2* experiment is given in Figure 4.4-1.

Figure 4.4-1: Timeline for *Rag2* experiment

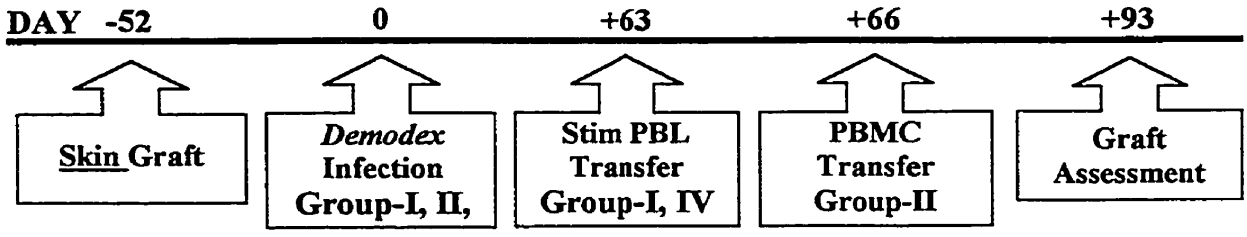

4.4.1.3 Experimental Protocol

Skin grafting: Thirty-three *Rag2* null mice were grafted with full-thickness canine skin and grafts were protected for 24 days with tape bandages (Method-B, Section 2.3.4).

Larger skin grafts (16 to 18 mm in diameter) were used compared to previous experiments.

Demodex graft Infection: At 51 days after skin grafting, grafts were subjectively graded and mice were allocated to four groups with skin grafts of comparable hair growth. Skin grafts on mice in Group-I, II, and III were infected with *D. canis* and received 150 to 250 viable mites with 80% adults and 20% nymphs, protonymphs, larvae, and eggs. Grafts were protected with tape bandages for five days (Method-B, Section 2.3.4). Skin grafts in Group-IV received mineral oil only.

Lymphocyte stimulation and lymphocyte transfer: Sixty days post *D. canis* infection, PBMC were isolated from the skin donor dog, placed into culture and stimulated *in vitro* with PHA and hr-IL-2. At 63 days post *D. canis* infection, 15×10^6 viable stimulated PBL were directly injected into each skin graft of Group-I (9 mice) and Group-IV (8 mice). The inoculum contained 99% lymphocytes with a cell viability of 81%. The calculated stimulation index was 32.3. At 66 days post *D. canis* infection, PBMC were again isolated from the skin donor dog and 25×10^6 unstimulated viable lymphocytes were directly injected into each skin graft of Group-II (8 mice). This second inoculum contained 76% lymphocytes and 93% PBMC, with a cell viability of 98%. Skin grafts in Group-III (8 mice) were injected with PBS only.

Skin graft and mouse evaluation: Mouse serum samples and skin grafts were collected 93 days after mite transfer. Skin graft hair growth was subjectively scored as 1 (>50% or more of graft) or as 2 (<50% of skin graft). A sample of each skin graft was collected for bacterial culture. Skin grafts, as well as liver, lung and spleen, were evaluated for the

stained with anti-CD3 antibody to detect T-cells. Necropsy examination was performed for all mice and the liver, lung, and spleen were examined by histology.

4.4.1.4 Statistical Methods

Statistical evaluation was performed as described for Section 4.2.1.4. For statistical purposes, skin grafts were considered culture positive if *S. intermedius* was recovered.

4.4.2 RESULTS

Thirty-two out of 33 *Rag2* knockout mice survived the five month experiment in good health. The skin graft on one mouse in Group-II developed crusting 85 days after *D. canis* infection; the mouse subsequently appeared ill and was removed from the study.

Skin grafts healed well after mild central crusting and were 13 to 15 mm in diameter. Grafts started to regrow hair by three to four weeks after transplantation and hair length and hair density were highest at the completion of the trial, resembling that of the donor. Approximately 75% of grafts grew hair over more than 95% of the graft surface and there was little or no visible scarring. Three skin grafts grew very little hair. Twenty-six grafts had a hair growth score of 1 and six grafts had a score of 2 (Appendix 4). The gross appearance of skin grafts did not change appreciably after infection with *D. canis* or after leukocyte injection. Similarly, there were no appreciable gross differences between the four experimental groups (Figure 4.4-2 through Figure 4.4-5).

Demodex canis was recovered from 25 out of 25 grafts infected with mites by NaOH digestion. Large numbers of mites were recovered from grafts and the range of calculated mite totals per graft sample were as follows: Group-I, 2,250 to 39,125; Group-

II, 2,425 to 10,750; and Group-III, 3,675 to 15,675. The calculated mean total number of mites per digest sample (mean ± SEM) for Groups-I, -II, and -III were 15,330.55 ± 3,583.55, 6,582.14 ± 1,118.92, and 8,931.25 ± 1,716.72, respectively. Mites were not recovered from the eight grafts in Group-IV that did not receive *D. canis*. Figure 4.4-6 shows the calculated number of mites and stages per digest sample. Immature stages tended to be more numerous on grafts than adults (Figure 4.4-6B). The calculated number of mites per digest sample are listed in Table 4.4-1.

There was a significant effect of treatment on calculated mite numbers ($P = 0.018$) that depended on the presence of bacteria and hair growth score in a three-way interaction. This was due to both a significant interaction between the presence of bacteria (as determined by culture) and treatment ($P = 0.008$) and a significant interaction between hair growth score and treatment ($P < 0.001$). Regardless of the hair growth score, when bacteria were not present, there were significantly more mites on grafts in Group-I than Group-II (hair growth score = 1, $P = 0.016$; hair growth score = 2, $P < 0.001$) or Group-III (hair growth score = 1, $P = 0.049$; hair growth score = 2, $P < 0.001$). Similarly, when bacteria (*S. intermedius)* were present and the hair growth score was equal to 2, there were significantly more mites in Group-I than Group-III ($P = 0.041$). However, when bacteria were present and the hair growth score was equal to 1, there were significantly fewer mites on skin grafts in Group-I than Group-III ($P = 0.012$). In summary, treatment with *in vitro* stimulated lymphocytes led to a significant increase in the number of mites on skin grafts, except when bacteria were present on grafts with good hair growth, then there were significantly fewer mites. There were no significant differences detected between Group-II and Group-III.

Histological evaluation did not identify differences between treatment and control groups and confirmed follicular *D. canis* infection of all 25 grafts that received mites (Figure 4.4-7 through Figure 4.4-10). Mites were located in the follicular lumen in the superficial 1/3 to 1/2 of primary and secondary hairs and were found occasionally in sebaceous gland ducts. Minimal changes were associated with mite colonization and included dilation of the hair follicle lumen with thinning of the hair follicle wall. Mites did not penetrate the hair follicle wall and an intact layer of keratin always separated mites from viable cells of the external root sheath. Mild to moderate follicular keratosis was present in nearly all grafts but did not appear to be associated with mite infection or lymphocyte treatment. Other than scattered dermal mast cells and histiocytes, inflammatory cells were rarely observed. A lymphocytic folliculitis was absent and inflammation did not target mite-infected hair follicles.

In 3 out of 32 skin grafts, regional to diffuse perivascular infiltrates of granulocytes and mononuclear cells, predominately histiocytes, were observed. These grafts were culture positive for *S. intermedius* and in two grafts inflammatory cell infiltrates were associated with bacterial colonies -consistent in morphology for *S. intermedius*. Epidermal hyperplasia accompanied these inflammatory changes. In occasional grafts, small focal accumulations of histiocytes at the graft margin accompanied hair shaft or keratin fragments.

Regardless of experimental group, 50 to 75% or more of hair follicles were in the anagen phase of the hair cycle. Remaining hair follicles were in the telogen phase or were atrophied. Hair follicles, sebaceous glands and apocrine glands resembled those of pregrafted normal skin. The surface epidermis resembled pregrafted skin and

keratinization of the stratum corneum was of the orthokeratotic basket weave type. Focal irregular epidermal hyperplasia was occasionally present at the margin of grafts. Mast cells were scattered individually throughout the dermis. Mild to moderate dermal fibrosis was present in several grafts.

Immunohistochemical staining for CD3 identified rare T-cells within skin grafts in all groups. Typically, 1 to 3 cells with positive membrane staining and lymphocyte cellular morphology were present in the entire skin graft section (less than 1 cell per 20 HPF). Individual cells were located in the dermis, surface epidermis and follicular epithelium. A few mice in each group had an occasional CD3 positive cell in the spleen.

Canine IgG was detected in mouse serum samples collected at completion of the trial from all surviving mice that were inoculated with canine leukocytes (24/24) (Appendix 5). Canine IgG mouse serum concentrations in Group-I (mean ± SEM, 34.01 ± 4.91) were significantly higher than canine IgG concentrations in either Group-II (mean ± SEM, 1.07 ± 0.25; $P < 0.001$) or Group-IV (mean ± SEM, 11.42 ± 5.42; $P = 0.002$). Canine IgG mouse serum levels in Group-IV were significantly higher then those in Group-II ($P = 0.007$). Figure 4.4-11 shows the mean IgG concentrations for the three groups. Canine IgG was not detected in serum samples from mice in Group-III that did not receive canine lymphocytes or in pre-experiment samples for all mice. The PCV for mice at the completion of trial ranged between 39 and 49 and was similar to that of pre-experimental values (Table 4.4-2).

Bacteriologic culture was performed for all 33 grafts. No bacterial growth was observed from 18 grafts. *S. intermedius* was recovered at 1 to 4+ colony growth from nine grafts (Appendix 6). These were distributed with between two to four culture

positive grafts in Group-I, -II, and -III, often affecting more than one graft per cage. A *Bacillus sp.* was recovered with 1+ growth from one graft in Group-I and from one graft in Group-II. There was bacterial growth for grafts in Group-IV.

There were no significant necropsy findings for the 32 *Rag2* null mice completing the study and there was no evidence of GVHD. One mouse had changes consistent with systemic bacterial infection, including multifocal hepatic necrosis and neutrophilic hepatitis (*S. intermedius* was cultured from the crusted skin graft of this mouse).

4.4.3 DISCUSSION

In the early 1970s, Scott *et al.* proposed that generalized demodicosis results from a defect in T-cell immunity (Scott *et al.*, 1974; Scott *et al.*, 1976). This widely referenced T-cell dysfunction hypothesis has generally found support from descriptive and *in vitro* studies (reviewed in Chapter 1). One objective of this study was to directly test the tacit hypothesis that lymphocytes of normal dogs control *D. canis* overgrowth on skin.

Direct transfer of *in vitro* stimulated canine PBL to *D. canis* infected skin grafts on *Rag2* null mice led to significantly more mites on grafts than control grafts or grafts receiving unstimulated lymphocytes. Similar to previous experiments (Section 4.2 and 4.3), these results provided evidence that canine lymphocytes could have a trophic effect on mite growth. The results were unexpected given that the literature supports a protective role for lymphocytes in demodicosis.

Although a sustained lymphocytic tissue reaction was not observed, serum canine IgG levels were significantly higher from *Rag2* null mice with mite infected grafts, confirming that lymphocytes interacted with mites. Only rare lymphocytes were

identified in nearly all skin grafts on *Rag2* null mice by CD3 staining, consistent with the presence of carrier lymphocytes in grafts. Carrier graft lymphocytes have been shown to survive human skin xenografting (Kaufmann *et al.*, 1993). Alternatively, an interaction between mites and lymphocytes may have resulted from the release of chemical mediators by mites, lymphocytes and/or graft cells and a tissue inflammatory response need not have necessarily developed to explain the results.

Because eggs out numbered adults on skin grafts on *Rag2* null mice, it is unlikely that the treatment caused retention of the more mobile mature mite stages on grafts. It is more likely that lymphocytes led to stimulation of mite replication. The finding of increased immature stages on grafts, compared to adults, after a 33 day incubation period is also more consistent with the estimated life cycle of *D. canis* (24 to 30 days) (Sako, 1964). Female mites have a sperm storage area in the uterus. Therefore, it is possible that female mites could produce a large number of fertile eggs in a short period of time (Desch, 1984).

The paradoxical stimulatory effect of lymphocytes on mite fecundity could be an adaptive mite response to increase mite survival after activation of host defense mechanisms. Comparative evidence from studies of unicellular or other multicellular parasites indicate that host cytokines could function as parasite growth factors and suggests a mechanism by which lymphocytes could lead to an increase in mite numbers (Damian, 1997; McKerrow, 1997). A related situation occurs with the rabbit flea – this ectoparasite responds to host hormone signals to cue its own replication (Rothschild & Ford, 1966; Rothschild & Ford, 1972). Given the evidence of extensive coevolutionary history of *Demodex spp*, molecular signaling interactions between *Demodex spp.* and

their host are expected and further investigations should focus on identifying these interactions (Nutting, 1985). Alternatively, experimental conditions may have selected for a lymphocyte population capable of stimulating mites. The relative balance of functional lymphocyte populations in demodicosis may affect mite proliferation and disease progression, similar to murine and human Th-1 and Th-2 lymphocyte models of parasite resistance (Kuby, 1997). Residual PHA in the washed lymphocyte inoculum could have stimulated mites.

There was no conclusive evidence that the canine lymphocytes homed to *D. canis* infected hair follicles in this experiment. Normal dogs were used in this study; the lack of a sustained cellular response in skin grafts could simply reflect the natural interaction of adult dogs with *D. canis*, that is a state of anergy. *Demodex canis* alone may not be antigenic/immunogenic – this finding is supported by the observation that mites do not appear to damage hair follicles on skin grafts. In the *Rag2* experiment, *S. intermedius* was present on several lymphocyte treated skin grafts yet a cellular response to *D. canis* was not observed. Bacterial interactions may not trigger an immune response to mites.

Experimental conditions could account for the fact that lymphocytic inflammation did not persist in *D. canis* infected skin grafts on *Rag2* null mice. First, it is entirely possible that a lymphocyte tissue reaction developed in grafts after transfer, but subsided by the time grafts were collected, 30 days later. Second, the lack of a canine regional lymph node in the mouse could have limited canine lymphocyte expansion in this model and the ability to generate a sustained cellular response. Third, expansion of a lymphocyte response could have been limited if dendritic cells did not survive in skin grafts after transplantation. While this possibility exists, monocytes present in human

PBMC transferred to scid mice differentiate into tissue dendritic cells capable of mediating aspects of allergic reactions in the mouse lung (Hammad *et al.*, 2000). Therefore, it is likely that monocytes transferred in the PBMC inocula could act as the antigen presenting cells needed. Furthermore, Kaufmann *et al.*(1993) demonstrated that human dentritic cells and macrophages survive in human skin grafts on scid mice for 12 months. Fourth, adequate numbers of *D. canis* specific lymphocyte clones might not have been delivered to skin grafts, survived transfer or circulated to skin grafts on mice. In this study, lymphocytes survived transfer to grafts and lymphocytes were delivered directly to skin grafts on *Rag2* null mice, thereby circumventing the need for lymphocyte recirculation to deliver effector cells to grafts. Finally, in some human studies, the lymphocytes transferred to scid mice appeared to have develop anergy in the mouse environment (Tary-Lehmann & Saxon, 1992; Tary-Lehmann *et al.*, 1994; Taylor, 1994). However, the presence of the test antigen in the mouse at the time of lymphocyte transfer and the presence of syngeneic host tissues can rescue lymphocytes from this anergic effect (Taylor, 1994). Delhem and others demonstrated an antigen specific human lymphocyte response to HIV glycoprotein in skin grafts on scid mice (Delhem *et al.*, 1998). In the current study, mite antigens and syngeneic skin grafts were present at the time of canine lymphocyte transfer.

Staphylococcus intermedius graft infection appeared to negate the stimulatory effect of lymphocytes on mite numbers in the *Rag2* experiment. This interaction was also affected by the degree of hair growth of skin grafts, perhaps because grafts with less hair were colonized differently by bacteria. The effect of bacteria on the lymphocyte-mite interactions is interesting in light of the clinical evidence that bacterial skin infection

impacts the severity of demodicosis (Scott *et al.*, 1995) and is associated with decreased *in vitro* lymphocyte blastogenesis for dogs with generalized demodicosis (Barta *et al.*, 1983). This experiment was not specifically designed to assess the effects of bacteria on lymphocyte mite interactions and further studies should address this interaction.

Rag2 null mice reconstituted with *in vitro* stimulated canine PBL *in vitro* had significantly higher levels of serum canine IgG (regardless of the presence or absence of mites) than mice reconstituted with PBMC. This finding is similar to human studies in which treatment with cytokines, including IL-2, or non specific *in vitro* activation of lymphocytes prior to transfer, led to increased engraftment of human lymphocytes in scid mice (Murphy *et al.*, 1993; Kaul *et al.*, 1995; Delhem *et al.*, 1998). In some human studies, exogenous IL-2 was delivered to the mouse environment in order to increase lymphocyte engraftment (Kaul *et al.*, 1995; Delhem *et al.*, 1998). Injection of skin grafts with hr-IL-2 after canine lymphocyte transfer in the current study would have necessitated an additional control group to evaluate the effect of hr-IL-2 on mite growth; this option was limited by the number of grafted mice and by the number of mites available. It does however, suggest another potential protocol for further investigation.

The level of canine IgG in sera from *Rag2* null mice reconstituted with unstimulated canine PBMC was low compared to previous experiments with tgε26 mice. The mean canine IgG concentration (± SEM) for *Rag2* null mice after intragraft injection of canine PBMC was a low 1.07 μg/mL (± 0.25) compared to 114.6 μg/mL (± 90.34) 4 weeks after IP injection of tgε26 mice with canine PBMC (Section 3.3). Direct inoculation of skin grafts on tgε26 mice with canine PBMC (Section 3.4) resulted in higher canine IgG titers (mean ± SEM, 226.66 ± 38.44) than was observed after intragraft

inoculation using *Rag2* null mice. Although a different antigenic stimulus was present in the two experiments, this result suggests that the route of injection was not the reason for lower canine IgG levels after transfer of unstimulated canine PBMC to *Rag2* null mice. Rather, individual dog factors or characteristics of *Rag2* null mice may have limited canine lymphocyte engraftment. Alternatively, the kinetics of canine IgG production or clearance in *Rag2* null mice may be altered compared to tgε26 mice. Finally, in the current experiment, the presence of bacteria on skin grafts (as determined by culture) did not appear to correlate with the level of canine IgG detected in *Rag2* mouse serum.

The *Rag2* null mice supported good quality, relatively uniform, canine skin grafts. At completion of the trial, the majority of the skin grafts had grown abundant hair that was comparable to that of the donor. Grafts developed less ischemic damage after transplantation and the improvement in graft quality was attributed primarily to the extended bandaging time (24 days versus 7 to 12 days for previous experiments). Furthermore, the full-thickness canine skin grafts used in this experiment were 16 to 18 mm in diameter at grafting and were significantly larger (over 50%) than has been previously reported (Caswell *et al.*, 1996). These results support the conclusions of the previous chapter, that stabilization and reperfusion of full-thickness grafts are essential to creating good quality grafts, and that graft diameter may not be a primary limiting factor for grafting canine skin to mice.

Rag2 null mice proved to be hardier than tgε26 mice and all of the 33 mice survived the duration of the experiment. The *Rag2* mice were also larger and more robust than tgε26 mice (data not shown) and were easier to manipulate surgically. Unlike scid/bg mice, ICR scid mice or tgε26 mice, there was no evidence of host graft rejection

by *Rag2* mice. *Rag2* null mice did not develop evidence of GVHD or hemolytic anemia, which complicated experiments with scid/bg mice (Caswell, 1995) and ICR scid mice (Section 4.2).

This experiment provided evidence, contrary to literature reports, that canine lymphocytes can stimulate the growth of *D. canis* on canine skin (Scott *et al.*, 1974; Scott *et al.*, 1976; Scott *et al.*, 1995). *In vitro* stimulation of canine lymphocytes led to increased production of canine IgG in *Rag2* null mice. *Rag2* null mice do not support unstimulated lymphocytes to the same degree as tgε26 mice, as measured by immunoglobulin levels. *Rag2* null mice are useful for the long-term experiments modeling demodicosis and do not succumb to the complications associated with other mice used this study. A large number of good quality skin xenografts were created, thereby demonstrating that the difficulties associated with grafting full-thickness canine skin to mice are no longer a limitation of the canine skin xenograft mouse model.

Figure 4.4-2: Appearance of canine skin grafts on *Rag2* null mice in Group-I at experiment completion. Skin lesions did not develop after *D. canis* infection or after injection of grafts with *in vitro* stimulated canine lymphocytes. Abundant hair regrowth is evident in central and peripheral areas on most grafts.

A

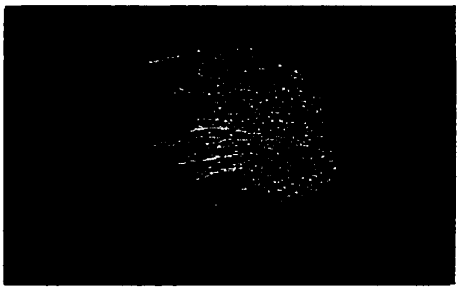

B

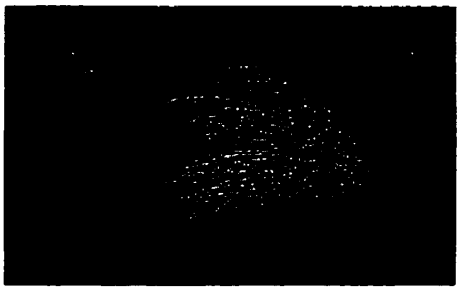

C

D

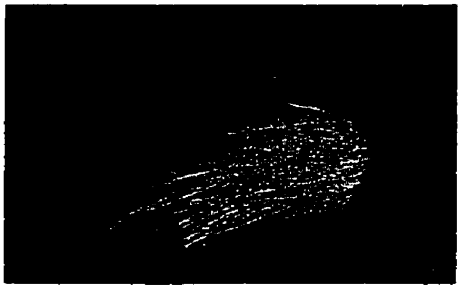

E

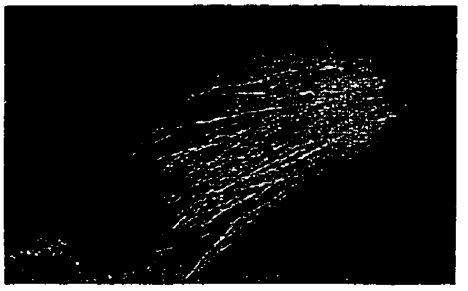

F

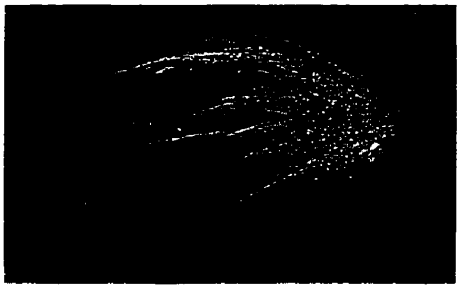

G

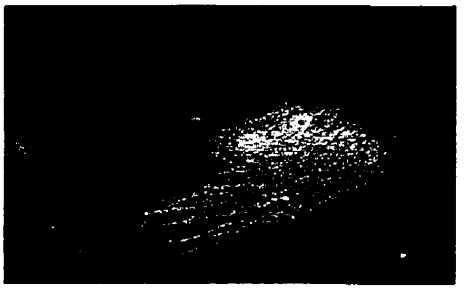

H

I

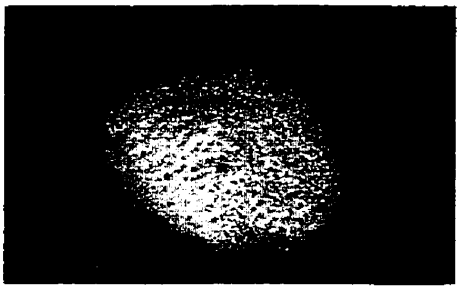

Figure 4.4-3: Appearance of canine skin grafts on *Rag2* null mice in Group-II at experiment completion. Skin lesions did not develop after *D. canis* infection or after injection of grafts with unstimulated canine PBMC. Prominent hair growth is present on the majority of skin grafts.

A

B

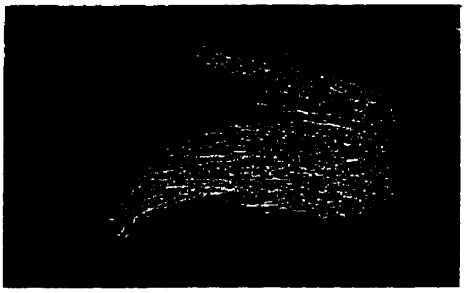

C

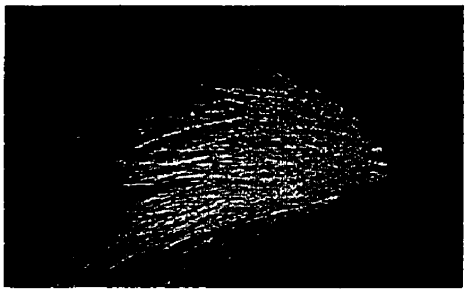

D

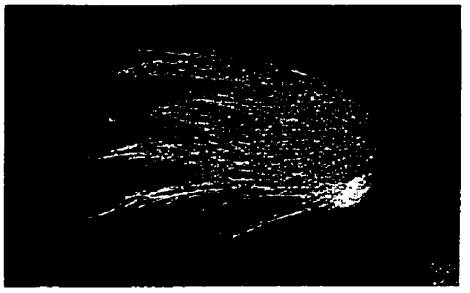

E

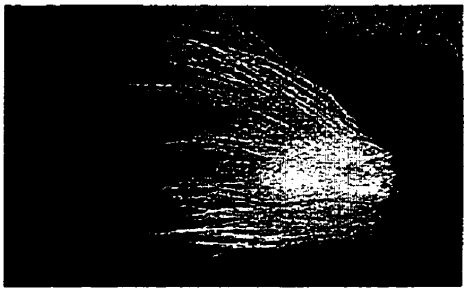

F

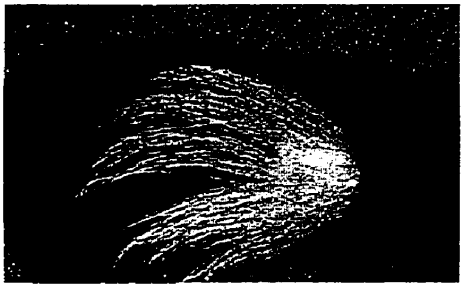

G

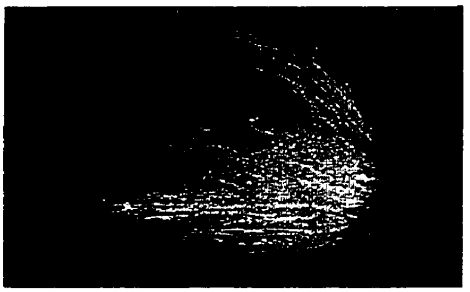

Figure 4.4-4: Appearance of canine skin grafts on *Rag2* null mice in Group-III at experiment completion. Skin lesions did not develop after *D. canis* infection or after injection of grafts with PBS. Prominent hair growth is present on the majority of skin grafts.

A

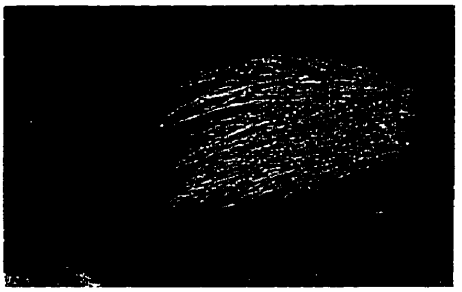

B

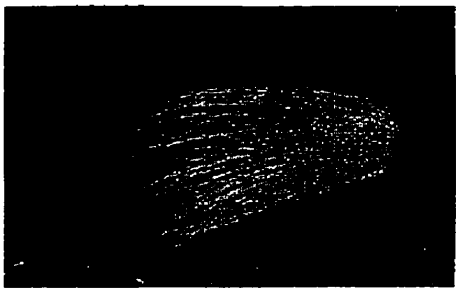

C

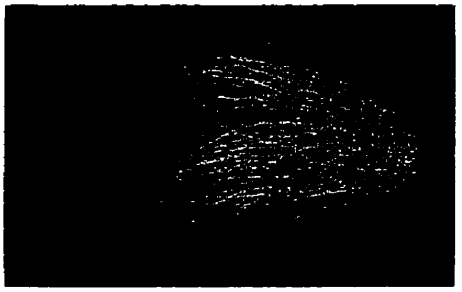

D

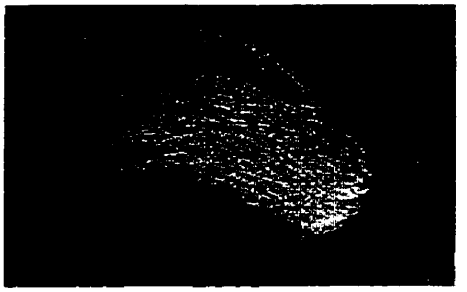

E

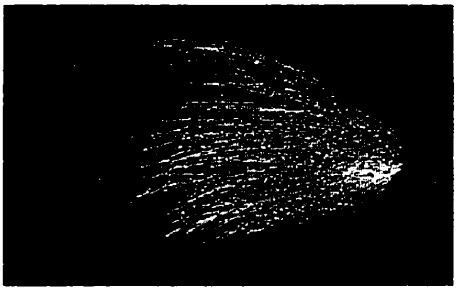

F

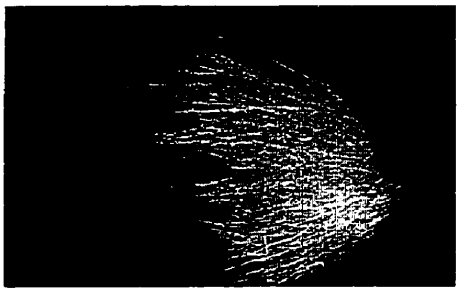

G

H

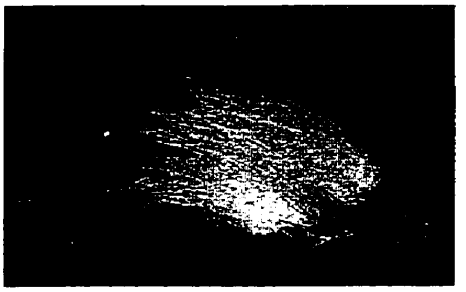

Figure 4.4-5: Appearance of canine skin grafts on *Rag2* null mice in Group-IV at experiment completion. Skin lesions did not develop after uninfected grafts were injected *in vitro* stimulated canine lymphocytes. Prominent hair growth is present on the majority of skin grafts.

A

B

C

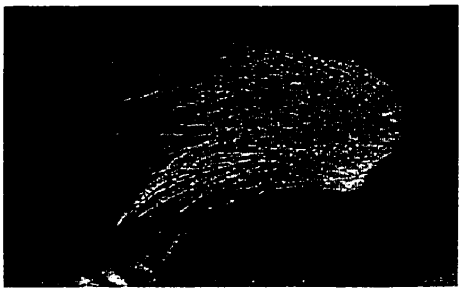

D

E

F

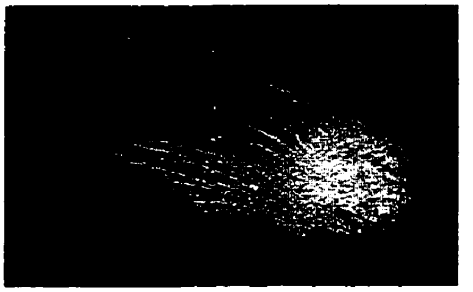

G

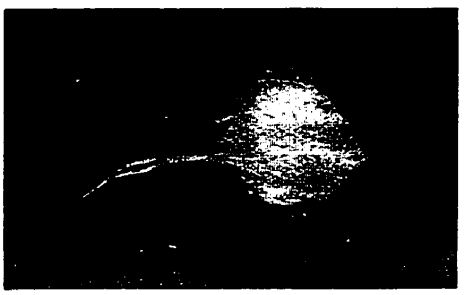

H

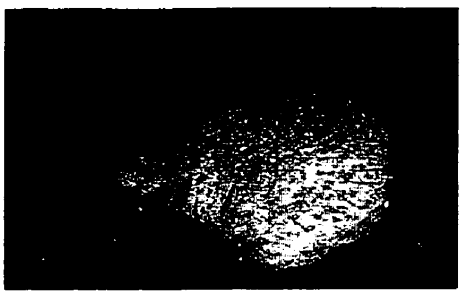

Figure 4.4-6: Bar graphs showing the results of *D. canis* enumeration for canine skin grafts, by NaOH digestion, at completion of the *Rag2* experiment. **(A)** The calculated total number of *D. canis* per graft digest sample (mean ± standard error) recovered from grafts that received *in vitro* stimulated PBL (Group-I), unstimulated PBMC (Group-II), or PBS (Group-III). Mites were not recovered from grafts that only received unstimulated PBMC (Group-IV) (not shown). **(B)** The calculated total number of each *D. canis* life-cycle stage per graft sample (mean ± standard error) recovered from grafts for Group-I, Group-II, and Group-III.

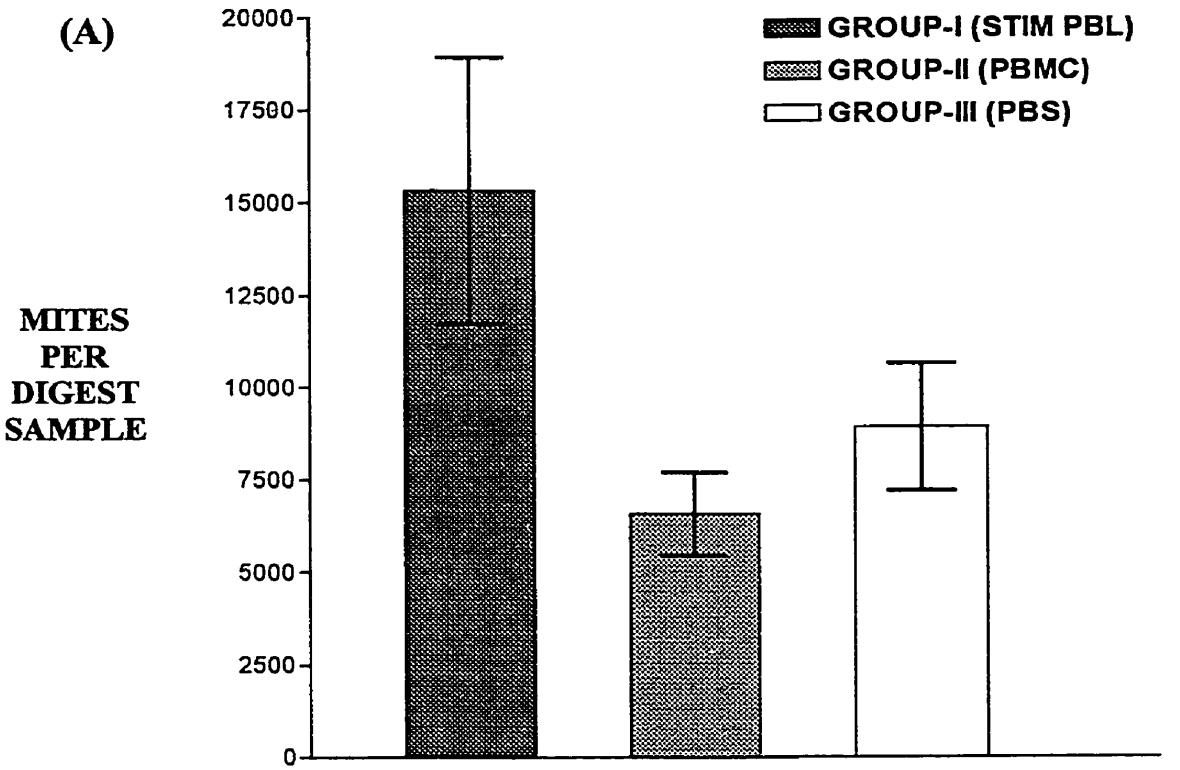
(A)
MITES PER DIGEST SAMPLE
20000
17500
15000
12500
10000
7500
5000
2500
0
GROUP-I (STIM PBL)
GROUP-II (PBMC)
GROUP-III (PBS)

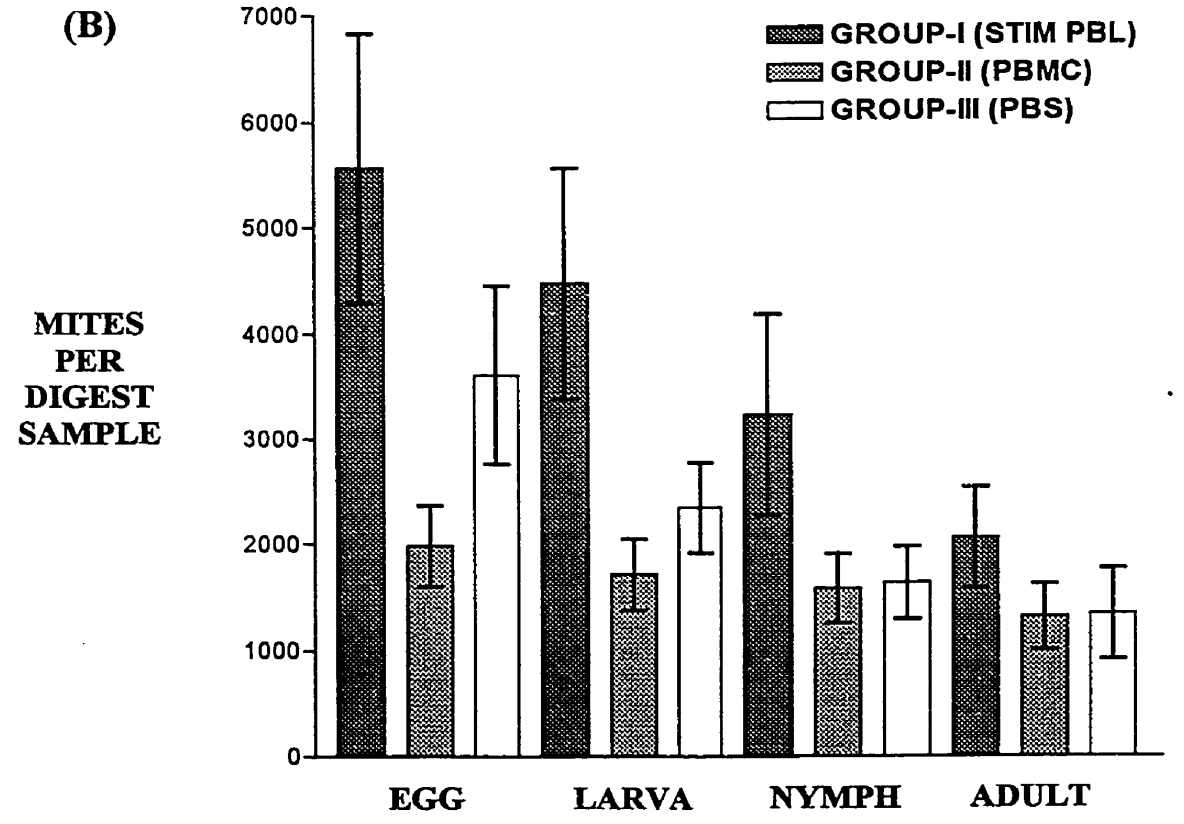
(B)
MITES PER DIGEST SAMPLE
7000
6000
5000
4000
3000
2000
1000
0
GROUP-I (STIM PBL)
GROUP-II (PBMC)
GROUP-III (PBS)
EGG
LARVA
NYMPH
ADULT

Figure 4.4-7: Photomicrographs of a representative canine skin graft, treated with *in vitro* stimulated PBL (Group-I), from a *Rag2* null mouse. **(A)** Low magnification shows graft morphology and lack of inflammation (magnification = X10). **(B)** Higher magnification shows cross sections of *D. canis* (arrow) in hair follicles (magnification = X25). Mites are associated with dilation of the follicle lumen. Hematoxylin and eosin stained, paraffin embedded, tissue sections

A

B

Figure 4.4-8: Photomicrographs of a representative canine skin graft, treated with unstimulated PBMC (Group-II), from a *Rag2* null mouse. **(A)** Low magnification shows graft morphology and the lack of inflammation (magnification = X10). **(B)** Higher magnification shows cross sections of *D. canis* (arrow) in hair follicles (magnification = X25). Mites are associated with dilation of the follicle lumen. Inflammation is not present. Hematoxylin and eosin stained, paraffin embedded, tissue sections

A

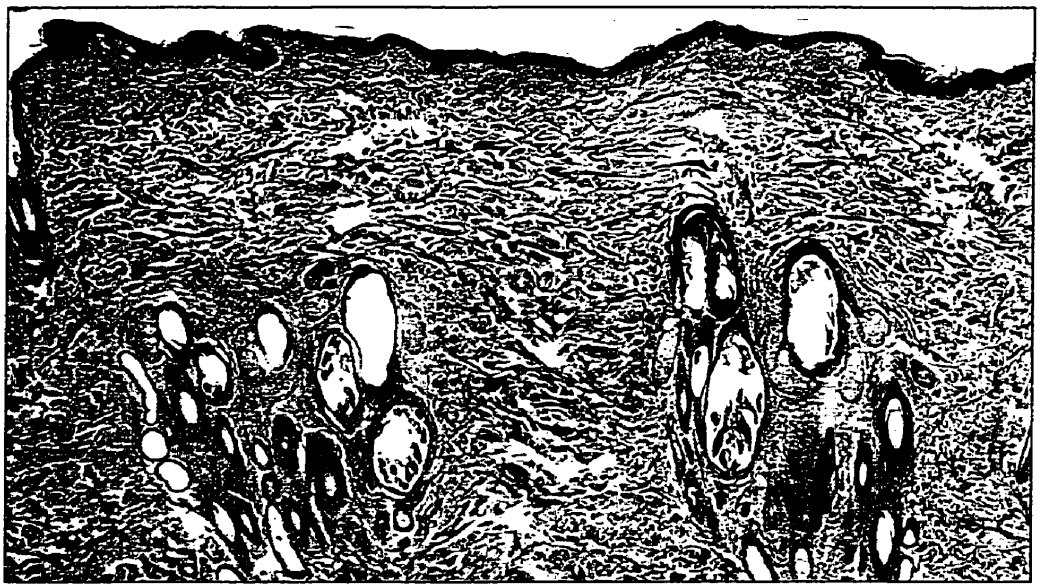

B

Figure 4.4-9: Photomicrographs of a representative canine skin graft, treated with PBS (Group-III), from a *Rag2* null mouse. **(A)** Low magnification shows graft morphology and lack of inflammation (magnification = X10). **(B)** Higher magnification shows *D. canis* (arrow) infection of hair follicles (magnification = X25). Mites are associated with dilation of the follicle lumen. Hematoxylin and eosin stained, paraffin embedded, tissue sections

A

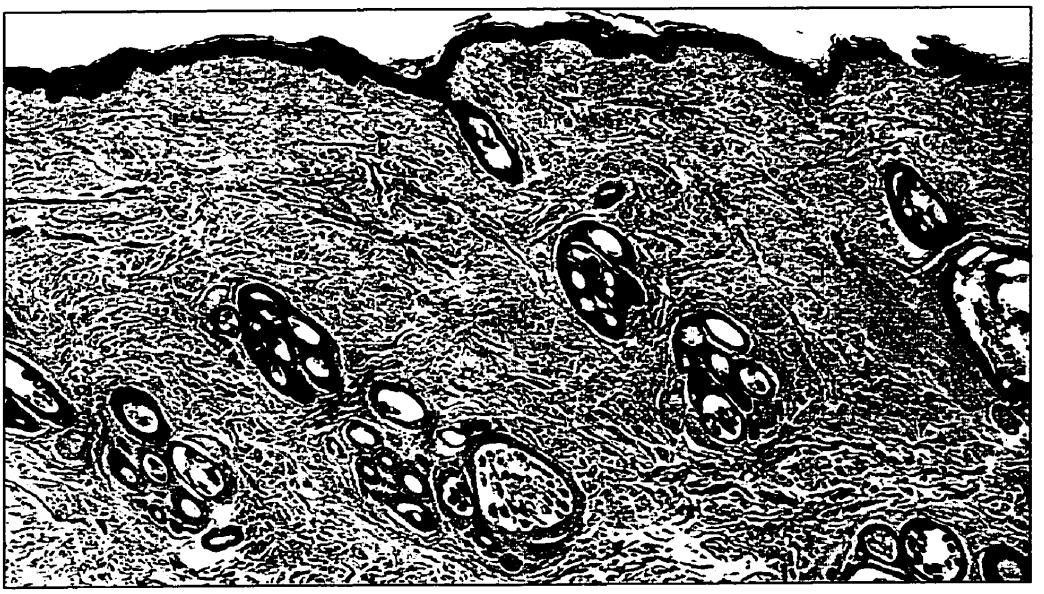

B

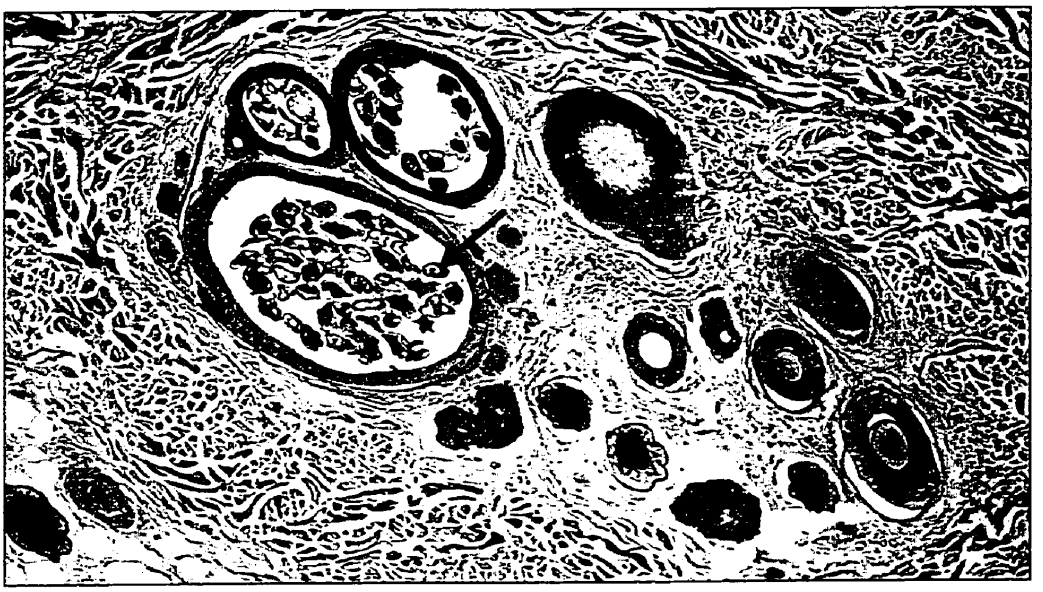

Figure 4.4-10: Photomicrographs of a representative canine skin graft, treated with *in vitro* stimulated PBL (Group-IV) but not infected with *D. canis*, from a *Rag2* null mouse. **(A)** Low magnification shows lack of inflammation or *D. canis* infection (magnification = X10). **(B)** Higher magnification shows hair follicle morphology (magnification = X25). Hematoxylin and eosin stained, paraffin embedded, tissue sections

A

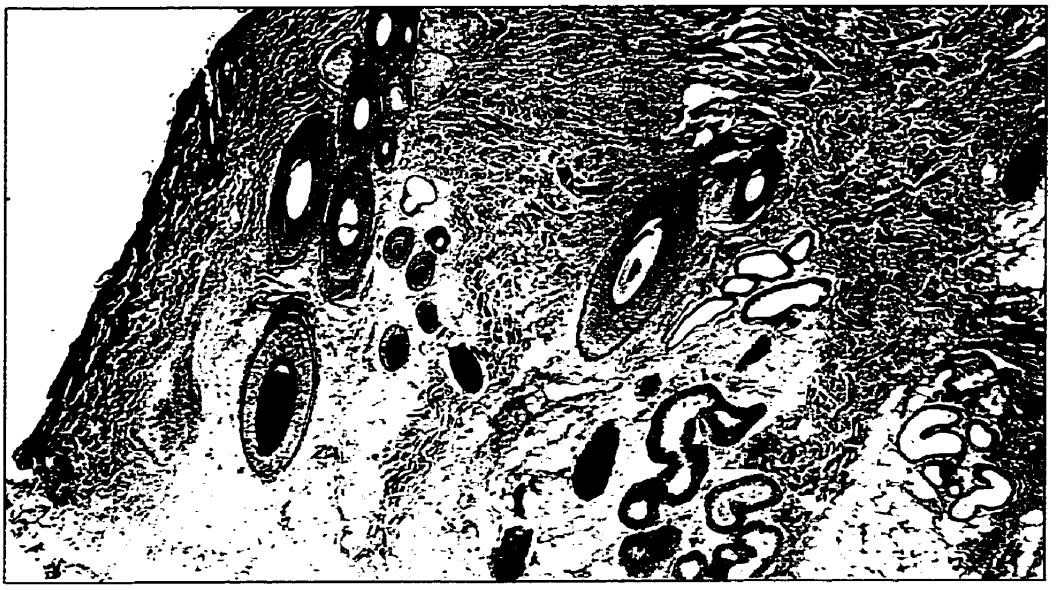

B

Figure 4.4-11: Bar graph showing canine IgG concentration (μg/mL, mean ± standard error) in sera from *Rag2* mice at experiment completion, approximately 4 weeks after intragraft transfer of canine leukocytes. Group-I (n = 9) and Group-IV (n = 8) received *in vitro* stimulated PBL, where as Group-II (n = 7) received unstimulated PBMC. Canine IgG was not detected in sera from mice in Group-III (n = 8) that did not receive canine lymphocytes (data not shown).

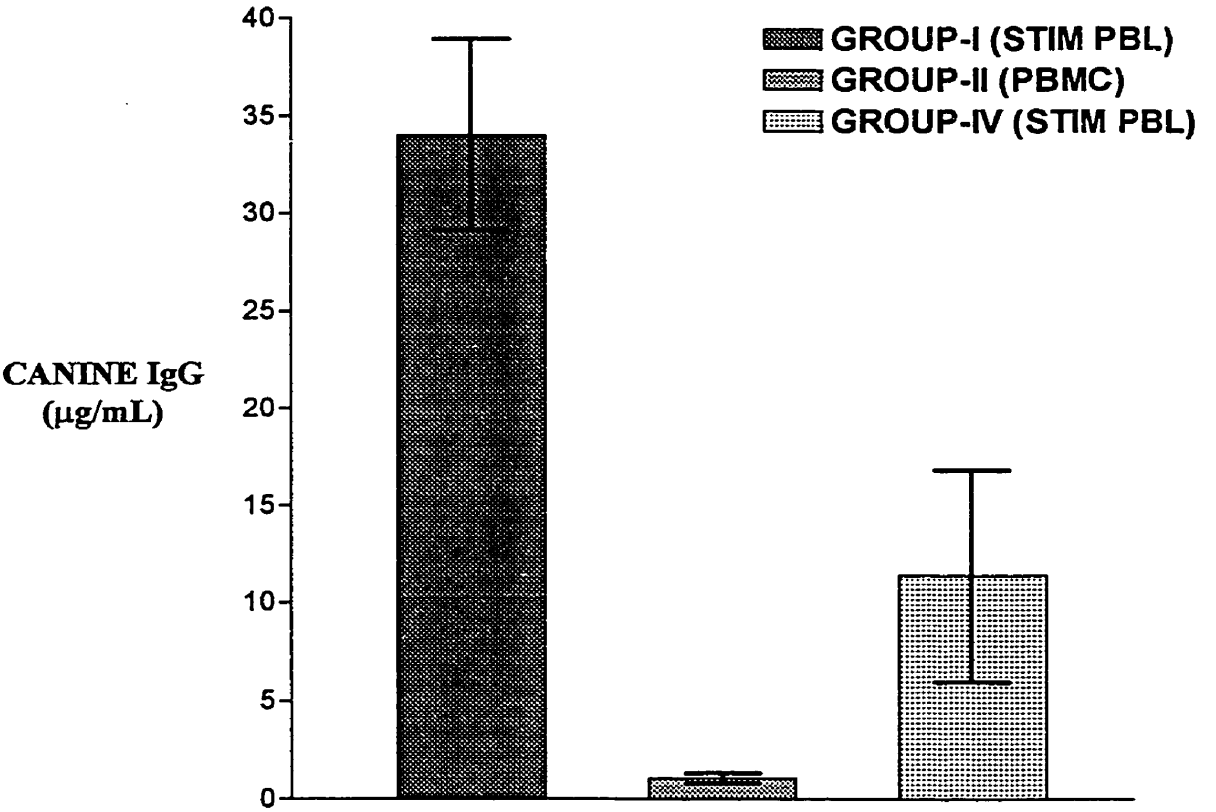
GROUP-I (STIM PBL)
GROUP-II (PBMC)
GROUP-IV (STIM PBL)
CANINE IgG
(µg/mL)
40
35
30
25
20
15
10
5
0

Table 4.4-1: Calculated Number of *D. canis* Per Skin Graft Digest Sample Collected from Grafts on *Rag2* Mice at Experiment Completion

Mouse	Calculated Stage Totals				Calculated Mite Totals
	Egg	Larva	Nymph	Adult	
Group-I (*D. canis* plus *in vitro* stimulated PBL)					
1	6075.00	4275.00	3100.00	1475.00	14925.00
2	1750.00	675.00	600.00	200.00	3225.00
3	825.00	475.00	550.00	400.00	2250.00
4	4900.00	5625.00	1050.00	3525.00	15100.00
5	14075.00	11425.00	10025.00	3600.00	39125.00
6	5650.00	4125.00	3275.00	2550.00	15600.00
7	6900.00	3325.00	2825.00	1075.00	14125.00
8	3650.00	3925.00	3400.00	1675.00	12650.00
9	6250.00	6425.00	4250.00	4050.00	20975.00
Mean ± SEM	5563.88 ±1269.68	4475.00 ±1090.71	3230.55 ±959.43	2061.11 ±477.17	15330.55 ±3583.55
Group-II (*D. canis* plus unstimulated PBMC)					
1	1550.00	1350.00	2525.00	2200.00	7625.00
2	400.00	875.00	600.00	550.00	2425.00
3	1725.00	1400.00	1775.00	2425.00	7325.00
4	1550.00	1100.00	450.00	675.00	3775.00
5	3075.00	3200.00	2650.00	1825.00	10750.00
6	2100.00	1275.00	1250.00	475.00	5100.00
7	3450.00	2750.00	1825.00	1050.00	9075.00
Mean ± SEM	1978.57 ±387.47	1707.14 ±337.56	1582.14 ±326.68	1314.29 ±310.38	6582.14 ±1118.92
Group-III (*D. canis* plus PBS)					
1	1625.00	1225.00	775.00	750.00	4375.00
2	5100.00	2875.00	1225.00	500.00	9700.00
3	4875.00	3425.00	3325.00	3825.00	15450.00
4	950.00	1475.00	725.00	675.00	3825.00
5	7200.00	4425.00	2250.00	1800.00	15675.00
6	5750.00	2750.00	1325.00	450.00	10275.00
7	1425.00	900.00	875.00	475.00	3675.00
8	1950.00	1700.00	2575.00	2250.00	8475.00
Mean ± SEM	3609.38 ±843.40	2346.88 ±432.04	1634.38 ±341.41	1340.63 ±427.85	8931.25 ±1716.72

Group-IV *Demodex canis* were not recovered from any skin grafts in Group-IV that received only *in vitro* stimulated PBMC.

Table 4.4-2: *Rag2* Mouse PCV Values at the Onset and at Experiment Completion

Mouse	Onset	Completion	Mouse	Onset	Completion
Group-I (*D. canis* + stimulated PBL)			**Group-II (*D. canis* + unstimulated PBMC)**		
1	44	43	1	46	40
2	47	44	2	46	39
3	46	45	3	47	40
4	46	46	4	45	38
5	48	46	5	43	44
6	45	45	6	40	42
7	42	46	7	45	48
8	45	47	8	45	48 **e**
9	45	47			
Group-III (*D. canis* + PBS)			**Group-IV (*D. canis* + stimulated PBL)**		
1	44	48	1	45	48
2	45	46	2	45	46
3	42	45	3	46	49
4	46	46	4	46	45
5	47	40	5	45	45
6	46	45	6	45	45
7	47	42	7	45	45
8	45	42	8	40	44

Mean PCV and 95% Confidence Intervals (CI) for mice (n=33) at the onset of the *Rag2* experiment: Mean = 44.97, Lower 95% CI = 44.32, Upper 95% CI = 45.62

e - Mouse euthanised due to illness

CHAPTER 5: GENERAL DISCUSSION AND CONCLUSIONS

5.1 INTRODUCTION

Investigating the pathogenesis of complex inflammatory skin conditions is often limited by the ability to recreate aspects of the natural disease (in a meaningful way) experimentally. Progress in our understanding of canine demodicosis suffers from this limitation and there have been few *in vivo* studies reported. Because of this, basic questions about the pathogenesis of this complex inflammatory disease and about the biology of *D. canis* remain unanswered. The first objective of this thesis was to develop the skin xenograft mouse model for experimentally recreating aspects of canine demodicosis. The second objective was to apply this model to assess the role of lymphocytes in host resistance to demodicosis, thereby addressing a central question in the pathogenesis of this disease. The results established the model as a useful tool for studying canine demodicosis and challenge the accepted dogma that lymphocytes (at least the population transferred from peripheral blood) play a protective role in this disease. New insights are provided about the relative role of local and systemic mechanisms of innate defense in limiting mite populations and about the contribution of *D. canis* to the development of skin lesions.

5.2 DEVELOPMENT OF THE CANINE SKIN XENOGRAFT MOUSE MODEL

Although the skin xenograft mouse model is well established in human dermatology, this model has not been optimized sufficiently for use with canine tissues. This thesis developed the basic components of the canine model.

5.2.1 Immunodeficient Mice

Four different genetically immunodeficient mice were used for experiments supporting canine tissues: scid/bg, ICR scid, tgε26 and *Rag2* knockout mice. Of these mice, *Rag2* mice were found to be most useful for the skin xenograft mouse model. *Rag2* null mice were robust; none of the 33 mice used in this study developed spontaneous complications. Unlike scid/bg, ICR scid, or tgε26 mice, development of the "leaky" phenotype and skin graft rejection were not observed. *Rag2* null mice did not develop evidence of GVHD after injection with canine lymphocytes, that was seen in scid/bg mice. Over the 5-month course of experiments, neoplasia was not detected in *Rag2* null mice. Table 5.1 compares the

Table 5.1: Comparison of Skin Xenografting Results, *D. canis* Infection Rates and Outcomes for the Different Strains of Mice Used to Model Canine Demodicosis

Mouse Strain	Skin donor	Graft quality[c]		Infective dose[d]	Infection (rate)		Usefulness / Outcome
Scid/bg	Dog 1[a]	+	(n=25)	60	yes	(NA)	Poor / Became "leaky" Developed GVHD
	Dog 2[a]	+/++	(n=20)	300	yes	(NA)	Poor / Became "leaky"
ICR scid	Dog 3[b]	++	(n=25)	220[e]	yes	(18/20)	Poor / Became "leaky"
Tgε26	Dog 4[a]	+	(n=12)	300	yes	(12/12)	Fair / Low survivability
	Dog 5[b]	++	(n=10)	100	yes	(9/10)	Fair / Low survivability Some graft rejection
Rag2	Dog 6[b]	+++	(n=33)	200	yes	(25/25)	Good / No complications

[a]Skin grafting methods according to Section 3.3 (Caswell *et al.*, 1996)
[b]Skin grafting methods according to materials and methods
[c]Graft quality score;
+ = hair growth at margin, extensive central scarring, wide variation
++ = hair growth at margin and center, mild / moderate central scarring, wide variation
+++ = hair growth over entire graft, little or no scarring, uniform grafts
[d]Average viable *D. canis* (adults and nymphs) dose applied to each graft. Each dose contained approximately 80-85% adults and 15-20% combined eggs, larvae and nymphs
[e]Total mite dose given. Grafts were infected on three occasions
GVHD: Graft-versus-host disease; NA: Not available

grafting results, graft infections and mouse qualities for the mice used in this study.

In preliminary experiments, scid/bg mice were found to accept canine skin and/or lymphocyte grafts; however, the development of the "leaky" phenotype and GVHD limited the use of this mouse type for modeling demodicosis. Although ICR scid mice did not develop GVHD, a large percentage of these mice (63%) produced murine immunoglobulin and rejected skin grafts and were considered "leaky". Similar to previous reports of scid mice in a CB-17 background strain, ICR scid mice appear prone to developing thymic lymphoma, observed in 12% mice in this study. For these reasons, scid/bg and ICR scid mice were found unsuitable for xenograft experiments modeling demodicosis.

The tgε26 mouse were found to accept canine skin and lymphocyte grafts and these mice did not develop GVHD. However, subsequent use of tgε26 mice for modeling demodicosis identified characteristics of this mouse that limit their use in long term studies. Tgε26 mice were not hardy; between 17 to 40% did not survive the duration of experiments, over 5 months. A common cause of death was not identified; however some mice developed splenic lymphoma, consistent with the finding that CD3-epsilon subunit (over-expressed in tgε26 mice) can act as an oncogene (Wang *et al.*, 1997).

In this study, CD3+ T-cells were identified in canine skin grafts on control tgε26 mice (that did not receive canine leukocytes) in association with graft rejection. Subsequently, immunohistochemical staining of serial graft sections with mouse specific anti-CD45 antibody identified the infiltrating T-cells to be of mouse origin. These findings indicated that a percentage of tgε26 mice produced functional mouse T-cells and had become "leaky" for T-cells.

The finding of "leaky" tgε26 mice could explain another observation made during this study. Occasional tgε26 mice in the mouse colony developed a wasting syndrome that was associated with colitis. A similar colitis was reported in adult tgε26 mice that had been reconstituted with wild type mouse bone marrow (Hollander *et al.*, 1995). The authors showed that thymic grafts protected mice from colitis and concluded that colitis in marrow-grafted mice resulted from auto-reactive T-cells. In the current study, tgε26 mice that developed the wasting syndrome had likely become "leaky", and because these mice lack a functional thymus (Wang *et al.*, 1994; Wang *et al.*, 1995), auto-reactive lymphocytes were not eliminated and induced colitis. This was supported by identifying CD3+ T-cells in colonic lesions of tgε26 mice that had not received any canine tissue grafts. One possible explanation is that the CD3-epsilon transgene copy number may not be stable in tgε26 mice and changes in copy number could affect the degree of immunodeficiency. Transgenic mice that were created with lower copy numbers of the CD3-epsilon gene (compared to tgε26 mice) do not show complete ablation of T-cells and NK-cells during development, as was reported for tgε26 mice (Wang *et al.*, 1994; Wang *et al.*, 1995). Instability of the immunodeficient phenotype and variable longevity limit the use tgε26 mice for long term experiments.

5.2.2 Canine Skin Xenografting

Canine skin xenografting has received little attention in veterinary dermatology and techniques were not available that produced adequate and reliable results needed for modeling demodicosis (Caswell *et al.*, 1996). The factors that are important for

developing good quality full-thickness skin grafts on immunodeficient mice have not been identified in the literature.

In this study, a comparison of split-thickness and full-thickness canine skin grafts identified the importance of maintaining vascular perfusion for reducing early ischemic damage and thereby promoting more rapid healing, better hair growth and decreased scarring. It was concluded that full-thickness grafts do not favor the formation of vascular anastomoses, do not stabilize well in the graft bed and are more susceptible to mouse grooming-related graft trauma, compared to split-thickness grafts. As a consequence, these thicker grafts suffer severe ischemic damage.

A simple solution was created for improving the quality of full-thickness canine skin grafts. Graft bandages were redesigned and mice were bandaged for longer periods of time thereby allowing for more robust vascular connections and increased graft anchoring to the graft bed. Success was greatest when bandages were left in place for the longest time (24 days) on *Rag2* null mice. More than 75 % of skin grafts in this experiment developed prominent hair regrowth involving over 95% of the skin graft surface. Furthermore, larger healed canine skin xenografts were created, 13-15 mm in diameter; these grafts were more than 50% larger when healed than grafts in previous canine xenografting experiments (Rosenquist *et al.*, 1988; Caswell *et al.*, 1996). The development of good quality, well-haired, full-thickness skin xenografts from animals with relatively thick skin has not been previously described and has eluded human researchers for years (Van Neste, 1996). The draw back of prolonged bandaging is an increase in experiment duration, which can increase cost and mouse mortality.

To accommodate the extended bandaging times, it was essential that skin graft bandages be redesigned to be lighter and to allow for more flexibility of mice. This was necessary to decrease stress of mice and the negative impact that excessive bandaging can have on mouse weight gain and wound healing. The new bandages did not leave adhesive residue on the graft therefore tended not to induce excessive mouse grooming and graft trauma. The tape bandage procedure finally adopted for these experiments is outlined in Method B (Section 2.3.4)

These experiments demonstrate for the first time that full-thickness canine skin can be grafted to ICR scid, tgε26 transgenic and *Rag2* knockout mice and will survive for extended periods of time, greater than 4 months.

5.2.3 Canine Leukocyte Mouse Chimeras

Caswell (1995) reconstituted scid/bg mice with canine PBMC and described the development of GVHD in the majority of mice. Circulating canine immunoglobulin was identified in scid/bg mice, indicating the mice partially reconstituted with canine lymphocytes. Preliminary experiments in the present study repeated these findings. Since the onset of this study, only two abstracts have been published describing the reconstitution of scid mice with canine PBMC (DeBoer *et al.*, 1998; DeBoer *et al.*, 1999). Specific results were provided in one of these abstracts (DeBoer *et al.*, 1998). Scid mice were reconstituted with 10 to 100 x 10^6 canine PBMC and canine IgG and IgE were subsequently measured in mouse sera. Canine IgG peaked at 1 to 6 mg/mL, 1 to 2 weeks post PBMC inoculation, and declined over 6 to 8 weeks. Canine IgE levels peaked at 2 to 9 μg/ml and declined similarly. The peak canine IgG levels reported were similar to

those in the current study using scid/bg mice and tgε26 mice, and the duration of immunoglobulin production was similar to that observed with tgε26 mice. Although not specifically addressed, evidence of GVHD was not reported. Scid mice were not evaluated at the end of the trial for development of the "leaky" phenotype (D. DeBoer, personal communication).

The current study is the first attempt to reconstitute tgε26 mice with canine lymphocytes. The detection of canine IgG in tgε26 mouse plasma for several weeks indicated that canine lymphocytes survived transfer. In addition to intraperitoneal injection, canine lymphocytes were shown to survive direct injection into canine skin grafts on tgε26 mice and to be capable of mediating skin allograft rejection. Tgε26 mice did not develop GVHD, but were found to be sub-optimal for use with the skin xenograft mouse model for other reasons, e.g. limited life span and development of functional lymphocytes.

Rag2 null mice were only reconstituted by direct injection of canine lymphocytes into canine skin grafts. Because canine IgG was detected in mouse serum after cell transfer, the experimental goal of delivering viable lymphocytes to *D. canis* infected skin grafts on *Rag2* null mice was achieved. However, low concentrations of canine IgG were detected, compared to intraperitoneal reconstitution experiments with scid or scid/bg mice (DeBoer *et al.*, 1998), (personal observation) or tgε26 mice reconstituted by intragraft injection. Lymphocytes were rarely identified in the spleens from these mice. The results suggest that the level of canine lymphocyte engraftment was low in *Rag2* null mice. *Rag2* mice were successfully engrafted with human lymphocytes, but the level of engraftment was also considered reduced compared that of scid mice (Steinsvik *et al.*,

1995). If canine lymphocyte recirculation in mice was required to develop a sustained lymphocyte response to mites on skin grafts, then the ability of *Rag2* mice to support systemic canine lymphocyte engraftment could have been a limiting factor in this experiment. Further development of the xenograft model for studying inflammatory skin conditions will depend on optimizing canine leukocyte chimeras.

In addition to varying the leukocyte inoculum and route of delivery, two general techniques have been used to improve engraftment of human lymphocytes in immunodeficient mice. First, different methods of treating mice have been attempted and include for example whole body irradiation, NK-cell depletion or cytokine administration (Taylor, 1994). Second, different recipient mice have been used that vary in their immunodeficient phenotype.

5.2.4 Newer Immunodeficient Mice

The development of immunodeficient mouse mutants over the last decade has provided potentially useful mice for skin xenografting studies. Importantly, several newer mouse mutants have been shown to support higher levels of engraftment with human leukocytes. Non-obese diabetic/scid (NOD/LtSz-scid/scid, hereafter referred to as NOD/scid) mice lack B-cells and T-cells, and exhibit diminished macrophage and NK-cell function (Shultz *et al.*, 1995). NOD/scid mice support higher levels of human leukocyte engraftment compared with scid mice and have been popular for studying human leukocyte chimeras and hematopoiesis (Greiner *et al.*, 1995; Wang *et al.*, 1998a; Rice *et al.*, 2000). Addition of the null mutation for beta2-microglobulin (b2m) to create NOD/scid/b2m null mice (NOD/LtSz-scid/scid + $B2m^{null}$) improved human leukocyte

engraftment (Christianson *et al.*, 1997). However, due to a high incidence of thymic lymphomas, the mean life span of NOD/scid mice is only 8.5 months and that of NOD/scid/b2m null mice is only 6.5 months, limiting the use of both mice for the long experiments required for modeling demodicosis (Greiner *et al.*, 1995; Shultz *et al.*, 1995; Christianson *et al.*, 1997).

Two potentially useful alternative mice were recently developed. First, NOD/*Rag1* mice have delayed onset of lymphoma, do not develop the "leaky" phenotype, and retain the ability to support higher levels of human leukocyte engraftment (Shultz *et al.*, 2000). Combined *Rag2* and γc (common cytokine receptor chain gamma) double knockout mice are T-cell, B-cell, and NK-cell deficient (Goldman *et al.*, 1998). *Rag2*/γc null mice appear to have a stable immunodeficient phenotype and support increased levels of human lymphocyte engraftment compared to NOD/scid mice (Goldman *et al.*, 1998; Mazurier *et al.*, 1999). The mean life span of *Rag2*/γc null mice is greater than 12 months and these mice do not exhibit the increased spontaneous neoplasia that is observed with NOD/scid or NOD/*Rag1* mice (Goldman *et al.*, 1998; Mazurier *et al.*, 1999).

Improved human leukocyte engraftment in some newer mice with combined mutations (compared to scid or *Rag* null mice) has been attributed to innate defense mechanism defects (diminished macrophage and/or NK-cell function) that are present in addition to T-cell deficiencies (Shultz *et al.*, 1995). These new mice have severe deficits in host defense (affecting innate defense mechanisms and acquired immunity) and may not survive the multiple procedures that are typically required of the xenograft model. Systemic bacterial infections are likely to become a more significant issue.

5.3 APPLICATION OF THE SKIN XENOGRAFT MOUSE MODEL TO STUDY CANINE DEMODICOSIS:

5.3.1 The Skin Xenograft Mouse Model of Canine Demodicosis

The development of a useful experimental model of a disease can be judged by a number of criteria. These include the biologic relevance, reproducibility, and availability of the model. The skin xenograft mouse model is biologically relevant because the skin xenografts represent an *in vivo* system using skin from the species being studied and because *D. canis* infections of grafts mimic naturally occurring demodicosis (discussed below).

The reproducibility of the xenograft model for demodicosis depends on the ability to establish adequate canine skin grafts and active *D. canis* infections. As described above, this study established that replicas of full-thickness canine skin grafts, which morphologically resemble donor skin and actively grow abundant hair, can be generated on immunodeficient mice. Canine skin grafts survive for the extended periods needed to culture *D. canis*. To achieve the skin grafting results needed for controlled experiments requires careful attention to surgical technique and the skills that are needed could be a limiting factor in the model's general use.

The ability to reproduce skin infections with *D. canis* was demonstrated using *D. canis* from different sources as well as donor skin from different dogs. Graft infection rates in the four experiments were 95% (19/20), 100% (12/12), 80% (8/10), and 100% (25/25). Large numbers of mites, including all life-cycle stages, were recovered from grafts at 90 to 117 days after infection, comparable to naturally canine demodicosis (Unsworth, 1946). The highest calculated total for one half of a skin graft (the approximate size of digest samples) was over 39,000 mites. The techniques developed in

this study significantly improved the graft infection results over those of Caswell *et al.* (1996), who reported an overall *D. canis* infection rate of 53% and generally less than 100 mites per digest sample. Because skin grafts were inoculated with between approximately 90 and 350 viable mites, it could be concluded that extensive mite proliferation occurred on grafts. More mites were generally recovered from grafts inoculated with higher mite doses. In the tgε26 and *Rag2* experiments, immature stages (eggs and larvae) were present on skin grafts in large numbers (greater than 50% of the population), whereas the mite inocula used to infect grafts contained few immature stages (15% or less). This finding suggested that mite populations on skin grafts were still expanding at the time graft digestion, 90 to 117 days after infection.

The components of the skin xenograft mouse model of canine demodicosis are readily accessible to researchers. The genetically immunodeficient mice used in these experiments are sold commercially, and *Rag2* knockout mice, identified as most useful, are currently available from Taconic (Germantown, New York, USA). Based on the preliminary work in this study, new mouse mutants should be sought to improve use of the model for inflammatory skin reactions, as discussed above. The cost of these specialized mice and the need for a barrier housing facility may limit the utility of the model for some researchers. Canine skin grafts can be collected from dogs without the need for euthanasia and availability is not a limiting factor. *Demodex canis* are retrievable, albeit intermittently, from dogs with naturally occurring demodicosis throughout North America (Sischo *et al.*, 1989). For this study, *D. canis* were collected from dogs with demodicosis by non-invasive methods. The ability to collect sufficient

numbers of mites for adequate infection of skin grafts at a desired point in time limited the number of skin grafts that could be infected in each experiment.

This study establishes the skin xenograft mouse model as the first reliable means for culturing *D. canis* in the laboratory and as a reliable method of recreating skin infections. Furthermore, the techniques developed make the canine skin xenograft mouse model a viable system for investigating the pathobiology of other canine skin diseases.

5.3.2 Investigating the Pathogenesis of Canine Demodicosis

Fundamental questions remain unresolved regarding the contribution of different host or mite factors to *D. canis* overgrowth and skin lesion development in canine demodicosis. Although the literature supports a central role for T-cells in mediating host resistance to the development of demodicosis, direct evidence is lacking. Other host mechanisms of resistance or mite factors have received little attention.

5.3.2.1 *Host resistance to Demodex canis overgrowth*

The experiments reported in Chapter 4 were designed to directly assess the effect of lymphocytes on *D. canis* populations on canine skin using a quantitative approach. This was accomplished by comparing mite numbers on lymphocyte treated and control grafts. Four replicas of these experiments were performed. While each experiment provided valuable information the *Rag2* experiment was considered the best assessment of the lymphocyte hypothesis. In this experiment, high numbers of mice survived in experimental groups, *D. canis* infection was 100% and complications, such as development of the "leaky" phenotype, were not detected.

The first important observation from these experiments was that the introduction of canine lymphocytes into the mouse skin chimera either had no effect on *D. canis* numbers or, in two experiments, was associated with a significant increase in mite numbers on skin grafts. These findings, which suggest that a lymphocytic response does not control *D. canis* overgrowth on the host but rather may exacerbate it, contradict conventional ideas about the role of lymphocytes in canine demodicosis (reviewed in Chapter 1).

The results of this study require a re-examination of the evidence that T-cells are responsible for controlling *D.canis* populations on the host. Dogs with demodicosis are not lymphopenic, do not have depleted lymphoid tissues and do not appear to be at increased risk of developing other infectious conditions known to be controlled by a lymphocyte response (Scott *et al.*, 1974; Scott *et al.*, 1976; Scott, 1979; Scott *et al.*, 1995). Therefore, dogs that develop generalized demodicosis do not have an overt lymphocyte deficit or a generalized T-cell dysfunction (Scott *et al.*, 1995). Dogs with generalized demodicosis were shown to have a decreased *in vitro* lymphocyte blastogenesis response and decreased cutaneous response to mitogens (reviewed in Chapter 1). However, these mitogen tests are not specific, and depressed lymphocyte responses observed with generalized disease do not clearly precede the onset of generalized demodicosis. Rather, it is likely that the depressed lymphocyte response observed is a consequence of severe inflammation in generalized demodicosis.

Owen (1972) and subsequently Healey and Gafaar (1977), associated experimental immunosuppression using antilymphocyte serum with the development of generalized demodicosis. In their experiments, antilymphocyte serum was derived from

animals treated with whole lymph node, spleen or thymus extracts. It is likely that this antiserum contained antibodies to many cellular and humoral components of the immune system (and possibly common tissue antigens) in addition to lymphocytes. Although not measured in these experiments, more than just lymphocyte suppression must have occurred, leaving open the possibility that other mechanisms, in addition to a T-cell response, were interrupted in these dogs, thus allowing generalized demodicosis to develop. In addition, in these studies, mites were collected from dogs with generalized disease, leaving open the possibility that intrinsic mite factors were important for controlling population size and lesion development.

The clinical evidence suggesting generalized demodicosis, especially in older dogs, is associated with immunosuppressive treatment or concurrent debilitating disease has been reported as indirect evidence that immune system dysfunction contributes to the development of demodicosis (Duclos *et al.*, 1994; Scott *et al.*, 1995; Lemarie, 1996; Lemarie *et al.*, 1996). Again, systemic alterations associated with immunosuppressive treatment in dogs or with debilitating disease are not limited to the T-cell arm of the immune system and are generally considered to impact multiple host systems in addition to other components of the immune system (Kuby, 1997). Immunosuppressive corticosteroid treatment is very common in veterinary medicine, yet it appears that dogs receiving this treatment rarely develop generalized demodicosis despite widespread carriage of *D. canis* (Scott *et al.*, 1995).

Dogs with acquired immunosuppression or dogs with naturally occurring immune deficiency syndromes (for example, dogs with X-linked severe combined immunodeficiency) have not been investigated to determine if normal carriage of *D.*

canis is altered in these conditions. In a human study, immunosuppressed renal transplant patients did not have increased numbers of *D. folliculorum* on their skin surface when compared to healthy controls (Aydingoz *et al.*, 1997). Numerous surveys of patients with acquired immune deficiency syndrome (AIDS) have not identified an increased incidence of skin lesions associated with *Demodex spp.*(Cockerell, 1993; Mirowski *et al.*, 1998; Munoz-Perez *et al.*, 1998; Aftergut & Cockerell, 1999; Jing & Ismail, 1999) despite widespread carriage of *D. folliculorum* and *D. brevis* on humans. These acquired conditions are known to exhibit severe T-cell deficiencies, yet *Demodex spp.* populations appear unaffected (Aydingoz *et al.*, 1997; Kuby, 1997). These findings suggest that T-cell function is not required to limit *Demodex spp.* populations on the human host.

While studying ectoparasite treatments for mice, Hill and colleagues discovered *D. musculi* on mice and subsequently transferred this mite to several different mouse mutants (Hill *et al.*, 1999). Although limited, non quantitative, data were reported, *D. musculi* were recovered from tgε26 mice (T-cell and NK-cell deficient) and prad-1 mice (epidermal proliferation defect, but immunocompetent). *Demodex musculi* were then successfully transferred to scid mice (T-cell and B-cell deficient), but did not appear to establish on *Rag1* knockout mice (T-cell and B-cell deficient), nude mice (T-cell deficient) or SSIN mice (immunocompetent). Mites were reported to be more readily recovered from tgε26 mice and scid mice (data not provided) than from immunocompetent prad-1 mice. This study does not identify a clear association between T-cell, NK-cell, or B-cell deficiency and increased colonization by *D. musculi.* Rather,

these experiments suggest that other host factors, aside from acquired immunity, could be involved in controlling mite numbers on mouse skin.

Finally, although there is good histological and immunohistochemical evidence that a lymphocyte mediated tissue response targets *D. canis* infected hair follicles, it is not clear that these lymphocytes limit mite populations (Caswell *et al.*, 1995; Caswell *et al.*, 1997). Mite numbers could be controlled by another mechanism, mediated either by the host or by mite factors, and lymphocytes are merely responding to mite antigens released by this mechanism and are not directly involved in mite clearance. Alternatively, *D. canis* could alter presentation of host antigen and induce a tissue specific autoimmune-like reaction mediated by lymphocytes that is not directed towards mites. The similarity between the interface folliculitis reaction pattern that occurs in demodicosis and the skin inflammatory reactions observed in autoimmune conditions, such as lupus, or conditions such as GVHD supports this latter possibility (Yager & Wilcock, 1994). The evidence in the literature leaves room for an expanded interpretation of the pathogenesis of demodicosis and the role of lymphocytes in this disease.

What mechanisms limit or promote *D. canis* overgrowth on dogs with demodicosis? In the experiments in this study, *D. canis* grew to large numbers on skin grafts that were derived from normal adult dogs and mite numbers reached levels similar to that of naturally occurring disease. Because skin grafts were isolated from systemic host factors, this observation suggests that local innate skin mechanisms of host resistance are not sufficient to control mite populations on the skin. Rather, it appears that either systemic host mechanisms or possibly intrinsic mite-related factors are

important in controlling mite numbers on canine skin. Regarding the possible systemic factors, lymphocyte treatment was not associated with a decrease in *D. canis* numbers on canine skin grafts. Other systemic factors, such as serum proteins or hormones should be investigated for the ability to limit mite colonization of skin grafts. In this study, *D. canis* continued to proliferate to high numbers on skin grafts after removal from the diseased host. This finding suggests that a continued stimulus from the diseased host is not required for mite replication and the role that intrinsic mite factors play in mite proliferation should be investigated further.

5.3.2.2 *Skin Lesion Development in Canine Demodicosis*

Controversy remains regarding the contribution of *Demodex spp.* to skin lesion development. Previous reports contend that mites contribute to the formation of skin lesions by directly damaging hair follicles, probably as a result of feeding (Nutting, 1976b; Nutting *et al.*, 1989). Hair loss, follicular wall erosion, external root sheath and epidermal hyperplasia, hyperpigmentation and follicular rupture are some of the changes that have been attributed to mite activity in hair follicles. These mites are thought to feed by piercing cells with their stylet-like chelicera and to ingest cellular contents after pre-oral digestion (Desch *et al.*, 1989). Except for the presence of epidermal "pits" associated with *D. criceti* on hamsters, there is minimal direct evidence for a cell-piercing mode of feeding or for direct damage to the hair follicle by mites (Nutting *et al.*, 1989). The functional effect of mites on hair growth or the effect of a large population of mites on hair follicle morphology, in the absence of host humoral or cellular immunity, has not been reported.

In the current study, *D. canis* infected skin xenografts provided a means to assess mite induced hair follicle damage and development of skin lesions in the absence of host inflammation. The conditions were suitable for allowing mite-related follicle damage to occur. Mite numbers reached into the thousands on skin grafts and mites were actively replicating on grafts, producing all life-cycle stages. There was ample time for follicular damage to occur; mites were incubated on grafts for at least 3 months.

Gross or histological lesions of demodicosis did not develop despite the presence of thousands of actively proliferating mites on grafts (Table 4.4-1). Besides dilation of the hair follicle lumen and attenuation of the hair follicle wall around larger numbers of mites, degenerative or adaptive changes were not observed for infected hair follicles. The number of mites on grafts, and their location in the superficial follicle, and less often in sebaceous gland ducts, was similar to naturally occurring cases of demodicosis (Unsworth, 1946; Nutting, 1976a). Instead of loosing hair, as is seen in demodicosis, grafts continued to grow more hair (when not complicated by bacterial infection) even though mite populations were expanding in hair follicles. As many as 60 mites occupied a hair follicle unit for grafts on tgε26 mice and did not induce hair loss (Table 4.3-1). Therefore, *D. canis* does not appear to have a functional effect on hair growth. These findings indicate that inflammation, and not mite colonization, is responsible for lesion development in demodicosis (Caswell *et al.*, 1995; Caswell *et al.*, 1997). The presence of mites in the dermis, observed in demodicosis, likely results from lymphocyte mediated destruction of the hair follicle wall, or the consequences of bacterial pyoderma, and not from active mite penetration (Caswell *et al.*, 1995). The results also support the conclusions by Sheahan and Gafaar that *D. canis* do not feed by piercing viable

keratinocytes but feed most likely on the lipid rich surface film and/or non-viable keratinocytes at the skin surface (Sheahan & Gaafar, 1970).

The observation that mites do not appear to directly damage hair follicles impacts our understanding of host recognition of *Demodex spp.* Keratinocytes are known to constitutively express pro-inflammatory mediators within the cytoplasm, such as interleukin-1 alpha (IL-1α), tumor necrosis factor-alpha (TNF-α), interleukin-6 (IL-6) and can be induced to express several others (Luger *et al.*, 1997). For example, feeding and burrowing by *Sarcoptes scabiei* on *in vitro* constructed human epidermis is associated with release of IL-1α and IL-1β from keratinocytes (Arlian *et al.*, 1996). If *D. canis* feed without disrupting keratinocytes, then mites may avoid activation of the host immune response by this mechanism. Furthermore, *Demodex spp.* do not have a posterior opening to their gastrointestinal tract and do not excrete feces that are potentially antigenic (Desch *et al.*, 1989). Finally, sebaceous dwelling *D. brevis* from humans are coated with a carbohydrate antigen that is also expressed in sebaceous glands and this may be an example of antigenic mimicry or host antigen acquisition being exploited by mites to avoid immune recognition (Kanitakis *et al.*, 1997). Together, these findings suggest that *Demodex spp.* may have evolved to evade host recognition as a means to avoid elimination by the host immune response.

Mite antigens could possibly be released and recognized by the host through two mechanisms. First, if mites die and their exoskeleton ruptures while the mite remains on the skin surface, then internal mite antigens could be released and become available for host recognition. Second, *Demodex spp.* require pre-oral digestion of their food and appear to secrete enzyme rich saliva from large paired salivary glands to accomplish this

(Desch *et al.*, 1989). Externalized salivary antigens may be available for host recognition. If mite antigens are recognized by the host, then the lack of mite induced tissue trauma may actually favor the development of tolerance, thereby facilitating maintenance of *D. canis* on the skin surface (Grabbe *et al.*, 1996; Matzinger, 1998; McFadden & Basketter, 2000). Further investigation is required to determine the specific mechanisms of host recognition of *Demodex spp.* antigens. These events at the host parasite interface are important for understanding the development of inflammation in demodicosis and the apparent host tolerance observed in normal dogs that harbor *D. canis* (Scott *et al.*, 1995).

5.3.3 Future Investigations of Canine Demodicosis

The results of the current study bring into question the accepted dogma that lymphocytes limit *D. canis* populations on canine skin and are protective for demodicosis. Future experiments should be directed towards: (1) confirming or refuting the findings of the current study with regard to the functional role of lymphocytes in demodicosis; (2) assessing other systemic factors (humoral, endocrine, etc.) in the control of *D. canis* on canine skin; and (3) evaluating *D. canis* biology and intrinsic mite factors that affect proliferation.

Three *in vivo* experimental techniques could be used to address mechanisms of host resistance to *D. canis* and the biology of this mite. First, in the current study, the skin xenograft mouse model was developed sufficiently that it could be used to assess the role of systemic humoral or endocrine factors in limiting mite populations on canine skin. Using the xenograft model, basic questions, such as "what is the life span of *D. canis*?"

could finally be addressed. Mites derived from normal dogs and those with localized or generalized demodicosis could be compared on syngeneic grafts to assess for population differences in proliferative capacity and to identify replication stimuli or inhibitors.

To address lymphocyte function, newer immunodificient mice, such as *Rag1/γc* double knockouts, could be used in attempts to improve canine lymphocyte engraftment. Coengraftment of a canine lymph node, in addition to canine skin, may enhance the ability to generate a more robust lymphocyte mediated tissue reaction by facilitating expansion of reacting clones (Carballido *et al.*, 2000). To insure that adequate numbers of *D. canis* specific lymphocyte clones are available for reconstituting mice, tissues could be collected from dogs that had recently recovered from localized demodicosis. These dogs would theoretically be known capable of clearing mites from the skin surface. These experiments are difficult because it is difficult to acquire acceptable dogs. Stimulation of lymphocytes *in vitro* with *D. canis* antigens, an alternative method for generating increased numbers of mite specific T-cell clones, is complicated by difficulties in obtaining mite antigens free of bacterial and/or allogeneic keratinocyte antigens (personal observation; T. Bell, personal communication).

A second method would be to experimentally deplete normal adult dogs of lymphocyte subsets using monoclonal antibodies before *D. canis* infection. Previous studies have used this method to immunosuppress dogs for organ transplant studies using antibodies to CD4 and CD8 lymphocyte cell surface antigens (Watson *et al.*, 1993; Watson *et al.*, 1995). The immunologic defect induced would be more specific than the severe immunosuppression induced in dogs with antilymphocyte serum in the *D. canis* studies of the 1970s (Owen, 1972; Healey & Gaafar, 1977a). However, dogs develop an

immune response to the foreign antibody and this complication has limited antibody treatment in canine and human organ transplant studies and has spurred the development of human chimeric antibodies (Watson *et al.*, 1993; Mourad *et al.*, 1998). A comparative benefit of the xenograft model is the ability to obtain larger numbers in treatment and control groups with syngeneic grafts. Additionally, *D. canis* replication is restricted to the skin xenograft (personal observation), whereas after infection of dogs, mites could disperse over the body making it difficult to assess a quantitative treatment effect.

Finally, a third *in vivo* approach is comparative and based on assessing the resistance of different immunodeficient mutant mice to *D. musculi* (introduced above) (Hill *et al.*, 1999). The use of mice with specific gene mutations affecting different host mechanisms of interest offers an attractive means to delineate those factors involved in host resistance to *Demodex spp.* skin colonization. A number of relevant knockout mice are commercially available for use in this approach; however, little is known about the natural distribution and availability of *D. musculi* (Hill *et al.*, 1999). Mouse strains exhibit different immune responses and therefore different mutations should be compared on the same background strain and to the same strain lacking the mutation (Charles *et al.*, 1999).

5.4 CONCLUSIONS

1) The skin xenograft mouse model was successfully adapted for use with canine tissues.
    a) Techniques for grafting full-thickness canine skin were developed that allowed the production of well-haired skin grafts on immunodeficient mice. Factors affecting early vascular perfusion of full-thickness skin grafts, graft stability and

mouse-related trauma were important for achieving good quality grafts. The first macroscopic and microscopic descriptions of canine skin xenografts are provided. Full-thickness and split-thickness canine skin grafts contract significantly and similarly during healing. Larger canine skin grafts were developed than previously reported. Canine skin was successfully grafted to tgε26 mice, ICR scid mice and *Rag2* knockout mice for the first time.

b) Canine lymphocytes can survive transfer to the immunodeficient mouse and are capable of producing immunoglobulin and mediating effector functions within canine skin grafts. Survival of canine lymphocytes, delivered in the form of PBMC, was generally higher in tgε26 mice than in *Rag2* null mice or ICR scid mice, as demonstrated by circulating canine IgG levels. *In vitro* stimulation of canine lymphocytes with PHA-P and hr-IL-2 was associated with increased production of canine IgG in *Rag2* mice. The half-life of canine IgG in tgε26 mice is 2.9 days.

2) It was demonstrated that the skin xenograft mouse model of canine demodicosis recreates aspects of the naturally occurring disease and is a useful experimental tool for studying canine demodicosis.

a) Canine skin grafts from different dogs, on different mouse mutants, could be repeatedly infected with *D. canis* and mites replicated to high numbers on grafts, similar to those observed in demodicosis. This study refined the skin xenograft mouse model into the first useful system for culturing *D. canis* in the laboratory.

b) Of the immunodeficient mice evaluated in this study, *Rag2* knockout mice were most useful for skin xenograft experiments modeling canine demodicosis.

3) In the canine skin xenograft mouse model, lymphocytes did not limit *D. canis* proliferation on skin grafts. Inoculation with canine lymphocytes, stimulated non-specifically *in vitro*, led to an increase in mite numbers on skin grafts.

4) Grafting experiments demonstrated that local mechanisms of skin innate defense alone do not control *D. canis* proliferation on canine skin. Systemic host mechanisms and/or intrinsic mite factors control mite proliferation on dog skin.

5) *Demodex canis*, collected from dogs with generalized demodicosis, continued to proliferate to high numbers when transferred to skin grafts from normal dogs on mice. Mite proliferation in demodicosis does not require a continued stimulus from the diseased canine host.

6) *Demodex canis* alone did not induce skin lesions in canine xenografts. *Demodex canis* activity does not contribute to skin lesion development and does not induce hair loss in demodicosis. Inflammation is required for development of skin lesions in demodicosis.

REFERECES:

Anonymous (1989) *Institute of Laboratory Animal Resources (U.S.) Commitee on Immunologically Compromised Rodents. Immunodeficient rodents: a Guide to Their Immunobiology, Husbandry, and Use.* National Academy Press, Washington D. C. p 69-71.

Abedi, M.R., Christenson, B., Islam, K.B., Hammarstrom, L. & Smith, C.I. (1992) Immunoglobulin production in severe combined immunodeficient (SCID) mice reconstituted with human peripheral blood mononuclear cells. *Eur J Immunol*, **22**, 823-828.

Aftergut, K. & Cockerell, C.J. (1999) Update on the cutaneous manifestations of HIV infection. Clinical and pathologic features. *Dermatol Clin*, **17**, 445-471.

Alegre, M.L., Peterson, L.J., Jeyarajah, D.R., Weiser, M., Bluestone, J.A. & Thistlethwaite, J.R. (1994) Severe combined immunodeficient mice engrafted with human splenocytes have functional human T cells and reject human allografts. *J Immunol*, **153**, 2738-2749.

Arlian, L.G., Vyszenski-Moher, D.L., Rapp, C.M. & Hull, B.E. (1996) Production of IL-1 alpha and IL-1 beta by human skin equivalents parasitized by *Sarcoptes scabiei*. *J Parasitol*, **82**, 719-723.

Atillasoy, E.S., Elenitsas, R., Sauter, E.R., Soballe, P.W. & Herlyn, M. (1997) UVB induction of epithelial tumors in human skin using a RAG-1 mouse xenograft model. *J Invest Dermatol*, **109**, 704-709.

Aydingoz, I.E., Mansur, T. & Dervent, B. (1997) *Demodex folliculorum* in renal transplant patients. *Dermatology*, **195**, 232-234.

Baker, D.W. & Fisher, W.F. (1969) The incidence of demodectic mites in the eyelids of various mammalian hosts. *J Econ Entomol*, **62**, 942.

Baker, K.P. (1969) The histopathology and pathogenesis of demodicosis in the dog. *J of Comp Path*, **79**, 321-327.

Baker, K.P. (1970) Observations on the epidemiology, diagnosis and treatment of demodicosis in dogs. *Vet Rec*, **86**, 90-91.

Baker, K.P. (1975) Hyperpigmentation of the skin in canine demodicosis. *Vet Parasitol*, **1**, 193-197.

Balson, G.A., Yager, J.A. & Croy, B.A. (1992) Scid/beige mice in the study of immunity to *Rhodococcus equi*. In: W. Plowright, P.D. Rossdale and J.F. Wade (Eds), *Equine Infectious Diseases*, Vol. VI. R & W Publications, Ltd., Newmarket, p. 49-53.

Balson, G.A., Croy, B.A., Ross, T.L. & Yager, J.A. (1993) Demonstration of equine immunoglobulin in sera from severe combined immunodeficiency/beige mice inoculated with equine lymphocytes. *Vet Immunol Immunopathol*, **39**, 315-325.

Bancroft, G.J., Schreiber, R.D. & Unanue, E.R. (1991) Natural immunity: a T-cell-independent pathway of macrophage activation, defined in the scid mouse. *Immunol Rev*, **124**, 5-24.

Barriga, O.O., Al Khalidi, N.W., Martin, S. & Wyman, M. (1992) Evidence of immunosuppression by *Demodex canis*. *Vet Immunol Immunopathol*, **32**, 37-46.

Barta, O., Waltman, C., Shaffer, L.M. & Oyekan, P.P. (1982) Effect of serum on lymphocyte blastogenesis. I. Basic characteristics of action by diseased dog serum. *Vet Immunol Immunopathol*, **3**, 567-583.

Barta, O., Waltman, C., Oyekan, P.P., McGrath, R.K. & Hribernik, T.N. (1983) Lymphocyte transformation suppression caused by pyoderma--failure to demonstrate it in uncomplicated demodectic mange. *Comp Immunol, Microbiol and Infect Dis*, **6**, 9-18.

Barta, O. & Barta, V. (1993) Immunological techniques evaluating cells and their functions. In: O. Barta (Ed) *Veterinary Clinical Immunology Laboratory*, Vol. 2. BAR-LAB Inc., Blacksburg. p. B1-7 - B5-12.

Bhalerao, D.P. & Bose, D.A. (1990) Cutaneous response to intradermal injection of phytohemagglutinin - M in dogs infested with *Demodex canis*. *J Bombay Vet Coll*, **2**, 61-63.

Billingham, R.E. & Medawar, P.B. (1951) The technique of skin grafting in mammals. *J Exp Bio*, **28**, 385-402.

Bivin, S. & Smith, G. (1984) Techniques of experimentation. In: J. Fox, B. Cohen and F. Loew (Eds), *Laboratory animal medicine*. Academic Press, Inc, San Diego. p. 563-594.

Black, K.E. & Jederberg, W.W. (1985) Athymic nude mice and human skin grafting. In: H.I. Maibach and N.J. Lowe (Eds), *Models in Dermatology*, Vol. 1. Karger, Basel, p. 228-239.

Blunt, T., Finnie, N.J., Taccioli, G.E., Smith, G.C., Demengeot, J., Gottlieb, T.M., Mizuta, R., Varghese, A.J., Alt, F.W., Jeggo, P.A. & *et al.* (1995a) Defective DNA-dependent protein kinase activity is linked to V(D)J recombination and DNA repair defects associated with the murine scid mutation. *Cell*, **80**, 813-823.

Blunt, T., Taccioli, G.E., Priestley, A., Hafezparast, M., McMillan, T., Liu, J., Cole, C.C., White, J., Alt, F.W., Jackson, S.P. & *et al.* (1995b) A YAC contig encompassing the

XRCC5 (Ku80) DNA repair gene and complementation of defective cells by YAC protoplast fusion. *Genomics*, **30**, 320-328.

Boehncke, W.H., Sterry, W., Hainzl, A., Scheffold, W. & Kaufmann, R. (1994) Psoriasiform architecture of murine epidermis overlying human psoriatic dermis transplanted onto SCID mice. *Arch Dermatol Res*, **286**, 325-330.

Boehncke, W.H., Zollner, T.M., Dressel, D. & Kaufmann, R. (1997) Induction of psoriasiform inflammation by a bacterial superantigen in the SCID-hu xenogeneic transplantation model. *J Cutan Pathol*, **24**, 1-7.

Bosca, A.R., Tinois, E., Faure, M., Kanitakis, J., Roche, P. & Thivolet, J. (1988) Epithelial differentiation of human skin equivalents after grafting onto nude mice. *J Invest Dermatol*, **91**, 136-141.

Bosma, G.C., Custer, R.P. & Bosma, M.J. (1983) A severe combined immunodeficiency mutation in the mouse. *Nature*, **301**, 527-530.

Bosma, G.C., Fried, M., Custer, R.P., Carroll, A., Gibson, D.M. & Bosma, M.J. (1988) Evidence of functional lymphocytes in some (leaky) scid mice. *J Exp Med*, **167**, 1016-1033.

Bosma, M.J. (1992) B and T cell leakiness in the scid mouse mutant. *Immunodefic Rev*, **3**, 261-276.

Brandsma, J.L., Brownstein, D.G., Xiao, W. & Longley, B.J. (1995) Papilloma formation in human foreskin xenografts after inoculation of human papillomavirus type 16 DNA. *J Virol*, **69**, 2716-2721.

Braverman, I.M. (1989) Ultrastructure and organization of the cutaneous microvasculature in normal and pathologic states. *J Invest Dermatol*, **93**, 2S-9S.

Breyere, E.J. (1972) A quantitative experimental skin-grafting technique in mice. *Med Ann Dist Columbia*, **41**, 51-55.

Briggaman, R.A. & Wheeler, C.E., Jr. (1976) Lamellar ichthyosis: long-term graft studies on congenitally athymic nude mice. *J Invest Dermatol*, **67**, 567-576.

Briggaman, R.A. (1980) Localization of the defect in skin diseases analyzed in the human skin graft-nude mouse model. *Curr Probl Dermatol*, **10**, 115-126.

Briggaman, R.A. (1985) Human skin graft-nude mouse model: techniques and application. In: D. Skerrow and C.J. Skerrow (Eds), *Methods of Skin Research*. Chischester, Toronto, p. 251-276.

Bukva, V. (1991) Structural reduction and topological retrieval: problems in taxonomy of demodecidae. In: F. Dusbabek and V. Bukva (Eds), *Modern Acarology*, Vol. 1. SPB Academic Publishing, Prague, p. 293-300.

Buller, R.M., Burnett, J., Chen, W. & Kreider, J. (1995) Replication of molluscum contagiosum virus. *Virology*, **213**, 655-659.

Burkett, G., Frank, L.A., Bailey, E.M., Schmeitzel, L.P. & Kania, S.A. (1996) Immunology of dogs with juvenile-onset generalized demodicosis as determined by lymphoblastogenesis and CD4:CD8 analysis. *J Vet Aller Clin Immunol*, **4**, 46-52.

Carballido, J.M., Namikawa, R., Carballido-Perrig, N., Antonenko, S., Roncarolo, M.G. & de Vries, J.E. (2000) Generation of primary antigen-specific human T- and B-cell responses in immunocompetent SCID-hu mice. *Nat Med*, **6**, 103-106.

Carpenter, B.A. (1992) Enzyme-Linked Immunoassays. In: N.R. Rose, E.C. DeMacrio, J.L. Fahey, H. Friedman and G.M. Penn (Eds), *Manual of Clinical Laboratory Immunology*. American Society for Microbiology, Washington, p. 2-9.

Carroll, A.M. & Bosma, M.J. (1988) Detection and characterization of functional T cells in mice with severe combined immune deficiency. *Eur J Immunol*, **18**, 1965-1971.

Carroll, A.M. & Bosma, M.J. (1989) Rearrangement of T cell receptor delta genes in thymus of scid mice. *Curr Top Microbiol Immunol*, **152**, 63-67.

Carroll, A.M., Hardy, R.R. & Bosma, M.J. (1989) Occurrence of mature B (IgM+, B220+) and T (CD3+) lymphocytes in scid mice. *J Immunol*, **143**, 1087-1093.

Caswell, J. (1995) Investigation of the immunopathology of canine demodicosis (DVSc Thesis). In: *Pathology*. University of Guelph, Guelph.

Caswell, J.L., Yager, J.A., Ferrer, L. & Weir, J.A.M. (1995) Canine demodicosis: a re-examination of the histopathologic lesions and description of the immunophenotype of infiltrating cells. *Vet Dermatol*, **6**, 9-19.

Caswell, J.L., Yager, J.A., Barta, J.R. & Parker, W. (1996) Establishment of *Demodex canis* on canine skin engrafted onto scid-beige mice. *J Parasitol*, **82**, 911-915.

Caswell, J.L., Yager, J.A., Parker, W.M. & Moore, P.F. (1997) A prospective study of the immunophenotype and temporal changes in the histologic lesions of canine demodicosis. *Vet Pathol*, **34**, 279-287.

Cayatte, S.M., Scott, D.W. & Miller, W.H. (1992) Perifollicular melanosis in the dog. *Vet Dermatol*, **3**, 165-170.

Charles, P.C., Weber, K.S., Cipriani, B. & Brosnan, C.F. (1999) Cytokine, chemokine and chemokine receptor mRNA expression in different strains of normal mice: implications for establishment of a Th1/Th2 bias. *J Neuroimmunol*, **100**, 64-73.

Chen, C. (1995) A short-tailed demodectic mite and *Demodex canis* infestation in a Chihuahua dog. *Vet Dermatol*, **6**, 227-229.

Chesney, C.J. (1999) Short form of *Demodex* species mite in the dog: occurrence and measurements. *J Small Anim Pract*, **40**, 58-61.

Christensen, N.D. & Kreider, J.W. (1990) Antibody-mediated neutralization in vivo of infectious papillomaviruses. *J Virol*, **64**, 3151-3156.

Christensen, N.D., Kreider, J.W., Cladel, N.M., Patrick, S.D. & Welsh, P.A. (1990) Monoclonal antibody-mediated neutralization of infectious human papillomavirus type 11. *J Virol*, **64**, 5678-5681.

Christensen, N.D. & Kreider, J.W. (1991) Neutralization of CRPV infectivity by monoclonal antibodies that identify conformational epitopes on intact virions. *Virus Res*, **21**, 169-179.

Christensen, N.D. & Kreider, J.W. (1993) Monoclonal antibody neutralization of BPV-1. *Virus Res*, **28**, 195-202.

Christianson, S.W., Greiner, D.L., Hesselton, R.A., Leif, J.H., Wagar, E.J., Schweitzer, I.B., Rajan, T.V., Gott, B., Roopenian, D.C. & Shultz, L.D. (1997) Enhanced human CD4+ T cell engraftment in beta2-microglobulin-deficient NOD-scid mice. *J Immunol*, **158**, 3578-3586.

Christofidou-Solomidou, M., Murphy, G.F. & Albelda, S.M. (1996) Induction of E-selectin-dependent leukocyte recruitment by mast cell degranulation in human skin grafts transplanted on SCID mice. *Am J Pathol*, **148**, 177-188.

Christofidou-Solomidou, M., Albelda, S.M., Bennett, F.C. & Murphy, G.F. (1997a) Experimental production and modulation of human cytotoxic dermatitis in human-murine chimeras. *Am J Pathol*, **150**, 631-639.

Christofidou-Solomidou, M., Longley, B.J., Whitaker-Menezes, D., Albelda, S.M. & Murphy, G.F. (1997b) Human skin/SCID mouse chimeras as an in vivo model for human cutaneous mast cell hyperplasia. *J Invest Dermatol*, **109**, 102-107.

Cockerell, C.J. (1993) Organ-specific manifestations of HIV infection. II. Update on cutaneous manifestations of HIV infection. *Aids*, **7**, S213-S218.

Coleman, S.R. (1997) Facial recontouring with lipostructure. *Clin Plast Surg*, **24**, 347-367.

Corbett, R., Banks, K., Hinrichs, D. & Bell, T. (1975) Cellular immune responsiveness in dogs with demodectic mange. *Transplant Proc*, 7, 557-559.

Cubie, H.A. (1976) Failure to produce warts on human skin grafts on 'nude' mice. *Br J Dermatol*, **94**, 659-665.

Custer, R.P., Bosma, G.C. & Bosma, M.J. (1985) Severe combined immunodeficiency (SCID) in the mouse. Pathology, reconstitution, neoplasms. *Am J Pathol*, **120**, 464-477.

Damian, R.T. (1997) Parasite immune evasion and exploitation: reflections and projections. *Parasitology*, **115 Suppl**, S169-S175.

Davisson, M.T. (1996) Rules and guidelines for gene nomenclature. In: M.F. Lyon, S. Rastan and S.D.M. Brown (Eds), *Genetic Variants and Strains of the Laboratory Mouse*, Vol. 1. Oxford University Press Inc., New York, p. 1-16.

Day, M.J. & Penhale, W.J. (1988) Serum immunoglobulin A concentrations in normal and diseased dogs. *Res Vet Sci*, **45**, 360-363.

Day, M.J. (1997) An immunohistochemical study of the lesions of demodicosis in the dog. *J Comp Pathol*, **116**, 203-216.

DeBoer, D., Volk, L. & Olivry, T. (1998) Canine antibody production in immunodeficient mice reconstituted with peripheral blood mononuclear cells from hypersensitive dogs (ABSRACT). *FASEB J*, **12**, 1062.

DeBoer, D., Volk, L., Blum, J. & Lawton, T. (1999) Anti-IgE induced reduction of canine immunoglobulin-E concentrations in a scid-canine chimeric mouse model. In: *Proceedings of the AAVD / ACVD annual meeting*, Maui, Hawaii, p. 103.

DeBoer, D.J., Ihrke, P.J. & Stannard, A.A. (1988) Circulating immune complex concentrations in selected cases of skin disease in dogs. *Am J Vet Res*, **49**, 143-146.

DeBoer, D.J. (1994) Immunomodulatory effects of staphylococcal antigen and antigen-antibody complexes on canine mononuclear and polymorphonuclear leukocytes. *Am J Vet Res*, **55**, 1690-1696.

Delhem, N., Hadida, F., Gorochov, G., Carpentier, F., de Cavel, J.P., Andreani, J.F., Autran, B. & Cesbron, J.Y. (1998) Primary Th1 cell immunization against HIVgp160 in SCID-hu mice coengrafted with peripheral blood lymphocytes and skin. *J Immunol*, **161**, 2060-2069.

Demarchez, M., Sengel, P. & Prunieras, M. (1986) Wound healing of human skin transplanted onto the nude mouse. I. An immunohistological study of the reepithelialization process. *Dev Biol*, **113**, 90-96.

Demarchez, M., Hartmann, D.J., Herbage, D., Ville, G. & Prunieras, M. (1987a) Wound healing of human skin transplanted onto the nude mouse. II. An immunohistological and ultrastructural study of the epidermal basement membrane zone reconstruction and connective tissue reorganization. *Dev Biol*, **121**, 119-129.

Demarchez, M., Hartmann, D.J. & Prunieras, M. (1987b) An immunohistological study of the revascularization process in human skin transplanted onto the nude mouse. *Transplantation*, **43**, 896-903.

Demarchez, M., Asselineau, D. & Czernielewski, J. (1993) Migration of Langerhans cells into human epidermis of "reconstructed" skin, normal skin, or healing skin, after grafting onto the nude mouse. *J Invest Dermatol*, **100**, 648-652.

Desch, C. & Nutting, W.B. (1972) *Demodex folliculorum* (Simon) and *D. brevis* akbulatova of man: redescription and reevaluation. *J Parasitol*, **58**, 169-177.

Desch, C.E. (1973) The biology of the demodicids of man (PhD Thesis). In: *Zoology*. University of Massechusetts, Boston.

Desch, C.E. & Nutting, W.B. (1978) Morphology and functional anatomy of *Demodex folliculorum* (Simon) of man. *Acarologia*, **19**, 422-462.

Desch, C.E., Jr. (1984) The reproductive anatomy of *Demodex folliculorum* (Simon). In: D.A. Griffiths and C.E. Bowman (Eds), *Acarology VI*. Chichester, Toronto, p. 464-469.

Desch, C.E., Jr., ChannaBasavanna, G.P. & Viraktamath, C.A. (1989) The digestive system of *Demodex folliculorum* (Acari: Demodicidae) of man: a light and electron microscope study. *Progress in acarology*, **1**, 187-195.

Desch, C.E., Jr. & Stewart, T.B. (1999) *Demodex gatoi*: new species of hair follicle mite (Acari: Demodecidae) from the domestic cat (Carnivora: Felidae). *J Med Entomol*, **36**, 167-170.

Duchosal, M.A., Eming, S.A., McConahey, P.J. & Dixon, F.J. (1992) The hu-PBL-SCID mouse model. Long-term human serologic evolution associated with the xenogeneic transfer of human peripheral blood leukocytes into SCID mice. *Cell Immunol*, **139**, 468-477.

Duclos, D.D., Jeffers, J.G. & Shanley, K.J. (1994) Prognosis for treatment of adult-onset demodicosis in dogs: 34 cases (1979-1990). *J Am Vet Med Assoc*, **204**, 616-619.

Eaton, G.J. (1976) Hair growth cycles and wave patterns in "nude" mice. *Transplantation*, **22**, 217-222.

Eming, S.A., Lee, J., Snow, R.G., Tompkins, R.G., Yarmush, M.L. & Morgan, J.R. (1995) Genetically modified human epidermis overexpressing PDGF-A directs the development of a cellular and vascular connective tissue stroma when transplanted to athymic mice--implications for the use of genetically modified keratinocytes to modulate dermal regeneration. *J Invest Dermatol*, **105**, 756-763.

Evans, S.S., Bain, M.D. & Wang, W.C. (2000) Fever-range hyperthermia stimulates alpha4beta7 integrin-dependent lymphocyte-endothelial adhesion. *Int J Hyperthermia*, **16**, 45-59.

Farooqui, J.Z., Robb, E., Boyce, S.T., Warden, G.D. & Nordlund, J.J. (1995) Isolation of a unique melanogenic inhibitor from human skin xenografts: initial in vitro and in vivo characterization. *J Invest Dermatol*, **104**, 739-743.

Fife, K.H., Whitfeld, M., Faust, H., Goheen, M.P., Bryan, J. & Brown, D.R. (1996) Growth of molluscum contagiosum virus in a human foreskin xenograft model. *Virology*, **226**, 95-101.

Flanagan, S.P. (1966) 'Nude', a new hairless gene with pleiotropic effects in the mouse. *Genet Res*, **8**, 295-309.

Folz, S.D., Geng, S., Nowakowski, L.H. & Conklin, R.D. (1978) Evaluation of a new treatment for canine scabies and demodecosis. *J Vet Pharmacol Therap*, **1**, 199-204.

French, F.E. (1962) Biology and Morphology of *Demodex canis* (PhD Thesis). In: *Entomology*. Iowa State University, Ames.

French, F.E. (1963) Two Larva Stadia of *Demodex canis* Legdig (Acarina: Trombidiformes). *Acarologia*, **5**, 34-38.

French, F.E., Raun, E.S. & Baker, D.L. (1964) Transmission of *Demodex canis* leydig to pups. *Iowa St J Sci*, **38**, 291-298.

Frey, M., Packianathan, N.B., Fehniger, T.A., Ross, M.E., Wang, W.C., Stewart, C.C., Caligiuri, M.A. & Evans, S.S. (1998) Differential expression and function of L-selectin on CD56bright and CD56dim natural killer cell subsets. *J Immunol*, **161**, 400-408.

Friedman, T., Shimizu, A., Smith, R.N., Colvin, R.B., Seebach, J.D., Sachs, D.H. & Iacomini, J. (1999) Human CD4+ T cells mediate rejection of porcine xenografts. *J Immunol*, **162**, 5256-5262.

Gafaar, S.M., Smalley, N.D. & Turk, R.D. (1958) The incidence of *Demodex* species on skins of apparently normal dogs. *J Am Vet Med Assoc*, **133**, 122-123.

Gilhar, A. & Krueger, G.G. (1987) Hair growth in scalp grafts from patients with alopecia areata and alopecia universalis grafted onto nude mice. *Arch Dermatol*, **123**, 44-50.

Gilhar, A., Pillar, T., Eidelman, S. & Etzioni, A. (1989a) Vitiligo and idiopathic guttate hypomelanosis. Repigmentation of skin following engraftment onto nude mice. *Arch Dermatol*, **125**, 1363-1366.

Gilhar, A., Pillar, T., Winterstein, G. & Etzioni, A. (1989b) The pathogenesis of lichen planus. *Br J Dermatol*, **120**, 541-544.

Gilhar, A., Pillar, T. & David, M. (1991a) Aged versus young skin before and after transplantation onto nude mice. *Br J Dermatol*, **124**, 168-171.

Gilhar, A., Pillar, T., David, M. & Eidelman, S. (1991b) Melanocytes and Langerhans cells in aged versus young skin before and after transplantation onto nude mice. *J Invest Dermatol*, **96**, 210-214.

Gilhar, A., Pillar, T., Assay, B. & David, M. (1992) Failure of passive transfer of serum from patients with alopecia areata and alopecia universalis to inhibit hair growth in transplants of human scalp skin grafted on to nude mice. *Br J Dermatol*, **126**, 166-171.

Gilhar, A., David, M., Ullmann, Y., Berkutski, T. & Kalish, R.S. (1997) T-lymphocyte dependence of psoriatic pathology in human psoriatic skin grafted to SCID mice. *J Invest Dermatol*, **109**, 283-288.

Gilhar, A., Ullmann, Y., Berkutzki, T., Assy, B. & Kalish, R.S. (1998) Autoimmune hair loss (alopecia areata) transferred by T lymphocytes to human scalp explants on SCID mice. *J Clin Invest*, **101**, 62-67.

Goldman, J.P., Blundell, M.P., Lopes, L., Kinnon, C., Di Santo, J.P. & Thrasher, A.J. (1998) Enhanced human cell engraftment in mice deficient in RAG2 and the common cytokine receptor gamma chain. *Br J Haematol*, **103**, 335-342.

Grabbe, S., Steinert, M., Mahnke, K., Schwartz, A., Luger, T.A. & Schwarz, T. (1996) Dissection of antigenic and irritative effects of epicutaneously applied haptens in mice. Evidence that not the antigenic component but nonspecific proinflammatory effects of haptens determine the concentration-dependent elicitation of allergic contact dermatitis. *J Clin Invest*, **98**, 1158-1164.

Graem, N., Dabelsteen, E. & Tommerup, N. (1984) Blood group substances, T6 antigen and heterochromatin pattern as species markers in the nude mouse/human skin model. *Exp Cell Biol*, **52**, 251-259.

Green, F.D., Lee, K.W. & Balish, E. (1982) Chronic *T. mentagrophytes* dermatophytosis of guinea pig skin grafts on nude mice. *J Invest Dermatol*, **79**, 125-129.

Greenwood, J.D. & Croy, B.A. (1993) A study on the engraftment and trafficking of bovine peripheral blood leukocytes in severe combined immunodeficient mice. *Vet Immunol Immunopathol*, **38**, 21-44.

Greenwood, J.D., Bos, N.A. & Croy, B.A. (1996) Offspring of xenogeneically-reconstituted scid/scid mice are capable of a primary xenogeneic immune response to DNP-KLH. *Vet Immunol Immunopathol*, **50**, 145-155.

Greenwood, J.D., Croy, B.A., Trout, D.R. & Wilcock, B.P. (1997) Xenogeneic (bovine) peripheral blood leukocytes engrafted into severe combined immunodeficient mice retain primary immune function. *Vet Immunol Immunopathol*, **59**, 93-112.

Greiner, D.L., Shultz, L.D., Yates, J., Appel, M.C., Perdrizet, G., Hesselton, R.M., Schweitzer, I., Beamer, W.G., Shultz, K.L., Pelsue, S.C. & et al. (1995) Improved engraftment of human spleen cells in NOD/LtSz-scid/scid mice as compared with C.B-17-scid/scid mice. *Am J Pathol*, **146**, 888-902.

Greve, J.H. & Gaafar, S.M. (1966) Natural transmission of Demodex canis in dogs. *J Am Vet Med Assoc*, **148**, 1043-1045.

Gross, T., Ihrke, P. & Walder, E. (1992) *Veterinary Dermatopathology: a Macroscopic and Microscopic Evaluation of Canine and Feline Skin Disease*. Mosby, St. Louis. p. 252-270.

Hammad, H., Duez, C., Fahy, O., Tsicopoulos, A., Andre, C., Wallaert, B., Lebecque, S., Tonnel, A.B. & Pestel, J. (2000) Human dendritic cells in the severe combined immunodeficiency mouse model: their potentiating role in the allergic reaction. *Lab Invest*, **80**, 605-614.

Hammerberg, B., Bevier, D., DeBoer, D.J., Olivry, T., Orton, S.M., Gebhard, D. & Vaden, S.L. (1997) Auto IgG anti-IgE and IgG x IgE immune complex presence and effects on ELISA-based quantitation of IgE in canine atopic dermatitis, demodectic acariasis and helminthiasis. *Vet Immunol Immunopathol*, **60**, 33-46.

Hashimoto, T., Kazama, T., Ito, M., Urano, K., Katakai, Y. & Ueyama, Y. (1996) Histological examination of human hair follicles grafted onto severe combined immunodeficent (SCID) mice. In: J. Van Neste and V. Randell (Eds), *Hair Research for the Next Millenium*. Elsevier Science, New York, p. 141-145.

Healey, M.C. & Gaafar, S.M. (1977a) Immunodeficiency in canine demodectic mange. I. experimental production of lesions using antilymphocyte serum. *Vet Parasitol*, **3**, 121-131.

Healey, M.C. & Gaafar, S.M. (1977b) Immunodeficiency in canine demodectic mange. I. Experimental production of lesions using antilymphocyte serum. II. Skin reactions to phytohemagglutinin and concanavalin A. *Vet Parasitol*, **3**, 121-140.

Hendrickson, E.A. (1993) The SCID mouse: relevance as an animal model system for studying human disease. *Am J Pathol*, **143**, 1511-1522.

Herz, U., Schnoy, N., Borelli, S., Weigl, L., Kasbohrer, U., Daser, A., Wahn, U., Kottgen, E. & Renz, H. (1998) A human-SCID mouse model for allergic immune response bacterial superantigen enhances skin inflammation and suppresses IgE production. *J Invest Dermatol*, **110**, 224-231.

Heslop, B.F. & Shaw, J.H. (1986) Early vascularization of syngeneic, allogeneic and xenogeneic skin grafts. *Aust N Z J Surg*, **56**, 357-362.

Hill, L., Kille, P., Weiss, D., Craig, T. & Coghlan, L. (1999) *Demodex musculi* in the skin of transgenic mice. *Contemp Topics*, **38**, 13-18.

Hill, P.B., Moriello, K.A. & DeBoer, D.J. (1995) Concentrations of total serum IgE, IgA, and IgG in atopic and parasitized dogs. *Vet Immunol Immunopathol*, **44**, 105-113.

Hillier, A. & Desch, C.E. (1997) A new species of demodex mite in the dog: case report. In: *13th annual proceedings of the ACVD and AAVD*, Nashville, Tennessee, p. 118-119.

Himonas, C.A., Theodorides, J.T. & Alexakis, A.E. (1975) Demodectic mites in the eyelids of domestic animals in greece. *J Parasitol*, **61**, 766.

Hirsh, D.C., Baker, B.B., Wiger, N., Yaskulski, S.G. & Osburn, B.I. (1975) Suppression of in vitro lymphocyte transformation by serum from dogs with generalized demodicosis. *Am J Vet Res*, **36**, 1591-1595.

Hoefakker, S., Balk, H.P., Boersma, W.J., van Joost, T., Notten, W.R. & Claassen, E. (1995) Migration of human antigen-presenting cells in a human skin graft onto nude mice model after contact sensitization. *Immunology*, **86**, 296-303.

Hollander, G.A., Simpson, S.J., Mizoguchi, E., Nichogiannopoulou, A., She, J., Gutierrez-Ramos, J.C., Bhan, A.K., Burakoff, S.J., Wang, B. & Terhorst, C. (1995) Severe colitis in mice with aberrant thymic selection. *Immunity*, **3**, 27-38.

Holub, M. (1989) Lymphatic tissues and cellular immune reactions. In: M. Holub (Ed) *Immunology of Nude Mice*. CRC Press Inc., Boca Raton, p. 111-129.

Jain, N. (1993) *Essentials of Veterinary Hematology*. Lea & Febiger, Philadelphia.

Jing, W. & Ismail, R. (1999) Mucocutaneous manifestations of HIV infection: a retrospective analysis of 145 cases in a Chinese population in Malaysia. *Int J Dermatol*, **38**, 457-463.

Johnson, C.M., Selleseth, D.W., Ellis, M.N., Childers, T.A., Tompkins, M.B. & Tompkins, W.A. (1994) Feline lymphoid tissues engrafted into scid mice maintain morphologic structure and produce feline immunoglobulin. *Lab Anim Sci*, **44**, 313-318.

Juhasz, I., Murphy, G.F., Yan, H.C., Herlyn, M. & Albelda, S.M. (1993) Regulation of extracellular matrix proteins and integrin cell substratum adhesion receptors on epithelium during cutaneous human wound healing in vivo. *Am J Pathol*, **143**, 1458-1469.

Juhasz, I., Simon, M., Jr, Herlyn, M. & Hunyadi, J. (1996) Repopulation of Langerhans cells during wound healing in an experimental human skin/SCID mouse model. *Immunol Lett*, **52**, 125-128.

Kaestner, K.H., Knochel, W. & Martinez, D.E. (2000) Unified nomenclature for the winged helix/forkhead transcription factors. *Genes Dev*, **14**, 142-6.

Kakutani, H. & Takahashi, S. (1987) Serial observations of tissue reaction in dermatophytosis experimentally induced in human skin graft to nude mouse. *Jap J Med Mycol*, **28**, 175-183.

Kamboj, D.S., Singh, K.B., Banga, H.S., Naresh, S., Nauriyal, D.C. & Sood, N. (1993) Study on the histopathological changes of canine demodicosis. *Int J Anim Sci*, **8**, 119-121.

Kanitakis, J., Al-Rifai, I., Faure, M. & Claudy, A. (1997) Demodex mites of human skin express Tn but not T (Thomsen-Friedenreich) antigen immunoreactivity [letter]. *J Cutan Pathol*, **24**, 454-5.

Kaufmann, R., Mielke, V., Reimann, J., Klein, C.E. & Sterry, W. (1993) Cellular and molecular composition of human skin in long-term xenografts on SCID mice. *Exp Dermatol*, **2**, 209-216.

Kaul, R., Sharma, A., Lisse, J.R. & Christadoss, P. (1995) Human recombinant IL-2 augments immunoglobulin and induces rheumatoid factor production by rheumatoid arthritis lymphocytes engrafted into severe combined immunodeficient mice. *Clin Immunol Immunopathol*, **74**, 271-282.

Kim, Y.H., Woodley, D.T., Wynn, K.C., Giomi, W. & Bauer, E.A. (1992) Recessive dystrophic epidermolysis bullosa phenotype is preserved in xenografts using SCID mice: development of an experimental in vivo model. *J Invest Dermatol*, **98**, 191-197.

Kotloff, D.B., Bosma, M.J. & Ruetsch, N.R. (1993a) V(D)J recombination in peritoneal B cells of leaky scid mice. *J Exp Med*, **178**, 1981-1994.

Kotloff, D.B., Bosma, M.J. & Ruetsch, N.R. (1993b) Scid mouse Pre-B cells with intracellular mu chains: analysis of recombinase activity and IgH gene rearrangements. *Int Immunol*, **5**, 383-391.

Koutz, F.R., Groves, H.F. & Gee, C.M. (1960) A survey of *Demodex canis* in the skin of clinically normal dogs. *Vet Med*, **55**, 52-53.

Krawiec, D.R. & Gaafar, S.M. (1980) Studies on the immunology of canine demodicosis. *J Am Anim Hosp Assoc*, **16**, 669-676.

Kreider, J.W., Bartlett, G.L. & Sharkey, F.E. (1979) Primary neoplastic transformation in vivo of xenogeneic skin grafts on nude mice. *Cancer Res*, **39**, 273-276.

Kreider, J.W., Howett, M.K., Wolfe, S.A., Bartlett, G.L., Zaino, R.J., Sedlacek, T. & Mortel, R. (1985) Morphological transformation in vivo of human uterine cervix with papillomavirus from condylomata acuminata. *Nature*, **317**, 639-641.

Kreider, J.W., Howett, M.K., Lill, N.L., Bartlett, G.L., Zaino, R.J., Sedlacek, T.V. & Mortel, R. (1986) In vivo transformation of human skin with human papillomavirus type 11 from condylomata acuminata. *J Virol*, **59**, 369-376.

Kreider, J.W., Howett, M.K., Leure-Dupree, A.E., Zaino, R.J. & Weber, J.A. (1987) Laboratory production in vivo of infectious human papillomavirus type 11. *J Virol*, **61**, 590-593.

Kreider, J.W., Patrick, S.D., Cladel, N.M. & Welsh, P.A. (1990) Experimental infection with human papillomavirus type 1 of human hand and foot skin. *Virology*, **177**, 415-417.

Krueger, G.G., Manning, D.D., Malouf, J. & Ogden, B. (1975) Long-term maintenance of psoriatic human skin on congenitally athymic (nude) mice. *J Invest Dermatol*, **64**, 307-312.

Krueger, G.G. & Briggaman, R.A. (1982) The Nude Mouse in Experimental and Clinical Research. In: J. Fogh and G. B.C. (Eds), *The Nude Mouse in the Biology and Pathology of Skin*, Vol. 2. Academic Press, New York, p. 301-322.

Kuby, J. (1997) *Immunology*. W.H. Freeman and Company, New York. p. 311-321.

Kwochka, K.W. (1987) Mites and related disease. In: F. Dusbabek and V. Bukva (Eds), *Veterinary Clinics of North America, Small Animal Practice*, Vol. 17. SPB Academic Publishing, Prague, p. 1263-1284.

Kyoizumi, S., Suzuki, T., Teraoka, S. & Seyama, T. (1998) Radiation sensitivity of human hair follicles in SCID-hu mice. *Radiat Res*, **149**, 11-18.

Lambert, P.B. (1971) Vascularization of skin grafts. *Nature*, **232**, 279-280.

Lane, A.T., Scott, G.A. & Day, K.H. (1989) Development of human fetal skin transplanted to the nude mouse. *J Invest Dermatol*, **93**, 787-791.

Latimer, K.S., Prasse, K.W., Mahaffey, E.A., Dawe, D.L., Lorenz, M.D. & Duncan, J.R. (1983) Neutrophil movement in selected canine skin diseases. *Am J Vet Res*, **44**, 601-605.

Lemarie, S.L. (1996) Canine demodicosis. *Comp Cont Edu Pract Vet*, **18**, 354-369.

Lemarie, S.L. & Horohov, D.W. (1996) Evaluation of interleukin-2 production and interleukin-2 receptor expression in dogs with generalized demodicosis. *Vet Dermatol*, 7, 213-219.

Lemarie, S.L., Hosgood, G. & Foil, C.S. (1996) A retrospective study of juvenile- and adult-onset generalized demodicosis in dogs (1986-91). *Vet Dermatol*, 7, 3-10.

Lemmens, P., Schrauwen, E., Rooster, H.d. & De Rooster, H. (1994) An uncommon species of *Demodex* in a dog. *Vlaams Diergeneeskundig Tijdschrift*, **63**, 19-21.

Limat, A., Stockhammer, E., Breitkreutz, D., Schaffner, T., Egelrud, T., Salomon, D., Fusenig, N.E., Braathen, L.R. & Hunziker, T. (1996) Endogeneously regulated site-specific differentiation of human palmar skin keratinocytes in organotypic cocultures and in nude mouse transplants. *Eur J Cell Biol*, **69**, 245-258.

Lin, R.Y., Sullivan, K.M., Argenta, P.A., Meuli, M., Lorenz, H.P. & Adzick, N.S. (1995) Exogenous transforming growth factor-beta amplifies its own expression and induces scar formation in a model of human fetal skin repair. *Ann Surg*, **222**, 146-154.

Lobe, D.C., Kreider, J.W. & Phelps, W.C. (1998) Therapeutic evaluation of compounds in the SCID-RA papillomavirus model. *Antiviral Res*, **40**, 57-71.

Luger, T., Beissert, S. & Schwarz, T. (1997) The epidermal cytokine network. In: J. Bos (Ed) *Skin immune system (SIS)*. CRC Press, New York, p. 271-310.

MacDougall, J.R., Croy, B.A., Chapeau, C. & Clark, D.A. (1990) Demonstration of a splenic cytotoxic effector cell in mice of genotype SCID/SCID.BG/BG. *Cell Immunol*, **130**, 106-117.

Manning, D.D., Reed, N.D. & Shaffer, C.F. (1973) Maintenance of skin xenografts of widely divergent phylogenetic origin of congenitally athymic (nude) mice. *J Exp Med*, **138**, 488-494.

Mason, K. (1993a) Clinical and pathophysiological aspects of parasitic skin diseases. In: P. Irkhle, I. Mason and S. White (Eds), *Advances in Veterinary Dermatology*, Vol. 2. Pergamon, Oxford, p. 177-206.

Mason, K.V. (1993b) A new species of demodex mite with D. canis causing canine demodecosis: a case report. *Vet Dermatol*, **4**, 37.

Matsumoto, K., Robb, E., Warden, G. & Nordlund, J. (1996) Hyperpigmentation of human skin grafted on to athymic nude mice: immunohistochemical study. *Br J Dermatol*, **135**, 412-418.

Matzinger, P. (1998) An innate sense of danger. *Semin Immunol*, **10**, 399-415.

Mazurier, F., Fontanellas, A., Salesse, S., Taine, L., Landriau, S., Moreau-Gaudry, F., Reiffers, J., Peault, B., Di Santo, J.P. & de Verneuil, H. (1999) A novel immunodeficient mouse model--RAG2 x common cytokine receptor gamma chain double mutants--requiring exogenous cytokine administration for human hematopoietic stem cell engraftment. *J Interferon Cytokine Res*, **19**, 533-541.

McCloghry, C.E., Hollis, D.E., Foldes, A., Rintoul, A.J., Baker, P., Vaughan, J.D., Maxwell, C.A., Kennedy, J.P. & Wynn, P.C. (1993a) The effects of exogenous melatonin and prolactin on wool follicle development in ovine foetal skin grafts. *Aust J Agric Res*, **44**, 993-1002.

McCloghry, C.E., Hollis, D.E., Raphael, K.A., Marshall, R.C., Foldes, A., Kennedy, J.P. & Wynn, P.C. (1993b) Wool follicles initiate, develop and produce wool fibres in ovine fetal skin grafts. *J Agric Sci*, **121**, 247-253.

McCune, J.M., Namikawa, R., Kaneshima, H., Shultz, L.D., Lieberman, M. & Weissman, I.L. (1988) The SCID-hu mouse: murine model for the analysis of human hematolymphoid differentiation and function. *Science*, **241**, 1632-1639.

McFadden, J.P. & Basketter, D.A. (2000) Contact allergy, irritancy and 'danger'. *Contact Dermatitis*, **42**, 123-127.

McKerrow, J.H. (1997) Cytokine induction and exploitation in schistosome infections. *Parasitology*, **115 Suppl**, S107-S112.

Medalie, D.A., Eming, S.A., Tompkins, R.G., Yarmush, M.L., Krueger, G.G. & Morgan, J.R. (1996) Evaluation of human skin reconstituted from composite grafts of cultured keratinocytes and human acellular dermis transplanted to athymic mice. *J Invest Dermatol*, **107**, 121-127.

Miller, W.H., Jr., Wellington, J.R. & Scott, D.W. (1992) Dermatologic disorders of Chinese Shar Peis: 58 cases (1981-1989). *J Am Vet Med Assoc*, **200**, 986-990.

Minato, N., Reid, L., Cantor, H., Lengyel, P. & Bloom, B.R. (1980) Mode of regulation of natural killer cell activity by interferon. *J Exp Med*, **152**, 124-137.

Mirowski, G.W., Hilton, J.F., Greenspan, D., Canchola, A.J., MacPhail, L.A., Maurer, T., Berger, T.G. & Greenspan, J.S. (1998) Association of cutaneous and oral diseases in HIV-infected men. *Oral Dis*, **4**, 16-21.

Mizuno, S., Fujinaga, T. & Hagio, M. (1993) Characterization of dog interleukin-2 activity. *J Vet Med Sci*, **55**, 925-930.

Moffat, J.F., Stein, M.D., Kaneshima, H. & Arvin, A.M. (1995) Tropism of varicella-zoster virus for human CD4+ and CD8+ T lymphocytes and epidermal cells in SCID-hu mice. *J Virol*, **69**, 5236-5242.

Moffat, J.F., Zerboni, L., Kinchington, P.R., Grose, C., Kaneshima, H. & Arvin, A.M. (1998a) Attenuation of the vaccine Oka strain of varicella-zoster virus and role of glycoprotein C in alphaherpesvirus virulence demonstrated in the SCID-hu mouse. *J Virol*, **72**, 965-974.

Moffat, J.F., Zerboni, L., Sommer, M.H., Heineman, T.C., Cohen, J.I., Kaneshima, H. & Arvin, A.M. (1998b) The ORF47 and ORF66 putative protein kinases of varicella-zoster virus determine tropism for human T cells and skin in the SCID-hu mouse. *Proc Natl Acad Sci USA*, **95**, 11969-11974.

Mombaerts, P., Iacomini, J., Johnson, R.S., Herrup, K., Tonegawa, S. & Papaioannou, V.E. (1992) RAG-1-deficient mice have no mature B and T lymphocytes. *Cell*, **68**, 869-877.

Mond, J.J., Scher, I., Cossman, J., Kessler, S., Mongini, P.K., Hansen, C., Finkelman, F.D. & Paul, W.E. (1982) Role of the thymus in directing the development of a subset of B lymphocytes. *J Exp Med*, **155**, 924-936.

Moore, F.M., White, S.D., Carpenter, J.L. & Torchon, E. (1987) Localization of immunoglobulins and complement by the peroxidase antiperoxidase method in autoimmune and non-autoimmune canine dermatopathies. *Vet Immunol Immunopathol*, **14**, 1-9.

Mosier, D.E., Gulizia, R.J., Baird, S.M. & Wilson, D.B. (1988) Transfer of a functional human immune system to mice with severe combined immunodeficiency. *Nature*, **335**, 256-259.

Mosier, D.E., Stell, K.L., Gulizia, R.J., Torbett, B.E. & Gilmore, G.L. (1993) Homozygous scid/scid;beige/beige mice have low levels of spontaneous or neonatal T cell-induced B cell generation. *J Exp Med*, **177**, 191-194.

Mourad, G.J., Preffer, F.I., Wee, S.L., Powelson, J.A., Kawai, T., Delmonico, F.L., Knowles, R.W., Cosimi, A.B. & Colvin, R.B. (1998) Humanized IgG1 and IgG4 anti-CD4 monoclonal antibodies: effects on lymphocytes in the blood, lymph nodes, and renal allografts in cynomolgus monkeys. *Transplantation*, **65**, 632-641.

Munoz-Perez, M.A., Rodriguez-Pichardo, A., Camacho, F. & Colmenero, M.A. (1998) Dermatological findings correlated with CD4 lymphocyte counts in a prospective 3 year study of 1161 patients with human immunodeficiency virus disease predominantly acquired through intravenous drug abuse. *Br J Dermatol*, **139**, 33-39.

Murphy, W.J., Conlon, K.C., Sayers, T.J., Wiltrout, R.H., Back, T.C., Ortaldo, J.R. & Longo, D.L. (1993) Engraftment and activity of anti-CD3-activated human peripheral blood lymphocytes transferred into mice with severe combined immune deficiency. *J Immunol*, **150**, 3634-3642.

Murphy, W.J., Taub, D.D., Anver, M., Conlon, K., Oppenheim, J.J., Kelvin, D.J. & Longo, D.L. (1994) Human RANTES induces the migration of human T lymphocytes into the peripheral tissues of mice with severe combined immune deficiency. *Eur J Immunol*, **24**, 1823-1827.

Murray, A.G., Schechner, J.S., Epperson, D.E., Sultan, P., McNiff, J.M., Hughes, C.C., Lorber, M.I., Askenase, P.W. & Pober, J.S. (1998) Dermal microvascular injury in the human peripheral blood lymphocyte reconstituted-severe combined immunodeficient (HuPBL-SCID) mouse/skin allograft model is T cell mediated and inhibited by a combination of cyclosporine and rapamycin. *Am J Pathol*, **153**, 627-638.

Nehls, M., Pfeifer, D., Schorpp, M., Hedrich, H. & Boehm, T. (1994) New member of the winged-helix protein family disrupted in mouse and rat nude mutations. *Nature*, **372**, 103-107.

Nickoloff, B.J., Kunkel, S.L., Burdick, M. & Strieter, R.M. (1995) Severe combined immunodeficiency mouse and human psoriatic skin chimeras. Validation of a new animal model. *Am J Pathol*, **146**, 580-588.

Nonoyama, S., Smith, F.O., Bernstein, I.D. & Ochs, H.D. (1993) Strain-dependent leakiness of mice with severe combined immune deficiency. *J Immunol*, **150**, 3817-3824.

Nutting, W.B. (1965) Host-parasite relations: demodicidae. *Acarology*, 7, 301-317.

Nutting, W.B. (1976a) Hair follicle mites (*Demodex* spp.) of medical and veterinary concern. *Cornell Vet*, **66**, 214-231.

Nutting, W.B. (1976b) Pathogenesis associated with hair follicle mites (Acari: Demodicidae). *Acarologia*, **17**, 493-507.

Nutting, W.B. & Desch, C.E. (1978) *Demodex canis*: redescription and reevaluation. *Cornell Vet*, **68**, 139-149.

Nutting, W.B. (1985) Prostigmata-mammalia: validation of coevolutionary phylogenies. In: K. Kim (Ed) *Coevolution of Parasitic Arthropods and Mammals*. John Wiley & Sons, New York, p. 569-640.

Nutting, W.B., Firda, K.E., Desch, C.E., Jr., ChannaBasavanna, G.P. & Viraktamath, C.A. (1989) Topology and histopathology of hair follicle mites (Demodicidae) of man. *Progress in Acarology*, **1**, 113-121.

Okada, T. (1986) Revascularisation of free full thickness skin grafts in rabbits: a scanning electron microscope study of microvascular casts. *Br J Plast Surg*, **39**, 183-189.

Owen, L.N. (1972) Demodectic mange in dogs immunosuppressed with antilymphocyte serum. *Transplantation*, **13**, 616-617.

Paradis, M. (1999) New approaches to the treatment of canine demodicosis. In: *Veterinary Clinics of North America: Small Animal Practice*, Vol. 29. SPB Academic Publishing, Prague, p. 1425-1436.

Paslin, D., Krowka, J. & Forghani, B. (1997) Molluscum contagiosum virus grows in human skin xenografts. *Arch Dermatol Res*, **289**, 486-488.

Paulik, S., Mojzisova, J., Bajova, V., Baranova, D. & Paulikova, I. (1996) Lymphocyte blastogenesis to concanavalin A in dogs with localized demodicosis according to duration of clinical disease. *Veterinarni Medicina*, **41**, 245-249.

Pavletic, M.M. (1991) Anatomy and circulation of the canine skin. *Microsurgery*, **12**, 103-112.

Petersen, M.J., Zone, J.J. & Krueger, G.G. (1984) Development of a nude mouse model to study human sebaceous gland physiology and pathophysiology. *J Clin Invest*, **74**, 1358-1365.

Petrini, J.H., Carroll, A.M. & Bosma, M.J. (1990) T-cell receptor gene rearrangements in functional T-cell clones from severe combined immune deficient (scid) mice: reversion of the scid phenotype in individual lymphocyte progenitors. *Proc Natl Acad Sci USA*, **87**, 3450-3453.

Petzelbauer, P., Groger, M., Kunstfeld, R., Petzelbauer, E. & Wolff, K. (1996) Human delayed-type hypersensitivity reaction in a SCID mouse engrafted with human T cells and autologous skin. *J Invest Dermatol*, **107**, 576-581.

Pilewski, J.M., Yan, H.C., Juhasz, I., Christofidou-Solomidou, M., Williams, J., Murphy, G.F. & Albelda, S.M. (1995) Modulation of adhesion molecules by cytokines in vivo

using human/severe combined immunodeficient (SCID) mouse chimeras. *J Clin Immunol*, **15**, 122S-129S.

Plenat, F., Vignaud, J.M., Guerret-Stocker, S., Hartmann, D., Duprez, K. & Duprez, A. (1992) Host-donor interactions in healing of human split-thickness skin grafts onto nude mice: in situ hybridization, immunohistochemical, and histochemical studies. *Transplantation*, **53**, 1002-1010.

Qintero, T.M. (1978) Frequencia de acaros *Demodex* en parpados de diferntes especies de animales domesticos (Frequency of *Demodex* mites in the skin of domestic animals). *Veterinaria Mex*, 111-113.

Randazzo, B.P., Kucharczuk, J.C., Litzky, L.A., Kaiser, L.R., Brown, S.M., MacLean, A., Albelda, S.M. & Fraser, N.W. (1996) Herpes simplex 1716--an ICP 34.5 mutant--is severely replication restricted in human skin xenografts in vivo. *Virology*, **223**, 392-395.

Ratner, D. (1998) Skin grafting. From here to there. *Dermatol Clin*, **16**, 75-90.

Reddy, N.R., Rao, P. & Yathiraj, S. (1992) Serum protein profiles and their significance in canine demodicosis. *Ind Vet J*, **96**, 762-764.

Reddy, N.R.J. & Rao, P.M. (1992) Immunological status of canine demodicosis based on the cutaneous response to mitogens. *Ind J Vet Med*, **12**, 4-7.

Reed, N.D. & Manning, D.D. (1973) Long-term maintenance of normal human skin on congenitally athymic (nude) mice. *Proc Soc Exp Biol Med*, **143**, 350-353.

Reed, N.D. & Manning, D.D. (1978) Present status of xenotransplantation of nonmalignant tissue to the nude mouse. In: *The Nude Mouse in Experimental and Clinical Research*, Vol. 1. Academic Press, New York, p. 167-185.

Revilla, Y., Pena, L., Mampaso, F., Vinuela, E. & Martinez-Alonso, C. (1994) Swine-reconstituted SCID mice as a model for African swine fever virus infection. *J Gen Virol*, **75**, 1983-1988.

Rice, A.M., Wood, J.A., Milross, C.G., Collins, C.J., McCarthy, N.F. & Vowels, M.R. (2000) Conditions that enable human hematopoietic stem cell engraftment in all NOD-SCID mice. *Transplantation*, **69**, 927-935.

Riechers, R. & Kopf, A.W. (1969) Cutaneous infestation with *Demodex folliculorum* in man. *J Invest Dermatol*, **52**, 103-106.

Robertson, M.T., Boyajian, M.J., Patterson, K. & Robertson, W.V. (1986) Modulation of the chloride concentration of human sweat by prolactin. *Endocrinology*, **119**, 2439-2444.

Rosenquist, M.D., Cram, A.E. & Kealey, G.P. (1988) Skin preservation at 4 degrees C: a species comparison. *Cryobiology*, **25**, 31-37.

Rothschild, H. & Ford, B. (1966) Hormones of the vertebrate host controlling ovarian regression and copulation of the rabbit flea. *Nature*, **211**, 261-266.

Rothschild, M. & Ford, B. (1972) Breeding cycle of the flea Cediopsylla simplex is controlled by breeding cycle of host. *Science*, **178**, 625-626.

Roye, O., Delhem, N., Trottein, F., Remoue, F., Nutten, S., Decavel, J.P., Delacre, M., Martinot, V., Cesbron, J.Y., Auriault, C. & Wolowczuk, I. (1998) Dermal endothelial cells and keratinocytes produce IL-7 in vivo after human Schistosoma mansoni percutaneous infection. *J Immunol*, **161**, 4161-4168.

Rufli, T. & Mumcuoglu, Y. (1981) The hair follicle mites *Demodex folliculorum* and *Demodex brevis*: biology and medical importance. A review. *Dermatologica*, **162**, 1-11.

Rygaard, J. (1969) Immunobiology of the mouse mutant "Nude". Preliminary investigations. *Acta Pathol Microbiol Scand*, 77, 761-762.

Rygaard, J. (1974) Skin grafts in nude mice. 3. Fate of grafts from man and donors of other taxonomic classes. *Acta Pathol Microbiol Scand [A.]*, **82**, 105-112.

Rygaard, J. (1991) History and Pathology. In: E. Boven and B. Winograd (Eds), *The Nude Mouse in Oncology Research.* CRC Press, Boca Raton, p. 1-9.

Sako, S. (1964) Studies on canine demodecosis. IV. Experimental infection of *Demodex foliculorum var canis* to dogs. *Trans Tottori Soc of Agric Sci*, **17**, 41-46.

Saridomichelakis, M., Koutinas, A., Papadogiannakis, E., Papazachariadou, M., Liapi, M. & Trakas, D. (1999) Adult-onset demodicosis in two dogs due to *Demodex canis* and a short-tailed demodectic mite. *J Small Anim Pract*, **40**, 529-532.

Scott, D.W., Farrow, B.R.H. & Schultz, R.D. (1974) Studies on the therapeutic and immunologic aspects of generalized demodectic mange in the dog. *J Am Anim Hosp Assoc*, **10**, 233-244.

Scott, D.W., Schultz, R.D. & Baker, E.B. (1976) Further studies on the therapeutic and immunologic aspects of generalized demodectic mange in the dog. *J Am Anim Hosp Assoc*, **12**, 203-213.

Scott, D.W. (1979) Canine demodicosis. In: E. Boven and B. Winograd (Eds), *Veterinary Clinics of North America: Small Animal Practice*, Vol. 9. CRC Press, Boca Raton, p. 79-92.

Scott, D.W. & Paradis, M. (1990) A survey of canine and feline skin disorders seen in a university practice: Small Animal Clinic, University of Montreal, Saint-Hyacinthe, Quebec, (1987-1988). *Can Vet J*, **31**, 830-835.

Scott, D.W., Miller, W.H. & Griffin, C.G. (1995) *Muller and Kirk's Small Animal Dermatology*. W.B. Saunders Company, Philadelphia. p. 417-434.

Scott, R.C. & Rhodes, C. (1988) The permeability of grafted human transplant skin in athymic mice. *J Pharm Pharmacol*, **40**, 128-129.

Segre, J.A., Nemhauser, J.L., Taylor, B.A., Nadeau, J.H. & Lander, E.S. (1995) Positional cloning of the nude locus: genetic, physical, and transcription maps of the region and mutations in the mouse and rat. *Genomics*, **28**, 549-59.

Sengbusch, H.G. & Hauswirth, J.W. (1986) Prevalence of hair follicle mites, *Demodex folliculorum* and *D. brevis* (Acari: Demodicidae), in a selected human population in western New York, USA. *J Med Entomol*, **23**, 384-388.

Sengbusch, H.G. (1991) Epidemiological studies of *Demodex spp.* (Acariformes: Demodecidae). In: F. Dusbabek and V. Bukva (Eds), *Modern Acarology*, Vol. 1. SPB Academic Publishing, Prague, p. 301-308.

Shaffer, C.F., Reed, N.D. & Jutila, J.W. (1973) Comparative survival of skin grafts from several donor species on congenitally athymic mice. *Transplant Proc*, **5**, 711-712.

Sheahan, B.J. & Gaafar, S.M. (1970) Histologic and histochemical changes in cutaneous lesions of experimentally induced and naturally occurring canine demodicidosis. *Am J Vet Res*, **31**, 1245-1254.

Shinkai, Y., Rathbun, G., Lam, K.P., Oltz, E.M., Stewart, V., Mendelsohn, M., Charron, J., Datta, M., Young, F., Stall, A.M. & et al. (1992) RAG-2-deficient mice lack mature lymphocytes owing to inability to initiate V(D)J rearrangement. *Cell*, **68**, 855-867.

Short, S.M., Paasch, B.D., Turner, J.H., Weiner, N., Daugherty, A.L. & Mrsny, R.J. (1996) Percutaneous absorption of biologically-active interferon-gamma in a human skin graft-nude mouse model. *Pharm Res*, **13**, 1020-1027.

Shultz, L.D., Schweitzer, P.A., Christianson, S.W., Gott, B., Schweitzer, I.B., Tennent, B., McKenna, S., Mobraaten, L., Rajan, T.V., Greiner, D.L. & et al. (1995) Multiple defects in innate and adaptive immunologic function in NOD/LtSz-scid mice. *J Immunol*, **154**, 180-191.

Shultz, L.D., Lang, P.A., Christianson, S.W., Gott, B., Lyons, B., Umeda, S., Leiter, E., Hesselton, R., Wagar, E.J., Leif, J.H., Kollet, O., Lapidot, T. & Greiner, D.L. (2000) NOD/LtSz-Rag1null mice: an immunodeficient and radioresistant model for engraftment

of human hematolymphoid cells, HIV infection, and adoptive transfer of NOD mouse diabetogenic T cells. *J Immunol*, **164**, 2496-2507.

Sigounas, G., Harindranath, N., Donadel, G. & Notkins, A.L. (1994) Half-life of polyreactive antibodies. *J Clin Immunol*, **14**, 134-140.

Sischo, W.M., Ihrke, P.J. & Franti, C.E. (1989) Regional distribution of ten common skin diseases in dogs. *J Am Vet Med Assoc*, **195**, 752-756.

Somberg, R.L., Robinson, J.P. & Felsburg, P.J. (1992) Detection of canine interleukin-2 receptors by flow cytometry. *Vet Immunol Immunopathol*, **33**, 17-24.

Spickett, S.G. (1961) Studies on *Demodex folliculorum* Simon (1842). *Parsitology*, **51**, 181-192.

Steinsvik, T.E., Gaarder, P.I., Aaberge, I.S. & Lovik. (1995) Engraftment and humoral immunity in SCID and RAG-2-deficient mice transplanted with human peripheral blood lymphocytes. *Scand J Immunol*, **42**, 607-616.

Sullivan, K.M., Lorenz, H.P., Meuli, M., Lin, R.Y. & Adzick, N.S. (1995) A model of scarless human fetal wound repair is deficient in transforming growth factor beta. *J Pediatr Surg*, **30**, 198-202.

Sumi, Y., Ueda, M., Kaneda, T., Oka, T. & Torii, S. (1984) Dynamic vascular changes in free skin grafts. *J Oral Maxillofac Surg*, **42**, 382-387.

Tary-Lehmann, M. & Saxon, A. (1992) Human mature T cells that are anergic in vivo prevail in SCID mice reconstituted with human peripheral blood. *J Exp Med*, **175**, 503-516.

Tary-Lehmann, M., Lehmann, P.V., Schols, D., Roncarolo, M.G. & Saxon, A. (1994) Anti-SCID mouse reactivity shapes the human CD4+ T cell repertoire in hu-PBL-SCID chimeras. *J Exp Med*, **180**, 1817-1827.

Taub, D.D., Longo, D.L. & Murphy, W.J. (1996) Human interferon-inducible protein-10 induces mononuclear cell infiltration in mice and promotes the migration of human T lymphocytes into the peripheral tissues and human peripheral blood lymphocytes-SCID mice. *Blood*, **87**, 1423-1431.

Taylor, P.C. (1994) *The Use of SCID Mice in the Investigation of Human Autoimmune Disease*. R. G. Landes Company, Austin. p. 1-129.

Toman, M., Svoboda, M., Rybnicek, J., Krejci, J. & Svobodova, V. (1998) Secondary immunodeficiency in dogs with enteric, dermatologic, infectious or parasitic diseases. *J Vet Med Series B*, **45**, 321-334.

Torbett, B.E., Picchio, G. & Mosier, D.E. (1991) hu-PBL-SCID mice: a model for human immune function, AIDS, and lymphomagenesis. *Immunol Rev*, **124**, 139-164.

Tsicopoulos, A., Pestel, J., Fahy, O., Vorng, H., Vandenbusche, F., Porte, H., Eraldi, L., Wurtz, A., Akoum, H., Hamid, Q., Wallaert, B. & Tonnel, A.B. (1998) Tuberculin-induced delayed-type hypersensitivity reaction in a model of hu-PBMC-SCID mice grafted with autologous skin. *Am J Pathol*, **152**, 1681-1688.

Tsuchida, M., Brown, S.A., Tutt, L.M., Tan, J., Seehafer, D.L., Harris, J.P., Xun, C.Q. & Thompson, J.S. (1997) A model of human anti-T-cell monoclonal antibody therapy in SCID mice engrafted with human peripheral blood lymphocytes. *Clin Transplant*, **11**, 522-528.

Unsworth, K. (1946) Studies on the clinical and parasitological aspects of canine demodectic mange. *J Comp Pathol Therapeut*, **56**, 114-127.

Vailly, J., Gagnoux-Palacios, L., Dell'Ambra, E., Romero, C., Pinola, M., Zambruno, G., De Luca, M., Ortonne, J.P. & Meneguzzi, G. (1998) Corrective gene transfer of keratinocytes from patients with junctional epidermolysis bullosa restores assembly of hemidesmosomes in reconstructed epithelia. *Gene Ther*, **5**, 1322-1332.

Van Genderen, J., Wolthuis, O.L., Ariens, A.T., Ericson, A.C. & Datema, R. (1987) The effects of topical foscarnet in a new model of herpes simplex skin infection. *J Antimicrob Chemother*, **20**, 547-556.

Van Neste, D., Warnier, G., Thulliez, M. & Van Hoof, F. (1989) Human hair follicle grafts onto nude mice: morphological study. In: D. Van Neste, J.M. Lachapelle and J.L. Antoine (Eds), *Trends in Human Hair Growth and Alopecia Research*. Kluwer Academic Publisher, Dordrecht, p. 117-131.

Van Neste, D. (1996) The use of scalp grafts onto nude mice as a model for human hair growth: Is there something new for hair growth drug screening programs? In: H.I. Maibach (Ed) *Dermatologic Research Techniques*. CRC Press. Inc., Boca Raton, p. 37-48.

Van Neste, D.J., Gillespie, J.M., Marshall, R.C., Taieb, A. & De Brouwer, B. (1993) Morphological and biochemical characteristics of trichothiodystrophy-variant hair are maintained after grafting of scalp specimens on to nude mice. *Br J Dermatol*, **128**, 384-387.

Van Vliet, E., Jenkinson, E.J., Kingston, R., Owen, J.J.T. & Van Ewijk, W. (1985) Stromal cell types in the developing thymus of the normal and nude mouse embryo. *Eur J Immunol*, **15**, 675-681.

Waldmann, T.A. & Strober, W. (1969) Metabolism of immunoglobulins. *Prog Allergy*, **13**, 1-110.

Wang, B., Biron, C., She, J., Higgins, K., Sunshine, M.J., Lacy, E., Lonberg, N. & Terhorst, C. (1994) A block in both early T lymphocyte and natural killer cell development in transgenic mice with high-copy numbers of the human CD3E gene. *Proc Natl Acad Sci USA*, **91**, 9402-9406.

Wang, B., Levelt, C., Salio, M., Zheng, D., Sancho, J., Liu, C.P., She, J., Huang, M., Higgins, K. & Sunshine, M.J. (1995) Over-expression of CD3 epsilon transgenes blocks T lymphocyte development. *Int Immunol*, 7, 435-448.

Wang, B., She, J., Salio, M., Allen, D., Lacy, E., Lonberg, N. & Terhorst, C. (1997) CD3-epsilon overexpressed in prothymocytes acts as an oncogene. *Mol Med*, **3**, 72-81.

Wang, J.C., Lapidot, T., Cashman, J.D., Doedens, M., Addy, L., Sutherland, D.R., Nayar, R., Laraya, P., Minden, M., Keating, A., Eaves, A.C., Eaves, C.J. & Dick, J.E. (1998a) High level engraftment of NOD/SCID mice by primitive normal and leukemic hematopoietic cells from patients with chronic myeloid leukemia in chronic phase. *Blood*, **91**, 2406-2414.

Wang, W.C., Goldman, L.M., Schleider, D.M., Appenheimer, M.M., Subjeck, J.R., Repasky, E.A. & Evans, S.S. (1998b) Fever-range hyperthermia enhances L-selectin-dependent adhesion of lymphocytes to vascular endothelium. *J Immunol*, **160**, 961-969.

Watanabe, M., Kobayashi, M., Iida, K., Ozeki, M., Doi, S. & Hoshino, T. (1996) Langerhans cells in mice with severe combined immunodeficiency (SCID). *Arch Histol Cytol*, **59**, 347-355.

Watson, C.J., Cobbold, S.P., Davies, H.S., Rebello, P.R., Waldmann, H., Calne, R.Y. & Metcalfe, S.M. (1993) CD4 and CD8 monoclonal antibody therapy: strategies to prolong renal allograft survival in the dog. *Br J Surg*, **80**, 1389-1392.

Watson, C.J., Davies, H.F., Cobbold, S.P., Rasmussen, A., Rebello, P.R., Thiru, S., Waldmann, H., Calne, R.Y. & Metcalfe, S.M. (1995) CD4 and CD8 monoclonal antibody therapy in the dog: strategies to induce tolerance to renal allografts. *Transplant Proc*, **27**, 123-124.

White, P.J., Fogarty, R.D., Liepe, I.J., Delaney, P.M., Werther, G.A. & Wraight, C.J. (1999) Live confocal microscopy of oligonucleotide uptake by keratinocytes in human skin grafts on nude mice. *J Invest Dermatol*, **112**, 887-892.

Wilkie, B.N., Markham, R.J.F. & Hazlett, C. (1979) Deficient cutaneous response to PHA-P in healthy puppies from a kennel with a high prevalence of demodicosis. *Can J Comp Med*, **43**, 415-419.

Wixson, S. & Smiler, K. (1997) Anesthesia and analgesia in rodents. In: D. Kohn, S. Wixson, W. White and G. Benson (Eds), *Anesthesia and Analgesia in Laboratory Animals*. Academic Press, New York. p. 181.

Wolfe, J.H. & Halliwell, R.E.W. (1980) Total hemolytic complement values in normal and diseased dog populations. *Vet Immunol Immunopathol*, **1**, 287-298.

Wortis, H.H., Nehlsen, S. & Owen, J.J. (1971) Abnormal development of the thymus in nude mice. *J Exp Med*, **134**, 681-692.

Xun, C.Q., Thompson, J.S., Jennings, C.D., Brown, S.A. & Widmer, M.B. (1994) Effect of total body irradiation, busulfan-cyclophosphamide, or cyclophosphamide conditioning on inflammatory cytokine release and development of acute and chronic graft-versus-host disease in H-2-incompatible transplanted SCID mice. *Blood*, **83**, 2360-2367.

Yager, J.A. & Wilcock, B.P. (1994) *Color Atlas and Text of Surgical Pathology of the Dog and Cat*. Wolfe Publishing, London. p. 85-197.

Yan, H.C., Juhasz, I., Pilewski, J., Murphy, G.F., Herlyn, M. & Albelda, S.M. (1993) Human/severe combined immunodeficient mouse chimeras. An experimental in vivo model system to study the regulation of human endothelial cell- leukocyte adhesion molecules. *J Clin Invest*, **91**, 986-996.

Yan, H.C., Delisser, H.M., Pilewski, J.M., Barone, K.M., Szklut, P.J., Chang, X.J., Ahern, T.J., Langer-Safer, P. & Albelda, S.M. (1994) Leukocyte recruitment into human skin transplanted onto severe combined immunodeficient mice induced by TNF-alpha is dependent on E-selectin. *J Immunol*, **152**, 3053-3063.

Yan, H.C., Williams, J.P., Christofidou-Solomidou, M., Delisser, H.M. & Albelda, S.M. (1996) The role of selectins and CD18 in leukotriene B4-mediated white blood cell emigration in human skin grafts transplanted on SCID mice. *Cell Adhes Commun*, **3**, 475-486.

Young, D.M., Greulich, K.M. & Weier, H.G. (1996) Species-specific in situ hybridization with fluorochrome-labeled DNA probes to study vascularization of human skin grafts on athymic mice. *J Burn Care Rehabil*, **17**, 305-310.

APPENDIX 1: FABRICATED SKIN BIOPSY TOOLS

Skin punches were formed with the same blade stock used in commercially available Acu-punch® skin biopsy instruments (Acuderm Inc., Ft. Lauderdale, Florida, USA) obtained directly from the manufacturer (Cardan Inc., Maple Wood, New Jersey, USA). Blade stock was machined into exactly 38 mm-long blanks **(A)**. Individual, 12 mm-in-diameter, cylindrical skin punch blades **(B)** were formed around the machined end of an aluminum mandrill **(C)** using a 12.5 mm shaft-clamp **(D, E)**. The completed skin punch was created by holding the cylindrical blade in the shaft clamp. To cut each graft, skin samples were gently held in place on a plastic cutting board using an applicator **(F)** and grafts were cut through the circular opening in the applicator. (bar = 2 cm)

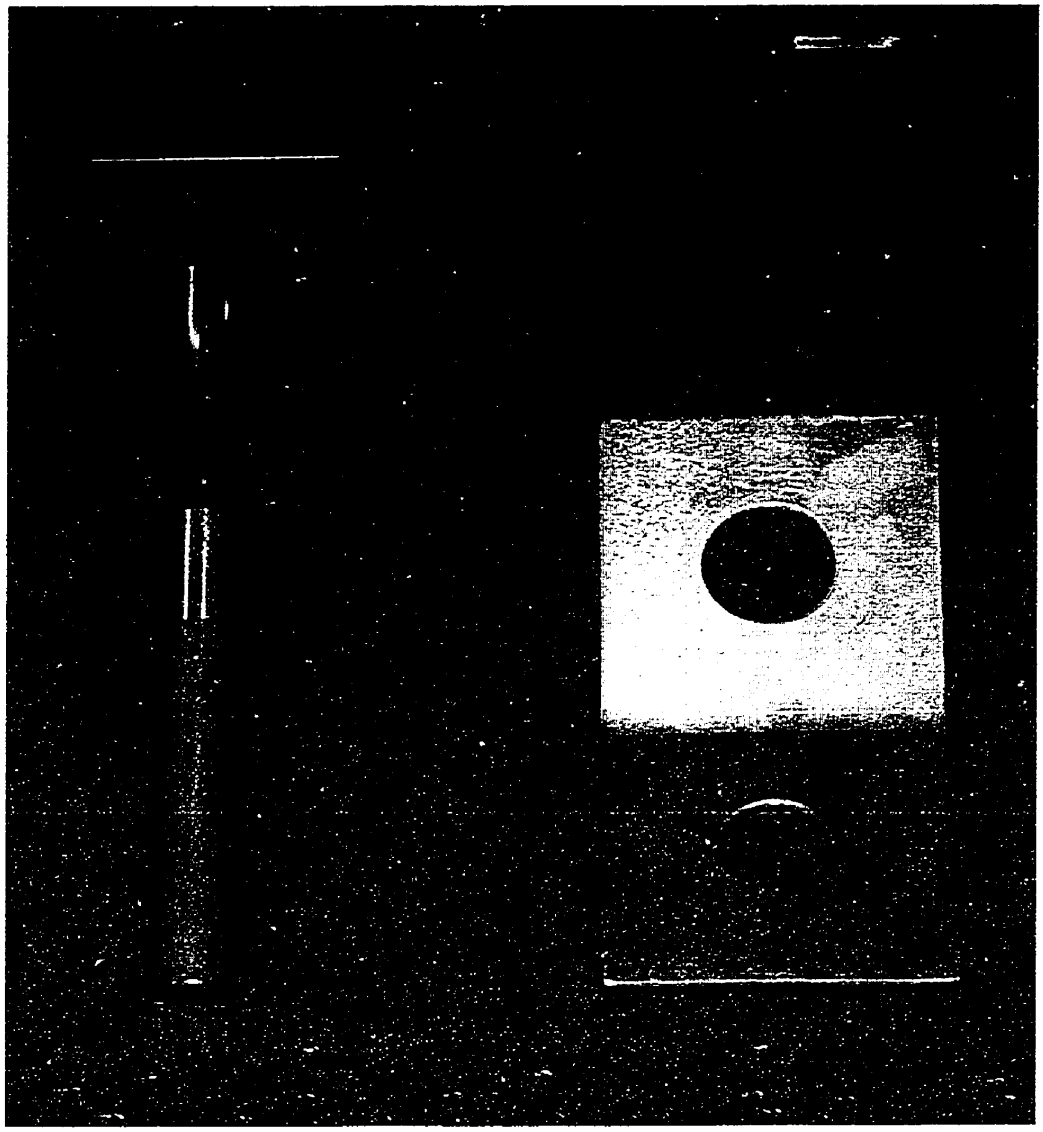

APPENDIX 2: MOUSE PLASMA CANINE IgG LEVELS (μg/mL) FOR PBMC RECONSTITUTED Tgε26 MICE EXPERIMENT, SECTION 3.3

GROUP-I (Mice received 22 x 10^6 canine lymphocytes by intraperitoneal injection)

WEEK	MOUSE-1	MOUSE-2	MOUSE-3	MOUSE-4	MOUSE-5	MEAN ±SD
2	6.60	5391.87	714.55	141.76	30.29	64.35 ±2329.35
4	2.57	18103.39*	1280.91	140.81	25.04	81.67 ±615.37
6	0.72	5736.52	1322.18	49.41	18.07	52.80 ±2474.88
8	0.31	6492.05	1692.73	31.61	17.11	15.83 ±2804.20

GROUP-II (Mice received 12 x 10^6 canine lymphocytes by intraperitoneal injection)

WEEK	MOUSE-1	MOUSE-2	MOUSE-3	MOUSE-4	MOUSE-5	MEAN ±SD
2	8.16	11.56	ND	†	†	9.86 ±2.40
4	0.34	7.61	-	-	-	3.98 ±5.14
6	ND	1.93	-	-	-	-
8	-	ND	-	-	-	-
10	-	-	-	-	-	-
12	-	-	-	-	-	-

*** = Value not included in calculations of mean and standard deviation**
ND = Canine IgG not detected
SD = Standard deviation
† = Mouse died prior to completion of the trial

APPENDIX 2: CONTINUED

GROUP-III (Mice received 25 x 10^6 canine lymphocytes by intraperitoneal injection)

WEEK	MOUSE-1	MOUSE-2	MOUSE-3	MOUSE-4	MOUSE-5	MEAN ±SD
2	8.34	6.47	1.94	7.55	7.24	6.31 ±2.53
4	6.05	4.82	ND	2.49	1.82	3.80 ±1.98
6	0.36	†	-	ND	ND	-
8	†		-	-	-	-
10			-	-	-	-
12			-	-	-	-

GROUP-IV (Mice received 14 x 10^6 canine lymphocytes by intraperitoneal injection)

WEEK	MOUSE-1	MOUSE-2	MOUSE-3	MOUSE-4	MEAN ±SD
2	64.35	2.14	128.2	27.78	55.62 ±54.71
4	81.67	5.37	26.92	17.67	32.91 ±33.69
6	52.80	ND	11.48	9.71	24.66 ±24.38
8	15.83	-	ND	6.08	10.96 ±6.89
10	10.31	-	1.10	1.83	4.41 ±5.12
12	3.18	-	ND	ND	-

ND = Canine IgG not detected
SD = Standard deviation
† = Mouse died prior to completion of the trial

APPENDIX 3: MOUSE PLASMA CANINE IgG LEVELS (μg/mL) FOR THE ICR Scid EXPERIMENT, SECTION 4.2

GROUP-I*

Mouse	(μg/mL)
1	11.88
2	0.0
3	0.67
4	8.86
5	24.93
Mean	11.42
±SD	±10.32

GROUP-III

Mouse	(μg/mL)
1	0.2
2	5290

Note, values are only reported for mice that completed the ICR scid experiment (Section 4.2).

***Experimental groups**

Group-I: *Demodex canis* plus canine PBMC
Group-II: *Demodex canis* plus PBS
Group-III: Canine PBMC only

Canine IgG was not detected in serum samples from mice in **GROUP-II** (n=8) that did not receive canine lymphocytes (data not shown).

SD = Standard deviation

APPENDIX 4: HAIR GROWTH SCORE FOR CANINE XENOGRAFTS IN THE *Rag2* EXPERIMENT, SECTION 4.4

GROUP-I*

Mouse		Score
1	(I)**	2
2	(A)	1
3	(H)	2
4	(B)	1
5	(G)	2
6	(C)	1
7	(D)	1
8	(E)	1
9	(F)	1

GROUP-II

Mouse		Score
1	(E)	1
2	(G)	1
3	(C)	1
4	(B)	1
5	(D)	1
6	(F)	1
7	(A)	1

GROUP-III

Mouse		Score
1	(A)	1
2	(B)	1
3	(C)	1
4	(G)	2
5	(D)	1
6	(E)	1
7	(H)	1
8	(F)	1

GROUP-IV

Mouse		Score
1	(A)	1
2	(H)	2
3	(B)	1
4	(C)	1
5	(D)	1
6	(G)	2
7	(E)	1
8	(F)	1

***Experimental groups**

Group-I: *Demodex canis* plus *in vitro* stimulated canine PBL
Group-II: *Demodex canis* plus unstimulated canine PBMC
Group-III: *Demodex canis* plus PBS
Group-IV: *In vitro* stimulated canine PBL only

** Note that the letters identify the pictures of each skin graft within figures provided in Section-4.4 for the *Rag2* experiment; Group-I (Figure-4.4-2), Group-II (Figure-4.4-3), Group-III (Figure-4.4-4) and Group-IV (Figure-4.4-5).

APPENDIX 5: MOUSE SERUM CANINE IgG LEVELS (μg/mL) FOR THE *Rag2* EXPERIMENT, SECTION 4.4

GROUP-I*

Mouse	(μg/mL)
1	52.97
2	27.93
3	27.59
4	46.12
5	5.7
6	38.45
7	21.26
8	43.58
9	42.53
Mean	34.01
±SEM	±4.91

GROUP-II

Mouse	(μg/mL)
1	0.51
2	0.56
3	1.66
4	1.78
5	0.32
6	1.87
7	0.79
Mean	1.07
±SEM	±0.25

GROUP-IV

Mouse	(μg/mL)
1	14.24
2	0.35
3	20.94
4	3.31
5	1.45
6	4.06
7	2.1
8	44.88
Mean	11.42
±SEM	±5.42

***Experimental groups**

Group-I: *Demodex canis* plus *in vitro* stimulated canine PBL
Group-II: *Demodex canis* plus unstimulated canine PBMC
Group-III: *Demodex canis* plus PBS
Group-IV: *In vitro* stimulated canine PBL only

Note, values are reported only for mice that completed the *Rag2* experiment. Canine IgG was not detected in serum samples from mice in **GROUP-III** (n = 8) that did not receive canine lymphocytes (data not shown).

SEM = Standard error of the mean

APPENDIX 6: BACTERIAL CULTURE RESULTS FOR THE *Rag2* EXPERIMENT, SECTION 4.4

GROUP-I*

Mouse	Culture
1 (I)**	*S. intermedius*
2 (A)	*S. intermedius*
3 (H)	*Bacillus sp.*
4 (B)	NBG
5 (G)	NBG
6 (C)	NBG
7 (D)	NBG
8 (E)	NBG
9 (F)	NBG

GROUP-II

Mouse	Culture
1 (E)	*S. intermedius*
2 (G)	NBG
3 (C)	NBG
4 (B)	*S. intermedius*
5 (D)	*S. intermedius*
6 (F)	NBG
7 (A)	*Bacillus sp.*

GROUP-III

Mouse	Culture
1 (A)	NBG
2 (B)	NBG
3 (C)	NBG
4 (G)	*S. intermedius*
5 (D)	*S. intermedius*
6 (E)	*S. intermedius*
7 (H)	NBG
8 (F)	NBG

GROUP-IV

Mouse	Culture
1 (A)	NBG
2 (H)	NBG
3 (B)	NBG
4 (C)	NBG
5 (D)	NBG
6 (G)	NBG
7 (E)	NBG
8 (F)	NBG

***Experimental groups**

Group-I: *Demodex canis* plus *in vitro* stimulated canine PBL
Group-II: *Demodex canis* plus unstimulated canine PBMC
Group-III: *Demodex canis* plus PBS
Group-IV: *In vitro* stimulated canine PBL only

****Note that the letters identify the pictures of each skin graft within figures provided in Section-4.4 for the *Rag2* experiment; Group-I (Figure-4.4-2), Group-II (Figure-4.4-3), Group-III (Figure-4.4-4) and Group-IV (Figure-4.4-5).